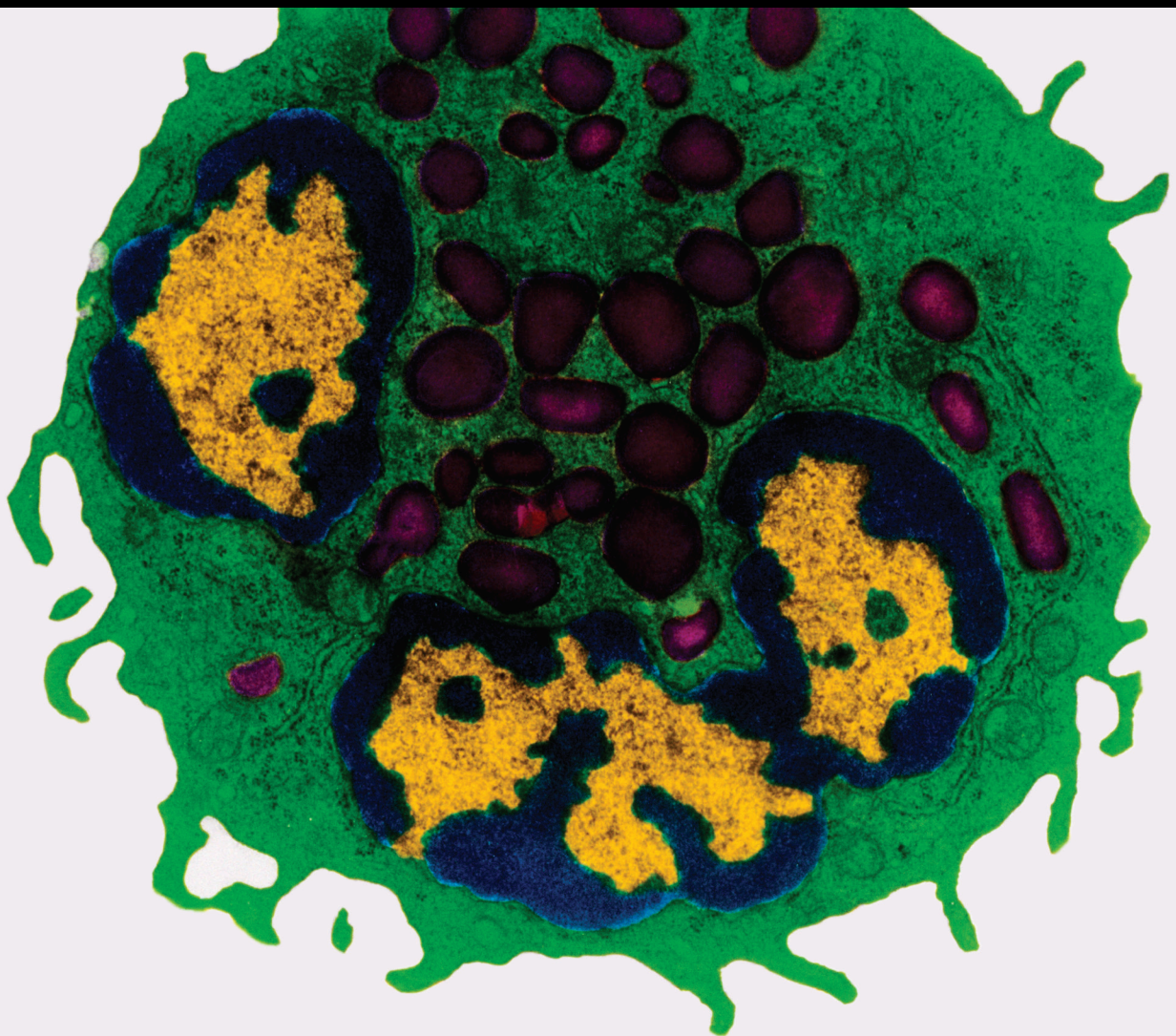


# Immune Regulatory Cells in Inflammation, Infection, Tumor, Metabolism, and Other Diseases 2019

Lead Guest Editor: Qingdong Guan

Guest Editors: Cheng Xiao and Minggang Zhang





---

**Immune Regulatory Cells in Inflammation,  
Infection, Tumor, Metabolism, and Other  
Diseases 2019**

Mediators of Inflammation

---

**Immune Regulatory Cells in Inflammation,  
Infection, Tumor, Metabolism, and Other  
Diseases 2019**

Lead Guest Editor: Qingdong Guan

Guest Editors: Cheng Xiao and Minggang Zhang



---

Copyright © 2019 Hindawi Limited. All rights reserved.

This is a special issue published in "Mediators of Inflammation." All articles are open access articles distributed under the Creative Commons Attribution License, which permits unrestricted use, distribution, and reproduction in any medium, provided the original work is properly cited.

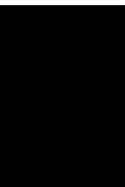
# Chief Editor

Anshu Agrawal, USA

## Editorial Board

Muzamil Ahmad, India  
Maria Jose Alcaraz, Spain  
Simi Ali, United Kingdom  
Amedeo Amedei, Italy  
Oleh Andrukhov, Austria  
Emiliano Antiga, Italy  
Zsolt J. Balogh, Australia  
Adone Baroni, Italy  
Jagadeesh Bayry, France  
Jürgen Bernhagen, Germany  
Tomasz Brzozowski, Poland  
Philip Bufler, Germany  
Elisabetta Buommino, Italy  
Daniela Caccamo, Italy  
Luca Cantarini, Italy  
Raffaele Capasso, Italy  
Calogero Caruso, Italy  
Maria Rosaria Catania, Italy  
Carlo Cervellati, Italy  
Cristina Contreras, Spain  
Robson Coutinho-Silva, Brazil  
Jose Crispin, Mexico  
Fulvio D'Acquisto, United Kingdom  
Eduardo Dalmarco, Brazil  
Pham My-Chan Dang, France  
Wilco de Jager, The Netherlands  
Beatriz De las Heras, Spain  
Chiara De Luca, Germany  
Clara Di Filippo, Italy  
Carlos Dieguez, Spain  
Agnieszka Dobrzyn, Poland  
Elena Dozio, Italy  
Emmanuel Economou, Greece  
Ulrich Eisel, The Netherlands  
Giacomo Emmi, Italy  
Fabiola B Filippin Monteiro, Brazil  
Antonella Fioravanti, Italy  
Stefanie B. Flohé, Germany  
Jan Fric, Czech Republic  
Tânia Silvia Fröde, Brazil  
Julio Galvez, Spain  
Mirella Giovarelli, Italy  
Denis Girard, Canada  
Ronald Gladue, USA

Markus H. Gräler, Germany  
Oreste Gualillo, Spain  
Qingdong Guan, Canada  
Elaine Hatanaka, Brazil  
Tommaso Iannitti, United Kingdom  
Byeong-Churl Jang, Republic of Korea  
Yoshihide Kanaoka, USA  
Yasumasa Kato, Japan  
Yona Keisari, Israel  
Alex Kleinjan, The Netherlands  
Marije I. Koenders, The Netherlands  
Elzbieta Kolaczowska, Poland  
Vladimir A. Kostyuk, Belarus  
Dmitri V. Krysko, Belgium  
Sergei Kusmartsev, USA  
Martha Lappas, Australia  
Philipp M. Lepper, Germany  
Eduardo López-Collazo, Spain  
Andreas Ludwig, Germany  
Ariadne Malamitsi-Puchner, Greece  
Joilson O. Martins, Brazil  
Donna-Marie McCafferty, Canada  
Barbro N. Melgert, The Netherlands  
Paola Migliorini, Italy  
Vinod K. Mishra, USA  
Eeva Moilanen, Finland  
Alexandre Morrot, Brazil  
Jonas Mudter, Germany  
Kutty Selva Nandakumar, China  
Hannes Neuwirt, Austria  
Nadra Nilsen, Norway  
Daniela Novick, Israel  
Marja Ojaniemi, Finland  
Sandra Helena Penha Oliveira, Brazil  
Olivia Osborn, USA  
Carla Pagliari, Brazil  
Martin Pelletier, Canada  
Vera L. Petricevich, Mexico  
Sonja Pezelj-Ribarić, Croatia  
Philenio Pinge-Filho, Brazil  
Michele T. Pritchard, USA  
Michal A. Rahat, Israel  
Zoltan Rakonczay Jr., Hungary  
Marcella Reale, Italy



---

Alexander Riad, Germany  
Emanuela Roschetto, Italy  
Carlos Rossa, Brazil  
Settimio Rossi, Italy  
Bernard Ryffel, France  
Carla Sipert, Brazil  
Helen C. Steel, South Africa  
Jacek Cezary Szepietowski, Poland  
Dennis D. Taub, USA  
Taina Tervahartiala, Finland  
Kathy Triantafilou, United Kingdom  
Fumio Tsuji, Japan  
Giuseppe Valacchi, Italy  
Luc Vallières, Canada  
Elena Voronov, Israel  
Kerstin Wolk, Germany  
Suowen Xu, USA  
Soh Yamazaki, Japan  
Shin-ichi Yokota, Japan  
Teresa Zelante, Singapore

## Contents

### **Immune Regulatory Cells in Inflammation, Infection, Tumor, Metabolism, and Other Diseases 2019**

Qingdong Guan , Cheng Xiao , and Minggang Zhang  
Editorial (2 pages), Article ID 3182198, Volume 2019 (2019)

### **Nephropathy in Hypertensive Animals Is Linked to M2 Macrophages and Increased Expression of the YM1/Chi3l3 Protein**

Paula Andréa Malveira Cavalcante , Natalia Alenina , Alexandre Budu, Leandro Ceotto Freitas-Lima , Thaís Alves-Silva , Juan Sebastian Henao Agudelo, Fatimunnisa Qadri, Niels Olsen Saraiva Camara , Michael Bader, and Ronaldo Carvalho Araújo   
Research Article (14 pages), Article ID 9086758, Volume 2019 (2019)

### **IL-10 Dampens the Th1 and Tc Activation through Modulating DC Functions in BCG Vaccination**

Hui Xu, Yanjuan Jia, Yonghong Li, Chaojun Wei, Wanxia Wang, Rui Guo, Jing Jia, Yu Wu, Zhenhao Li, Zhenhong Wei, Xiaoming Qi, Yuanting Li, and Xiaoling Gao   
Research Article (10 pages), Article ID 8616154, Volume 2019 (2019)

### **Noncanonical IFN Signaling, Steroids, and STATs: A Probable Role of V-ATPase**

Howard M. Johnson , Ezra Noon-Song, and Chulbul M. Ahmed  
Review Article (11 pages), Article ID 4143604, Volume 2019 (2019)

### **Rosiglitazone Improves Glucocorticoid Resistance in a Sudden Sensorineural Hearing Loss by Promoting MAP Kinase Phosphatase-1 Expression**

Liang Xia, Jingjing Liu, Yuanyuan Sun, Haibo Shi , Guang Yang , Yanmei Feng , and Shankai Yin   
Research Article (10 pages), Article ID 7915730, Volume 2019 (2019)

### **Dendritic Cells in Subcutaneous and Epicardial Adipose Tissue of Subjects with Type 2 Diabetes, Obesity, and Coronary Artery Disease**

Miloš Mráz, Anna Cinkajzlová, Jana Kloučková, Zdeňka Lacinová, Helena Kratochvílová, Michal Lipš, Michal Pořízka, Petr Kopecký, Jaroslav Lindner, Tomáš Kotulák , Ivan Netuka, and Martin Haluzík   
Research Article (7 pages), Article ID 5481725, Volume 2019 (2019)

### **Epigenetic Regulation of IL-17-Induced Chemokines in Lung Epithelial Cells**

Jiadi Luo , Xiaojing An, Yong Yao, Carla Erb, Annabel Ferguson, Jay K. Kolls, Songqing Fan, and Kong Chen   
Research Article (11 pages), Article ID 9050965, Volume 2019 (2019)

### **The Effect of Taxifolin on Cisplatin-Induced Pulmonary Damage in Rats: A Biochemical and Histopathological Evaluation**

Edhem Unver , Mustafa Tosun, Hasan Olmez, Mehmet Kuzucu, Ferda Keskin Cimen, and Zeynep Suleyman  
Research Article (6 pages), Article ID 3740867, Volume 2019 (2019)

**Leukotriene Involvement in the Insulin Receptor Pathway and Macrophage Profiles in Muscles from Type 1 Diabetic Mice**

João Pedro Tôrres Guimarães , Luciano Ribeiro Filgueiras, Joilson Oliveira Martins , and Sonia Jancar   
Research Article (8 pages), Article ID 4596127, Volume 2019 (2019)

**Innate Lymphoid Cells: A Link between the Nervous System and Microbiota in Intestinal Networks**

Lin Han , Xin-miao Wang, Sha Di , Ze-zheng Gao , Qing-wei Li , Hao-ran Wu , Qing Wang, Lin-hua Zhao , and Xiao-lin Tong   
Review Article (11 pages), Article ID 1978094, Volume 2019 (2019)

**Chemokines and Growth Factors Produced by Lymphocytes in the Incompetent Great Saphenous Vein**

Ewa Grudzińska , Sławomir Grzegorzczyn, and Zenon P. Czuba   
Research Article (10 pages), Article ID 7057303, Volume 2019 (2019)

**Phenotypic and Functional Diversities of Myeloid-Derived Suppressor Cells in Autoimmune Diseases**

Huijuan Ma and Chang-Qing Xia   
Review Article (8 pages), Article ID 4316584, Volume 2018 (2018)

## Editorial

# Immune Regulatory Cells in Inflammation, Infection, Tumor, Metabolism, and Other Diseases 2019

**Qingdong Guan** <sup>1,2,3,4</sup> **Cheng Xiao** <sup>5</sup> and **Minggang Zhang**<sup>6</sup>

<sup>1</sup>Cellular Therapy Laboratory, Manitoba Blood and Marrow Transplant Program, CancerCare Manitoba, Winnipeg, Canada

<sup>2</sup>Department of Internal Medicine, University of Manitoba, Winnipeg, Canada

<sup>3</sup>Department of Immunology, University of Manitoba, Winnipeg, Canada

<sup>4</sup>Research Institute in Oncology and Hematology, CancerCare Manitoba, Winnipeg, Canada

<sup>5</sup>Institute of Clinical Medicine, China-Japan Friendship Hospital, Beijing, China

<sup>6</sup>Immunology Program, Memorial Sloan-Kettering Cancer Center, New York, USA

Correspondence should be addressed to Qingdong Guan; [qguan@hsc.mb.ca](mailto:qguan@hsc.mb.ca)

Received 11 September 2019; Accepted 12 September 2019; Published 23 October 2019

Copyright © 2019 Qingdong Guan et al. This is an open access article distributed under the Creative Commons Attribution License, which permits unrestricted use, distribution, and reproduction in any medium, provided the original work is properly cited.

The immune regulatory components of the immune system, such as immune regulatory cells and regulatory cytokines, either natural or induced, play important roles in controlling a variety of physiological and pathological immune responses [1]. In the past years, great advances have been made in studying the physiopathological and therapeutic roles of immune regulator cells in inflammation, infection, tumor, transplantation, autoimmune diseases, and other diseases, such as mesenchymal stromal/stem cells (MSC) and regulatory T cells. MSC are being tested widely as a cellular therapy for autoimmune diseases and other diseases through modulating immune responses and/or promoting tissue repair [2–4]. Through proteomic analysis, we developed a reliable, rapid, and relevant potency assay for clinical grade MSC which is correlated with immunological function of MSC, and this may enhance the standardization of MSC cell products and ultimately promote the development of new MSC treatments [5, 6].

Myeloid-derived suppressor cells (MDSCs) are a heterogeneous population of immature cells that are imbalanced during cancer, transplantation, allergy, and other diseases and have a remarkable ability to suppress various T cell responses and to promote regulatory T cell expansion through multiple mechanisms [7–10]. The adoptive transfer of MDSCs sorted from animal models or generated in vitro could improve transplantation and autoimmune diseases, while targeting MDSC can improve cancer treatment. In this special issue, H. Ma and C.-Q. Xia summarized the phenotype

and functional characteristics of MDSC and reviewed recent advances on their roles in the pathogenesis of autoimmune diseases and potential therapeutic applications.

Dendritic cells and macrophages are professional antigen-presenting cells with the ability to suppress or instigate immune responses and to bridge innate and adaptive immunity. In this issue, M. Mraz et al. evaluated the presence of HLA-DR<sup>+</sup> lineage<sup>−</sup> DC and their subtype in peripheral blood and subcutaneous and epicardial adipose tissue in subjects with T2DM and with T2DM undergoing elective cardiac surgery and showed that T2DM decreased the amount of total DC but increased plasmacytoid DC in subcutaneous adipose tissue. H. Xu et al. showed that IL-10 deficiency restored the type 1 immune response through DC activation, thus providing better protection against TB infection. Using marrow cells from male FVB/N (control) and transgenic hypertensive animals, cells treated with M-CSF and subsequently with LPS and IFN- $\gamma$  polarized into M1 macrophages and with IL-4 and IL-13 treatment cells polarized to M2 phenotype. P. A. M. Cavalcante et al. compared stimulated macrophages in vitro and found that cells from hypertensive mice were predisposed toward polarization to an M2 phenotype.

Proinflammatory cytokines and regulatory cytokines also play important roles in the physiopathology of diseases. In this special issue, E. Grudzinska et al. evaluated the levels of chemokines and growth factors produced by lymphocytes

in the incompetent great saphenous vein. J. P. T. Guimaraes et al. explored the leukotriene involvement in the insulin receptor pathway and macrophage profiles in muscles from type I diabetic mice and showed that diabetic 5LO<sup>-/-</sup> mice (lack of leukotriene synthesis) had a higher expression of insulin receptor and AKT phosphorylation and increased the expression of anti-inflammatory molecules IL-10, Arg1, and Ym1 and reduced the expression of proinflammatory cytokine IL-6 in muscle macrophage.

In response to IL-17, airway epithelial cells can produce antimicrobial proteins and neutrophil chemoattractants such as CXCR2 ligands. In order to understand how IL-17 exerts downstream effects on its target cells through epigenetic mechanisms, J. Luo et al. showed that IL-17-induced CXCR2 ligand productions are dependent on histone acetylation specifically through repressing HDAC5, and the recognition of acetylated histones plays a pivotal role. However, IL-17 responses were regulated differently by the DNA methylation mechanisms in specific lineages. By focusing on IFN signaling, H. M. Johnson et al. showed that ligand, IFN receptor, the JAKs, and the STATs all undergo endocytosis and ATP-dependent nuclear translocation to promoters of genes specifically activated by IFNs, which indicated that the vacuolar ATPase (V-ATPase) proton pump probably plays a key role in endosomal membrane crossing by IFNs for receptor cytoplasmic binding.

Innate lymphoid cells (ILCs) are a novel family of innate immune cells, which are shown to be critical for integrated mucosal immunity. L. Han et al. summarized studies about ILCs in inflammatory bowel disease (IBD), crosstalk of ILCs with intestinal microbiota, and the relationship of ILCs in enteric nervous system (ENS).

Using a guinea pig model of lipopolysaccharide- (LPS-) induced sudden sensorineural hearing loss (SSHL), L. Xia et al. studied the role of MAP kinase phosphatase-1 (MKP-1) and rosiglitazone (RSG) in glucocorticoid resistance/sensitivity. Severe hearing loss was observed in the LPS group, as opposed to the protection from hearing loss in the treatment of LPS, DEX, and RSG. A positive correlation was found between MKP-1 levels and protection from hearing loss. RSG and DEX synergistically influenced inner ear inflammation may result from impaired MKP-1 function in inner ear tissues, suggesting a novel target to develop potential therapeutics for inflammatory diseases of the inner ear.

Overall, we believe that these articles may improve our knowledge of immune regulatory cell-mediated immune mechanisms in infection, inflammation, tumor, and other diseases, providing insights into designing effective immunodiagnostic and potential therapeutic strategies.

## Conflicts of Interest

The authors declare no financial conflict of interest.

## Acknowledgments

We would like to thank the authors for their cutting-edge research data and thought-provoking reviews. We also

express our gratitude to all the reviewers for their kind assistance and valuable insights.

Qingdong Guan  
Cheng Xiao  
Minggang Zhang

## References

- [1] Q. Guan, C. Xiao, and M. Zhang, "Immune regulatory cells in inflammation, infection, tumor, metabolism, and other diseases," *Mediators of Inflammation*, vol. 2018, Article ID 4170780, 2 pages, 2018.
- [2] F. van den Akker, S. C. de Jager, and J. P. Sluiter, "Mesenchymal stem cell therapy for cardiac inflammation: immunomodulatory properties and the influence of toll-like receptors," *Mediators of Inflammation*, vol. 2013, 181013 pages, 2013.
- [3] J. Y. Oh, T. W. Kim, H. J. Jeong et al., "Intraperitoneal infusion of mesenchymal stem/stromal cells prevents experimental autoimmune uveitis in mice," *Mediators of Inflammation*, vol. 2014, Article ID 624640, 9 pages, 2014.
- [4] J. Galipeau and L. Sensebe, "Mesenchymal stromal cells: clinical challenges and therapeutic opportunities," *Cell Stem Cell*, vol. 22, no. 6, pp. 824–833, 2018.
- [5] Q. Guan, P. Ezzati, V. Spicer, O. Krokhin, D. Wall, and J. A. Wilkins, "Interferon  $\gamma$  induced compositional changes in human bone marrow derived mesenchymal stem/stromal cells," *Clinical Proteomics*, vol. 14, no. 1, p. 26, 2017.
- [6] Q. Guan, Y. Li, T. Shpiruk, S. Bhagwat, and D. A. Wall, "Inducible indoleamine 2, 3-dioxygenase 1 and programmed death ligand 1 expression as the potency marker for mesenchymal stromal cells," *Cytotherapy*, vol. 20, no. 5, pp. 639–649, 2018.
- [7] D. I. Gabrilovich, "Myeloid-derived suppressor cells," *Cancer Immunology Research*, vol. 5, pp. 3–8, 2017.
- [8] Q. Zhang, M. Fujino, J. Xu, and X. K. Li, "The role and potential therapeutic application of myeloid-derived suppressor cells in allo- and autoimmunity," *Mediators of Inflammation*, vol. 2015, Article ID 421927, 14 pages, 2015.
- [9] Q. Guan, A. R. Blankstein, K. Anjos et al., "Functional myeloid-derived suppressor cell subsets recover rapidly after allogeneic hematopoietic stem/progenitor cell transplantation," *Biology of Blood and Marrow Transplantation*, vol. 21, no. 7, pp. 1205–1214, 2015.
- [10] Q. Guan, B. Yang, R. J. Warrington et al., "Myeloid-derived suppressor cells: roles and relations with Th2, Th17 and Treg cells in asthma," *Allergy*, 2019.

## Research Article

# Nephropathy in Hypertensive Animals Is Linked to M2 Macrophages and Increased Expression of the YM1/Chi3l3 Protein

Paula Andréa Malveira Cavalcante <sup>1,2,3</sup>, Natalia Alenina <sup>2,4</sup>, Alexandre Budu,<sup>1,3</sup>  
Leandro Ceotto Freitas-Lima <sup>1,3</sup>, Thaís Alves-Silva <sup>1,3</sup>, Juan Sebastian Henao Agudelo,<sup>5</sup>  
Fatimunnisa Qadri,<sup>2</sup> Niels Olsen Saraiva Camara <sup>5,6</sup>, Michael Bader,<sup>2,7,8,9</sup>  
and Ronaldo Carvalho Araújo <sup>1,3</sup>

<sup>1</sup>Department of Biophysics, Federal University of São Paulo (UNIFESP), São Paulo, SP, Brazil

<sup>2</sup>Max-Delbrück-Center for Molecular Medicine (MDC), Berlin, Germany

<sup>3</sup>Laboratory of Exercise Genetics and Metabolism, Federal University of São Paulo (UNIFESP), São Paulo, SP, Brazil

<sup>4</sup>German Center for Cardiovascular Research (DZHK), Partner Site Berlin, Germany

<sup>5</sup>Department of Immunology, Institute of Biomedical Sciences, University of São Paulo, São Paulo, Brazil

<sup>6</sup>Laboratory of Renal Pathophysiology, Department of Medicine, School of Medicine, University of São Paulo, São Paulo, Brazil

<sup>7</sup>Institute for Biology, University of Lübeck, Germany

<sup>8</sup>Berlin Institute of Health (BIH), Berlin, Germany

<sup>9</sup>Charité University Medicine, Berlin, Germany

Correspondence should be addressed to Ronaldo Carvalho Araújo; araujorona@gmail.com

Received 6 February 2019; Revised 3 June 2019; Accepted 16 June 2019; Published 10 July 2019

Guest Editor: Minggang Zhang

Copyright © 2019 Paula Andréa Malveira Cavalcante et al. This is an open access article distributed under the Creative Commons Attribution License, which permits unrestricted use, distribution, and reproduction in any medium, provided the original work is properly cited.

Macrophages contribute to a continuous increase in blood pressure and kidney damage in hypertension, but their polarization status and the underlying mechanisms have not been clarified. This study revealed an important role for M2 macrophages and the YM1/Chi3l3 protein in hypertensive nephropathy in a mouse model of hypertension. Bone marrow cells were isolated from the femurs and tibia of male FVB/N (control) and transgenic hypertensive animals that overexpressed the rat form of angiotensinogen (TGM(rAOPEN)123, TGM123-FVB/N). The cells were treated with murine M-CSF and subsequently with LPS+IFN- $\gamma$  to promote their polarization into M1 macrophages and IL-4+IL-13 to trigger the M2 phenotype. We examined the kidneys of TGM123-FVB/N animals to assess macrophage polarization and end-organ damage. mRNA expression was evaluated using real-time PCR, and protein levels were assessed through ELISA, CBA, Western blot, and immunofluorescence. Histology confirmed high levels of renal collagen. Cells stimulated with LPS+IFN- $\gamma$  *in vitro* showed no significant difference in the expression of CD86, an M1 marker, compared to cells from the controls or the hypertensive mice. When stimulated with IL-4+IL-13, however, macrophages of the hypertensive group showed a significant increase in CD206 expression, an M2 marker. The M2/M1 ratio reached 288%. Our results indicate that when stimulated *in vitro*, macrophages from hypertensive mice are predisposed toward polarization to an M2 phenotype. These data support results from the kidneys where we found an increased infiltration of macrophages predominantly polarized to M2 associated with high levels of YM1/Chi3l3 (91,89%), suggesting that YM1/Chi3l3 may be a biomarker of hypertensive nephropathy.

## 1. Introduction

Recent studies have established a strong association between immunoinflammatory processes, hypertension, and chronic

forms of kidney disease [1–4]. These pathologies are marked by progressive renal fibrosis and ultimately organ failure [5, 6]. Nephropathy in the wake of sustained hypertension is the second leading cause of end-stage renal disease

(ESRD), a condition whose incidence is increasing worldwide [7, 8]. Studies of both animal models of CKD and human hypertension have revealed high levels of proinflammatory cytokines and have exposed inflammation as the most significant factor in the progression of fibrosis, regardless of the initial cause [9, 10]. Thus, immunoinflammatory mechanisms are now recognized as crucial contributors to both acute and chronic forms of kidney disease [3].

Hypertension is marked by an infiltration of immune cells into the kidneys, vessel walls, perivascular regions, and nervous system; simultaneously, there is a high release of cytokines, a production of reactive oxygen species (ROS), and an increase in the expression of adhesion molecules [4, 11, 12]. These events are mediated by the innate and adaptive immune systems and have been shown to contribute to the sustained elevation of blood pressure [4].

Several studies [9, 10, 11] have implicated macrophages in the pathogenesis of hypertension. An elegant study by Wenzel et al. [13] provided strong evidence that monocytes and macrophages mediate angiotensin II- (Ang II-) induced hypertension and vascular dysfunction.

Studies of hypertension have revealed that Ang II activates angiotensin II receptor type 1 (AT1R). Upon hemodynamic injury, this leads to the recruitment of monocytes to the vasculature, kidney, and heart [13–16]. After infiltration, monocytes differentiate into at least two phenotypes: M1 or M2 [17, 18].

M1 cells express high levels of proinflammatory cytokines including interleukin-1 beta (IL-1 $\beta$ ) and tumor necrosis factor-alpha (TNF $\alpha$ ) and produce high amounts of ROS, which strongly promote microbicidal and tumoricidal activity. In contrast, M2 macrophages, also known as “alternatively activated,” have anti-inflammatory effects and mediate tissue repair through the secretion of IL-10 and transforming growth factor-beta (TGF- $\beta$ ) [19, 20].

The M2 response has been shown to depend on a sustained stimulus. Persistent lesions also cause irreversible fibrosis and the destruction of tissue [21, 22]. Studies have shown that the M2 phenotype enters a prorepair stage with the expression of chitinase-like protein-3 (YM1/Chi3l3) and acquires pathogenic functions [23–26].

YM1/Chi3l3 is a marker expressed by M2 macrophages in diverse tissues in the mouse and has been associated with recovery and function restoration [27, 28]. This protein displays chemotactic activity for T lymphocytes, bone marrow cells, and eosinophils [29]. Here, we attempt to determine whether the YM1/Chi3l3 marker has functions in arterial hypertension and hypertensive nephropathy, where its roles have not yet been clarified.

YM1/Chi3l3 exhibits a significant homology to microbial chitinases and several “chitinase-like” proteins reported recently (in tissues including human cartilage- (HC-) gp39, human macrophage chitotriosidase, porcine smooth muscle gp38k, and *Drosophila* DS-47) [30]. A recent study [31] has shown that YKL-40 serve as a new biomarker for predicting hypertension in a population of prehypertensive subjects.

As Ang II promotes macrophage recruitment [32, 33], we decided to study the cells in a mouse model in which the renin-angiotensin system could be controlled. Ang II arises

from the precursor angiotensinogen (AOPEN), making it one of the most important factors in the regulation of human blood pressure.

Mice lacking AOPEN presented drastic hypotension, pathomorphological alterations in the kidney, and reduced survival [34–36]. In contrast, transgenic mice overexpressing the rat AOPEN gene (TGM(rAOPEN)123, TGM123-FVB/N) developed hypertension, cardiac hypertrophy, impaired heart function, high levels of albuminuria, and pronounced fibrosis [34, 37, 38]. This suggests that besides being a good model of arterial hypertension, this animal model can also be used in studies of hypertensive nephropathy. We hypothesized that macrophages of these hypertensive animals from 10 to 12 weeks of age would be predisposed to polarize to an M2 phenotype and high levels of YM1/Chi3l3 would be found in their kidneys. This could make the protein a marker for hypertensive nephropathy.

## 2. Materials and Methods

**2.1. Animals.** The study was approved by the Federal University of São Paulo Ethics Committee (approval number CEUA 2384220216 in 29/Feb/2016). 10- to 12-week-old hypertensive (TGM123-FVB/N) male mice and normotensive controls (FVB/N) were used in the experiments. Mice overexpressing rat AOPEN (TGM(rAOPEN)123), originally generated on NMRI background [37], were crossed with FVB/N mice for 8 generations to transfer the rAOPEN transgene to the FVB/N background and generate the hypertensive model. The animals were maintained under standardized conditions with an artificial 12 h dark-light cycle and free access to food and water. Mice from the control group (FVB/N) ( $n = 9$ ) and hypertensive group (TGM123-FVB/N) ( $n = 9$ ) were euthanized by cervical dislocation; then, the femurs, tibia, and kidneys were extracted.

The transgenic animals used in this study (TGM123-FVB/N) are considered a valid model of arterial hypertension and hypertensive nephropathy since they presented mean blood pressure around 158 mmHg in males and 132 mmHg in females and developed high levels of albuminuria and pronounced renal fibrosis [34, 37, 38].

**2.2. Cell Culture.** Bone marrow-derived macrophages (BMDM) were isolated from the femur and tibia of the control (FVB/N) and hypertensive (TGM123-FVB/N) male mice. Cells were filtered using a Cell Steiner 70  $\mu$ m filter (Corning, USA), and the flow-through cells were washed twice with PBS by centrifugation at 300 g for 5 min. Subsequently, cells were lysed with 0.83% NH<sub>4</sub>Cl (3 min/4°C) and cultured in RPMI 1640 (Gibco) and DMEM High Glucose Medium (Gibco) supplemented with 10% FBS (Gibco), 1% penicillin-streptomycin (Gibco), and murine M-CSF (macrophage colony-stimulating factor) (PeproTech, USA). The culture medium was refreshed on day 3 and maintained until day 7 to promote BMDM differentiation. On day 8, the cells were polarized to M1 by 10  $\mu$ g/ml IFN- $\gamma$  (R&D Systems) and 1 mg/ml LPS (*E. coli*-LPS, Sigma-Aldrich, USA) and to M2 by 10  $\mu$ g/ml IL-4 (R&D Systems) and 10  $\mu$ g/ml IL-13 (R&D Systems). After induction of polarization, cells were

TABLE 1: The gene-specific primer sequences.

Gene name	Direction	Primer sequence (5'-3')
$\beta$ -Actin	Forward	CTG GCC TCA CTG TCC ACC TT
	Reverse	CGG ACT CAT CGT ACT CCT GCT T
iNOS	Forward	CTG CTG GTG GTG ACA AGC ACA TTT
	Reverse	ATG TCA TGA GCA AAG GCG CAG AAC
F4/80	Forward	CTTTGGCTATGGGCTTCCAGTC
	Reverse	GCAAGGAGGACAGAGTTTATCGTG
CD86	Forward	TCT CCA CGG AAA CAG CAT CT
	Reverse	CTT ACG GAA GCA CCC ATG AT
TNF $\alpha$	Forward	CCC ACG TCG TAG CAA ACC AC
	Reverse	CAC AGA GCA ATG ACT CCA AAG TAG
IL-1 $\beta$	Forward	GGC TCA TCT GGG ATC CTC TC
	Reverse	TCA TCT TTT GGG GTC CGT CA
MMP-9	Forward	ACG GAC CCG AAG CGG ACA TT
	Reverse	TTG CCC AGC GAC CAC AAC TC
IL-6	Forward	TAGTCCTTCCTACCCCAATTTC
	Reverse	TTGGTCCTTAGCCACTCCTCC
CD206	Forward	CAA GGA AGG TTG GCA TTT GT
	Reverse	CCT TTC AGT CCT TTG CAA GC
Collagen I	Forward	GAC ATG TTC AGC TTT GTG GAC CTC
	Reverse	GGG ACC CTT AGG CCA TTG TGT A
Fibronectin	Forward	CCT ACG GCC ACT GTG TCA CC
	Reverse	AGT CTG GGT CAC GGC TGT CT
KIM-1	Forward	TGT CGA GTG GAG ATT CCT GGA TGG T
	Reverse	GGT CTT CCT GTA GCT GTG GGC C
YM1	Forward	CCC CTG GAC ATG GAT GAC TT
	Reverse	AGC TCC TCT CAA TAA GGG CC
TGF- $\beta$ 1	Forward	CAA CAA TTC CTG GCG TTA CCT TGG
	Reverse	GAA AGC CCT GTA TTC CGT CTC CTT
MCP-1	Forward	CTCACCTGCTGCTACTCATT
	Reverse	TTACGGCTCAACTTCACATTCA
Collagen III	Forward	TCCTAACCAAGGCTGCAAGATGGA
	Reverse	AGGCCAGCTGTACATCAAGGACAT
AT1a	Forward	CAAGTCGCACTCAAGCCTG
	Reverse	CTCAGAACAAGACGCAGGC

cultured for 48 h and thereafter used for the RNA extraction, one well per condition per animal.

**2.3. Real-Time Quantitative PCR.** Real-time quantitative PCR (qPCR) was used to evaluate the mRNA expression of macrophage polarization marker genes. RNA isolation from the kidney and the macrophage cultures was performed using TRIzol (TRIzol Reagent, Invitrogen, Germany) according to the manufacturer's instructions. The RNA pellet was resuspended in RNase-free water and kept at  $-80^{\circ}\text{C}$  until used. RNA concentration was quantified using spectrophotometry (NanoDrop, München, Germany), and  $1\ \mu\text{g}$  of RNA was taken for the synthesis of cDNA using M-MLV

Reverse Transcriptase (Invitrogen). The reaction product was amplified using the GoTaq qPCR Master Mix (Promega; Germany) by real-time quantitative PCR (ABI 7900HT Real-Time PCR System, Applied Biosystems, Germany). The gene-specific primer sequences are listed in Table 1.

**2.4. Histology.** Paraffinized sections of renal tissue ( $5\ \mu\text{m}$  thick) were deparaffinized, rehydrated, and incubated with 1% sirius red in a saturated solution of picric acid for 60 min. Unbound sirius red was removed by treating the sections with acidified water and coverslipped using Eukit. The sections were examined and photographed at a magnification of 2x with a Keyence BZ-9000 microscope

(Keyence, Germany). The quantification of fibrosis was performed using the Keyence digital image analysis software (Keyence BZII).

**2.5. Protein Extraction.** Kidney tissue (ca. 1 g) was homogenized in extraction buffer containing phosphatases and protease inhibitors 100 mM Tris-HCl (pH 7.5), 1% Triton X-100, 10% sodium dodecyl sulfate (SDS), 10 mM EDTA, 100 mM sodium fluoride, 10 mM sodium pyrophosphate, 10 mM sodium orthovanadate, 2 mM phenylmethylsulfonyl fluoride (PMSF), and 0.1 mg aprotinin/ml at 14000 rpm by 40 minutes at 4°C. Protein concentrations were determined by the Bradford assay (Bio-Rad Laboratories, Hercules, CA, USA). Extracts were used for Western blotting, CBA, and ELISA analysis.

**2.6. Enzyme-Linked Immunosorbent Assay (ELISA).** Renal levels of IL-10, IL-1 $\beta$ , and TNF $\alpha$  were determined using Quantikine Mouse ELISA kits (R&D Systems, MN, USA) according to the manufacturer's instructions.

**2.7. Detection of TGF- $\beta$  and YM1/YM2 by Western Blot (WB).** Proteins extracted from the mouse kidney were submitted to SDS-PAGE (25  $\mu$ g of protein/well) and transferred to a PVDF membrane at 300 mA, for 2 h, in ice-cold buffer (3 g/l Tris, 14.4 g/l glycine, and 20% methanol). Membrane blocking was executed overnight, at 4°C, in PBS-T (137 mM NaCl, 2.7 mM KCl, 8.1 mM Na<sub>2</sub>HPO<sub>4</sub>, 1.5 mM KH<sub>2</sub>PO<sub>4</sub>, 0.05% Tween-20, pH 7.2), containing 5% (*m/v*) of bovine serum albumin (Sigma). The membrane was then incubated with 1:1000 anti-TGF- $\beta$  antibody (Cell Signaling Technology, #3709) in PBS-T or anti-YM-1+YM-2 and 1:10000 (Abcam, #ab192029) in PBS-T+5% BSA overnight at room temperature on a shaker. After washing the membrane (three times, 10 min), the secondary antibody (anti-IgG rabbit, HRP-conjugated, Sigma, #A6154, 1:5000) was added and incubation proceeded for 1 h on a shaker. After three washes as above, the substrate SuperSignal West Pico (Pierce) was used to detect the bands in an imager. The antibodies were removed from the membrane with two subsequent 10-minute incubations in mild stripping buffer (15 g/l glycine, 1 g/l SDS, 10 ml Tween-20, pH 2.2). The membrane was washed twice (10 min each) with PBS and twice (5 min each) in PBS-T, blocked as above, and incubated for 2 h in PBS-T with the primary anti- $\beta$ -actin antibody (1:5000, raised in rabbit) used as a loading control. Secondary antibody incubation and detection of the bands were performed as above. The densitometry was obtained using the software Scion Image (Release Alpha 4.0.3.2), and relative protein expression was determined by dividing TGF- $\beta$  and YM1/YM2 by  $\beta$ -actin densitometry data.

**2.8. Cytokine Assessment in Kidney Sample (CBA).** Levels of concentrations of interleukin-6 (IL-6), Monocyte Chemoattractant Protein-1 (MCP-1), Interferon- $\gamma$  (IFN- $\gamma$ ), and tumor necrosis factor (TNF) in a kidney sample were measured using the BD™ CBA Mouse Inflammation Kit (Becton Dickinson (BD), USA). Controls and samples were processed according to the manufacturer's instructions. The

results were normalized according to the total value of the protein and expressed as pg/mg protein.

**2.9. Immunofluorescence (IF).** Immunofluorescence for F4/80, iNOS, and YM1 was performed by incubating the sections with Alexa Fluor 594 (1:300, ThermoFisher, #A11007) anti-mouse and Alexa Fluor 488 anti-rabbit (1:300, ThermoFisher, #A11034) anti-mouse sections. The nuclei were stained with DAPI (1:600, ThermoFisher, #D1306). The kidney slices were incubated with primary mouse anti-F4/80 antibodies (1:500, Abcam, #ab6640) overnight at 4°C, rabbit anti-iNOS (1:100, Abcam, #ab15323), and rabbit anti-YM-1+YM-2, (1:10000, Abcam, #ab192029). Nonspecific binding was controlled by the replacement of a negative control by the primary antibody.

**2.10. 3D Confocal Microscopy.** Immunopositive signals were detected by 3D confocal microscopy (Zeiss LSM 780, Germany). The images were analyzed with ImageJ software.

The images were acquired employing a PlanNeofluar 40x objective with 1.3 numerical aperture. DAPI, Alexa 594, and Alexa 488 were excited with 405 nm, 594 nm, and 488 nm lasers, while emission was collected between 421 nm-488 nm, 597 nm, and 646 nm and 498 nm and 554 nm, respectively. Slices on the Z plane were taken. The stacked images were rendered at the maximum precision available, and three-dimensional projection was performed using the "surface" option (ZEN software, Carl Zeiss, Germany).

**2.11. Statistical Analysis.** Data are presented as means  $\pm$  SEM. The statistical analysis was performed with Prism software (GraphPad Software, La Jolla, CA, USA). Multiple groups were compared through a one-way analysis of variance (ANOVA) followed by the Bonferroni post hoc test. The two-group analysis was performed using Student's *t*-test. *p* values < 0.05 were considered statistically significant.

### 3. Results

**3.1. The Macrophages of Hypertensive Animals Have a Predisposition toward the M2 Phenotype.** Initially, we cultured macrophages extracted from the bone marrow of hypertensive TGM123-FVB/N and control mice (FVB/N) over 10 days. After *in vitro* stimulation, we observed no differences in the expression of CD86 (an M1 marker) between the groups (Figure 1(a)). The hypertensive group, however, revealed a significant increase in the expression of CD206 (M2 marker) compared to controls (Figure 1(b)). In this group, the M2/M1 ratio reached 288% (Figure 1(c)). These results showed that the macrophages of hypertensive animals had a predisposition toward the M2 phenotype.

**3.2. The Kidneys of Hypertensive Animals Show High Levels of Collagen and Macrophage Polarization to the M2 Phenotype.** Histological examinations confirmed that hypertensive animals TGM123-FVB/N exhibited higher levels of collagen, indicative of both interstitial and perivascular fibrosis, compared to control animals (FVB/N) (Figures 2(a) and 2(b)).

We analyzed the association between F4/80 gene expression and the presence of macrophages in the kidneys of

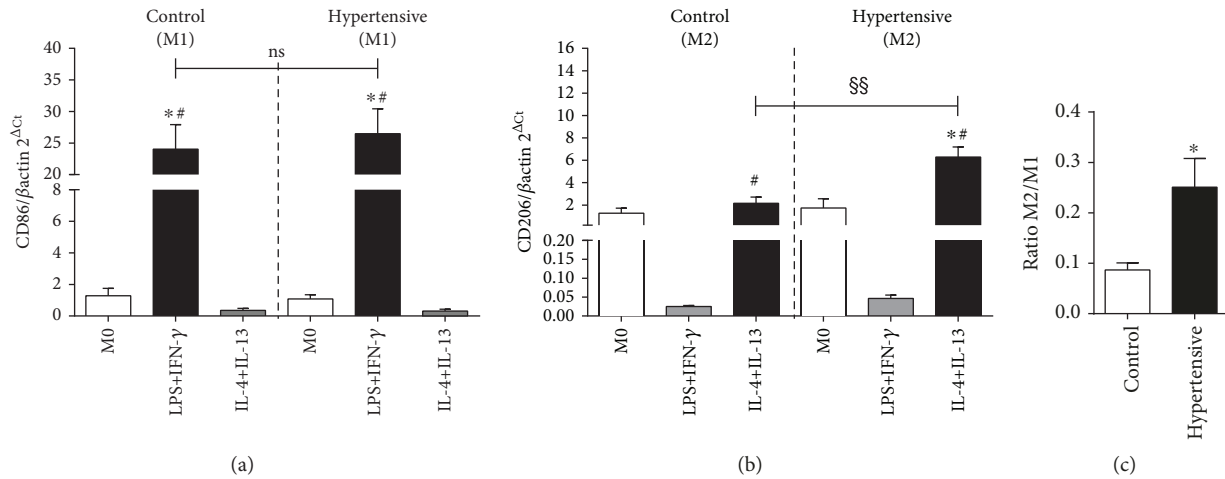


FIGURE 1: The macrophages of hypertensive animals have a predisposition toward the M2 phenotype. Four mice for each group, 6 wells per animal. (a) CD86 gene expression. Values were expressed as the mean ± SEM. \**p* < 0.05 compared to M0 groups and #*p* < 0.05 relative to IL-4+IL-13 groups, with ANOVA followed by Bonferroni correction for multiple comparisons. (b) CD206 gene expression. Values expressed as the mean ± SEM. \**p* < 0.05 compared to M0 groups, #*p* < 0.05 relative to LPS+IFN-γ groups, and §§*p* < 0.05 compared to IL-4+IL-13 from control mice, with ANOVA followed by Bonferroni correction for multiple comparisons. (c) Ratio M2/M1. Values are expressed as the mean ± SEM. \**p* < 0.05 compared to the control group with the *t*-test. The M2/M1 ratio reached 288%.

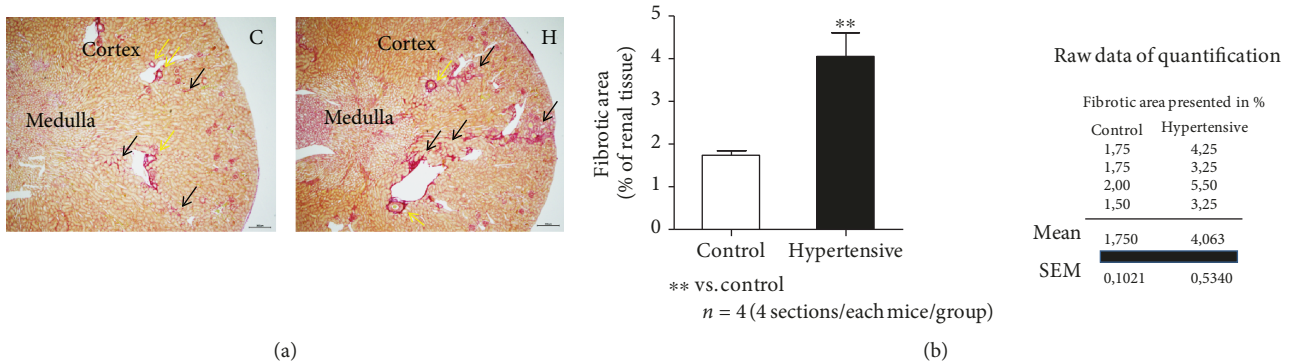


FIGURE 2: High levels of collagen were found in the kidneys of the hypertensive group. (a) Picro sirius red stained renal paraffin sections (renal cortex and medulla) of nonhypertensive control (C) and of rAOGEN transgenic hypertensive (H) mice at the age of 12 weeks. Light microscopic images were taken using a Keyence microscope (BZ-9000). Yellow arrows represent the perivascular fibrosis and black arrows the interstitial fibrosis. The scale bar = 300 μm. (b) Analysis and quantification of total fibrosis (interstitial and perivascular) were performed on digital renal images using a Keyence BZII analyzer. Data were presented as the area of fibrosis in % of whole renal section (4 sections/animal/groups). Histology with four mice of each group.

hypertensive and control mice, which revealed significant differences in the hypertensive group (Figure 3(a)). Hypertensive groups exhibited no increase in the expression of AT1aR (Figure 3(b)), suggesting that the Ang II-AT1R interaction tends to shift the M1/M2 balance toward M2 predominance.

We evaluated the expression of genes related to the polarization to M1 (iNOS, CD86, TNFα, IL-1β, MCP-1, MMP-9, and IL-6). Statistically significant differences were found for transcripts of iNOS, TNFα, and IL-1β (Figure 4). However, these differences were smaller than twofold. Karlen et al. [39] showed that real-time qPCR yields reliable estimates only in cases when the relative expression is twofold or higher.

In addition, these gene expression data do not support the results from measurements of protein levels, in which

we did not find a significant difference in the M1 marker protein levels relative to the respective control groups. This was the case for TNFα (Figures 5(a) and 6(a)), IL-1β (Figure 5(b)), IL-6 (Figure 6(b)), IFN-γ (Figure 6(c)), MCP-1 (Figure 6(d)), and iNOS (Figure 7(c)).

Next, we evaluated the expression of genes related to polarization to the M2 phenotype (Arg-1, IL-10, type I collagen, type III collagen, fibronectin, KIM-1, YM1, and TGF-β1). Statistically significant differences were found for the expression of YM1, TGF-β1, type I collagen, type III collagen, fibronectin, and KIM-1 (Figure 8).

We verified this at the protein level for IL-10, where no significant difference was again detected (Figures 8 and 9).

We confirmed the high levels of other M2 markers, including TGF-β1 and YM1, by Western blot (Figures 10(a) and 10(b)).

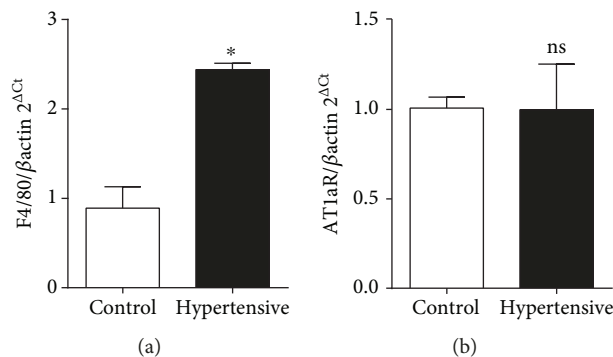


FIGURE 3: F4/80 gene expression indicates the presence of macrophages in the kidneys of hypertensive mice. Ang II levels are elevated, but Ang II is probably not binding to AT1aR. (a) F4/80 gene presented a significant difference when compared to the respective controls. Values are expressed as the mean ± SEM. \* $p < 0.05$  compared to the control group with the  $t$ -test. (b) AT1aR gene presented no significant difference when compared to the respective controls. Values are expressed as the mean ± SEM. \* $p < 0.05$  compared to the control group with the  $t$ -test. Five mice for each group.

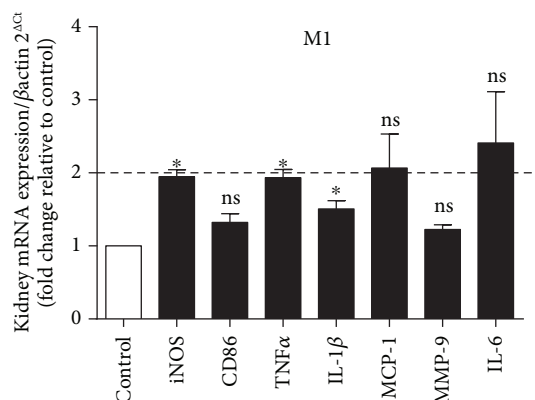


FIGURE 4: Three markers of the M1 phenotype showed an increase, but the changes were smaller than twofold. Values are expressed as the mean ± SEM. \* $p < 0.05$  compared to the control group with the  $t$ -test. The genes iNOS, TNFα, and IL-1β presented a significant difference when compared to the respective controls. Five mice for each group.

3.3. *High Levels of YM1/Chi3l3 Were Found in the Kidneys of Hypertensive Animals.* Alongside a general increase in F4/80 levels (Figure 7(a)), other M2 markers exhibited a sharp rise of expression in hypertensive kidneys (Figures 7, 8, 10(a) and 10(b)).

In addition, quantitative immunofluorescence showed a significant jump in the expression of YM1 in hypertensive animals (Figure 7(b)) but no difference in the M1 marker gene iNOS (Figure 7(c)), as can be observed in Figures 11(a)–11(d).

#### 4. Discussion

Despite strong evidence that macrophage polarization plays an important role in the development of hypertension

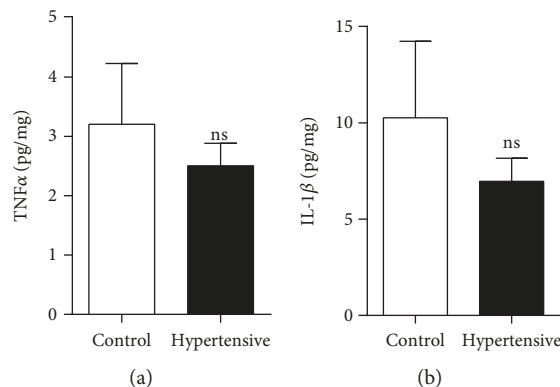


FIGURE 5: There was no increase in levels of the M1 marker proteins TNFα and IL-1β. (a) Renal levels of TNFα by ELISA. (b) Renal levels of IL-1β by ELISA. Values are expressed as the mean ± SEM. \* $p < 0.05$  compared to the control group with the  $t$ -test. Five mice for each group.

[9, 10, 11], few studies have addressed the role of these cells in the disease. We carried out a study of the polarization of these cells from hypertensive animals *in vitro* and *in vivo*, with the aim of developing insights into their possible functions in the kidney and roles in renal pathologies.

This study revealed an important role for M2 macrophages during hypertensive nephropathy. Our main finding was that the kidneys of 10- to 12-week-old hypertensive TGM123-FVB/N mice exhibited high levels of collagen, indicative of perivascular and interstitial fibrosis and confirming earlier studies on this model [34, 38]. These symptoms were accompanied by an increase in the expression of marker genes for the M2 phenotype, suggesting that hypertensive kidneys had undergone an infiltration of macrophages polarized preferentially toward M2. This effect reflected the results of our *in vitro* investigation, in which macrophages from hypertensive animals also had a predisposition toward the M2 type.

Ang II, a peptide hormone whose effects are similar to those of proinflammatory cytokines, plays a key role in the progression of chronic renal damage and may be involved in the development of fibrosis [40–42]. This vasoactive peptide activates mesangial and tubular cells and interstitial fibroblasts, increasing the expression and synthesis of extracellular matrix proteins. Studies have shown that blocking Ang II action through ACE inhibitors and Ang II receptor antagonists prevents proteinuria and fibrosis, as well as the infiltration of inflammatory cells into the kidneys [40, 41].

During disease, kidneys are infiltrated by neutrophils and subsequently by monocytes, which differentiate into macrophages and contribute to tubular injury [43]. Proinflammatory macrophages are known to contribute to the initiation and progression of renal diseases [44–49], renal injury related to cisplatin nephrotoxicity [50, 51], and renal allograft injury [52, 53].

The main feature of renal fibrosis is an excessive production and accumulation of ECM (extracellular matrix) proteins, which leads to the formation of scar tissue and

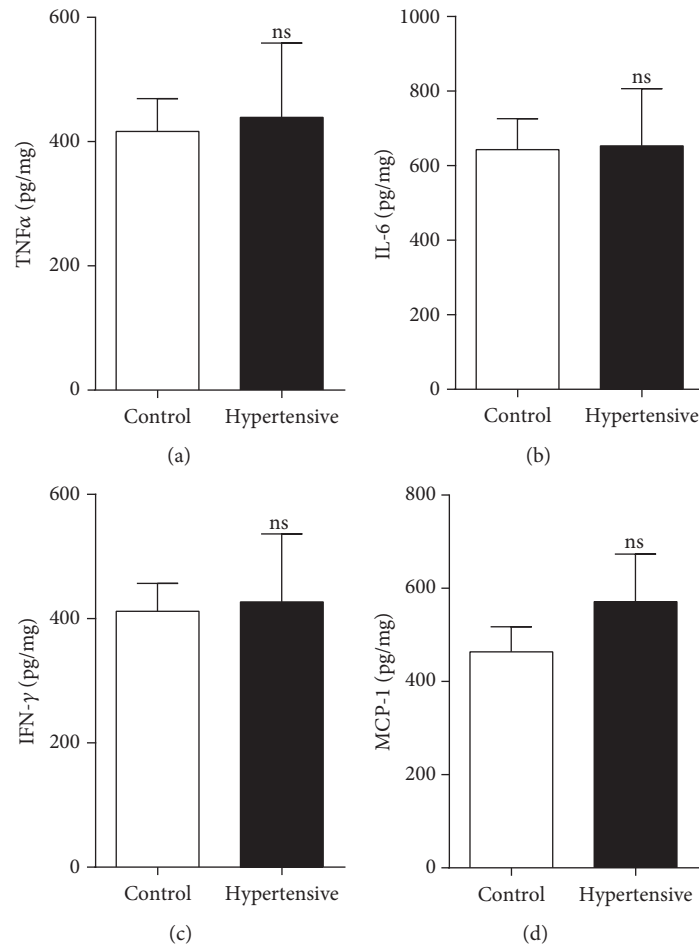


FIGURE 6: There was no increase in levels of M1 marker proteins TNFα, IL-6, IFN-γ, and MCP-1: (a) renal levels of TNFα by CBA; (b) renal levels of IL-6 by CBA; (c) renal levels of IFN-γ by CBA; (d) renal levels of MCP-1 by CBA. Values were expressed as the mean ± SEM. \**p* < 0.05 compared to the control group with the *t*-test. Five mice for each group.

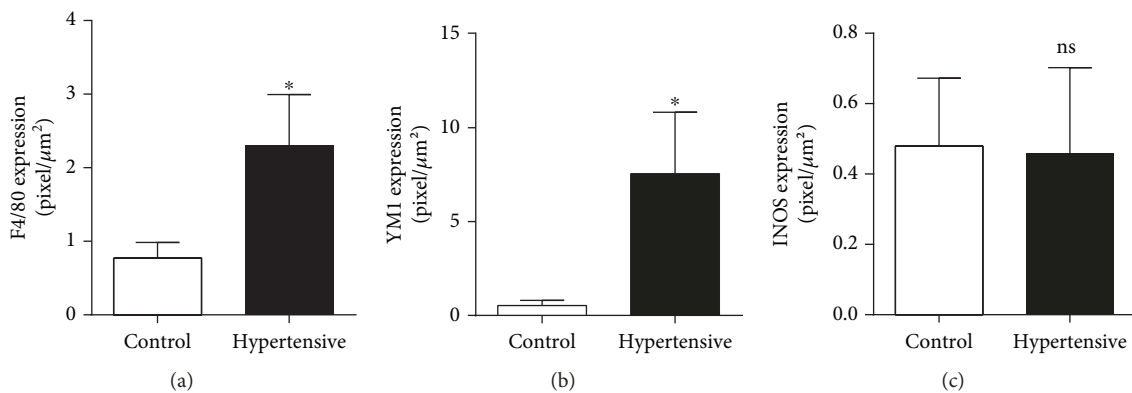


FIGURE 7: High levels of F4/80 in the hypertensive group indicate the presence of macrophages, and the YM1 marker shows the predominance for the M2 phenotype. There was no increase in iNOS, an M1 phenotype marker: (a) renal levels of F4/80 by IF; (b) renal levels of YM1 by IF; (c) renal levels of iNOS by IF. Values were expressed as the mean ± SEM. \**p* < 0.05 compared to the control group with the *t*-test. Seven sections/animal/groups. Four mice for each group.

subsequently to renal dysfunction and organ failure [41, 54]. The implication is that M1 macrophages are responsible for triggering the fibrotic process due to their release of proinflammatory cytokines, which indirectly promote the

proliferation of myofibroblasts and the recruitment of fibrocytes [21, 55].

TNFα is known to have an autocrine effect on the activation of macrophages [56] in a process which mediates kidney

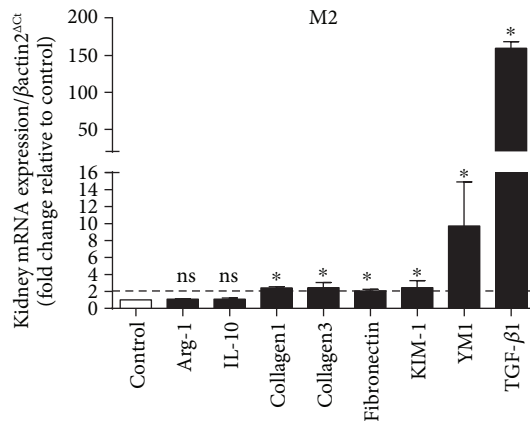


FIGURE 8: Increase in markers related to the M2 phenotype in the kidneys. The genes YM1, TGF- $\beta$ 1, KIM-1, fibronectin, type I collagen, and type III collagen presented a significant difference when compared to the respective controls, and these results were higher than twofold. Values were expressed as the mean  $\pm$  SEM. \* $p < 0.05$  compared to the control group with the  $t$ -test. Five mice for each group.

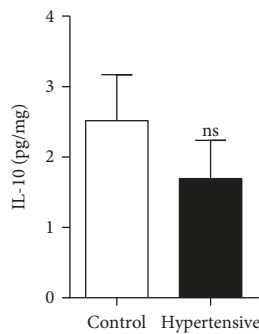


FIGURE 9: IL-10 do not represent a form of protection against renal fibrosis in the hypertensive animals. Values were expressed as the mean  $\pm$  SEM. Five mice for each group.

injury [57]. M1 macrophages release inflammatory mediators including ROS and TNF $\alpha$ , which augment an injury in a positive feedback loop, to cause renal fibrosis [1, 21]. Studies have shown that M1 proinflammatory macrophages are recruited into the kidney within the first hours after ischemia-reperfusion-induced acute kidney injury [58–60], whereas M2 anti-inflammatory macrophages predominate at a later time.

In the hypertensive animal model studied in this work, however, we found no increase in protein levels of TNF $\alpha$ , IL-1 $\beta$ , IL-6, IFN- $\gamma$ , MCP-1, and iNOS in the kidneys. Thus, our data do not support the polarization of macrophages to an M1 phenotype, suggesting that at this stage of hypertension, there is no renal inflammatory process. We also found no increase in the expression of AT1R. Prior work in a model of rats that develop hypertension has shown that the infusion of Ang II increased the number of type 1 T helper (Th1) cytokine IFN- $\gamma$ -secreting cells and decreased type 2 T helper (Th2) cytokine IL-4-secreting cells [61].

After the inflammatory phase orchestrated by the M1 phenotype, Th2 cytokines are produced and promote polarization to the M2 phenotype, which is known to create an anti-inflammatory environment [22, 43]. This response is generally associated with the resolution of inflammation and tissue healing. But when a lesion persists, these cells assume prorepair functions and promote irreversible fibrosis and the progressive destruction of renal tissue [21, 22].

M2 macrophages are initially anti-inflammatory, although the healing process depends on the termination of the initial injury [62]. In chronic conditions, on the other hand, M2 can activate resident fibroblasts through the release of transforming growth factor-beta (TGF- $\beta$ ), platelet-derived growth factor (PDGF), vascular endothelial growth factor (VEGF), insulin-like growth factor 1 (IGF-1), and galectin-3 [63, 64]. This suggests that the severity of fibrosis depends on the type of polarization macrophages undergo and the persistence of the inflammatory injury [21].

An elegant study by Ma et al. [65] suggested that after blocking AT1R with losartan, Ang II polarized macrophages into the M2 phenotype with a high expression of YM1/Chi3l3 and suppressed the expression of M1 markers in WT animals. It is important to note that this occurred in an obesogenic environment where the lean WT and AT1aKO animals showed no change in YM1/Chi3l3 protein levels.

Here, in contrast, we showed for the first time that the lean hypertensive animals presented macrophage polarization to the M2 phenotype with high levels of YM1/Chi3l3. Our transgenic animals come from a hypertensive environment and exhibit an overexpression of AOPEN.

In inflammation, the RAAS appears to act in an antagonistic way involving two different situations regarding the polarization of macrophages [9, 65], but the mechanisms have yet to be clarified. The activation of RAAS by AT1R in macrophages promotes the infiltration and activation of macrophages polarized to the M1 phenotype [1, 9, 65]. A systemic infusion of Ang II is known to induce the expression of proinflammatory mediators, such as MCP-1, TNF $\alpha$ , and IL-6, in vascular smooth muscle and kidney cells [66]. The other situation is related to M2 macrophages induced by Ang II stimulation. Moore et al. [32] confirmed Ang II-induced aortic infiltration with Ly6C<sup>hi</sup> monocytes, but at 7–14 days, these cells began to express the M2 phenotype, with increased CD206 and arginase. In addition, macrophage-specific AT1R receptor deficiency exacerbates renal fibrosis induced by a unilateral ureteral obstruction [67].

In light of the data from our experiments, we suggest that at this stage of hypertension, elevated AOPEN levels contribute to the development of renal damage toward the predominance of the M2 phenotype. In our experiments, we did not block AT1aR, but the animals presented elevated levels of AOPEN, and it seems that the AT1aR in the kidneys from the hypertensive animals were not activated. This fact suggests that the hypertensive environment plus the increase of AOPEN contributes to M2 macrophage polarization. However, we cannot state that Ang II is the mediator of M2 macrophage polarization (Figures 3 and 12) in our animal model, since other members of the RAAS may be involved.

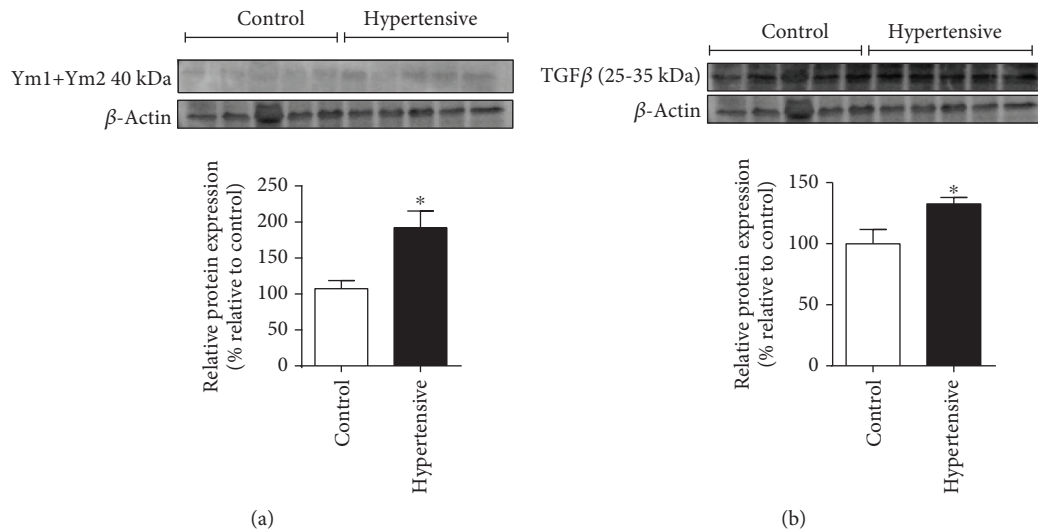


FIGURE 10: Levels of M2 marker proteins. M2 macrophages produced high levels of YM1 protein (91,89%): (a) renal levels of YM1/YM2/ $\beta$ -actin by WB; (b) renal levels of TGF- $\beta$ 1/ $\beta$ -actin by WB. Values were expressed as the mean  $\pm$  SEM. \* $p < 0.05$  compared to the control group with the  $t$ -test. Five mice for each group.

Some M2 markers, such as YM1/Chi3l3 from mice, were first identified as proteins that were secreted during infections by parasites and allergic inflammations [29, 68, 69]. It is known that YM1/Chi3l3 is a marker specific for the M2 macrophage phenotype [65], but little is known about its function in arterial hypertension and hypertensive nephropathy.

In this analysis, it has recently been shown that YKL-40, a member of the chitinase protein family, found in humans and homologous to YM1/Chi3l3, is positively associated with the incidence of hypertension among prehypertensive patients. The case-control study by Xu et al. [31] included an extraction of plasma samples from 20343 prehypertensive or normotensive Chinese subjects. This study suggested that YKL-40 may be a new biomarker for predicting hypertension in the prehypertensive population.

The analysis of the kidneys of our 10- to 12-week-old hypertensive mice revealed a chronic activation of macrophages with an M2 phenotype. In addition, we found significant increases in levels of YM1/Chi3l3 protein (91,89%) and collagen depositions.

Previous experiments by our group verified that the YM1/Chi3l3 gene was expressed in the hearts of these animals (unpublished data) but did not find significant differences in the hypertensive group compared to the control group at this stage. This suggests that at this point in the development of arterial hypertension, this protein is found in the kidney, but not in the heart of these animals, and may serve as a marker specific for hypertensive nephropathy.

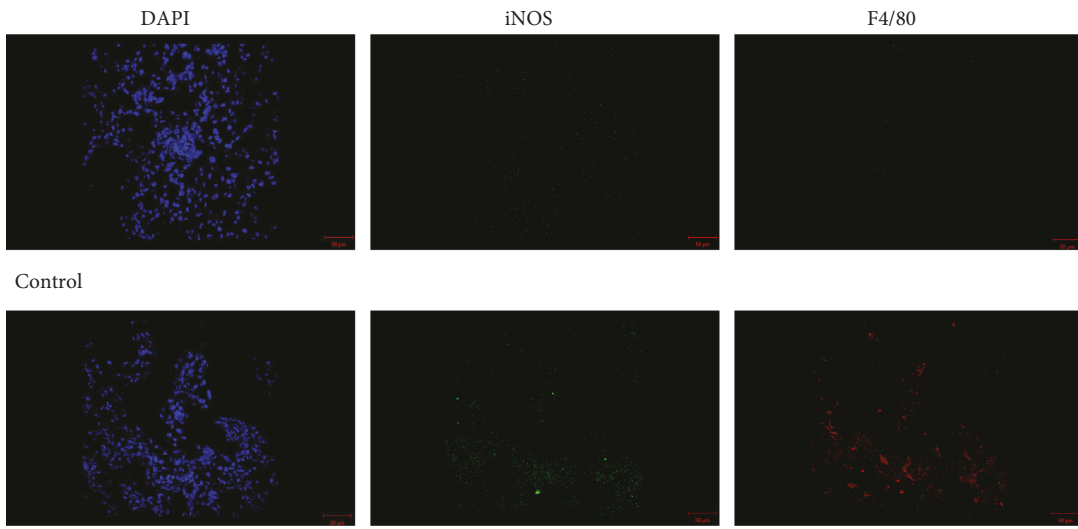
Our data support the idea that M2 macrophages help promote the development of kidney fibrosis at a specific stage of hypertension; this is in agreement with studies [70, 71] pointing to macrophages as sources of profibrotic factors. TGF- $\beta$ 1 has already been identified as a central mediator of renal fibrosis [72–74] and plays an important role in the progression of CKD.

In contrast, studies of experimental kidney disease models have produced a body of evidence indicating a multifunctional role of TGF- $\beta$  in inducing both profibrotic and protective effects [54]. This study did not reveal any protective effects from TGF- $\beta$ 1. On the contrary, our work suggests that high levels of TGF- $\beta$ 1 may be involved in the development of fibrosis.

This work also revealed that the kidneys of hypertensive animals experienced no change in IL-10. This cytokine is produced by several cell types, including macrophages, which polarize to an M2 phenotype, modulate the inflammatory response, and promote tissue repair [60, 75]. IL-10 is also known as an antifibrotic cytokine that is downregulated in CKD [76].

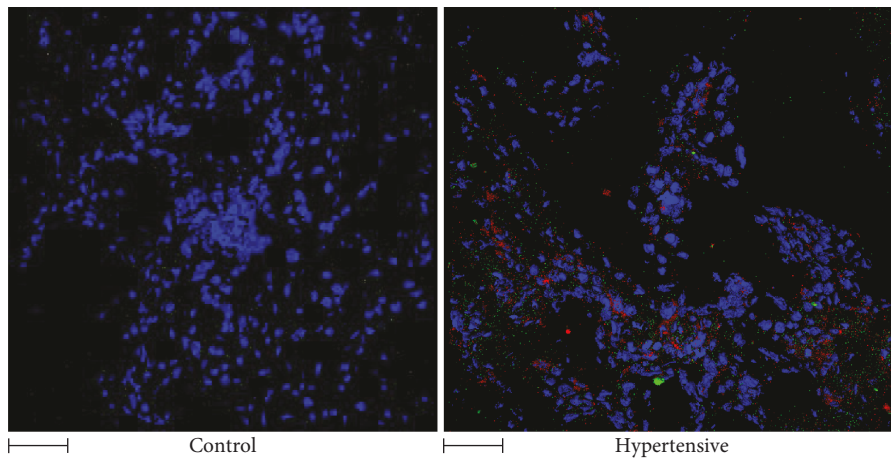
IL-10 controls inflammatory processes by suppressing the production of proinflammatory cytokines such as IL-1 $\beta$  and TNF $\alpha$ , which are known to be regulated by NF- $\kappa$ B transcription [77–79]. In general, IL-10 improves vascular and renal functions in hypertension [80], although little has been reported on the effects of this cytokine on hypertension, particularly in immune environments that favor the development of fibrosis. Our work suggests that basal levels of IL-10 do not represent a form of protection against renal fibrosis in the hypertensive animals (Figure 12).

In conclusion, our work shows for the first time that hypertensive animals are predisposed to a polarization of macrophages to an M2 phenotype *in vitro*, revealing features that suggest a profibrotic profile. This fits with our findings that the kidneys of these hypertensive animals showed a high deposition of collagen, accompanied by an increase in the expression of macrophage markers with a clear predominance toward the M2 phenotype. Taken together, these data suggest that M2 macrophages, associated with high levels of YM1/Chi3l3, are linked to renal damage and fibrosis. Furthermore, it suggests that YM1/Chi3l3 may serve as a new biomarker of hypertensive nephropathy.

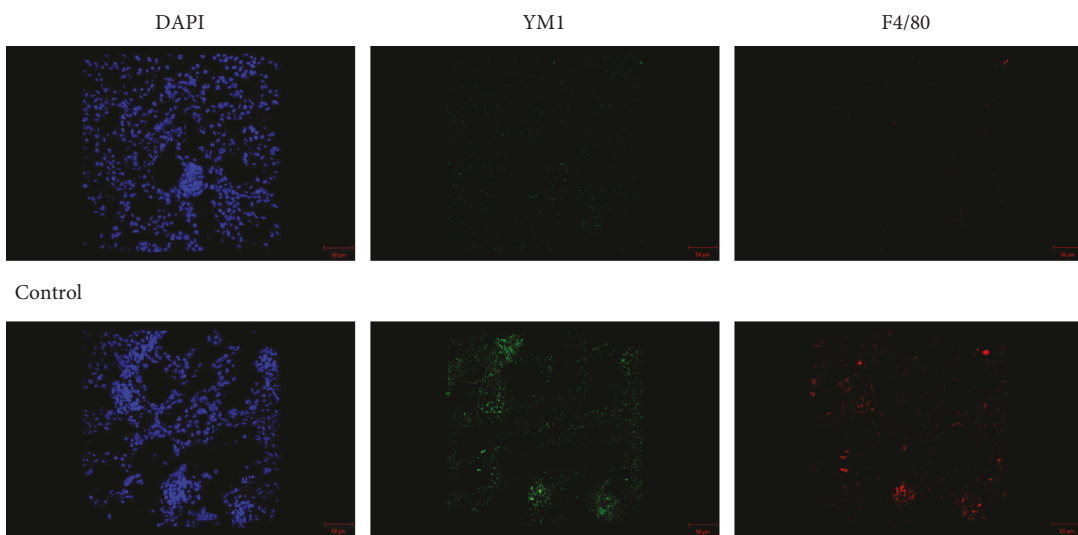


Hypertensive

(a)



(b)



Hypertensive

(c)

FIGURE 11: Continued.

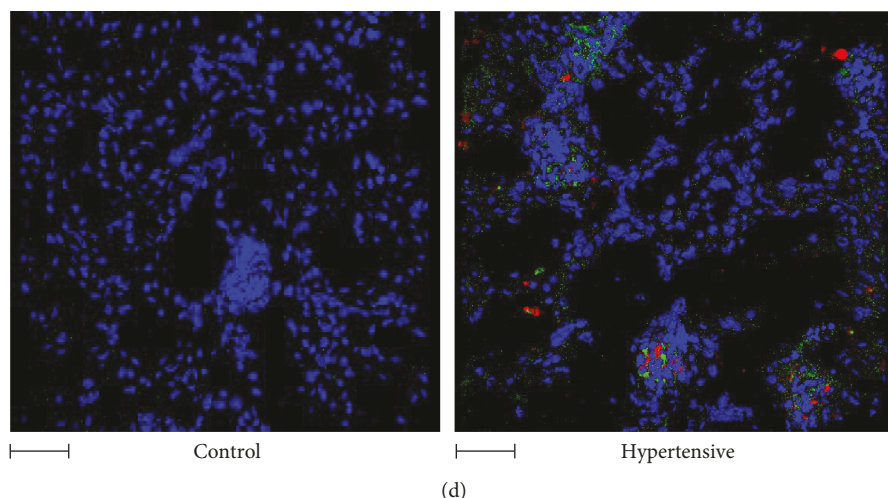


FIGURE 11: Immunofluorescence images of renal tissue showed colocalization between the F4/80, a macrophage marker, and YM1, suggesting that high levels of the YM1 protein were secreted by M2 macrophages. On the other hand, there was no increase in iNOS, an M1 marker: (a) DAPI, iNOS, and F4/80 by IF; (b) 3D overlapping images of DAPI, iNOS, and F4/80 by IF; (c) panel of DAPI, YM1, and F4/80 by IF; (d) 3D overlapping images of DAPI, YM1, and F4/80 by IF. The scale bar = 5 μm.

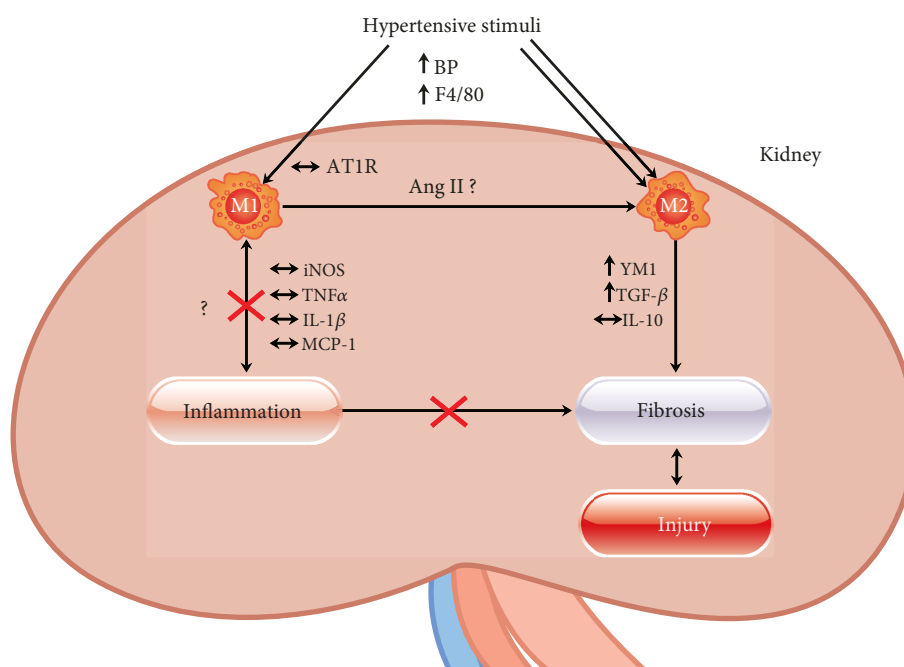


FIGURE 12: Macrophage polarization in the kidneys of 10- to 12-week-old hypertensive mice. The hypertensive stimuli from RAAS, as high levels of AOPEN contributed to macrophage polarization in the kidneys of hypertensive mice with a clear predominance of the M2 phenotype. The high levels of TGF-β1 may be involved in the development of fibrosis. Basal levels of IL-10 do not represent a form of protection against renal fibrosis in the hypertensive animals. In addition, at this stage of hypertension, our data do not support the polarization of macrophages to an M1 phenotype. It seems that the AT1aR in the kidneys from the hypertensive animals were not activated. High levels of AOPEN plus the hypertensive environment contribute to the M2 macrophage polarization. M2 macrophages produced high levels of YM1/Chi3l3 protein (91,89%).

Future studies are needed involving both YM1/Chi3l3 in mice and YKL-40 in humans at different time points to confirm whether reducing levels of these proteins may be beneficial in delaying the development of hypertensive nephropathy.

### Data Availability

We will send the information if necessary. All authors Paula Andréa Malveira Cavalcante, Natalia Alenina, Alexandre Budu, Leandro Ceotto Freitas-Lima, Thaís Alves-Silva, Juan

Sebastian Henao Agudelo, Fatimunnisa Qadri, Niels Olsen Saraiva Camara, Michael Bader, and Ronaldo Carvalho Araújo declare that all data as real-time quantitative PCR, histology, enzyme-linked immunosorbent assay (ELISA), Western blot, cytokine assessment in kidney sample (CBA), and immunofluorescence used to support the findings of this study are included within the article.

## Conflicts of Interest

The authors declare no conflicts of interest.

## Acknowledgments

We gratefully acknowledge funding provided by FAPESP (2015/20082-7), CAPES, PROBRAL (427/15), and the German Research Foundation (DFG, SFB1365), as well as a CNPq fellowship to Paula Andréa Malveira Cavalcante. We thank Russ Hodge (<https://goodsciencewriting.wordpress.com/about/>) for assisting in writing the manuscript.

## References

- [1] Q. Cao, D. C. H. Harris, and Y. Wang, "Macrophages in kidney injury, inflammation, and fibrosis," *Physiology*, vol. 30, no. 3, pp. 183–194, 2015.
- [2] N. Idris-Khodja, M. O. R. Mian, P. Paradis, and E. L. Schiffrin, "Dual opposing roles of adaptive immunity in hypertension," *European Heart Journal*, vol. 35, no. 19, pp. 1238–1244, 2014.
- [3] J. D. Imig and M. J. Ryan, "Immune and inflammatory role in renal disease," *Comprehensive Physiology*, vol. 3, no. 2, pp. 957–976, 2013.
- [4] W. G. McMaster, A. Kirabo, M. S. Madhur, and D. G. Harrison, "Inflammation, immunity, and hypertensive end-organ damage," *Circulation Research*, vol. 116, no. 6, pp. 1022–1033, 2015.
- [5] Y. M. Barri, "Hypertension and kidney disease: a deadly connection," *Current Hypertension Reports*, vol. 10, no. 1, pp. 39–45, 2008.
- [6] J. M. Krzesinski and E. P. Cohen, "Hypertension and the kidney," *Acta Clinica Belgica*, vol. 62, no. 1, pp. 5–14, 2007.
- [7] M. V. Rao, Y. Qiu, C. Wang, and G. Bakris, "Hypertension and CKD: Kidney Early Evaluation Program (KEEP) and National Health and Nutrition Examination Survey (NHANES), 1999–2004," *American Journal of Kidney Diseases*, vol. 51, no. 4, pp. S30–S37, 2008.
- [8] S. Udani, I. Lazich, and G. L. Bakris, "Epidemiology of hypertensive kidney disease," *Nature Reviews Nephrology*, vol. 7, no. 1, pp. 11–21, 2011.
- [9] S. C. Harwani, "Macrophages under pressure: the role of macrophage polarization in hypertension," *Translational Research*, vol. 191, pp. 45–63, 2018.
- [10] A. Justin Rucker and S. D. Crowley, "The role of macrophages in hypertension and its complications," *Pflügers Archiv - European Journal of Physiology*, vol. 469, no. 3–4, pp. 419–430, 2017.
- [11] M. O. R. Mian, P. Paradis, and E. L. Schiffrin, "Innate immunity in hypertension," *Current Hypertension Reports*, vol. 16, no. 2, p. 413, 2014.
- [12] E. L. Schiffrin, "Immune mechanisms in hypertension and vascular injury," *Clinical Science*, vol. 126, no. 4, pp. 267–274, 2014.
- [13] P. Wenzel, M. Knorr, S. Kossmann et al., "Lysozyme M-positive monocytes mediate angiotensin II-induced arterial hypertension and vascular dysfunction," *Circulation*, vol. 124, no. 12, pp. 1370–1381, 2011.
- [14] D. N. Muller, E. Shagdarsuren, J. K. Park et al., "Immunosuppressive treatment protects against angiotensin II-induced renal damage," *The American Journal of Pathology*, vol. 161, no. 5, pp. 1679–1693, 2002.
- [15] Y. Ozawa, H. Kobori, Y. Suzaki, and L. G. Navar, "Sustained renal interstitial macrophage infiltration following chronic angiotensin II infusions," *American Journal of Physiology-Renal Physiology*, vol. 292, no. 1, pp. F330–F339, 2007.
- [16] C. A. Papaharalambus and K. K. Griendling, "Basic mechanisms of oxidative stress and reactive oxygen species in cardiovascular injury," *Trends in Cardiovascular Medicine*, vol. 17, no. 2, pp. 48–54, 2007.
- [17] C. D. Mills, K. Kincaid, J. M. Alt, M. J. Heilman, and A. M. Hill, "M-1/M-2 macrophages and the Th1/Th2 paradigm," *The Journal of Immunology*, vol. 164, no. 12, pp. 6166–6173, 2000.
- [18] C. Mills, "M1 and M2 macrophages: oracles of health and disease," *Critical Reviews in Immunology*, vol. 32, no. 6, pp. 463–488, 2012.
- [19] S. Gordon and F. O. Martinez, "Alternative activation of macrophages: mechanism and functions," *Immunity*, vol. 32, no. 5, pp. 593–604, 2010.
- [20] A. Sica and A. Mantovani, "Macrophage plasticity and polarization: in vivo veritas," *The Journal of Clinical Investigation*, vol. 122, no. 3, pp. 787–795, 2012.
- [21] T. T. Braga, J. S. H. Agudelo, and N. O. S. Camara, "Macrophages during the fibrotic process: M2 as friend and foe," *Frontiers in Immunology*, vol. 6, 2015.
- [22] S. D. Ricardo, H. van Goor, and A. A. Eddy, "Macrophage diversity in renal injury and repair," *The Journal of Clinical Investigation*, vol. 118, no. 11, pp. 3522–3530, 2008.
- [23] C. Draijer and M. Peters-Golden, "Alveolar macrophages in allergic asthma: the forgotten cell awakes," *Current Allergy and Asthma Reports*, vol. 17, 2017.
- [24] C. Draijer, P. Robbe, C. E. Boorsma, M. N. Hylkema, and B. N. Melgert, "Dual role of YM1+ M2 macrophages in allergic lung inflammation," *Scientific Reports*, vol. 8, no. 1, p. 5105, 2018.
- [25] F. O. Martinez, A. Sica, A. Mantovani, and M. Locati, "Macrophage activation and polarization," *Frontiers in Bioscience*, vol. 13, no. 13, pp. 453–461, 2008.
- [26] B. N. Melgert, N. H. ten Hacken, B. Rutgers, W. Timens, D. S. Postma, and M. N. Hylkema, "More alternative activation of macrophages in lungs of asthmatic patients," *The Journal of Allergy and Clinical Immunology*, vol. 127, no. 3, pp. 831–833, 2011.
- [27] S. Bhatia, M. Fei, M. Yarlagadda et al., "Rapid host defense against *Aspergillus fumigatus* involves alveolar macrophages with a predominance of alternatively activated phenotype," *PLoS One*, vol. 6, no. 1, article e15943, 2011.
- [28] G. Raes, W. Noël, A. Beschin, L. Brys, P. de Baetselier, and G. G. Hassanzadeh, "FIZZ1 and Ym as tools to discriminate between differentially activated macrophages," *Developmental Immunology*, vol. 9, no. 3, pp. 151–159, 2002.
- [29] N.-C. A. Chang, S. I. Hung, K. Y. Hwa et al., "A macrophage protein, Ym1, transiently expressed during inflammation is a

- novel mammalian lectin," *The Journal of Biological Chemistry*, vol. 276, no. 20, pp. 17497–17506, 2001.
- [30] B. E. Hakala, C. White, and A. D. Recklies, "Human cartilage gp-39, a major secretory product of articular chondrocytes and synovial cells, is a mammalian member of a chitinase protein family," *The Journal of Biological Chemistry*, vol. 268, no. 34, pp. 25803–25810, 1993.
- [31] T. Xu, C. Zhong, A. Wang et al., "YKL-40 is a novel biomarker for predicting hypertension incidence among prehypertensive subjects: a population-based nested case-control study in China," *Clinica Chimica Acta*, vol. 472, pp. 146–150, 2017.
- [32] J. P. Moore, A. Vinh, K. L. Tuck et al., "M2 macrophage accumulation in the aortic wall during angiotensin II infusion in mice is associated with fibrosis, elastin loss, and elevated blood pressure," *American Journal of Physiology-Heart and Circulatory Physiology*, vol. 309, pp. H906–H917, 2015.
- [33] D. L. Rateri, D. A. Howatt, J. J. Moorleghen, R. Charnigo, L. A. Cassis, and A. Daugherty, "Prolonged infusion of angiotensin II in *apoE*<sup>-/-</sup> mice promotes macrophage recruitment with continued expansion of abdominal aortic aneurysm," *The American Journal of Pathology*, vol. 179, no. 3, pp. 1542–1548, 2011.
- [34] N. Kang, T. Walther, X.-L. Tian et al., "Reduced hypertension-induced end-organ damage in mice lacking cardiac and renal angiotensinogen synthesis," *Journal of Molecular Medicine*, vol. 80, no. 6, pp. 359–366, 2002.
- [35] F. Niimura, P. A. Labosky, J. Kakuchi et al., "Gene targeting in mice reveals a requirement for angiotensin in the development and maintenance of kidney morphology and growth factor regulation," *The Journal of Clinical Investigation*, vol. 96, no. 6, pp. 2947–2954, 1995.
- [36] K. Tanimoto, F. Sugiyama, Y. Goto et al., "Angiotensinogen-deficient mice with hypotension," *The Journal of Biological Chemistry*, vol. 269, no. 50, pp. 31334–31337, 1994.
- [37] S. Kimura, J. J. Mullins, B. Bunnemann et al., "High blood pressure in transgenic mice carrying the rat angiotensinogen gene," *The EMBO Journal*, vol. 11, no. 3, pp. 821–827, 1992.
- [38] P. Xu, Y. Wang, A. Sterner-Kock, M. Bader, H. P. Schultheiss, and T. Walther, "Excessive hypertension and end-organ damage in a transgenic mouse line carrying the rat angiotensinogen gene," *Journal of Cardiovascular Pharmacology*, vol. 53, no. 1, pp. 38–43, 2009.
- [39] Y. Karlen, A. McNair, S. Perseguers, C. Mazza, and N. Mermod, "Statistical significance of quantitative PCR," *BMC Bioinformatics*, vol. 8, p. 131, 2007.
- [40] S. A. Mezzano, M. Ruiz-Ortega, and J. E. Egidio, "Angiotensin II and renal fibrosis," *Hypertension*, vol. 38, no. 3, pp. 635–638, 2001.
- [41] T. A. Wynn, "Cellular and molecular mechanisms of fibrosis," *The Journal of Pathology*, vol. 214, no. 2, pp. 199–210, 2008.
- [42] C. Lavozy, R. Rodrigues-Diez, A. Benito-Martin et al., "Angiotensin II contributes to renal fibrosis independently of Notch pathway activation," *PLoS One*, vol. 7, no. 7, article e40490, 2012.
- [43] M. A. Alikhan and S. D. Ricardo, "Mononuclear phagocyte system in kidney disease and repair," *Nephrology*, vol. 18, no. 2, pp. 81–91, 2013.
- [44] H.-J. Anders, B. Banas, Y. Linde et al., "Bacterial CpG-DNA aggravates immune complex glomerulonephritis: role of TLR9-mediated expression of chemokines and chemokine receptors," *Journal of the American Society of Nephrology*, vol. 14, no. 2, pp. 317–326, 2003.
- [45] H.-J. Anders, V. Vielhauer, V. Eis et al., "Activation of toll-like receptor-9 induces progression of renal disease in MRL-Fas(lpr) mice," *The FASEB Journal*, vol. 18, no. 3, pp. 534–536, 2004.
- [46] Q. Cao, Y. Wang, X. M. Wang et al., "Renal F4/80<sup>+</sup>CD11c<sup>+</sup> mononuclear phagocytes display phenotypic and functional characteristics of macrophages in health and in Adriamycin nephropathy," *Journal of the American Society of Nephrology*, vol. 26, no. 2, pp. 349–363, 2014.
- [47] Y. Ikezumi, R. C. Atkins, and D. J. Nikolic-Paterson, "Interferon- $\gamma$  augments acute macrophage-mediated renal injury via a glucocorticoid-sensitive mechanism," *Journal of the American Society of Nephrology*, vol. 14, no. 4, pp. 888–898, 2003.
- [48] R. D. Pawar, P. S. Patole, A. Ellwart et al., "Ligands to nucleic acid-specific toll-like receptors and the onset of lupus nephritis," *Journal of the American Society of Nephrology*, vol. 17, no. 12, pp. 3365–3373, 2006.
- [49] Y. Wang, Y. Wang, Q. Cai et al., "By homing to the kidney, activated macrophages potentially exacerbate renal injury," *The American Journal of Pathology*, vol. 172, no. 6, pp. 1491–1499, 2008.
- [50] P. Chauhan, A. Sodhi, and A. Shrivastava, "Cisplatin primes murine peritoneal macrophages for enhanced expression of nitric oxide, proinflammatory cytokines, TLRs, transcription factors and activation of MAP kinases upon co-incubation with L929 cells," *Immunobiology*, vol. 214, no. 3, pp. 197–209, 2009.
- [51] G. Ramesh and W. B. Reeves, "p38 MAP kinase inhibition ameliorates cisplatin nephrotoxicity in mice," *American Journal of Physiology-Renal Physiology*, vol. 289, no. 1, pp. F166–F174, 2005.
- [52] M. D. Jose, Y. Ikezumi, N. van Rooijen, R. C. Atkins, and S. J. Chadban, "Macrophages act as effectors of tissue damage in acute renal allograft rejection," *Transplantation*, vol. 76, no. 7, pp. 1015–1022, 2003.
- [53] A. Matuschek, M. Ulbrich, S. Timm et al., "Analysis of parathyroid graft rejection suggests alloantigen-specific production of nitric oxide by iNOS-positive intragraft macrophages," *Transplant Immunology*, vol. 21, no. 4, pp. 183–191, 2009.
- [54] A. Sureshbabu, S. A. Muhsin, and M. E. Choi, "TGF- $\beta$  signaling in the kidney: profibrotic and protective effects," *American Journal of Physiology-Renal Physiology*, vol. 310, no. 7, pp. F596–F606, 2016.
- [55] T. A. Wynn and L. Barron, "Macrophages: master regulators of inflammation and fibrosis," *Seminars in Liver Disease*, vol. 30, no. 3, pp. 245–257, 2010.
- [56] T. A. Wynn, Y. R. Freund, and D. M. Paulnock, "TNF- $\alpha$  differentially regulates Ia antigen expression and macrophage tumoricidal activity in two murine macrophage cell lines," *Cellular Immunology*, vol. 140, no. 1, pp. 184–196, 1992.
- [57] M. Ryu, O. P. Kulkarni, E. Radoska, N. Miosge, O. Gross, and H.-J. Anders, "Bacterial CpG-DNA accelerates Alport glomerulosclerosis by inducing an M1 macrophage phenotype and tumor necrosis factor- $\alpha$ -mediated podocyte loss," *Kidney International*, vol. 79, no. 2, pp. 189–198, 2011.
- [58] J. J. Friedewald and H. Rabb, "Inflammatory cells in ischemic acute renal failure," *Kidney International*, vol. 66, no. 2, pp. 486–491, 2004.

- [59] H. R. Jang and H. Rabb, "The innate immune response in ischemic acute kidney injury," *Clinical Immunology*, vol. 130, no. 1, pp. 41–50, 2009.
- [60] S. Lee, S. Huen, H. Nishio et al., "Distinct macrophage phenotypes contribute to kidney injury and repair," *Journal of the American Society of Nephrology*, vol. 22, no. 2, pp. 317–326, 2011.
- [61] J. Shao, M. Nangaku, T. Miyata et al., "Imbalance of T-cell subsets in angiotensin II-infused hypertensive rats with kidney injury," *Hypertension*, vol. 42, no. 1, pp. 31–38, 2003.
- [62] T. A. Wynn and T. R. Ramalingam, "Mechanisms of fibrosis: therapeutic translation for fibrotic disease," *Nature Medicine*, vol. 18, no. 7, pp. 1028–1040, 2012.
- [63] M. Lech and H.-J. Anders, "Macrophages and fibrosis: how resident and infiltrating mononuclear phagocytes orchestrate all phases of tissue injury and repair," *Biochimica et Biophysica Acta (BBA) - Molecular Basis of Disease*, vol. 1832, no. 7, pp. 989–997, 2013.
- [64] Y.-H. Lin, C. H. Chou, X. M. Wu et al., "Aldosterone induced galectin-3 secretion in vitro and in vivo: from cells to humans," *PLoS One*, vol. 9, no. 9, article e95254, 2014.
- [65] L. J. Ma, B. A. Corsa, J. Zhou et al., "Angiotensin type 1 receptor modulates macrophage polarization and renal injury in obesity," *American Journal of Physiology-Renal Physiology*, vol. 300, no. 5, pp. F1203–F1213, 2011.
- [66] M. Ruiz-Ortega, M. Ruperez, O. Lorenzo et al., "Angiotensin II regulates the synthesis of proinflammatory cytokines and chemokines in the kidney," *Kidney International*, vol. 62, pp. S12–S22, 2002.
- [67] J. D. Zhang, M. B. Patel, R. Griffiths et al., "Type 1 angiotensin receptors on macrophages ameliorate IL-1 receptor-mediated kidney fibrosis," *The Journal of Clinical Investigation*, vol. 124, no. 5, pp. 2198–2203, 2014.
- [68] H. M. Jin, N. G. Copeland, D. J. Gilbert, N. A. Jenkins, R. B. Kirkpatrick, and M. Rosenberg, "Genetic characterization of the murine Ym1 gene and identification of a cluster of highly homologous genes," *Genomics*, vol. 54, no. 2, pp. 316–322, 1998.
- [69] S. K. Biswas and A. Mantovani, "Macrophage plasticity and interaction with lymphocyte subsets: cancer as a paradigm," *Nature Immunology*, vol. 11, no. 10, pp. 889–896, 2010.
- [70] V. A. Fadok, D. L. Bratton, A. Konowal, P. W. Freed, J. Y. Westcott, and P. M. Henson, "Macrophages that have ingested apoptotic cells in vitro inhibit proinflammatory cytokine production through autocrine/paracrine mechanisms involving TGF-beta, PGE2, and PAF," *The Journal of Clinical Investigation*, vol. 101, no. 4, pp. 890–898, 1998.
- [71] M. A. Vernon, K. J. Mylonas, and J. Hughes, "Macrophages and renal fibrosis," *Seminars in Nephrology*, vol. 30, no. 3, pp. 302–317, 2010.
- [72] W. A. Border and N. A. Noble, "Transforming growth factor  $\beta$  in tissue fibrosis," *New England Journal of Medicine*, vol. 331, no. 19, pp. 1286–1292, 1994.
- [73] Y. Ding and M. E. Choi, "Regulation of autophagy by TGF- $\beta$ : emerging role in kidney fibrosis," *Seminars in Nephrology*, vol. 34, no. 1, pp. 62–71, 2014.
- [74] S.-Y. Lee, S. I. Kim, and M. E. Choi, "Therapeutic targets for treating fibrotic kidney diseases," *Translational Research*, vol. 165, no. 4, pp. 512–530, 2015.
- [75] Y. Wang, Y. P. Wang, G. Zheng et al., "Ex vivo programmed macrophages ameliorate experimental chronic inflammatory renal disease," *Kidney International*, vol. 72, no. 3, pp. 290–299, 2007.
- [76] W. Lv, G. W. Booz, Y. Wang, F. Fan, and R. J. Roman, "Inflammation and renal fibrosis: recent developments on key signaling molecules as potential therapeutic targets," *European Journal of Pharmacology*, vol. 820, pp. 65–76, 2018.
- [77] M. F. Romano, A. Lamberti, A. Petrella et al., "IL-10 inhibits nuclear factor-kappa B/Rel nuclear activity in CD3-stimulated human peripheral T lymphocytes," *The Journal of Immunology*, vol. 156, no. 6, pp. 2119–2123, 1996.
- [78] P. Wang, P. Wu, M. I. Siegel, R. W. Egan, and M. M. Billah, "IL-10 inhibits transcription of cytokine genes in human peripheral blood mononuclear cells," *The Journal of Immunology*, vol. 153, no. 2, pp. 811–816, 1994.
- [79] P. Wu, "Interleukin (IL)-10 inhibits nuclear factor [IMAGE]B (NF[IMAGE]B) activation in human monocytes," *Journal of Biological Chemistry*, vol. 270, no. 16, pp. 9558–9563, 1995.
- [80] Y. Wen and S. D. Crowley, "Renal effects of cytokines in hypertension," *Current Opinion in Nephrology and Hypertension*, vol. 27, no. 2, pp. 70–76, 2018.

## Research Article

# IL-10 Dampens the Th1 and Tc Activation through Modulating DC Functions in BCG Vaccination

Hui Xu, Yanjuan Jia, Yonghong Li, Chaojun Wei, Wanxia Wang, Rui Guo, Jing Jia, Yu Wu, Zhenhao Li, Zhenhong Wei, Xiaoming Qi, Yuanting Li, and Xiaoling Gao 

The Institute of Clinical Research and Translational Medicine, Gansu Provincial Hospital, China

Correspondence should be addressed to Xiaoling Gao; [gaoxl008@hotmail.com](mailto:gaoxl008@hotmail.com)

Received 3 February 2019; Accepted 8 May 2019; Published 12 June 2019

Guest Editor: Xiao Chen

Copyright © 2019 Hui Xu et al. This is an open access article distributed under the Creative Commons Attribution License, which permits unrestricted use, distribution, and reproduction in any medium, provided the original work is properly cited.

BCG, the only registered vaccine against *Mycobacterial Tuberculosis* (TB) infection, has been questioned for its protective efficacy for decades. Although lots of efforts were made to improve the BCG antigenicity, few studies were devoted to understand the role of host factors in the variability of the BCG protection. Using the IL-10KO mice and pulmonary tuberculosis infection model, we have addressed the role of IL-10 in the BCG vaccination efficacy. The data showed that IL-10-deficient dendritic cells (DCs) could promote the immune responses through upregulation of the surface costimulatory molecule expression and play an orchestra role through activating CD4<sup>+</sup>T cell. IL-10-deficient mice had higher IFN  $\gamma$ , TNF  $\alpha$ , and IL-6 production after BCG vaccination, which was consistent with the higher proportion of IFN  $\gamma$ <sup>+</sup>CD3<sup>+</sup>, IFN  $\gamma$ <sup>+</sup>CD4<sup>+</sup>, and IFN  $\gamma$ <sup>+</sup>CD8<sup>+</sup> T cells in the spleen. Particularly, the BCG-vaccinated IL-10KO mice showed less inflammation after TB challenge compared to WT mice, which was supported by the promoted Th1 and Tc, as well as the downregulated Treg responses in IL-10 deficiency. In a conclusion, we demonstrated the negative relationship between Th1/Tc responses with IL-10 production. IL-10 deficiency restored the type 1 immune response through DC activation, which provided better protection against TB infection. Hence, our study offers the first experimental evidence that, contrary to the modulation of BCG, host immunity plays a critical role in the BCG protective efficacy against TB.

## 1. Introduction

*Mycobacterial Tuberculosis* (MTB) remains a detrimental contagious disease responsible for about 3 billion infection. According to the World Health Organization's (WHO) statistics, its scourge claims close to 1.6 million deaths worldwide each year (World Health Organization. Available at: <http://www.who.int/mediacentre/factsheets/fs104/en/>) aided by an endemic of multiple drug resistant strains, poor adherence to a long duration of therapy, HIV infection-induced immune compromise, and social and economic public health constraints [1].

The Bacillus Calmette-Guerin (BCG) is the only approved antituberculous vaccine developed through the serial in vitro passage of *M. bovis* until it becomes unpathogenic [2], but its efficacy had been questioned for decades.

Even it can confer reliable protection in children, it is inconsistent in limiting adult TB infection [3]. More interestingly, BCG decreases overall morbidity and mortality to other infectious diseases, which suggests that BCG offers the protective immune response to non-TB pathogens. Furthermore, BCG possesses potent immunostimulatory properties in the treatment of bladder cancer, multiple sclerosis, and type 1 diabetes [2, 4–6]. Given its potentials, beyond doubt, BCG is still the successful, affordable, and promising vaccine, especially in a resource-limited area.

New anti-TB vaccine development focuses on the improving BCG by enhancing its immunogenicity or applying the prime-boost strategies to amplify the protective response [7–11]. However, the suppressive host microenvironment would circumvent the protective immune responses. Before we move forward with the development

of a new or an improved TB vaccine to combat this pathogen, it is vital for better exploring the host limitations on BCG-induced protection.

Currently, there is limited efforts on defining the host factors in modulating the efficacy of BCG. The ability of host to control TB infection is largely dependent on the antigen-presenting cells such as macrophage and dendritic cells (DCs) to initial adaptive immune responses. Even both macrophage and DCs can be infected by TB, macrophage is rather equipped to control internalized TB through the NO production, while the TB can hijack the macrophage to escape the immune surveillance. On the other hand, DCs are best-known as the main participants in mounting the effective T cell-mediated immune responses against TB [12]. As a result, DCs are considered as a target for novel TB vaccine strategies [8]. Since DCs are a heterogeneous population, different DC subtypes contribute differently on the activation and polarization of TB-specific T cells. The phenotypic and functional alterations in DCs have been reported in individuals with TB infection. The type-1 polarized DCs (DC1s) induce Th1 responses and CTLs in TB infection [13]. Furthermore, regulatory DCs (DCreg) possess the suppressive potentials by secreting a number of soluble factors, e.g., PGE2, IL-10, and NO, which are capable to inhibit T cell responses [14–16]. Although we and others have previously shown the critical role of DCs in protective immunity in TB infection, the power of DCs in vaccine development has yet to be realized [17–19].

Cytokine interleukin-10 (IL-10) has been implicated in the pathogenesis of TB [20]. IL-10 is an important immunoregulatory cytokine mainly produced by macrophages, DC, monocytes, T cells, et al. [21]. Turner et al. demonstrated that increased susceptibility of reactivation of latent infection was strongly related to the expression of IL-10 during the chronic or latent phase of the infection [22]. IL-10 helps TB persistence in human by blocking phagosome maturation in macrophages [23]. The ability of IL-10 to downregulate immune responses and the fact that IL-10 can be detected in tuberculosis patients have led us to investigate whether IL-10 plays a role in BCG vaccination efficacy [24, 25].

In current study, we implied IL-10KO mice to explore the potential role of IL-10 in the BCG vaccination efficacy. Our data supported that DC activation was hampered after BCG vaccination due to the IL-10 production. IL-10 prevented the development the protective Th1 immune response which may be associated with the increased Treg activity.

## 2. Materials and Methods

**2.1. Mice and Culture Medium.** The animal was handled in compliance with the Guidelines for Animal Use set by the Ethic Committee on animal care and use. C57BL/6 female mice (6–8 weeks) and IL-10KO mice (Nanjing Junke Bioengineering Co., China) were housed for 2 weeks before the study. This study was approved by the Ethics Committee of Gansu Provincial Hospital. RPMI 1640 medium (Biological Industries, Israel) supplemented with 10% HI-FBS (heat-inactivated fetal bovine serum), 1% L-glu-

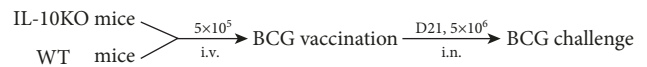


FIGURE 1: The chart of BCG vaccination and challenge to establish the BCG vaccine/challenge mouse model. The IL-10KO and WT mice were housed for 2 weeks after arriving. For vaccination, the mice were intravenously injected with  $5 \times 10^5$  CFU BCG in 200  $\mu$ L PBS; the control group was given PBS only. For challenge, at D21 after vaccination, the mice were infected intranasally with  $5 \times 10^6$  CFU BCG. The immune responses were detected after 21 days.

tamine, 25  $\mu$ L/mL gentamycin, and  $5 \times 10^{-5}$  M<sub>2</sub> was used as complete medium for cell culture. PBS was used as the control.

**2.2. Organism and Model of BCG Vaccination and Challenge (Figure 1).** The BCG strain was made by Wuhan Biological Products Research Institute Co. LTD. For expansion of the vaccine, the protocol was applied based on previous study [12]. Briefly, BCG was grown in the Middlebrook's 7H9 broth (BD Difco, USA) containing 0.2% (v/v) glycerol and 0.05% (v/v) Tween-80 and supplied with 10% (v/v) Middlebrook ADC enrichment (Difco) for 21 days. The stock of BCG was detected for the numbers of bacilli before it was stored at  $-80^\circ\text{C}$  before use. The colony-forming units (CFUs) were measured by plating diluted culture on plates of Middlebrook 7H11 agar (Difco) containing 0.5% (v/v) glycerol and supplied with Middlebrook OADC enrichment (Difco). BCG was put at  $65^\circ\text{C}$  for 1 hour for inactivation, which led to complete killing of BCG confirmed by viability testing (HK BCG). Mice were immunized intravenously with  $5 \times 10^5$  CFU BCG in 200  $\mu$ L sterile protein-free PBS and sacrificed at day 21 after immunization as previously described [26, 27]. Spleens were aseptically isolated and digested in 1.5 mg/mL collagenase D (Sigma, USA) at  $37^\circ$  for 30 min. The single cells were prepared after cell suspension went through cell strainer (70  $\mu$ m). DC surface marker expression was collected by Aria II flow cytometer (BD, CA, USA) and analyzed using FlowJo software. Vaccinated mice were challenged intranasally (i.n.) with  $5 \times 10^6$  CFUs of BCG. Mice were euthanized 21 d later and analyzed for immune responses.

**2.3. Lung, Spleen, and Local Lymph Node Cell Isolation.** Single cells isolated from the lungs, spleen, and draining lymph node (dLN) were set for bulk culture and flow cytometry analysis as described [28, 29]. Briefly, spleens were cut into small pieces and digested in 1.5 mg/mL collagenase D in RPMI 1640 for 30 min at  $37^\circ\text{C}$ . The cell suspension was filtered through cell strainer (70  $\mu$ m), and RBCs were removed by ammonium-chloride-potassium (ACK) lysis buffer (150 mmol/L  $\text{NH}_4\text{Cl}$ , 10 mmol/L  $\text{KHCO}_3$ , and 0.1 mmol/L EDTA). Lung tissues were harvested aseptically and digested in 2 mg/mL collagenase XI (Sigma, USA) in RPMI 1640 for 1 h at  $37^\circ\text{C}$ . After digestion, 35% (volume/volume) Percoll (Pharmacia, USA) was used to collect lung single cells. And ACK lysis buffer was used to remove red blood cells (RBCs). For dLN mononuclear cell isolation, the dLNs were homogenized in 3 mL RPMI 1640

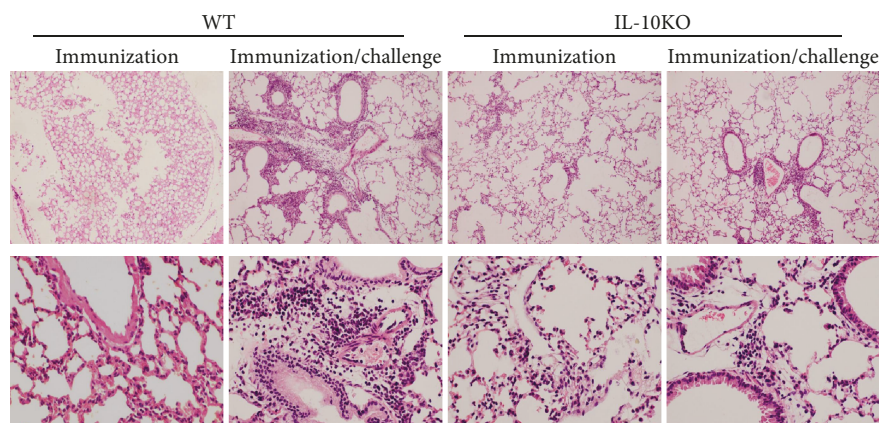


FIGURE 2: The pathological changes in vaccinated IL-10KO and WT mice following intranasally (i.n.) challenge infection after BCG vaccination. Pretreated mice were challenged intranasally with  $5 \times 10^6$  CFUs BCG and analyzed for histopathological changes in the lungs at day 21 postchallenge infection. Lung tissue sections ( $6 \mu\text{m}$ ) were stained with H&E for inflammation. (a) Low magnification ( $\times 10$ ), (b) High magnification ( $\times 40$ ). The representative of three independent experiments ( $n = 5$ ) with similar results was shown.

and RBCs were removed by ACK lysis buffer. All of the cells were washed and resuspended in complete RPMI-1640 medium. Single-cell suspensions were cultured in 48-well plates at a concentration of  $7.5 \times 10^6$  (spleen) and  $5 \times 10^6$  (lungs and dLNs) cells/well with HK BCG ( $5 \times 10^5$  CFU/mL). The supernatants were collected from the cell cultures after 3 d and assayed for IFN  $\gamma$ , IL-4, IL-6, and TNF  $\alpha$  production by Enzyme-Linked Immunosorbent Assay (ELISA) using antibodies purchased from eBioscience or BD Biosciences [12].

**2.4. Isolation of CD4<sup>+</sup>T Cell and DC Coculture.** Spleen CD4<sup>+</sup>T cells were isolated from WT mice after BCG vaccination as we previously described [30]. DCs were purified from the spleens of WT and IL-10KO BCG-vaccinated mice by flow cytometric sorting. DCs ( $7.5 \times 10^5$  cells/mL) from WT or IL-10KO BCG-vaccinated mice were cocultured with CD4<sup>+</sup>T cells ( $7.5 \times 10^6$  cells/mL) in 96-well plates in the presence of HK-BCG ( $5 \times 10^4$  CFU/mL) in 200  $\mu\text{L}$  complete RPMI medium. For testing IFN  $\gamma$  and IL-4 production, the supernatants were collected at 72 h and tested by ELISA.

**2.5. Analysis of Lung Pathology.** The lungs of WT or IL-10KO mice after BCG challenge were collected and fixed in 10% buffered formalin. Lung tissues were embedded, sectioned, and stained by H&E as described [26, 31]. Infiltrating inflammatory cells were identified based on cellular morphology and characteristics. Slides were examined for pathological changes by 2 independent pathologists using a light microscopy.

**2.6. Flow Cytometric Analysis.** The intracellular IFN  $\gamma$ - or Foxp3-positive T cells were analyzed by intracellular cytokine staining as described previously [28]. Briefly, the cells were stimulated with phorbolmyristate acetate (PMA; 50 ng/mL) and ionomycin (1 g/mL) for 2 hours, then brefeldin A was added to the culture, and the cells were cultured for another 4 h to accumulate cytokine intracellularly. The cells were collected and stained with anti-CD3 $\epsilon$ -fluorescein iso-

thiocyanate (FITC), anti-CD4-phycoerythrin (PE) mAbs, and anti-CD8-PerCy5.5 (BD, CA, USA). After being fixed and washed in permeabilization buffer twice, cells were stained with anti-IFN  $\gamma$  allophycocyanin (APC). For Treg detection, cells were stained with FITC-anti-CD3 $\epsilon$ , PerCy5.5 anti-CD4, APC anti-CD25, and PE-Foxp3. All of the sample data were collected using an Aria II flow cytometer (BD, CA, USA) and analyzed using FlowJo software.

**2.7. Statistical Analysis.** Statistical analysis of the data was performed using analysis of variance (ANOVA) and *t* tests (GraphPad Prism software, version 5.0 (GraphPad Software, La Jolla, CA, USA)), and values of  $p < 0.05$  were considered significantly. Data are presented as mean  $\pm$  standard deviation (SD). The presented data were collected from four to five mice of each group. All the experiments were repeated at least three times with similar results.

### 3. Results

**3.1. Less Inflammation after IL-10KO in TB Challenge.** To further assess the role of IL-10 in BCG vaccination efficacy, we challenged the BCG-vaccinated mice intranasally with high dose of BCG ( $5 \times 10^6$ ) and detected inflammation in the lungs. As shown in Figure 2, IL-10KO mice pretreated with BCG showed mild infiltrated inflammation in the lungs against challenge. In contrast, the WT mice immunized and challenged with BCG have much more severe pathological inflammatory reactions. Interestingly, both WT and IL-10KO mice have very mild inflammatory cells in their lungs after BCG immunization without challenge. The data suggested that IL-10KO deficiency can dramatically modulate the pathological inflammatory responses in the local tissues [12].

**3.2. IL-10 Deficiency Enhances Th1 and Cytotoxic T Cells after BCG Challenge Intranasally.** To examine the immune responses in BCG-challenged IL-10KO mice and WT mice, we performed the intracellular cytokine staining for T cells

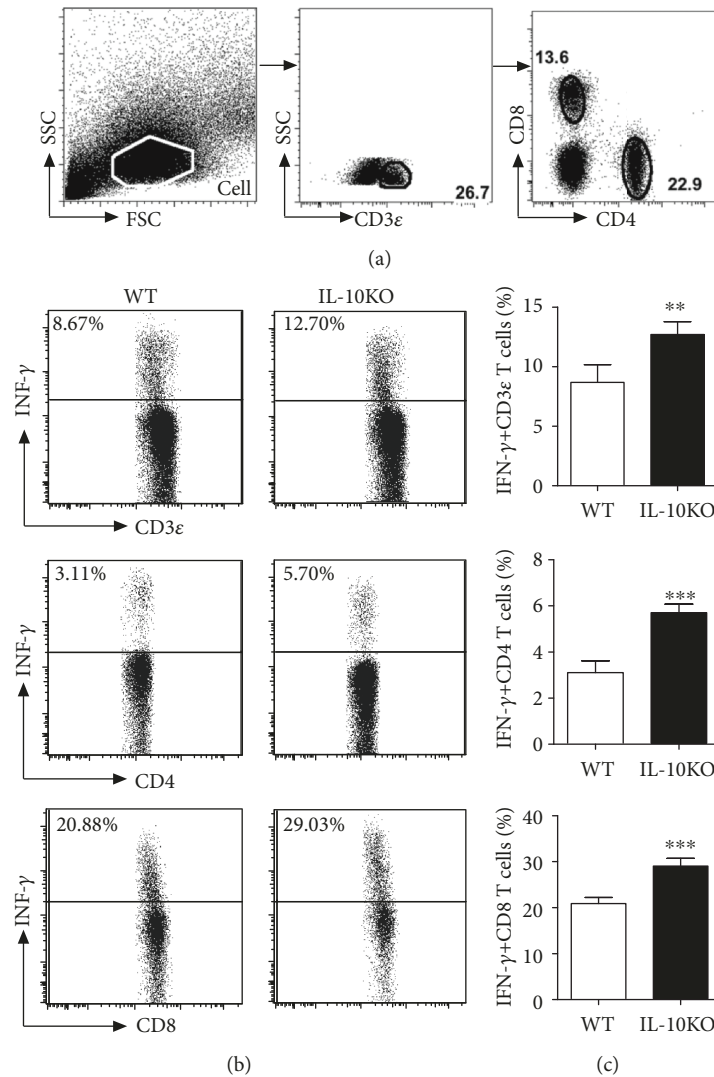


FIGURE 3: IL-10KO mice showed higher IFN  $\gamma$  production after BCG challenge in the lungs. The mice were treated as described in the legend of Figure 4. The lungs were digested as described in Materials and Methods. The intracellular IFN  $\gamma$ -positive T cells were analyzed by intracellular cytokine staining as described previously [29]. (a) Gating strategy: firstly, the major cells were gated for further gated based on the CD3 $\epsilon$  expression. Then, the CD3 $\epsilon$ <sup>+</sup> cells were gated on the CD4 and CD8 expression for CD4<sup>+</sup> and CD8<sup>+</sup> T cells. (b) The figures from FAC analysis for the IFN- $\gamma$ <sup>+</sup> expression were shown. (c) Summary of the percentage of the IFN- $\gamma$ <sup>+</sup>CD3 $\epsilon$ <sup>+</sup>, CD4<sup>+</sup>, and CD8<sup>+</sup> T cells in the lungs, and Student's *t* test was used for analysis. The representative of three independent experiments ( $n = 5$ ) with similar results was shown. \*\* $p < 0.01$ , \*\*\* $p < 0.001$ .

from the lungs and draining lymph nodes collected from mice after BCG challenge. As shown in Figures 3 and 4, IL-10-deficient mice showed higher IFN  $\gamma$  production in CD3 $\epsilon$ <sup>+</sup>T cells, which was consistent with the protective responses observed in lung pathogenesis changes, same to IFN  $\gamma$ <sup>+</sup> CD4<sup>+</sup> and IFN  $\gamma$ <sup>+</sup> CD8<sup>+</sup>T cells in both lungs and dLN in IL-10KO mice. Taken together, the results suggest that IL-10 blocks the Th1 responses, as well as cytotoxic T cell development in mycobacterial infection. IL-10 production might be partially responsible for the ineffective BCG vaccination.

**3.3. Th1 and Tc Responses Were Restricted by IL-10 Production in BCG Vaccination.** It is well known that Th1 and Tc were critical for TB infection control. To further

explore the role of IL-10 in Th1 and Tc development during the BCG vaccination, the T cell subsets were then examined in the IL-10KO and WT mice after BCG vaccination. The cells isolated from the spleen were analyzed by multicolor staining. As shown in Figure 5, IL-10KO promoted dominant Th1 (IFN  $\gamma$ <sup>+</sup>CD4<sup>+</sup>T cells) production and Tc production (IFN  $\gamma$ <sup>+</sup>CD8<sup>+</sup>T cells). It suggested that, without IL-10, BCG vaccination could induce better Th1 and Tc immune responses that might offer better protection against TB infection.

**3.4. IL-10KO Mice Showed Significantly Higher Protective Cytokine Production after BCG Vaccination in the Spleen.** To further explore the systemic immune responses in WT vs. IL-10KO mice after BCG immunization, the spleen, lungs,

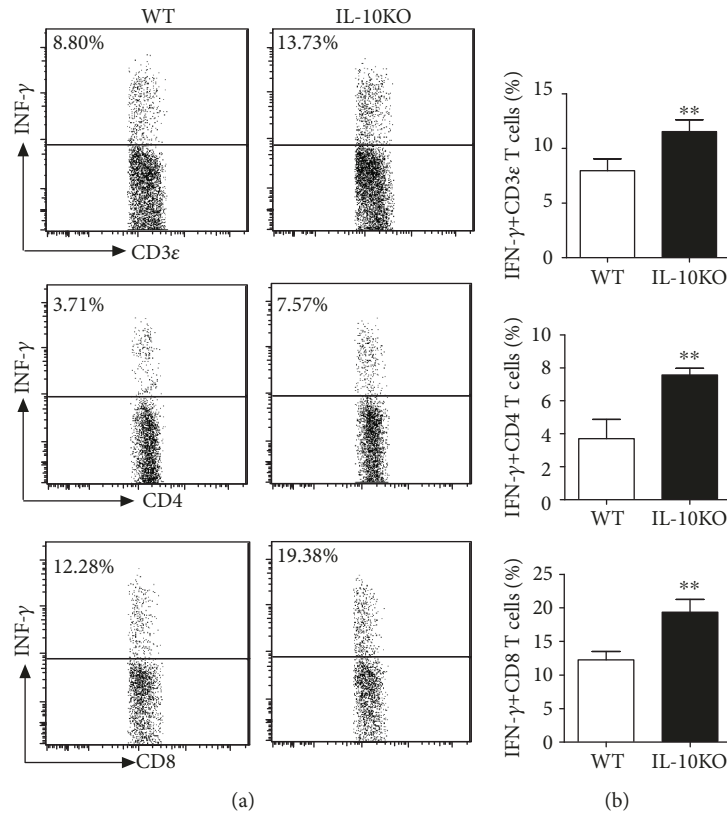


FIGURE 4: IL-10KO mice showed higher IFN  $\gamma$  production after BCG challenge in dLN. The mice were treated as described in the legend. The single cells from dLN were stained, and the intracellular IFN  $\gamma$ -positive T cells were analyzed by intracellular cytokine staining as described previously [29]. (a) Representative figures from FAC analysis were shown. (b) Summary of percentage of the IFN  $\gamma$ +CD3 $\epsilon$ +, CD4+, and CD8+ T cells in dLN. Data are shown as the representative of three independent experiments with similar results ( $n = 5$ ) and Student's  $t$  test was used for analysis. \*\* $p < 0.01$ .

and draining lymph nodes were collected aseptically and the bulk culture of splenocytes and the cells isolated from draining LN and lung tissues were used to detect the cytokine production in the supernatant in both IL-10KO and WT mice after BCG vaccination. As shown in Figure 6, IFN  $\gamma$  and IL-6 levels showed significantly higher in the IL-10KO mice compared to WT mice, but comparable levels of IL-4 were found in the spleen, lungs, and dLN in both types of mice. Rather surprisingly, the TNF  $\alpha$  levels of IL-10KO mice were higher than those in WT mice in the spleen and dLN but not in the lungs. The data suggest that IL-10 inhibited the protective IFN  $\gamma$  and TNF  $\alpha$  expression, as well as IL-6 production, even with the comparable TNF  $\alpha$  expression in the lungs from both types of mice.

**3.5. IL-10 Inhibits the T Cell Activation by DCs in BCG Vaccination.** To detect the role of IL-10 in the DC function of directing the T cell differentiation, the spleen DCs from WT and IL-10KO mice after BCG vaccination were purified by the FACs. The CD4+T cells were isolated from the spleen of BCG-vaccinated WT mice. The DCs were cocultured with BCG-boosted CD4+T cells. The IL-4 and IFN  $\gamma$  production in the culture supernatants were detected. As shown in Figure 7, the DCs from IL-10KO mice initiated higher IL-4 and IFN  $\gamma$  production by

CD4+T cells than those from WT mice ( $p < 0.01$ ). The results demonstrated that IL-10 signaling may contribute to the DC dysfunction in BCG vaccination.

**3.6. IL-10 Prevents the Activation of DC after BCG Vaccination.** The functions of DC in initiating immune responses largely depend on their expression of costimulatory molecules on their surface. To detect the role of IL-10 production in modulating DC functions in BCG vaccination, FACs were applied to detect the surface marker expression on the spleen DCs after BCG immunization. As shown in Table 1, there is no much jump between WT and IL-10KO mice regarding the CD80, CD86, and CD40 expression before the vaccination. However, after BCG immunization, the spleen DCs from IL-10-deficient mice expressed higher CD80 (89.79% vs. 58.32%), CD86 (32.66% vs. 25.73%), and CD40 (20.95% vs. 15.38%) molecules in comparison with the DCs from WT mice. It suggested that BCG vaccination can activate DCs which were suppressed by the IL-10 production.

**3.7. IL-10KO Mice Showed Reduced Tregs after BCG Vaccination.** The role of regulatory T cells (Tregs), especially Foxp3+ Tregs, was investigated after TB challenge infection. It was shown that the increased Treg was related to the

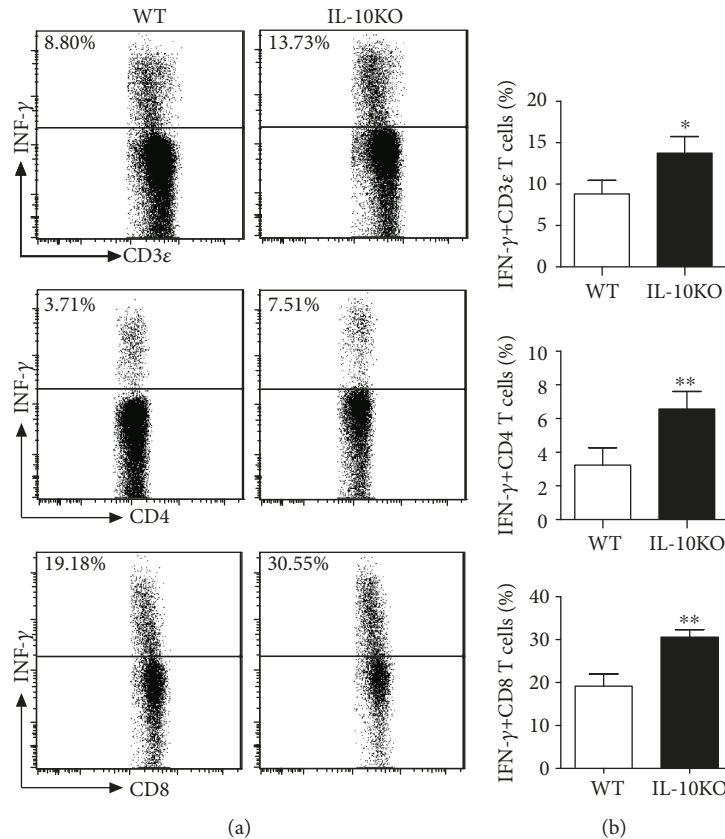


FIGURE 5: IL-10KO mice had higher IFN  $\gamma$  production after BCG vaccination in the spleen. The spleen was digested with enzyme as described in Materials and Methods. The cells were stained with FITC anti-CD3 $\epsilon$ , PE anti-CD4, PerCy5.5 anti-CD8, and APC anti-IFN  $\gamma$ . The intracellular IFN  $\gamma$ -positive cells were analyzed by intracellular cytokine staining when cells were gated on CD3 $\epsilon$ , CD4, and CD8 as described previously [29]. (a) Representative figures from FAC analysis were shown. (b) Summary of percentage of the IFN  $\gamma$ +CD3 $\epsilon$ +, CD4+, and CD8+ T cells in the spleen, and Student's *t* test was used for analysis. \**p* < 0.05, \*\**p* < 0.01. The representative of three independent experiments (*n* = 5) with similar results was shown.

pathogenesis in TB infection [32]. Treg analysis in the lung tissues by FACs showed less Foxp3+CD25+CD4+ T cells in the lungs of IL-10KO mice after BCG challenge (Figure 8). Collectively, the results demonstrated the increased IFN  $\gamma$  expression without IL-10 but reduced Treg responses following BCG challenge.

#### 4. Discussion

The protective efficacy of BCG is variable against TB infection. Some studies were devoted to BCG engineering for increasing its antigenicity to drive a desirable immune response against TB [33, 34]. The potential to modulate host immunity is critical for the success of a vaccine. The host genetic heterogeneity is partially responsible for the BCG failure that the host factors might be targeted to enhance the potency of this vaccine. In this study, we aimed to investigate the roles of host factor IL-10 in BCG vaccination efficacy. The data supported that BCG vaccination in IL-10-deficient host can boost the DC activation through upregulation of the surface molecule expression. In vivo BCG immunization in IL-10KO mice promotes IFN  $\gamma$  production, which was consistent with the protective effects after BCG challenge. The mild lung pathologic changes after BCG vaccination/challenge

supported that IL-10 deficiency resulted in higher protective responses. In clinical practice, an increased susceptibility toward the development of progressive tuberculosis in humans with increased IL-10 levels was reported [35]. Our study explored the molecular mechanisms of the notorious role of IL-10 in the BCG vaccination.

The ability of the host to control TB infection depends on recruited Th1 cells to release and activate the killing mechanisms of the infected cells. In the current study, to assess Th1-polarizing capacity after comparing the immunoregulatory cytokine IL-6, IFN  $\gamma$ , IL-4, and TNF  $\alpha$  production, we found that IL-10KO mice produced more IFN  $\gamma$  and TNF  $\alpha$  compared to the WT mice. The predisposition of IFN  $\gamma$  gene-deficient mice to TB and the therapeutic role of IFN  $\gamma$  support an essential role for this cytokine in the protective immune response against TB. Additionally, the clinical application of anti-TNF  $\alpha$  leads to reactivation of TB infection or patients succumbed to the TB disease. It is known that, after TB infection, activated type 1 T cells, particularly CD4+ T cells, are the most abundant cellular source of IFN  $\gamma$ . Consistent with the data of bulk culture, there was a much less frequency of IFN  $\gamma$  producing CD3 $\epsilon$ +, CD4+, and CD8+ T cells in the spleen in WT mice than those in IL-10 KO mice.

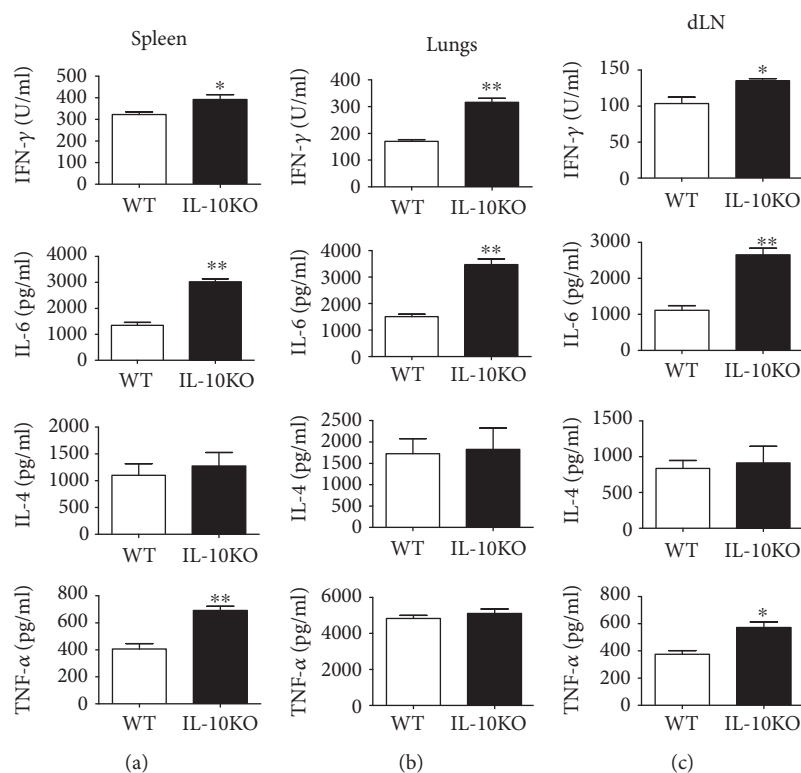


FIGURE 6: Cytokine levels after BCG vaccination in IL-10KO mice compared to WT mice. IL-10KO and WT mice were immunized with BCG as described in Materials and Methods. At d 21 after vaccination, the single cells prepared from the spleen, lungs, and dLN were cultured for 72 h stimulated with HK-BCG ( $5 \times 10^5$  CFUs/mL) before supernatant collection. The cytokines were measured by the ELISA. Data were summarized and representative of three independent experiments with similar results were shown. \* $p < 0.05$ , \*\* $p < 0.01$ .

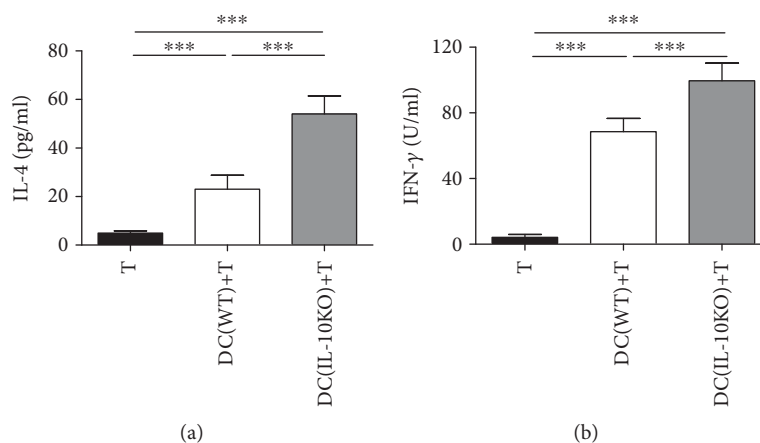


FIGURE 7: Cytokine production from DC-CD4<sup>+</sup>T cell coculture system. Spleen DCs ( $7.5 \times 10^5$  cells/mL) from WT and IL-10KO BCG-vaccinated mice were cocultured with BCG-educated CD4<sup>+</sup>T cells ( $7.5 \times 10^6$  cells/mL) as described in Materials and Methods. Cell supernatants were collected at 72 h for IFN  $\gamma$  and IL-4 detection by ELISA. Data were summarized as mean  $\pm$  SD ( $n = 5$ ) and representative of three independent experiments with similar results were shown. \*\* $p < 0.01$ , \*\*\* $p < 0.001$ .

The role of IL-10 in the immune response during TB infection had been studied previously. Several papers had shown that IL-10 is mainly produced by hematopoietic cells and play an important role in suppressing macrophage and dendritic cell (DC) functions. Thus, IL-10 is responsible for the ability of TB to evade immune responses [36]. Another study investigated the role of IL-10 in BCG efficacy too.

The authors showed that IL-10 signaling deficiency during BCG vaccination enhanced Th1 and Th17 responses that improved the protection against TB infection [37]. Our study focuses on and detects the functions of dendritic cells, the orchestra of immune response, and found that IL-10 hinders the activation of DCs that delays the fully activation of T cell responses. Further, our study firstly showed that IL-10

TABLE 1: The surface molecular expression on DC from WT/IL-10KO mice ( $\bar{x} \pm SD$ ).

	BCG immunization		PBS (naïve)	
	WT ( $n = 5$ )	IL-10KO ( $n = 5$ )	WT ( $n = 5$ )	IL-10KO ( $n = 5$ )
CD80 (%)	58.32 $\pm$ 2.50	89.79 $\pm$ 9.20*	22.14 $\pm$ 3.12	23.47 $\pm$ 2.90
CD86 (%)	25.70 $\pm$ 4.47	32.66 $\pm$ 3.16*	11.06 $\pm$ 2.20	10.66 $\pm$ 2.33
CD40 (%)	15.38 $\pm$ 3.54	20.95 $\pm$ 3.03*	7.17 $\pm$ 3.54	5.32 $\pm$ 1.10

\* $p < 0.05$ , compared to the WT mice.

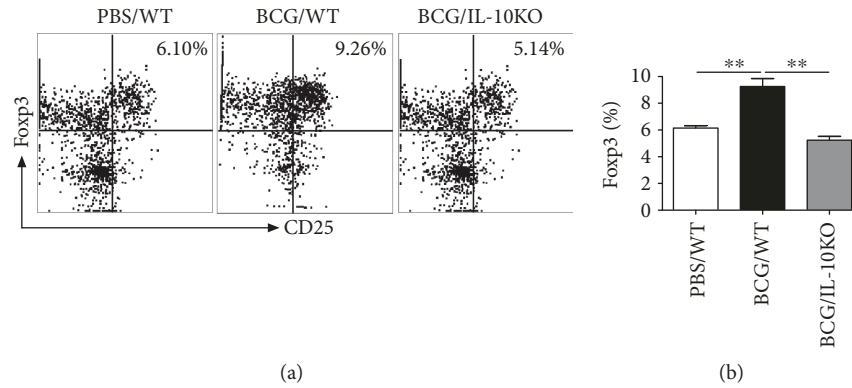


FIGURE 8: Lung Foxp3<sup>+</sup> Treg cells were analyzed after BCG challenged in IL-10KO and WT mice. The mice were treated as described in the legend of Figure 7. Lung single cells were stained with FITC anti-CD3<sub>ε</sub>, PerCy5.5 anti-CD4, APC anti-CD25, and PE-Foxp3. The Foxp3 expression was analyzed by flow cytometry when cells were gated on CD3<sub>ε</sub><sup>+</sup>CD4<sup>+</sup>T cells. (a) The representative pictures of Foxp3<sup>+</sup>CD3<sub>ε</sub><sup>+</sup>CD4<sup>+</sup>CD25<sup>+</sup>Tregs were shown. (b) Summary of the frequency of Foxp3<sup>+</sup>CD25<sup>+</sup>CD4<sup>+</sup>T cells in total T cells in the lungs. Data are shown as mean  $\pm$  SD ( $n = 5$ ) and are representative of three independent experiments with similar results. \*\* $p < 0.01$ .

promoted the Treg development. We found that the frequency of regulatory T cells increased in the IL-10-competent mice, while decreased in IL-10 compromised ones. Our study indicated that the host factors, especially the dendritic cell function, maybe of importance in understanding the efficacy of vaccine. It is a great benefit to develop a proper adjuvant for the efficacious vaccination strategy.

It is believed that BCG “educated” DCs interact with CD4<sup>+</sup>T cells that they reciprocally affect each other’s activation. Interestingly, we found that IL-10-deficient DCs can induce both higher IL-4 and IFN  $\gamma$  production by the CD4<sup>+</sup>T cell in vitro coculture system. It is well known that Th2 responses promote TB progression by inhibiting Th1 responses. Given an activation of both Th1 and Th2 T cells in the DC-CD4<sup>+</sup>T cell coculture system (Figure 7), we examined the impact of IL-10 deficiency on the T cell activation by using intracellular cytokine staining after BCG immunization (Figure 5). To this end, the total T cell, CD4<sup>+</sup>, and CD8<sup>+</sup>T cell subsets isolated from IL-10KO mice showed enhanced IFN  $\gamma$  production in the spleen. It indicated that in vivo host immunity lean to Th1 responses without IL-10 in BCG vaccination. In line with this finding, the IL-10-deficient mice did not show any Th2 response after BCG vaccination/challenge. We speculated that both Th2 and Th1 cells were released without IL-10 production, but the extent and level of Th2 are much less than Th1 in vivo that IL-4 production is comparable in IL-10KO and WT mice. Another reason for the inconsistent IL-4 production between in vivo T cell responses and in vitro coculture study is that T cells in the in vitro

coculture system were capable to produce IL-10 due to its isolation from WT mice, while in vivo BCG vaccination and challenge were conducted in the IL-10KO mice that T cell responses in the background of IL-10 deficiency.

After BCG challenge in immunized mice, IL-10KO mice had much higher Th1 responses in both lungs (Figure 3) and dLN (Figure 4). It is consistent with the lung inflammation detected by the professional pathologists that much less pro-inflammatory response in the IL-10KO mice compared to that in WT mice. It is keeping with Shaler et al. who showed that IL-10 deficiency can restore the Th1 response in a granuloma using IL-10KO mice [38].

It is noteworthy that an attenuated strain of mycobacteria (BCG, *M. bovis*), but not virulent *Mtb*, was applied in our current study that the same antigen was used for both vaccination and challenge. However, studies worked on the comparison of BCG and virulent strain of *Mtb* in mice showed that the overall kinetics and cellular response were comparable, same to the protective roles of IFN  $\gamma$  and Th1 responses in either BCG or *Mtb* exposure in mice [39–41]. Despite all these described similarities, we must caution to explain our findings in the clinical setting since *Mtb* is significantly more virulent compared to BCG.

Given that BCG vaccination efficacy is far from satisfied and much efforts focuses on the antigen modification, our current findings provide a new strategy for better vaccine adjuvant development, as well as a plausible mechanism to explain the heterogeneous outcomes after BCG vaccination in different populations.

## Data Availability

The scientific and statistical data used to support the findings of this study are included within the article. Requests for access to these data should be addressed to Xiaoling Gao at Gaoxl008@hotmail.com.

## Conflicts of Interest

The authors declare no conflict of interest.

## Authors' Contributions

All the authors have accepted responsibility for the entire content of this submitted manuscript and approved submission.

## Acknowledgments

This work was supported by the National Natural Science Foundation (grant nos. 81860372 and 31860598), the Talent Innovation and Entrepreneurship Project of Lanzhou (grant no. 2017-RC-43), the Natural Science Foundation of Gansu Province (grant no. 18JR3RA044), and the Health Industry Research Project of Gansu Province (grant no. GSWSKY2017-16).

## References

- [1] GBD 2017 Mortality Collaborators, "Global, regional, and national age-sex-specific mortality and life expectancy, 1950-2017: a systematic analysis for the Global Burden of Disease Study 2017," *The Lancet*, vol. 392, no. 10159, pp. 1684–1735, 2018.
- [2] W. M. Kühtreiber and D. L. Faustman, "BCG therapy for type 1 diabetes: restoration of balanced immunity and metabolism," *Trends in Endocrinology & Metabolism*, vol. 30, no. 2, pp. 80–92, 2018.
- [3] R. Basu Roy, E. Whittaker, J. A. Seddon, and B. Kampmann, "Tuberculosis susceptibility and protection in children," *The Lancet Infectious Diseases*, vol. 19, no. 3, pp. e96–e108, 2018.
- [4] G. Ristori, M. G. Buzzi, U. Sabatini et al., "Use of Bacille Calmette-Guerin (BCG) in multiple sclerosis," *Neurology*, vol. 53, no. 7, pp. 1588–1589, 1999.
- [5] S. Kodama, M. Davis, and D. L. Faustman, "The therapeutic potential of tumor necrosis factor for autoimmune disease: a mechanistically based hypothesis," *Cellular and Molecular Life Sciences CMLS*, vol. 62, no. 16, pp. 1850–1862, 2005.
- [6] A. B. Alexandroff, A. M. Jackson, M. A. O'Donnell, and K. James, "BCG immunotherapy of bladder cancer: 20 years on," *The Lancet*, vol. 353, no. 9165, pp. 1689–1694, 1999.
- [7] T. Elvang, J. P. Christensen, R. Billeskov et al., "CD4 and CD8 T cell responses to the *M. tuberculosis* Ag85B-TB10.4 promoted by adjuvanted subunit, adenovector or heterologous prime boost vaccination," *PLoS One*, vol. 4, no. 4, article e5139, 2009.
- [8] E. Z. Tchilian, C. Desel, E. K. Forbes et al., "Immunogenicity and Protective Efficacy of Prime-Boost Regimens with Recombinant *ΔureC hly<sup>+</sup>Mycobacterium bovis* BCG and Modified Vaccinia Virus Ankara Expressing *M. tuberculosis* Antigen 85A against Murine Tuberculosis," *Infect Immun*, vol. 77, no. 2, pp. 622–631, 2009.
- [9] Y. A. W. Skeiky, J. Dietrich, T. M. Lasco et al., "Non-clinical efficacy and safety of HyVac4:IC31 vaccine administered in a BCG prime-boost regimen," *Vaccine*, vol. 28, no. 4, pp. 1084–1093, 2010.
- [10] H. M. Vordermeier, B. Villarreal-Ramos, P. J. Cockle et al., "Viral booster vaccines improve *Mycobacterium bovis* BCG-induced protection against bovine tuberculosis," *Infect Immun*, vol. 77, no. 8, pp. 3364–3373, 2009.
- [11] K. T. Whelan, A. A. Pathan, C. R. Sander et al., "Safety and immunogenicity of boosting BCG vaccinated subjects with BCG: comparison with boosting with a new TB vaccine, MVA85A," *PLoS One*, vol. 4, no. 6, article e5934, 2009.
- [12] X. Gao, S. Wang, Y. Fan, H. Bai, J. Yang, and X. Yang, "CD8<sup>+</sup> DC, but Not CD8<sup>-</sup> DC, isolated from BCG-infected mice reduces pathological reactions induced by mycobacterial challenge infection," *PLoS One*, vol. 5, no. 2, article e9281, 2010.
- [13] Y. Satake, Y. Nakamura, M. Kono et al., "Type-1 polarized dendritic cells are a potent immunogen against *Mycobacterium tuberculosis*," *The International Journal of Tuberculosis and Lung Disease*, vol. 21, no. 5, pp. 523–530, 2017.
- [14] Q. Li, Z. Guo, X. Xu, S. Xia, and X. Cao, "Pulmonary stromal cells induce the generation of regulatory DC attenuating T-cell-mediated lung inflammation," *European Journal of Immunology*, vol. 38, no. 10, pp. 2751–2761, 2008.
- [15] M. Svensson and P. M. Kaye, "Stromal-cell regulation of dendritic-cell differentiation and function," *Trends in Immunology*, vol. 27, no. 12, pp. 580–587, 2006.
- [16] M. Svensson, A. Maroof, M. Ato, and P. M. Kaye, "Stromal cells direct local differentiation of regulatory dendritic cells," *Immunity*, vol. 21, no. 6, pp. 805–816, 2004.
- [17] M. Shakouri, S. M. Moazzeni, M. Ghanei, A. Arashkia, M. H. Etemadzadeh, and K. Azadmanesh, "A novel dendritic cell-targeted lentiviral vector, encoding Ag85A-ESAT6 fusion gene of *Mycobacterium tuberculosis*, could elicit potent cell-mediated immune responses in mice," *Molecular Immunology*, vol. 75, pp. 101–111, 2016.
- [18] J. K. Sia, E. Bizzell, R. Madan-Lala, and J. Rengarajan, "Engaging the CD40-CD40L pathway augments T-helper cell responses and improves control of *Mycobacterium tuberculosis* infection," *PLoS Pathogens*, vol. 13, no. 8, article e1006530, 2017.
- [19] M. Ahmed, H. Jiao, R. Domingo-Gonzalez et al., "Rationalized design of a mucosal vaccine protects against *Mycobacterium tuberculosis* challenge in mice," *Journal of Leukocyte Biology*, vol. 101, no. 6, pp. 1373–1381, 2017.
- [20] N. E. Corral-Fernandez, J. D. Cortes-García, R.-S. Bruno et al., "Analysis of transcription factors, microRNAs and cytokines involved in T lymphocyte differentiation in patients with tuberculosis after directly observed treatment short-course," *Tuberculosis*, vol. 105, pp. 1–8, 2017.
- [21] R. V. Sutavani, I. R. Phair, R. Barker et al., "Differential control of Toll-like receptor 4-induced interleukin-10 induction in macrophages and B cells reveals a role for p90 ribosomal S6 kinases," *Journal of Biological Chemistry*, vol. 293, no. 7, pp. 2302–2317, 2018.
- [22] J. Turner, M. Gonzalez-Juarrero, D. L. Ellis et al., "In vivo IL-10 production reactivates chronic pulmonary tuberculosis in C57BL/6 mice," *The Journal of Immunology*, vol. 169, no. 11, pp. 6343–6351, 2002.

- [23] S. O'Leary, M. P. O'Sullivan, and J. Keane, "IL-10 blocks phagosome maturation in *Mycobacterium tuberculosis*-infected human macrophages," *American Journal of Respiratory Cell and Molecular Biology*, vol. 45, no. 1, pp. 172–180, 2011.
- [24] X. Zhang, T. Y. Huang, Y. Wu et al., "Inhibition of the PI3K-Akt-mTOR signaling pathway in T lymphocytes in patients with active tuberculosis," *International Journal of Infectious Diseases*, vol. 59, pp. 110–117, 2017.
- [25] L. Xu, G. Cui, H. Jia et al., "Decreased IL-17 during treatment of sputum smear-positive pulmonary tuberculosis due to increased regulatory T cells and IL-10," *Journal of Translational Medicine*, vol. 14, no. 1, p. 179, 2016.
- [26] X. Yang, Y. Fan, S. Wang et al., "Mycobacterial infection inhibits established allergic inflammatory responses via alteration of cytokine production and vascular cell adhesion molecule-1 expression," *Immunology*, vol. 105, no. 3, pp. 336–343, 2002.
- [27] X. Yang, S. Wang, Y. Fan, and L. Zhu, "Systemic mycobacterial infection inhibits antigen-specific immunoglobulin E production, bronchial mucus production and eosinophilic inflammation induced by allergen," *Immunology*, vol. 98, no. 3, pp. 329–337, 1999.
- [28] C. S. Hirsch, J. Baseke, J. L. Kafuluma, M. Nserko, H. Mayanja-Kizza, and Z. Toossi, "Expansion and productive HIV-1 infection of Foxp3 positive CD4 T cells at pleural sites of HIV/TB co-infection," *Journal of Clinical & Experimental Immunology*, vol. 1, no. 1, p. 1, 2016.
- [29] B. M. Kagina, N. Mansoor, E. P. Kpamegan et al., "Qualification of a whole blood intracellular cytokine staining assay to measure mycobacteria-specific CD4 and CD8 T cell immunity by flow cytometry," *Journal of Immunological Methods*, vol. 417, pp. 22–33, 2015.
- [30] A. G. Joyee, H. Qiu, Y. Fan, S. Wang, and X. Yang, "Natural killer T cells are critical for dendritic cells to induce immunity in Chlamydial pneumonia," *American Journal of Respiratory and Critical Care Medicine*, vol. 178, no. 7, pp. 745–756, 2008.
- [31] R. Anuradha, S. Munisankar, Y. Bhootra et al., "Anthelmintic therapy modifies the systemic and mycobacterial antigen-stimulated cytokine profile in helminth-latent *Mycobacterium tuberculosis* Coinfection," *Infection and Immunity*, vol. 85, no. 4, 2017.
- [32] M. Tarique, H. Naz, S. V. Kurra et al., "Interleukin-10 producing regulatory B cells transformed CD4<sup>+</sup>CD25<sup>-</sup> into Tregs and enhanced regulatory T cells function in human leprosy," *Frontiers in Immunology*, vol. 9, article 1636, 2018.
- [33] N. C. Bull, D. A. Kaveh, M. C. Garcia-Pelayo, E. Stylianou, H. McShane, and P. J. Hogarth, "Induction and maintenance of a phenotypically heterogeneous lung tissue-resident CD4<sup>+</sup> T cell population following BCG immunisation," *Vaccine*, vol. 36, no. 37, pp. 5625–5635, 2018.
- [34] S. A. F. El-Sahrigy, A. M. O. Abdel Rahman, D. Y. Samaha et al., "The influence of interferon- $\beta$  supplemented human dendritic cells on BCG immunogenicity," *Journal of Immunological Methods*, vol. 457, pp. 15–21, 2018.
- [35] A. A. Awomoyi, A. Marchant, J. M. M. Howson, K. P. W. J. McAdam, J. M. Blackwell, and M. J. Newport, "Interleukin-10, polymorphism in *SLC11A1* (formerly *NRAMP1*), and susceptibility to tuberculosis," *The Journal of Infectious Diseases*, vol. 186, no. 12, pp. 1808–1814, 2002.
- [36] P. S. Redford, P. J. Murray, and A. O'Garra, "The role of IL-10 in immune regulation during *M. tuberculosis* infection," *Mucosal Immunology*, vol. 4, no. 3, pp. 261–270, 2011.
- [37] J. M. Pitt, E. Stavropoulos, P. S. Redford et al., "Blockade of IL-10 signaling during bacillus Calmette-Guerin vaccination enhances and sustains Th1, Th17, and innate lymphoid IFN- $\gamma$  and IL-17 responses and increases protection to *Mycobacterium tuberculosis* infection," *The Journal of Immunology*, vol. 189, no. 8, pp. 4079–4087, 2012.
- [38] C. R. Shaler, K. Kugathasan, S. McCormick et al., "Pulmonary mycobacterial granuloma: increased IL-10 production contributes to establishing a symbiotic host-microbe microenvironment," *The American Journal of Pathology*, vol. 178, no. 4, pp. 1622–1634, 2011.
- [39] A. Zganiacz, M. Santosuosso, J. Wang et al., "TNF- $\alpha$  is a critical negative regulator of type 1 immune activation during intracellular bacterial infection," *The Journal of Clinical Investigation*, vol. 113, no. 3, pp. 401–413, 2004.
- [40] N. D. Pecora, S. A. Fulton, S. M. Reba et al., "*Mycobacterium bovis* BCG decreases MHC-II expression *in vivo* on murine lung macrophages and dendritic cells during aerosol infection," *Cellular Immunology*, vol. 254, no. 2, pp. 94–104, 2009.
- [41] S. A. Fulton, T. D. Martin, R. W. Redline, and W. Henry Boom, "Pulmonary Immune Responses during Primary *Mycobacterium bovis*- Calmette-Guerin Bacillus Infection in C57Bl/6 Mice," *Am J Respir Cell Mol Biol*, vol. 22, no. 3, pp. 333–343, 2000.

## Review Article

# Noncanonical IFN Signaling, Steroids, and STATs: A Probable Role of V-ATPase

Howard M. Johnson , Ezra Noon-Song, and Chulbul M. Ahmed

*Department of Microbiology and Cell Science, University of Florida, Gainesville, FL, USA*

Correspondence should be addressed to Howard M. Johnson; johnsonh@ufl.edu

Received 9 December 2018; Accepted 15 April 2019; Published 28 May 2019

Guest Editor: Xiao Chen

Copyright © 2019 Howard M. Johnson et al. This is an open access article distributed under the Creative Commons Attribution License, which permits unrestricted use, distribution, and reproduction in any medium, provided the original work is properly cited.

A small group of only seven transcription factors known as STATs (signal transducer and activator of transcription) are considered to be canonical determinants of specific gene activation for a plethora of ligand/receptor systems. The activation of STATs involves a family of four tyrosine kinases called JAK kinases. JAK1 and JAK2 activate STAT1 in the cytoplasm at the heterodimeric gamma interferon (IFN $\gamma$ ) receptor, while JAK1 and TYK2 activate STAT1 and STAT2 at the type I IFN heterodimeric receptor. The same STATs and JAKs are also involved in signaling by functionally different cytokines, growth factors, and hormones. Related to this, IFN $\gamma$ -activated STAT1 binds to the IFN $\gamma$ -activated sequence (GAS) element, but so do other STATs that are not involved in IFN $\gamma$  signaling. Activated JAKs such as JAK2 and TYK2 are also involved in the epigenetics of nucleosome unwrapping for exposure of DNA to transcription. Furthermore, activated JAKs and STATs appear to function coordinately for specific gene activation. These complex events have not been addressed in canonical STAT signaling. Additionally, the function of noncoding enhancer RNAs, including their role in enhancer/promoter interaction is not addressed in the canonical STAT signaling model. In this perspective, we show that JAK/STAT signaling, involving membrane receptors, is essentially a variation of cytoplasmic nuclear receptor signaling. Focusing on IFN signaling, we showed that ligand, IFN receptor, the JAKs, and the STATs all undergo endocytosis and ATP-dependent nuclear translocation to promoters of genes specifically activated by IFNs. We argue here that the vacuolar ATPase (V-ATPase) proton pump probably plays a key role in endosomal membrane crossing by IFNs for receptor cytoplasmic binding. Signaling of nuclear receptors such as those of estrogen and dihydrotestosterone provides templates for making sense of the specificity of gene activation by closely related cytokines, which has implications for lymphocyte phenotypes.

## 1. Introduction

Our understanding of signaling by cytokines such as the interferons (IFNs) at the level of gene activation is stunningly deficient in mechanisms when compared to that of nuclear receptor signaling, as seen, for example, in the case of steroids and their receptors. The canonical model of type I and type II IFN signaling is a representative in fundamentals to that of cytokine or hormone signaling by any protein or peptide signaling via the JAK/STAT pathway.

According to this model, IFN $\gamma$  (type II IFN) signaling involves basically heterodimeric receptors IFNGR1 and IFNGR2, Janus kinases JAK1 and JAK2, and transcription factor signal transducer and activator of transcription 1 $\alpha$  (STAT1 $\alpha$ , reviewed in [1–3]). IFN $\gamma$  binds to the receptors,

mostly to the IFN $\gamma$  receptor (IFNGR1), causing autophosphorylation (activation) of and binding of the JAKs to IFNGR1. Somewhere in the activation process, JAK2 moves from IFNGR2 to IFNGR1 by some unknown mechanism. Also, somewhere in the process, IFNGR1 becomes phosphorylated in the cytoplasmic domain. These events cause binding, phosphorylation, and asymmetric dimer formation of STAT1 $\alpha$ . The activated STAT1 $\alpha$ , via an intrinsic nuclear localization sequence (NLS), undergoes energy-dependent nuclear translocation to promoters associated with genes that are activated by IFN $\gamma$ .

Type I IFN signaling is quite similar to that of IFN $\gamma$ , except that there are over 16 different type I IFN subtypes, all of which bind to the same heterodimeric IFNAR1 and IFNAR2 receptor complex. They all use JAK1 and TYK2

tyrosine kinases to phosphorylate STAT1 and STAT2, which in the activated state form a heterodimer, but some are toxic (apoptotic) at high doses while others are not. The toxic type I IFNs such as human IFN $\alpha$ 2 bind the receptor with a 10-fold higher binding affinity than does the nontoxic bovine IFN $\tau$ , yet they have the same specific antiviral activity on the same cells [4]. There is a third protein, called IFN response factor 9 (IRF9), that associates with activated STAT1 and STAT2 to form a trimeric complex called IFN-stimulated gene factor 3 (ISGF3) [1–3]. Similar to activated STAT1 $\alpha$  for IFN $\gamma$ , ISGF3 undergoes nuclear translocation, presumably via an intrinsic NLS. Also, according to the canonical model, ISGF3 is responsible for the specific activation of genes specific for type I IFNs. Thus, signal transduction via JAK/STAT does not explain the unique biological activities of different type I IFNs.

A comparison of type I IFN signaling with that of type III IFNs (IFN $\lambda$ s) further illuminates the inadequacy of the canonical model of JAK/STAT signaling in explaining the mechanism of the specificity of cytokine signaling. Unlike type I IFNs, interleukin 10 receptor 2 (IL10R2) and IFN $\lambda$  receptor (IFN $\lambda$ R) form the heterodimeric receptor for IFN $\lambda$  [5–7]. However, like type I IFNs, IFN $\lambda$ s use JAK1 and TYK2 kinases to activate STAT1 and STAT2 for signal transduction. Although the type I IFN receptor is ubiquitous on cells, the type III receptor is cell specific, appearing in particular on epithelial cells and some other cells such as neutrophils. The induction of reactive oxygen species (ROS) in neutrophils is inhibited by IL28A type III IFN, but not by the IFN $\beta$  type I IFN [8]. Consistent with ROS inhibition, IL28A is therapeutic in neutrophil-mediated inflammatory arthritis and colitis [8–10]. Other neutrophil functions such as phagocytosis and cytokine production are similarly affected by the two IFNs. These results beg a revisit of the conventional canonical JAK/STAT pathway as the basis for the specificity of cytokine signaling.

The specificity of IFN signaling as well as that of over 100 other different types of cytokines, growth factors, and hormones that use the canonical JAK/STAT pathway has been attributed solely to the STATs. Although there may be some overlap in their different functions, these different factors possess unique ligand specific functions at the level of the gene, cell, and organism. The problem is that there are not enough different STATs to provide a basis for the uniqueness of all these different functions as there are only seven different STATs that function mostly as homodimers [3, 11]. This means that there are cytokines that use the same STATs, but function differently. There is no evidence that a given STAT possesses functions at the level of gene activation that are unique to the activating cytokine beyond recognition of the response element [3].

The recent demonstration of activated JAK2 in the nucleus of cells by gain-of-function mutation (JAK2V617F) or by wild-type JAK2 activated by cytokines or growth factors provides profound insight into the mechanism of cytokine signaling [12]. It also challenges the canonical model of JAK/STAT signaling. In the case of a specific cytokine such as IFN $\gamma$ , treatment of cells results in nuclear translocation of both activated JAK2 (pJAK2) and activated STAT1 $\alpha$

(pSTAT1 $\alpha$ ) [13]. The earlier study with JAKV617F and cytokine-activated wild-type pJAK2 showed a novel and important epigenetic function of these nuclear JAKs [12]. The activated JAKs phosphorylate histone H3 at tyrosine residue 41 (Y41). Phosphorylated H3Y41, H3pY41, causes the dissociation of heterochromatin protein 1 $\alpha$  (HP1 $\alpha$ ) from histone H3, resulting in transcription of genes repressed by HP1 $\alpha$ . Activation of JAKs in the nucleus is an important epigenetic event not considered in the canonical model, but is addressed in the noncanonical model of IFN signaling later. We will first discuss briefly the nuclear receptor signaling as it is a big indicator and a guidepost for understanding cytokine signaling as well as that of other peptide/protein signaling in terms of nuclear kinases as well as the role of enhancers/enhancer noncoding RNAs (eRNAs) in such signaling.

## 2. Nuclear Receptor Signaling, Promoters, Enhancers, and Enhancer RNAs: A Comparison with Canonical IFN $\gamma$ Signaling

As suggested, we do not have comparable understanding of mechanisms of specific gene activation between nuclear receptor systems such as steroid/steroid receptor and canonical JAK/STAT signaling as exemplified by IFN $\gamma$  and its receptor. A comparison of the two at the level of the promoter and enhancer region of genes that are activated by steroids versus those activated by IFN $\gamma$  readily illustrates the difference in knowledge. In canonical signaling, IFN $\gamma$  binds to its heterodimeric receptor subunits IFNGR1 and IFNGR2, with IFNGR1 playing a dominant role in the binding [2, 14]. JAK1 is present on IFNGR1, and the binding results in movement of JAK2 from IFNGR2 to IFNGR1. These events result in JAK autophosphorylation, phosphorylation of IFNGR1, and binding and phosphorylation of STAT1 $\alpha$ , which forms an asymmetric homodimer and undergoes active nuclear transport to the promoters of genes that are activated by IFN $\gamma$ . The canonical model does not provide insight into the movement of JAK2 from IFNGR2 to IFNGR1. Importantly, it does not show the connection between activated STAT1 $\alpha$  at promoters of genes that are activated by IFN $\gamma$  and specific IFN $\gamma$  function as many cytokines with their own unique functions also activate STAT1 $\alpha$  [11]. Next-generation sequencing (NGS) studies provide important insight in genome-wide activity of cytokines, but the problem of specificity as per IFN $\gamma$  above is not addressed [3]. NGS also does not connect the dots of activated JAK2 in the nucleus along with activated STAT1 $\alpha$  in terms of their coordinated function as activated JAK2 in the nucleus is not considered in the NGS studies.

We have previously presented an overview of nuclear receptor signaling as per steroid hormone (SH)/steroid receptor (SR) signaling [15]. We briefly revisit this and then show how mechanistic events are embedded into nuclear receptor (NR) signaling beyond promoters and extend to providing insight into the role of enhancers and long-noncoding RNAs called enhancer RNAs (eRNAs) in steroid signaling. We will then show why this is important, via

noncanonical IFN signaling, in understanding signaling by cytokines like IFN $\gamma$  not only at promoters, but also at enhancers and eRNAs.

In a nutshell, SH/SR signaling proceeds as follows. There are many reviews on the subject with considerable detail, but this overview makes our point [16]. SH binds to SR in the cytoplasm and/or the nucleus at hormone response promoter elements (HRE). SR is a transcription factor. Scaffolding proteins called steroid coactivators (SRC) bind to SH/SR through their LXXLL motifs, of which there are three [16]. They do not bind DNA directly. SRCs recruit secondary coactivators such as histone acetyltransferase p300/CBP, methyltransferases such as PRMT1 and CARM1, and chromatin remodeling complex SWT/SNF. Serine/threonine and tyrosine kinases also become a part of this machinery [16, 17]. The SH/SR complex at the promoter is a key to the mechanistic insight of gene activation, including key epigenetic events. The canonical model of IFN $\gamma$  signaling by contrast, with only STAT at the promoter, tells us very little and is even primitive relative to that of SH/SR signaling.

The abundance of genetic and epigenetic mechanisms in SH/SR signaling as well as in other NR signaling at the promoters of genes activated by NRs provides a picture that contrasts not only with IFN $\gamma$  signaling but also in general with peptide and protein ligands of hormone, growth factor, and cytokine signaling. The role of enhancers in gene activation is vague and even unknown for almost all ligand/receptor systems except for the case of NRs. Most of the transcribed RNA in the genome does not result in protein production, but rather plays a regulatory role in gene regulation. Of particular interest in the context of enhancers is a subgroup of long-noncoding RNAs (lncRNAs) called enhancer RNAs (eRNAs) [18–20]. eRNAs are transcribed from enhancers, and SH/SR and other NR signaling provide important insight into how eRNAs are transcribed and how enhancers interact with promoters and the role of eRNAs in this interaction [21, 22].

Chromatin immunoprecipitation (ChIP) has been applied to NGS procedures such as ChIP-seq to demonstrate that the estrogen receptor (ER) binds to 5,000 to 10,000 locations across the genome [23]. Another powerful weapon in the toolbox of NGS goes by the acronym of GRO-seq, which stands for global run-on sequencing [24]. GRO-seq is a direct, high-throughput sequencing procedure for finding RNAs and is adapted from conventional nuclear run-on methodologies. These technologies provide insight into the binding of ER and androgen receptor (AR) to enhancers and subsequent transcription of eRNAs and interaction or cross talk with ER and AR promoters.

Active enhancers are known by the company they keep. Thus, high levels of histone 3 lysine 4 monomethylation (H3K4me), low levels of H3K4 trimethylation (H3K4me3), and increased H3K27 acetylation (H3K27Ac) are associated with active enhancers [25]. These types of alterations in H3 along with other epigenetic signals such as tyrosine kinase activity result in the exposure/unwrapping of the DNA for transcription [26]. Accordingly, these epigenetic modifications usually precede transcription of the noncod-

ing eRNA from the enhancer DNA. The transcription of eRNA is carried out by enhancer-associated RNA polymerase II (Pol II) [25].

In the case of human breast cancer cells, treatment with 17 $\beta$ -estradiol (E2) results in E2-bound estrogen receptor  $\alpha$  (ER $\alpha$ ) association with enhancers adjacent to genes that are upregulated by E2 [22]. E2/ER $\alpha$  is thus bound to both the enhancers and promoters of genes that are activated by ER $\alpha$ . Similar to the ER $\alpha$  results, studies with dihydrotestosterone- (DHT-) treated prostate cancer cells also showed AR association with an enhancer involved in AR activation of specific genes [21]. ChIP assay on DHT-treated LNCaP prostate cancer cells showed a dynamic interaction of AR with the promoter and enhancer, where AR loaded onto enhancers to a greater extent, but enhancer association was more transient than that to the promoter [21]. Further, studies showed that eRNA may function as a scaffold that guides an AR-linked protein complex to target chromatin so that DHT-stimulated transcription either occurs intrachromosomally (cis activity) or interchromosomally (trans activity), depending on the promoter target of eRNA. Importantly, this finding ascribes a key function to eRNA as a bridge between the enhancer and promoter. Using steady-state histone acetyltransferase (HAT) assays, it has recently been shown that eRNA binds directly to CREB-binding protein (CBP) to enhance the HAT activity of CBP at enhancers [27]. The interaction increases CBP HAT activity by increasing its binding to histone. These studies provide insight into how eRNAs function in gene activation.

A current picture of the players at the enhancers and at the promoters of genes activated by steroid hormones such as estrogen and testosterone is presented in Figure 1(a). For both the promoter and enhancer, there are a collection of similar players. Nuclear receptors such as ER and AR with ligand attached function as transcription factors at both the promoter and enhancer. Thus, at the enhancer, eRNA is transcribed, while at the promoter, messenger RNA (mRNA) is transcribed. The SRC cofactors and platforms are present at both sites as well as are the epigenetic factors such as CBP/300. Pol II catalyzes the synthesis of both eRNA and mRNA, and eRNA synthesis is bidirectional. The mediator complex in Figure 1(a) consists of 26 or more subunits in mammals and plays a key role in Pol II activity, such as pre-initiation, initiation, reinitiation, pausing, and elongation [28]. Topoisomerase I is recruited to AR-bound enhancers in order to nick DNA to relieve supercoiling and allow DHT-regulated eRNA synthesis to occur [29]. The looping shown in Figure 1(a) brings the enhancer complex into close proximity to the promoter for coordinated activity. There are other players in these enhancer-promoter complexes, but the foundation factors for specific gene activation are typified by E2 or DHT steroid ligands bound to their respective ER or AR nuclear receptor. Specific gene activation does not occur without them. Cytokine, growth factor, and polypeptide (or protein) ligand signaling does not entertain many of these steroid signaling counterparts and their receptors in complexes such as in Figure 1(a). We show with particular focus on IFN below that this hinders access to specific mechanisms in signaling by these factors.

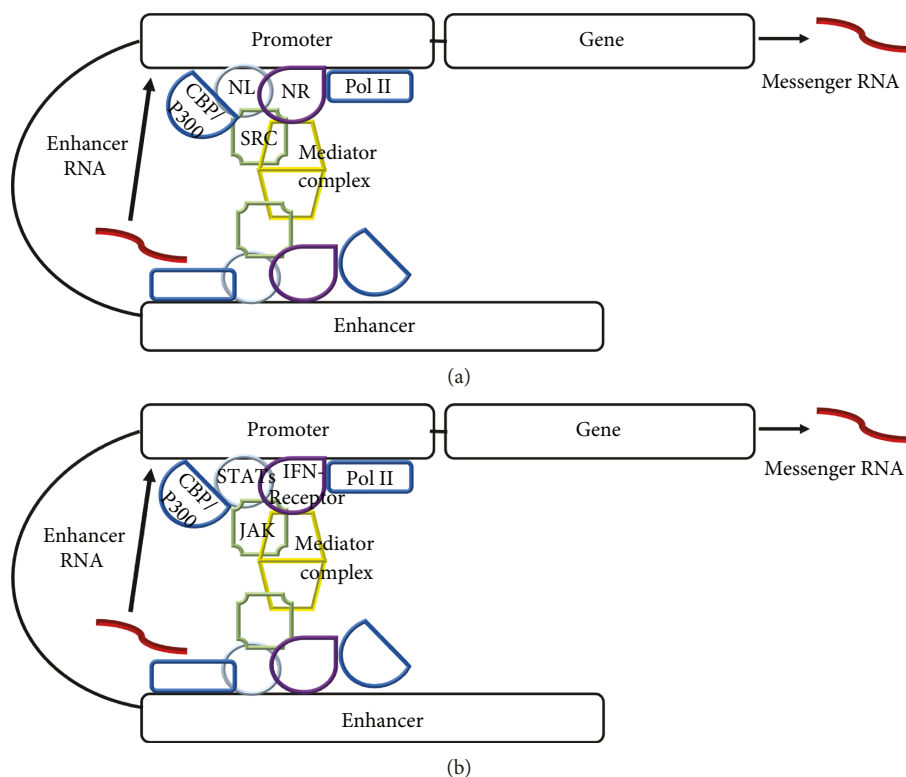


FIGURE 1: Nuclear receptor signaling as the template for IFN signaling via the JAK/STAT pathway. (a) Steroid hormones such as estrogen and dihydrotestosterone nuclear receptor ligands (NL) signal through cytoplasmic soluble nuclear receptors (NRs). NR signaling involves scaffolding proteins called steroid receptor coactivators (SRC) which serve as the platform for other factors such as histone acetyltransferases (CBP/p300) and kinases as well as other players such as a mediator complex consisting of 26 or more protein subunits. These factors are present at both the promoter and enhancer of genes specifically activated by steroids and their receptors. Specific transcription occurs at both the promoter (mRNA) and enhancer (eRNA) by RNA polymerase II. (b) We have shown that interferon (IFN) signaling involves the presence of IFN $\gamma$ , IFN $\gamma$  receptor, activated JAKs, activated STATs, and transferases at the promoters of genes activated by IFNs. It is predicted that similar players are present at the relevant enhancer of genes activated by IFNs, a prediction that can readily be tested. Adherents of the canonical model of IFN signaling do not conceptually accept retrograde trafficking of plasma membrane receptors to the nucleus, although this has been widely shown in JAK/STAT signaling as well as in receptor tyrosine kinase signaling (see text).

### 3. The Foundations of the Steroid-Like Noncanonical IFN Signaling Model

Structural studies of protein/peptide ligands binding to the membrane receptor extracellular domain are generally looked upon as key to gaining mechanistic insight to signaling that occurs at the cytoplasmic domain of the receptor. In the case of IFN $\gamma$ , details of IFN $\gamma$  interaction with the IFNGR1 receptor subunit were obtained using X-ray crystallography [30]. IFNGR1 plays the key role in IFN $\gamma$  binding to receptors in intact cells. The structural studies focused on interaction between IFN $\gamma$  and IFNGR1 extracellular domain via well-defined secondary structures. The C-terminus of IFN $\gamma$ , which contains a polycationic tail, did not form a clearly defined secondary structure and did not show interaction with the IFNGR1 extracellular domain. Interestingly, the C-terminus polycationic tail functions as a classic nuclear localization sequence (NLS) [31]. To date, this fact has not received much attention by the adherents of the canonical signaling pathway of IFNs even though the NLS is required for IFN $\gamma$  function [32].

In our early studies of binding sites on IFN $\gamma$  for the IFN $\gamma$  receptor in intact cells, IFN $\gamma$  N-terminus peptide IFN $\gamma$  (1-39), but not the NLS-containing C-terminus peptide IFN $\gamma$  (95-132), inhibited IFN $\gamma$  binding to the receptor on cells [33]. This was unexpected as antibodies to both the N-terminus and C-terminus peptides had similar neutralizing effects on IFN $\gamma$ . We next used a full-length IFNGR1 soluble receptor and carried out bindings with IFN $\gamma$  and with overlapping peptides, including IFN $\gamma$  (1-39) and IFN $\gamma$  (95-132). We also used overlapping IFNGR1 extracellular and cytoplasmic domain peptides. We discovered that the N-terminus peptide of IFN $\gamma$  bound to the IFNGR1 extracellular domain and that the C-terminus peptide bound to the IFNGR1 cytoplasmic domain [33]. Specifically, murine IFN $\gamma$  (95-132), as well as the human counterpart peptide, bound to the IFNGR1 cytoplasmic domain region (253-287), adjacent to the binding site of activated JAK2. The binding was specifically blocked by anti-(253-287)-specific antibodies in fixed, permeabilized cells. Related to this, the binding of Sepharose-coupled JAK2 to labeled soluble IFNGR1 was enhanced by IFN $\gamma$  and IFN $\gamma$  (95-132), but

not by the N-terminus IFN $\gamma$  (1-39) peptide. Binding was specifically blocked by IFNGR1-binding site peptide IFNGR1(253-287). Such enhanced binding could explain the movement of JAK2 from receptor subunit IFNGR2 to the receptor subunit IFNGR1.

The challenge was to show functional and physical evidence of intracellular IFN $\gamma$  and IFN $\gamma$  (95-132) in treated cells. The first step was to show that internalized IFN $\gamma$  (95-132) possessed IFN activity. Thus, macrophages with active pinocytosis internalized IFN $\gamma$  (95-132) and induced antiviral activity as well as upregulation of MHC class II antigens [34]. Attachment of a palmitate residue to IFN $\gamma$  (95-132), Pal-IFN $\gamma$  (95-132), for internalization by fibroblasts, similarly resulted in the induction of antiviral activity and upregulation of MHC class II antigens [35]. Knockout of the IFNGR1 gene in fibroblasts resulted in loss of IFN $\gamma$  peptide Pal-IFN $\gamma$  (95-132) function which is evidence that the C-terminus peptide functions through IFNGR1.

There has long been evidence that internalized IFN $\gamma$  also possesses biological activity across species. For example, the following have been reported: (1) liposome-encapsulated human IFN $\gamma$  induced an antitumor effect in murine macrophages [36], (2) intracellular human IFN $\gamma$  induced an antitumor effect in murine fibroblast cells [37], and (3) human IFN $\gamma$  microinjected into murine macrophages induced MHC class II antigen expression in murine macrophages [38]. These intracellular effects of human IFN $\gamma$  are odd for two reasons. First, protein ligands like IFN $\gamma$  are supposed to function by binding to extracellular receptor domains [1, 2]. Second, human IFN $\gamma$  does not have a biological effect on murine cells when simply added to these cells in cultures, because the murine IFN $\gamma$  receptor extracellular domain does not recognize human IFN $\gamma$  [39]. These cross-species intracellular effects of human IFN $\gamma$  have had to sit in limbo, waiting for a mechanism of IFN signaling that did not exist at the time of these discoveries.

Considerable insight has been gleaned concerning trafficking of the IFN $\gamma$  ligand and IFNGR1 receptor subunit from the plasma membrane to the nucleus. Specifically, we showed that endocytosed IFN $\gamma$  associates with the cytoplasmic domain of the receptor IFNGR1 subunit in the following manner [32]. Unlabeled IFN $\gamma$  but not IFNGR1(253-287) intracellular binding site peptide blocked binding of  $^{125}$ I-IFN $\gamma$  to the IFNGR1 extracellular domain. Internalized IFNGR1(253-287), however, blocked intracellular cytoplasmic binding of  $^{125}$ I-IFN $\gamma$  to IFNGR1 subsequent to extracellular binding. In the determination of internalization dynamics of IFN $\gamma$  receptors, we showed that the presence of IFNGR1 and IFNGR2 in the lipid microdomain on the surface of the cell was central to the endocytic events that are linked to the IFN $\gamma$  noncanonical signaling pathway [40]. In human epithelial WISH cells, the receptor subunits IFNGR1 and IFNGR2 are constitutively present in lipid microdomains, while in Jurkat cells, the receptor subunits migrate to the lipid microdomain. While IFNGR1 undergoes nuclear translocation in cells treated with IFN $\gamma$ , receptor subunit IFNGR2 remains in the plasma membrane [40, 41]. This raises questions about how the receptor subunits are cross-linked by IFN $\gamma$  or if cross-linking in fact occurs in a IFN-

GR1/IFNGR2 manner [42, 43]. The cytoplasmic domain of IFNGR1 with IFN $\gamma$  attached is exposed to the cytoplasm in endocytic vesicles, since the microinjection of antibodies to IFN $\gamma$  C-terminus in cells blocked IFNGR1 nuclear translocation as well as STAT1 $\alpha$  activation [44]. The antibodies had no effect on IFN $\alpha$  activation of STAT1 $\alpha$ .

The question arises as to whether there are existing mechanisms to explain the dissociation of IFN $\gamma$  from the IFNGR1 extracellular domain in the lumen of the endosome and subsequent association with the IFNGR1 cytoplasmic domain in the cytosol of the cell. The mechanism of these events are illustrated in Figure 2. As indicated, we showed that it is the endocytosis of IFN $\gamma$  receptors present in lipid microdomains that are key to our noncanonical model of signal transduction [40]. Lipid microdomains and caveolae are rich in proton pumps known as vacuolar H $^{+}$ -ATPases or V-ATPases (reviewed in [45-47]). These pumps are central to pH control in organelles such as endosomes and are, in fact, a key to signal transduction associated with endocytosis. V-ATPases are structurally and functionally related to F-ATPases which are well known in synthesis of ATP against a proton gradient in mitochondria. Unlike F-ATPases, V-ATPases do not synthesize ATP under physiological conditions but rather are ATP-driven proton pumps [45]. Thus, V-ATPases associated with the endosome lower the pH in the lumen to about 4.5 [48]. This results in dissociation of complexes such as IFN $\gamma$ /IFNGR1 [48, 49]. The cationic NLS tail of IFN $\gamma$  becomes protonated in the low pH which facilitates crossing of the endosome membrane into the cytosol. In the cytosol, the pH is 7 and above [48], and the IFN $\gamma$  then binds to the IFNGR1 cytoplasmic domain at residues 253-287 [33]. The experimental support for these events is as follows. The cationic NLS is very similar for IFN $\gamma$  and the prototypical NLS of SV40 large T antigen [49]. We showed that an IFN $\gamma$  mutant that lacked the cationic NLS was inactive and that the SV40 NLS restored complete antiviral activity [49]. In studies where SV40 NLS was coupled to an siRNA for nuclear transport of the RNA, it was shown that V-ATPase acidification of lipid membrane-derived endosomes resulted in SV40 NLS penetration of the endosome membrane and movement from the lumen side to the cytosol [50, 51]. Thus, the data of reference [32] and Figure 2 are consistent with well-known endocytic events involving V-ATPase and acidification of endocytic endosomes.

Receptor tyrosine kinases (RTKs), such as epidermal growth factor receptor (EGFR), have also been shown by different laboratories to undergo energy-dependent nuclear translocation [52, 53]. In fact, EGFR was the first RTK as well as the first plasma membrane receptor to be shown to function as a cotranscription factor [54]. The mechanism of retrograde trafficking of EGFR from the cell surface into the nucleus has been extensively elucidated [55, 56]. Endocytosis is triggered by binding of EGF to EGFR, with fusion of the endocytic vesicles with early endosomes, which then traffic to Golgi. Trafficking was blocked by treatment with either brefeldin A or by use of cells with dominant negative mutation of the small GTPase ARF (ADP-ribosylation factor). Both treatments resulted in coat protein complex I (COPI) disassembly, which is consistent with COPI regulation of

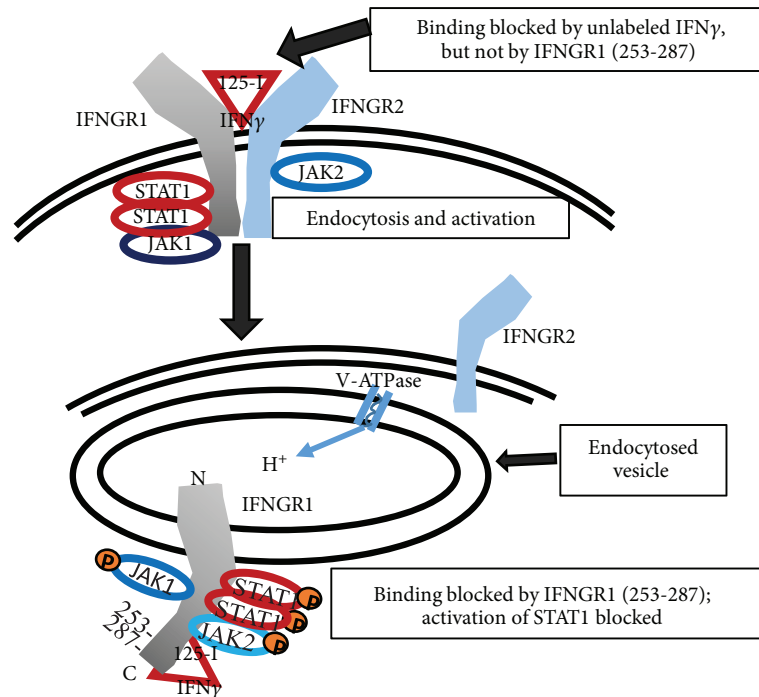


FIGURE 2: Schematic of IFN $\gamma$  binding to the receptor subunit IFNGR1 extracellular domain with endocytosis of the complex and subsequent movement of IFN $\gamma$  to the cytoplasmic domain of IFNGR1 at a site encompassing residues 253 to 287. Endosome-associated V-ATPase proton pump lowers the lumen pH for IFN $\gamma$  movement to the cytosol. Accordingly, extracellular binding of  $^{125}\text{I}$ -IFN $\gamma$  is blocked by unlabeled IFN $\gamma$  but not peptide IFNGR1(253-287). Cytoplasmic binding of  $^{125}\text{I}$ -IFN $\gamma$  is blocked by IFNGR1(253-287). Details of the experiment illustrated in this schematic are contained in the text [32]. Similar movement for ligands of RTKs from the receptor extracellular domain to the cytoplasm of the cell has been shown [15].

retrograde vesicular trafficking of EGFR from the Golgi to the endoplasmic reticulum [55]. EGFR movement from the ER into the nucleus was shown to require the Sec 61 translocon [56]. Epigenetic changes such as tyrosine phosphorylation of histone H4 at residue H4Y72, which is associated with enhanced methylation at H4K20, accompanied nuclear translocation of EGFR [57]. Nuclear translocation and epigenetic effects have also been reported for other RTKs [58, 59].

#### 4. Noncanonical IFN $\gamma$ Signaling at the Promoter

The data presented here show a remarkable similarity between IFN $\gamma$  noncanonical signaling and that of NRs and their ligands. The combination of immunoprecipitation with Western blotting, ChIP assay followed by PCR, nuclear confocal immunofluorescence, and other focused techniques showed that IFN $\gamma$ , STAT $\alpha$ , JAK1, and JAK2 were all present at the GAS element of genes activated by IFN $\gamma$  [13, 15, 44, 60]. Initial focus was on the role of IFN $\gamma$  NLS in translocation of IFNGR1 into the nucleus. Thus, treatment of cells with IFN $\gamma$  or with the internalizable C-terminus peptide Pal-IFN $\gamma$  (95-132) resulted in IFNGR1 translocation to the nucleus with the NLS of IFN $\gamma$  playing a key role for importin  $\alpha/\beta$  and nuclear pore complex recognition [60]. ChIP assay has been particularly useful in showing that activated STAT1 $\alpha$ , pSTAT1 $\alpha$ , and activated JAKs, pJAK1 and pJAK2, form a complex with IFN $\gamma$  and IFNGR1 at or in the vicinity of promoters of genes that are activated by IFN $\gamma$  [13, 60].

There is evidence that IFNGR1 plays a role in gene activation by IFN $\gamma$ . GAS-luciferase reporter gene transfection, along with IFNGR1 and nonsecreted IFN $\gamma$ , resulted in enhanced reporter activity. Further, fusion of IFNGR1 to yeast GAL-4 DNA-binding domain resulted in enhanced transcription from the GAL4 response element, consistent with a transactivation domain in IFNGR1 [60]. These results suggest a transcriptional/cotranscriptional role for IFN $\gamma$ /IFNGR1 in specific gene activation by IFN $\gamma$ . In NR signaling, the factors at the promoter seem also to be present at the enhancer and we feel that IFN $\gamma$ , IFNGR1, and pJAK2 should be included in specific gene studies as well as in genome-wide studies.

Within the IFN family, noncanonical signaling is not limited to IFN $\gamma$ , but was also found in the type I IFN system [61]. Cells treated with IFN $\alpha$  under the same protocol conditions as for IFN $\gamma$  showed IFN $\alpha$ 2, receptor subunits IFNAR1 and IFNAR2, and the type I IFN tyrosine kinase TYK2, all at the response element ISRE of the oligoadenylate synthetase (OAS) promoter [61]. An unrelated gene promoter for  $\beta$ -actin did not show these IFN players in the same cells treated with IFN $\alpha$ 2. Similarities between noncanonical IFN signaling and steroid signaling are presented in Figures 1(a) and 1(b).

As indicated, it has been shown that both wild-type and gain-of-function mutated JAK2 perform key epigenetic functions in the nucleus [12]. Mutated JAK2, JAK2V617F, plays a key epigenetic role in leukemias involving the erythropoietin (EpoR), thrombopoietin, and granulocyte colony stimulator receptors [62]. The key epigenetic effect of JAK2V617F was

to phosphorylate H3 at tyrosine (Y) 41, H3Y41 to H3pY41, which results in dissociation of the inhibitor protein HP1 $\alpha$  from H3. This, in conjunction with other epigenetic effects (see below) on H3, plays a key role in euchromatin activity related to gene expression in the associated cancers [12]. It has been shown that in the case of Epo, the EpoR is required for the activation of JAK2V617F [62]. The question arises as to how EpoR activated JAK2V617F then goes on to play a key role in leukemias that possess an EpoR phenotype. Thus, it would be interesting to determine if EpoR-coupled JAK2V617F is the activator of Epo genes rather than just JAK2V617F alone. There is a *Drosophila* HP1 and mutant JAK counterpart of JAK2V617F [63].

Essentially lost in the JAK2V617F discovery is the fact that wild-type JAK2, as indicated, also phosphorylated H3 at Y41 (H3pY41) with the same epigenetic result [12]. Activation of the wild-type JAK2 was dependent on treatment of cells with growth factors like platelet-derived growth factor (PDGF) and interleukin 3 (IL-3).

ChIP-seq has recently been used to study the genomic effects of nuclear JAK1 in an autocrine IL-6 and IL-10 activated B-cell lymphoma [64]. Specifically, it was shown that JAK1 regulated the expression of almost 3,000 genes in a B-cell lymphoma cell line (ABC DLBCL), with the interesting finding that many of these same genes showed phosphorylation of tyrosine 41 at histone H3, H3pY41, in the surrounding chromatin. A JAK1 inhibitor blocked the phosphorylation. Possible association of JAK1 and IL-6-related STAT3 at the genome level was not determined by ChIP-seq, but focus on the MYC gene did show H3pY41 and pSTAT at the MYC gene as determined by quantitative ChIP analysis. The question is as follows: are they physically linked, and if so, were there IL-6 receptor players present?

An important functional role of the induction of H3pY41 by the kinase activity of JAK2 and TYK of the IFNs, as discussed here, would be evidence of related nucleosome unwrapping, so that the IFN/receptor complexes have access to the DNA. In this regard, it has been shown that JAK2 induction of H3pY41 increased nucleosome unwrapping for access to transcription factor binding by several folds [26]. Lysine 56 (H3K56) is located in the same DNA interface as H3Y41. Thus, acetylated H3K56 (H3K56ac) also caused nucleosome unwrapping by several folds. The combination of H3pY41 and H3K56ac had a multiplicative effect with 17-fold unwrapping of the nucleosome. The authors concluded that it was the combination of these two epigenetic events that resulted in optimal DNA exposure to transcription factors. The nucleosome unwrapping mechanisms described here probably apply to both promoters and enhancers and are revisited in that context in the next section.

Changes in H3K9 have also been shown to be associated with gene activation [13]. For example, we observed in type I IFN-treated cells that trimethylated H3K9, H3K9me3, underwent demethylation in association with acetylation of the same residue (H3k9ac) at the region of the OAS1 promoter [13]. Tyrosine phosphorylation of H3, H3pY41, was observed in the same experiment. All of these events show a remarkable similarity to that of NR signaling as presented above.

## 5. IFNs, Enhancers, and eRNAs

The players at the promoters and enhancers of NR signaling as presented in the previous section on signaling by E2/ER $\alpha$  and DHT/AR paint a picture that is visual and communicative. Promoters contain NR, SRCs, and secondary cofactors like p300/CBP HATs, kinases, and Pol II for transcription (reviewed in [25, 65, 66]). It is important to note that enhancers also contain many of these players, in particular NRs and their ligands, as well as a mediator complex [25, 28, 65, 66]. All of these factors play a key role in NR-specific enhancer transcription of eRNA, which in turn plays a role in enhancer/promoter interaction for NR-specific transcription of mRNA by Pol II.

Genome-wide NGS with the primary focus on STATs and superenhancer (SE) markers, such as p300 HAT and H3K4me1, showed different patterns for T helper1 (Th1) versus Th2 cells [3, 67]. There are also lineage-determining transcription factors present at SEs adjacent to promoters of genes whose products define the different T cell phenotypes, for example, T-BET/STAT1/STAT4 at relevant SEs in Th1 cells, GATA3/STAT6 at the key SEs for Th2 cells, and ROR- $\gamma$ t/STAT3 at Th17 cell SEs [67]. The potential role of eRNAs in the determination of phenotypes was not addressed. The precise role of the lineage-determining T cell phenotype transcription factors in T cell differentiation is not clear and may be to function as negative regulators of phenotypes that differ from the signature phenotypes that they are associated with [67].

It appears that the cytokines may play a major role as inducers and possibly direct participants of signal-dependent transcription at the enhancers that participate in phenotype-specific gene activation. With regard to STATs and Th1 and Th2 cells and the respective roles of STAT4 (Th1) and STAT6 (Th2), recruitment of p300 and other enhancer signals have been attributed to these STATs based on the absence of p300 at enhancers where STATs are deficient [68]. Master regulators such as T-bet do not restore enhancer activity that is lost as a result of the STAT deficiency. As we indicated earlier, there is a problem in assigning specificity solely to STATs in cytokine signaling at the level of enhancers and promoters (reviewed in [3]). For example, IFN $\gamma$  treatment of cells results in a dramatic increase in STAT1 at putative enhancers of IL-6 and tumor necrosis factor [3]. Interaction of STATs with enhancers and other noncoding DNA sites is greater in terms of binding than with promoters as there is more of the noncoding DNA [3]. In some respects, rather than solving the problem of cytokine specificity regarding STATs at promoters, it is just been moved on to include enhancers.

All STATs bind to the GAS element, but how they recognize enhancer DNA is not clear. Cytokines that preferentially activate particular STATs may use another STAT or STATs if there is a deficiency of the preferred STAT. For example, STAT3 may substitute for STAT1 or STAT6 may substitute for STAT5 [3]. Different STATs may congregate at the same DNA elements and/or interact with other transcription factors and even compete with each other for the same DNA element [3]. Presumably, this also

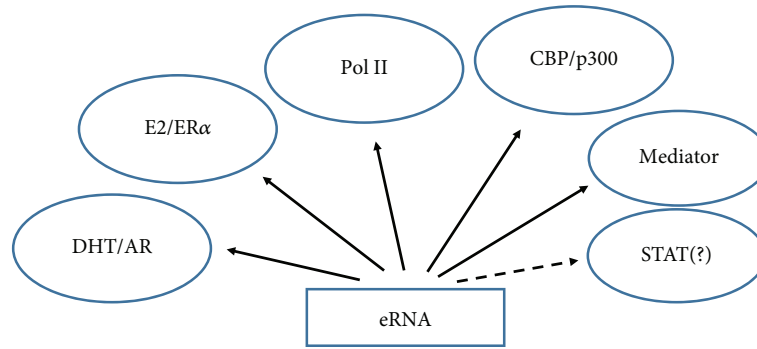


FIGURE 3: Binding of eRNA to various players in gene activation provides insight into its function. DHT/AR and E2/ER $\alpha$  binding places eRNA at the enhancer and promoter, as these nuclear receptor systems have been shown to be present at both sites. CBP/p300 histone acetyl transferase interaction with eRNA suggests epigenetic functions, while RNA polymerase II (Pol II) is involved in transcription at both the promoter and enhancer. STAT association with eRNA has not been definitively determined yet. Determination of complexes at the promoter and enhancer is key to understanding which factors directly bind to eRNA and which bind indirectly as members of transcriptional complexes. Nuclear receptor studies suggest that eRNA plays a role in looping of the enhancer and promoter via the interactions such as those shown here.

applies to enhancers. Additionally, cytokines may preferentially activate a particular STAT but also activate to a lesser extent the other STATs [3]. These and other complex STAT behaviors have recently been dubbed “the STAT specificity paradox” [3].

We are not aware that any of the extensive NGS studies with STATs has differentiated between activated (phosphorylated) or nonactivated (unphosphorylated) STATs at enhancers or at other regions of the genome. Activated STATs have been reported to be associated with euchromatin, while nonactivated STATs were associated with heterochromatin [63, 69]. Euchromatin indicates active DNA while heterochromatin indicates silent DNA. We thus feel that the discovery of cytokine and growth factor treatment of cells, where activated JAK2 underwent nuclear translocation, has profound importance for epigenetic activity of the genome. We have addressed earlier the histone H3Y41 to H3pY41 phosphorylation, which results in dissociation of the epigenetic inhibitor protein HP1 $\alpha$  from histone H3, resulting in unwrapping of the nucleosome and exposure of the DNA, presumably at both the promoter and enhancer [12, 26]. We determined that in cells treated with IFN $\gamma$ , activated JAK2 (pJAK2) underwent nuclear translocation along with activated STAT1 $\alpha$  (pSTAT1 $\alpha$ ) [13, 70]. Similarly, when we treated cells with IFN $\alpha$ , activated TYK2 (pTYK2) underwent nuclear translocation [61]. In both cases, activated STAT1 also underwent nuclear translocation to the same promoters in a complex that contained the activated JAKs. The presence of pJAKs and pSTAT1 at the same enhancers was not determined but is likely very important for enhancer function. The fact that a particular cytokine/receptor interaction results in nuclear import of pJAKs and pSTATs intuitively tells us that there is probably cross talk between the two at enhancers and promoters of genes that are activated by the particular cytokine. The data in Section 4 is based on our finding that IFN $\gamma$  and receptor subunit IFNGR1 are part of these nuclear events involving pJAK2 and pSTAT1 $\alpha$ , analogous to NR signaling, which could help resolve “the STAT specificity paradox” [3].

One does not need to fully subscribe to our NR-related noncanonical model of IFN signaling in order to have interest in associations of STATs at promoters and enhancers. We do not yet know if STATs bind to eRNAs, but there is a report of a lncRNA that is involved in conventional dendritic cell (cDC) differentiation which associates with and plays a role in STAT3 phosphorylation in the cytoplasm [71]. Nuclear colocalization of the two was not observed, which suggested that the lncRNA function was restricted to the cytoplasm. A series of experiments showed that the lncRNA protected pSTAT3 from the protein tyrosine phosphatase SHP1. Knockdown of lncRNA promoted the association of SHP1 with pSTAT3. An lncRNA associated with influenza virus infection called negative regulator of antiviral response (NRAV) was downregulated in virus-infected cells, which was associated with the suppression of IFN-stimulated gene transcription [72]. In terms of players at enhancers and promoters, STATs have been shown to associate with the HAT p300. A HAT CBP/p300 has recently been shown to associate with eRNA in RNA-dependent acetylation such as H3K27ac [27]. All of this suggests that STATs, presumably at enhancers, bind to CBP/p300, which in turn has been shown to bind to eRNA. How, then, are STATs associated with eRNAs?

It should be noted that CBP/p300 is highly prone to interactions with intrinsically disordered proteins (IDPs) as well as with proteins with intrinsically disordered regions (IDRs) [73]. IDPs and IDRs are particularly abundant in eukaryotic transcription factors. STATs and NF-kappaB as well as CBP/p300 are all IDPs and/or IDR proteins [73]. IFN $\gamma$  has a C-terminus that qualifies as an IDR [30]. It has been proposed that IDPs have functional advantages in the mediation of transcriptional events involving small recognition motifs with flexibility for multiple target interactions, thus giving rise to efficient use of small binding regions, as well as possessing the ability for high specificity with modest affinity for ease of reversible interactions [73]. The proteins in our noncanonical IFN signaling model from the ligand and receptor to genetic and epigenetic proteins at promoters

and enhancers all qualify as IDPs or IDR proteins. It seems that those fuzzy nonstructured regions of many impressive structural studies may contain more than what meets the eye.

Figure 3 summarizes some of the proteins that bind to eRNA as presented in the text. There is evidence that in the case of nuclear receptor systems, such as E2/ER $\alpha$  and DHT/AR, eRNA binds to these receptors as well as to complexes of the mediator, CBP/p300, various other transcription factors, and other players at the enhancer and promoter [21, 22, 25, 27]. These interactions are thought to facilitate the looping that brings the distal enhancer and promoter into close proximity for specific gene transcription.

## 6. Conclusion

The heart and soul of studies of ligand/receptor signaling is elucidation of the mechanism of specific gene activation. For the case of NRs, the foundations are in place with the NR and ligand at promoters and enhancers of genes specifically activated by the ligand. For example, E2 and ER $\alpha$  orchestrate the transcription of eRNA at the enhancers. The eRNA appears to be involved in mRNA transcription at the promoter, which also contains E2 and ER $\alpha$ . Other factors comprise the supporting cast. In canonical JAK/STAT signaling, STAT is the counterpart of the NR and we think that herein is the problem with the interpretation of NGS studies with STATs across the genome that has resulted in “the STAT specificity paradox.” For IFN $\gamma$  signaling, the inclusion of IFN $\gamma$ , IFNGR1, and activated JAKs in NGS studies in the context of the noncanonical model could potentially help resolve the paradox.

## Conflicts of Interest

The authors declare that there is no conflict of interest regarding the publication of this paper.

## References

- [1] A. H. Brivanlou and Darnell JE Jr, “Signal transduction and the control of gene expression,” *Science*, vol. 295, no. 5556, pp. 813–818, 2002.
- [2] L. C. Platanius, “Mechanisms of type-I- and type-II-interferon-mediated signalling,” *Nature Reviews Immunology*, vol. 5, no. 5, pp. 375–386, 2005.
- [3] A. V. Villarino, Y. Kanno, and J. J. O’Shea, “Mechanisms and consequences of Jak-STAT signaling in the immune system,” *Nature Immunology*, vol. 18, no. 4, pp. 374–384, 2017.
- [4] P. S. Subramaniam, S. A. Khan, C. H. Pontzer, and H. M. Johnson, “Differential recognition of the type I interferon receptor by interferons tau and alpha is responsible for their disparate cytotoxicities,” *Proceedings of the National Academy of Sciences of the United States of America*, vol. 92, no. 26, pp. 12270–12274, 1995.
- [5] P. Sheppard, W. Kinsvogel, W. Xu et al., “IL-28, IL-29 and their class II cytokine receptor IL-28R,” *Nature Immunology*, vol. 4, no. 1, pp. 63–68, 2003.
- [6] S. V. Kotenko, G. Gallagher, V. V. Baurin et al., “IFN-lambdas mediate antiviral protection through a distinct class II cytokine receptor complex,” *Nature Immunology*, vol. 4, no. 1, pp. 69–77, 2003.
- [7] S. V. Kotenko and J. E. Durbin, “Contribution of type III interferons to antiviral immunity: location, location, location,” *Journal of Biological Chemistry*, vol. 292, no. 18, pp. 7295–7303, 2017.
- [8] K. Blazek, H. L. Eames, M. Weiss et al., “IFN- $\lambda$  resolves inflammation via suppression of neutrophil infiltration and IL-1 $\beta$  production,” *Journal of Experimental Medicine*, vol. 212, no. 6, pp. 845–853, 2015.
- [9] A. Broggi, Y. Tan, F. Granucci, and I. Zanoni, “IFN- $\lambda$  suppresses intestinal inflammation by non-translational regulation of neutrophil function,” *Nature Immunology*, vol. 18, no. 10, pp. 1084–1093, 2017.
- [10] E. A. Hemann, J. Schwerk, and R. Savan, “IFN- $\lambda$  ‘guts’ neutrophil-mediated inflammation,” *Nature Immunology*, vol. 18, no. 10, pp. 1061–1062, 2017.
- [11] P. S. Subramaniam, B. A. Torres, and H. M. Johnson, “So many ligands, so few transcription factors: a new paradigm for signaling through the STAT transcription factors,” *Cytokine*, vol. 15, no. 4, pp. 175–187, 2001.
- [12] M. A. Dawson, A. J. Bannister, B. Göttgens et al., “JAK2 phosphorylates histone H3Y41 and excludes HP1 $\alpha$  from chromatin,” *Nature*, vol. 461, no. 7265, pp. 819–822, 2009.
- [13] E. N. Noon-Song, C. M. Ahmed, R. Dabelic, J. Canton, and H. M. Johnson, “Controlling nuclear JAKs and STATs for specific gene activation by IFN $\gamma$ ,” *Biochemical and Biophysical Research Communications*, vol. 410, no. 3, pp. 648–653, 2011.
- [14] H. M. Johnson, P. S. Subramaniam, S. Olsnes, and D. A. Jans, “Trafficking and signaling pathways of nuclear localizing protein ligands and their receptors,” *BioEssays*, vol. 26, no. 9, pp. 993–1004, 2004.
- [15] H. M. Johnson, E. N. Noon-Song, K. Kemppainen, and C. M. Ahmed, “Steroid-like signalling by interferons: making sense of specific gene activation by cytokines,” *Biochemical Journal*, vol. 443, no. 2, pp. 329–338, 2012.
- [16] A. B. Johnson and B. W. O’Malley, “Steroid receptor coactivators 1, 2, and 3: critical regulators of nuclear receptor activity and steroid receptor modulator (SRM)-based cancer therapy,” *Molecular and Cellular Endocrinology*, vol. 348, no. 2, pp. 430–439, 2012.
- [17] L. S. Trevino and N. L. Weigel, “Phosphorylation: a fundamental regulator of steroid receptor action,” *Trends in Endocrinology and Metabolism*, vol. 24, no. 10, pp. 515–524, 2013.
- [18] F. De Santa, I. Barozzi, F. Mietton et al., “A large fraction of extragenic RNA pol II transcription sites overlap enhancers,” *PLoS Biology*, vol. 8, no. 5, article e1000384, 2010.
- [19] T. K. Kim, M. Hemberg, J. M. Gray et al., “Widespread transcription at neuronal activity-regulated enhancers,” *Nature*, vol. 465, no. 7295, pp. 182–187, 2010.
- [20] D. Wang, I. Garcia-Bassets, C. Benner et al., “Reprogramming transcription by distinct classes of enhancers functionally defined by eRNA,” *Nature*, vol. 474, no. 7351, pp. 390–394, 2011.
- [21] C.-L. Hsieh, T. Fei, Y. Chen et al., “Enhancer RNAs participate in androgen receptor-driven looping that selectively enhances gene activation,” *Proceedings of the National Academy of Sciences of the United States of America*, vol. 111, no. 20, pp. 7319–7324, 2014.

- [22] W. Li, D. Notani, Q. Ma et al., "Functional roles of enhancer RNAs for oestrogen-dependent transcriptional activation," *Nature*, vol. 498, no. 7455, pp. 516–520, 2013.
- [23] J. S. Carroll and M. Brown, "Estrogen receptor target gene: an evolving concept," *Molecular Endocrinology*, vol. 20, no. 8, pp. 1707–1714, 2006.
- [24] N. Hah and W. L. Kraus, "Hormone-regulated transcriptomes: lessons learned from estrogen signaling pathways in breast cancer cells," *Molecular and Cellular Endocrinology*, vol. 382, no. 1, pp. 652–664, 2014.
- [25] W. Li, D. Notani, and M. G. Rosenfeld, "Enhancers as non-coding RNA transcription units: recent insights and future perspectives," *Nature Reviews Genetics*, vol. 17, no. 4, pp. 207–223, 2016.
- [26] M. Brehove, T. Wang, J. North et al., "Histone core phosphorylation regulates DNA accessibility," *Journal of Biological Chemistry*, vol. 290, no. 37, pp. 22612–22621, 2015.
- [27] D. A. Bose, G. Donahue, D. Reinberg, R. Shiekhhattar, R. Bonasio, and S. L. Berger, "RNA binding to CBP stimulates histone acetylation and transcription," *Cell*, vol. 168, no. 1–2, pp. 135–149.e22, 2017, e122.
- [28] B. L. Allen and D. J. Taatjes, "The mediator complex: a central integrator of transcription," *Nature Reviews Molecular Cell Biology*, vol. 16, no. 3, pp. 155–166, 2015.
- [29] J. Puc, P. Kozbial, W. Li et al., "Ligand-dependent enhancer activation regulated by topoisomerase-I activity," *Cell*, vol. 160, no. 3, pp. 367–380, 2015.
- [30] M. R. Walter, W. T. Windsor, T. L. Nagabhushan et al., "Crystal structure of a complex between interferon- $\gamma$  and its soluble high-affinity receptor," *Nature*, vol. 376, no. 6537, pp. 230–235, 1995.
- [31] P. S. Subramaniam, M. G. Mujtaba, M. R. Paddy, and H. M. Johnson, "The carboxyl terminus of interferon- $\gamma$  contains a functional polybasic nuclear localization sequence," *Journal of Biological Chemistry*, vol. 274, no. 1, pp. 403–407, 1999.
- [32] C. M. I. Ahmed, M. A. Burkhart, M. G. Mujtaba, P. S. Subramaniam, and H. M. Johnson, "The role of IFN $\gamma$  nuclear localization sequence in intracellular function," *Journal of Cell Science*, vol. 116, no. 15, pp. 3089–3098, 2003.
- [33] B. E. Szente, P. S. Subramaniam, and H. M. Johnson, "Identification of IFN-gamma receptor binding sites for JAK2 and enhancement of binding by IFN-gamma and its C-terminal peptide IFN-gamma(95-133)," *The Journal of Immunology*, vol. 155, no. 12, pp. 5617–5622, 1995.
- [34] B. E. Szente, J. M. Soos, and H. M. Johnson, "The C-terminus of IFN- $\gamma$  is sufficient for intracellular function," *Biochemical and Biophysical Research Communications*, vol. 203, no. 3, pp. 1645–1654, 1994.
- [35] K. Thiam, E. Loing, A. Delanoye et al., "Unrestricted agonist activity on murine and human cells of a lipopeptide derived from IFN- $\gamma$ ," *Biochemical and Biophysical Research Communications*, vol. 253, no. 3, pp. 639–647, 1998.
- [36] I. J. Fidler, W. E. Fogler, E. S. Kleinerman, and I. Saiki, "Abrogation of species specificity for activation of tumoricidal properties in macrophages by recombinant mouse or human interferon-gamma encapsulated in liposomes," *The Journal of Immunology*, vol. 135, no. 6, pp. 4289–4296, 1985.
- [37] J. Sancéau, P. Sondermeyer, F. Béranger, R. Falcoff, and C. Vaquero, "Intracellular human gamma-interferon triggers an antiviral state in transformed murine L cells," *Proceedings of the National Academy of Sciences of the United States of America*, vol. 84, no. 9, pp. 2906–2910, 1987.
- [38] M. R. Smith, K. Muegge, J. R. Keller, H. F. Kung, H. A. Young, and S. K. Durum, "Direct evidence for an intracellular role for IFN-gamma. Microinjection of human IFN-gamma induces Ia expression on murine macrophages," *The Journal of Immunology*, vol. 144, no. 5, pp. 1777–1782, 1990.
- [39] V. C. Gibbs, S. R. Williams, P. W. Gray et al., "The extracellular domain of the human interferon gamma receptor interacts with a species-specific signal transducer," *Molecular and Cellular Biology*, vol. 11, no. 12, pp. 5860–5866, 1991.
- [40] P. S. Subramaniam and H. M. Johnson, "Lipid microdomains are required sites for the selective endocytosis and nuclear translocation of IFN- $\gamma$ , its receptor chain IFN- $\gamma$  receptor-1, and the phosphorylation and nuclear translocation of STAT1 $\alpha$ ," *The Journal of Immunology*, vol. 169, no. 4, pp. 1959–1969, 2002.
- [41] J. Larkin III, H. M. Johnson, and P. S. Subramaniam, "Differential nuclear localization of the IFNGR-1 and IFNGR-2 subunits of the IFN- $\gamma$  receptor complex following activation by IFN- $\gamma$ ," *Journal of Interferon & Cytokine Research*, vol. 20, no. 6, pp. 565–576, 2000.
- [42] C. D. Krause, C. A. Lunn, L. S. Izotova et al., "Signaling by covalent heterodimers of interferon- $\gamma$ . Evidence for one-sided signaling in the active tetrameric receptor complex," *Journal of Biological Chemistry*, vol. 275, no. 30, pp. 22995–23004, 2000.
- [43] A. Landar, B. Curry, M. H. Parker et al., "Design, characterization, and structure of a biologically active single-chain mutant of human IFN- $\gamma$ ," *Journal of Molecular Biology*, vol. 299, no. 1, pp. 169–179, 2000.
- [44] P. S. Subramaniam, J. Larkin, M. G. Mujtaba, M. R. Walter, and H. M. Johnson, "The COOH-terminal nuclear localization sequence of interferon gamma regulates STAT1 alpha nuclear translocation at an intracellular site," *Journal of Cell Science*, vol. 113, pp. 2771–2781, 2000.
- [45] M. Forgac, "Vacuolar ATPases: rotary proton pumps in physiology and pathophysiology," *Nature Reviews Molecular Cell Biology*, vol. 8, no. 11, pp. 917–929, 2007.
- [46] S. Breton and D. Brown, "Regulation of luminal acidification by the V-ATPase," *Physiology*, vol. 28, no. 5, pp. 318–329, 2013.
- [47] G. H. Sun-Wada and Y. Wada, "Role of vacuolar-type proton ATPase in signal transduction," *Biochimica et Biophysica Acta (BBA) - Bioenergetics*, vol. 1847, no. 10, pp. 1166–1172, 2015.
- [48] M. E. Maxson and S. Grinstein, "The vacuolar-type H<sup>+</sup>-ATPase at a glance - more than a proton pump," *Journal of Cell Science*, vol. 127, no. 23, pp. 4987–4993, 2014.
- [49] P. S. Subramaniam, M. M. Green, J. Larkin III, B. A. Torres, and H. M. Johnson, "Nuclear translocation of IFN- $\gamma$  is an intrinsic requirement for its biologic activity and can be driven by a heterologous nuclear localization sequence," *Journal of Interferon & Cytokine Research*, vol. 21, no. 11, pp. 951–959, 2001.
- [50] J. K. W. Lam, W. Liang, Y. Lan et al., "Effective endogenous gene silencing mediated by pH responsive peptides proceeds via multiple pathways," *Journal of Controlled Release*, vol. 158, no. 2, pp. 293–303, 2012.
- [51] Y. Xu, W. Liang, Y. Qiu et al., "Incorporation of a nuclear localization signal in pH responsive LAH4-L1 peptide

- enhances transfection and nuclear uptake of plasmid DNA," *Molecular Pharmaceutics*, vol. 13, no. 9, pp. 3141–3152, 2016.
- [52] G. Carpenter, "Nuclear localization and possible functions of receptor tyrosine kinases," *Current Opinion in Cell Biology*, vol. 15, no. 2, pp. 143–148, 2003.
- [53] H. H. Lee, Y. N. Wang, and M. C. Hung, "Non-canonical signaling mode of the epidermal growth factor receptor family," *American Journal of Cancer Research*, vol. 5, no. 10, pp. 2944–2958, 2015.
- [54] S. Y. Lin, K. Makino, W. Xia et al., "Nuclear localization of EGF receptor and its potential new role as a transcription factor," *Nature Cell Biology*, vol. 3, no. 9, pp. 802–808, 2001.
- [55] Y. N. Wang, H. Wang, H. Yamaguchi, H. J. Lee, H. H. Lee, and M. C. Hung, "COPI-mediated retrograde trafficking from the Golgi to the ER regulates EGFR nuclear transport," *Biochemical and Biophysical Research Communications*, vol. 399, no. 4, pp. 498–504, 2010.
- [56] Y. N. Wang, H. Yamaguchi, L. Huo et al., "The translocon Sec61 $\beta$  localized in the inner nuclear membrane transports membrane-embedded EGF receptor to the nucleus," *Journal of Biological Chemistry*, vol. 285, no. 49, pp. 38720–38729, 2010.
- [57] R. H. Chou, Y. N. Wang, Y. H. Hsieh et al., "EGFR modulates DNA synthesis and repair through Tyr phosphorylation of histone H4," *Developmental Cell*, vol. 30, no. 2, pp. 224–237, 2014.
- [58] S. Olsnes, O. Klingenberg, and A. Wiedlocha, "Transport of exogenous growth factors and cytokines to the cytosol and to the nucleus," *Physiological Reviews*, vol. 83, no. 1, pp. 163–182, 2003.
- [59] D. M. Bryant and J. L. Stow, "Nuclear translocation of cell-surface receptors: lessons from fibroblast growth factor," *Traffic*, vol. 6, no. 10, pp. 947–953, 2005.
- [60] C. M. I. Ahmed and H. M. Johnson, "IFN- $\gamma$  and its receptor subunit IFNGR1 are recruited to the IFN- $\gamma$ -activated sequence element at the promoter site of IFN- $\gamma$ -activated genes: evidence of transactivational activity in IFNGR1," *The Journal of Immunology*, vol. 177, no. 1, pp. 315–321, 2006.
- [61] C. M. Ahmed, E. N. Noon-Song, K. Kemppainen, M. P. Pascalli, and H. M. Johnson, "Type I IFN receptor controls activated TYK2 in the nucleus: implications for EAE therapy," *Journal of Neuroimmunology*, vol. 254, no. 1-2, pp. 101–109, 2013.
- [62] X. Lu, R. Levine, W. Tong et al., "Expression of a homodimeric type I cytokine receptor is required for JAK2V617F-mediated transformation," *Proceedings of the National Academy of Sciences of the United States of America*, vol. 102, no. 52, pp. 18962–18967, 2005.
- [63] S. Shi, H. C. Calhoun, F. Xia, J. Li, L. Le, and W. X. Li, "JAK signaling globally counteracts heterochromatic gene silencing," *Nature Genetics*, vol. 38, no. 9, pp. 1071–1076, 2006.
- [64] L. Rui, A. C. Drennan, M. Ceribelli et al., "Epigenetic gene regulation by Janus kinase 1 in diffuse large B-cell lymphoma," *Proceedings of the National Academy of Sciences of the United States of America*, vol. 113, no. 46, pp. E7260–E7267, 2016.
- [65] C. E. Foulds, A. K. Panigrahi, C. Coarfa, R. B. Lanz, and B. W. O'Malley, "Long noncoding RNAs as targets and regulators of nuclear receptors," *Current Topics in Microbiology and Immunology*, vol. 394, pp. 143–176, 2016.
- [66] T. K. Kim and R. Shiekhhattar, "Architectural and functional commonalities between enhancers and promoters," *Cell*, vol. 162, no. 5, pp. 948–959, 2015.
- [67] J. J. Paiano, J. L. Johnson, and G. Vahedi, "Enhancing our understanding of enhancers in T-helper cells," *European Journal of Immunology*, vol. 45, no. 11, pp. 2998–3001, 2015.
- [68] G. Vahedi, H. Takahashi, S. Nakayama et al., "STATs shape the active enhancer landscape of T cell populations," *Cell*, vol. 151, no. 5, pp. 981–993, 2012.
- [69] L. Silver-Morse and W. X. Li, "JAK-STAT in heterochromatin and genome stability," *JAKSTAT*, vol. 2, no. 3, article e26090, 2013.
- [70] H. M. Johnson and C. M. Ahmed, "Noncanonical IFN signaling: mechanistic linkage of genetic and epigenetic events," *Mediators of Inflammation*, vol. 2016, Article ID 9564814, 9 pages, 2016.
- [71] P. Wang, Y. Xue, Y. Han et al., "The STAT3-binding long non-coding RNA lnc-DC controls human dendritic cell differentiation," *Science*, vol. 344, no. 6181, pp. 310–313, 2014.
- [72] J. Ouyang, X. Zhu, Y. Chen et al., "NRAV, a long noncoding RNA, modulates antiviral responses through suppression of interferon-stimulated gene transcription," *Cell Host & Microbe*, vol. 16, no. 5, pp. 616–626, 2014.
- [73] H. J. Dyson and P. E. Wright, "Role of intrinsic protein disorder in the function and interactions of the transcriptional coactivators CREB-binding protein (CBP) and p300," *Journal of Biological Chemistry*, vol. 291, no. 13, pp. 6714–6722, 2016.

## Research Article

# Rosiglitazone Improves Glucocorticoid Resistance in a Sudden Sensorineural Hearing Loss by Promoting MAP Kinase Phosphatase-1 Expression

Liang Xia,<sup>1</sup> Jingjing Liu,<sup>2</sup> Yuanyuan Sun,<sup>1</sup> Haibo Shi ,<sup>1</sup> Guang Yang ,<sup>1</sup> Yanmei Feng ,<sup>1</sup> and Shankai Yin <sup>1</sup>

<sup>1</sup>Department of Otolaryngology, Shanghai Jiao Tong University Affiliated Sixth People's Hospital, No. 600, Yishan Road, Xuhui District, 200233 Shanghai, China

<sup>2</sup>Department of Interventional Radiology, Shanghai Jiao Tong University Affiliated Sixth People's Hospital, No. 600, Yishan Road, Xuhui District, 200233 Shanghai, China

Correspondence should be addressed to Guang Yang; [gyang321@hotmail.com](mailto:gyang321@hotmail.com) and Yanmei Feng; [feng.yanmei@126.com](mailto:feng.yanmei@126.com)

Received 31 December 2018; Accepted 20 March 2019; Published 14 May 2019

Guest Editor: Minggang Zhang

Copyright © 2019 Liang Xia et al. This is an open access article distributed under the Creative Commons Attribution License, which permits unrestricted use, distribution, and reproduction in any medium, provided the original work is properly cited.

In this study, we investigated the role of MAP kinase phosphatase-1 (MKP-1) and rosiglitazone (RSG) in glucocorticoid resistance and glucocorticoid sensitivity, respectively, using a guinea pig model of lipopolysaccharide- (LPS-) induced sudden sensorineural hearing loss (SSHL). The pigs were divided into control, LPS, LPS+dexamethasone (DEX), LPS+RSG, and LPS+DEX+RSG groups. Their hearing was screened by auditory brainstem response measurement. Immunofluorescence staining was used to identify the location of MKP-1 in the inner ear. The expression levels of MKP-1 and the related proteins in the inner ear were detected using western blotting. The morphological changes in the cochlea were observed via hematoxylin-eosin staining. Severe hearing loss was observed in the LPS group, as opposed to the protection from hearing loss observed in the LPS+DEX+RSG group. A positive correlation was observed between MKP-1 expression levels and protection from hearing loss. RSG and DEX synergistically influenced inner ear inflammation. In conclusion, resistance of LPS-induced SSHL guinea pig models to glucocorticoids may result from impaired MKP-1 function in inner ear tissues, induced by glucocorticoids, impairing the inhibition of inflammation. Our findings present novel targets to develop potential therapeutics to treat inflammatory diseases of the inner ear.

## 1. Introduction

An increasing number of studies have reported that inflammation and oxidative stress may lead to sudden sensorineural hearing loss (SSHL) and affect prognosis [1–3]. Glucocorticoids are the main treatment option for SSHL. They play a major role in maintaining homeostasis, including immune function regulation. Dexamethasone (DEX), a synthetic glucocorticoid, has been widely used for the treatment of inner ear disorders such as SSHL, Ménière disease, and acute tinnitus. Although recent clinical studies have shown that glucocorticoid therapy is effective against inner ear diseases, a considerable number of patients are insensitive and thus resistant to glucocorticoids. Thus, there is an urgent need for effective drugs

that prevent disease progression. Proinflammatory cytokines and other mediators are presumed to contribute to the development of glucocorticoid insensitivity or resistance. For instance, reduced expression of glucocorticoid receptor (GR) and histone deacetylase-2 (HDAC2) leads to glucocorticoid insensitivity or resistance [4, 5]. A recent study suggested that the activity of mitogen-activated protein kinase (MAPK) phosphatase 1 (MKP-1: NCBI official full name, dual-specificity phosphatase 1 (DUSP1)) is related to corticosteroid insensitivity or resistance [6].

MKPs belong to the family of DUSPs, which play a role in dephosphorylating their substrates [7–9]. The MAPK family comprises of three stress-activated protein kinase pathways: p38, c-Jun N-terminal kinase (JNK), and extracellular regulating kinase (ERK) [10]. The ERK pathway is mainly

activated by mitogenic and proliferative stimuli, while the p38 MAPK and JNK pathways respond to environmental stresses [11]. MKP-1 is a protein that exerts anti-inflammatory function by efficaciously dephosphorylating the JNK and p38 MAPK pathways and deactivating the nuclear factor- $\kappa$ B (NF- $\kappa$ B) pathway in immune cells [12–14]. In addition, MKP-1 plays a critical role in controlling the extent and duration of proinflammatory MAPK signaling *in vivo*. However, alveolar macrophages from patients with severe asthma (glucocorticoid-resistant) showed reduced induction of MKP-1 expression, due to the activation of p38 MAPK [15]. In patients with chronic obstructive pulmonary disease and patients who smoke, MKP-1 may be inactive owing to its oxidation, which may contribute to glucocorticoid resistance [6]. However, the role of MKP-1 in the cochlea has not been reported.

Rosiglitazone (RSG), a peroxisome proliferator-activated receptor gamma (PPAR- $\gamma$ ) agonist, was reported to induce MKP-1 expression [16]. Another study showed that RSG can potentially be used as a therapeutic agent for acute inflammatory conditions and acute liver injury [17].

In this, as in other studies, a guinea pig model of SSHL was induced by intracochlear injection of lipopolysaccharides (LPS) [5, 18, 19]. Using this model, we demonstrate for the first time how MKP-1 protects inner ear tissue against inflammation-induced morphological damage and dysfunction. We also elucidated the synergistic effect of RSG and DEX on MKP-1 expression and glucocorticoid resistance. Therefore, this study may offer novel targets for potential therapeutics for treating inflammatory diseases of the inner ear.

## 2. Materials and Methods

**2.1. Drugs.** LPS and RSG were purchased from Sigma-Aldrich Chemical Co. (St. Louis, USA). DEX was purchased from Shanghai Jiao Tong University Affiliated Sixth People's Hospital (Shanghai, China).

**2.2. Ethics and Animals.** All animal experiments were approved by the Ethics Committee of the Shanghai Jiao Tong University Affiliated Sixth People's Hospital. And the care and handling of guinea pigs were approved by the Institutional Animal Care and Use Committee and preceded in accordance with the Animals (Scientific Procedures) Act 1986 (amended 2013) [20]. All guinea pigs were housed in individually ventilated cages (two or three per cage) under specific pathogen-free (SPF) conditions.

**2.3. Animal Models and Drug Treatments.** Thirty male albino guinea pigs with an average body weight of 250 g were randomly divided into five groups ( $n=6$ ) including the AP (artificial perilymph), LPS, LPS+DEX, LPS+RSG, and LPS+DEX+RSG groups. AP cochlear perfusion was performed on the pigs in the AP group. LPS cochlear perfusion was performed on the pigs in the LPS group. LPS cochlear perfusion performed on and DEX was intraperitoneally injected into the pigs in the LPS+DEX group. LPS cochlear perfusion was performed on and RSG was

intraperitoneally injected into the pigs in the LPS+RSG group. LPS cochlear perfusion was performed on and DEX and RSG were intraperitoneally injected into the pigs in the LPS+DEX+RSG group. DEX (1 mg/kg) or RSG (3 mg/kg, diluted in dimethyl sulfoxide) or both were intraperitoneally injected 30 min before surgery and 24 h after surgery. The subjects were placed in a heating pad with thermostatic control to maintain their body temperature at 38°C. Cochleostomy was performed on inhalant isoflurane-anesthetized pigs (4% for induction, 2% for maintenance, and 0.3 L/min O<sub>2</sub> flow rate) for injecting LPS (5 mg/mL) or AP (NaCl 145 mM, KCl 2.7 mM, MgSO<sub>4</sub> 2.0 mM, CaCl<sub>2</sub> 1.2 mM, and HEPES, C<sub>8</sub>H<sub>18</sub>N<sub>2</sub>O<sub>4</sub>S 5.0 mM). Lidocaine (1%) was subcutaneously administered in their postauricular regions. The posterior part of their auditory bulla was bluntly dissected. Holes, 0.3 mm in diameter, were punctured into their mastoid bulla to expose the basal turn of the cochlea. The holes were accessed through the bony wall of the scala tympani of the basal turn in the cochlea. Cochlear injections were administered using a glass tip made from a 34 G microfilm, connected to a microsyringe pump (Micro4; WPI, Kissimmee, USA) through a polyethylene tube. Then, 5  $\mu$ L of LPS/AP was injected at a rate of 50 nL/s into the scala tympani. The cochleostomy holes were closed with muscle tissue, while the holes made in their bulla were closed with muscle suture and skin incision.

**2.4. Auditory Brainstem Response (ABR) Tests.** ABR thresholds were determined before surgery and 48 h after surgery in all subjects. The mean threshold shifts were averaged from two ears in all subjects. First, the guinea pigs were anesthetized with ketamine (40 mg/kg) mixed with xylazine (4 mg/kg, ip). Body temperature was maintained at 38°C. For closed field ABR tests, sound signal was passed through a plastic tube to the tested ear. Three subcutaneous electrodes were used to record the reaction. The recording electrode was inserted at the vertex, while the reference and grounding electrodes were inserted behind the external auditory canal. The ends of the three electrodes were connected to a RA16PA preamplifier. TDT System III (Tucker-Davis Technologies, Alachua, FL, USA) was used for stimuli generation. The stimuli were played through a broadband speaker (MF1; TDT). The sound level was decreased by 5 dB steps from 90 dB SPL until the response disappeared. The ABR thresholds were tested at 1, 2, 4, 8, 16, and 32 kHz, which are the lowest levels at which repeatable wave III responses can be recorded.

**2.5. Immunofluorescence.** To investigate the expression of MKP-1 in the cochlea of guinea pigs, the cochlea was removed after the ABR tests. The cochlea was fixed in 4% paraformaldehyde in phosphate-buffered saline (PBS) for 2 h at 4°C. Then, the cochlea was transferred into PBS and its bony shell was removed. After removing the tectorial membrane, the basilar membrane and spiral ganglion (SGN) were carefully peeled off, followed by immersion in PBS containing 1% Triton X-100 for 1 h and incubation in 5% goat serum for 1 h. Next, the basilar membrane and spiral ganglion were incubated with primary rabbit anti-MKP-1 antibody (1:100) (Affinity Biosciences, USA) for 20 h at 4°C. This was followed

by incubation with the Alexa Fluor® 488 goat anti-rabbit IgG (secondary antibody) (1:500) (Abcam, Cambridge, UK) for 2 h at 25°C. Fluorescein isothiocyanate- (FITC-) phalloidin (1:500) (Cytoskeleton Inc., CO, USA) was used to stain hair cell stereocilia bundles. 4',6-Diamidino-2-phenylindole (DAPI) (Sigma-Aldrich, USA) was used for nucleic acid staining. The sections were cover-slipped, examined with the LSM 710 confocal microscope (Zeiss, Oberkochen, Germany), and analyzed by the ZEN 2011 software (Zeiss, Oberkochen, Germany).

**2.6. Hematoxylin-Eosin Staining.** Pathological changes in the cochlea of guinea pigs were observed using hematoxylin-eosin (HE) staining. The cochlea of pigs in all groups was decalcified in ethylenediaminetetraacetic acid (EDTA) and then dehydrated in ethanol. They were then imbedded in paraffin. Thereafter, they were sectioned to a 3  $\mu\text{m}$  thickness and stained with HE. The sections were observed with the LSM 710 META confocal laser scanning microscope (Zeiss, Shanghai, China). SGN cells from base to the apex in each section of Rosenthal's canal were counted. Lastly, SGN cell density (number/10000  $\mu\text{m}^2$ ) was analyzed.

**2.7. Western Blot Analysis.** Extracted proteins from cochlea samples were prepared in radioimmunoprecipitation assay (RIPA) buffer mixed with the protease inhibitor phenylmethanesulfonyl fluoride (PMSF) at a 100:1 ratio (Beyotime Institute of Biotechnology, Shanghai, China). The protein concentrations were detected using the Bicinchoninic Acid (BCA) Protein Assay Kit (Beyotime Institute of Biotechnology). Sample lysates (30  $\mu\text{g}$  protein per lane) were then subjected to 10% sodium dodecyl sulfate-polyacrylamide gel electrophoresis (SDS-PAGE) and transferred to polyvinylidene difluoride (PVDF) membranes with a pore size of 0.22  $\mu\text{m}$  (Millipore, Billerica, MA, USA). The membranes were blocked for 2 h at room temperature with 5% nonfat milk in Tris-buffered saline with Tween-20 (TBST) and then incubated with the appropriate primary antibodies (1:800–1:1000 dilution) at 4°C for 20 h. After washing three times for 10 min with TBST, the membranes were incubated with HRP-conjugated secondary antibodies (1:5000, Proteintech, Chicago, IL, USA) for 1 h at 25°C. The antibodies binding to the blots were visualized on a GE Amersham Imager 600 imaging system using an enhanced chemiluminescence detection kit (Cell Signaling Technology, Boston, MA, USA). The results are expressed as a percentage of GAPDH to express relative protein levels. Antibodies to p38 MAPK (cat. no. 8690S), phospho-p38 MAPK (cat. no. 4511S), NF- $\kappa\text{B}$  p65 (cat. no. 8242S), phospho-NF- $\kappa\text{B}$  p65 (cat. no. 3033S), and GAPDH (cat. no. 5174S) were purchased from Cell Signaling Technology. Anti-MKP-1 (cat. no. AF5286) was purchased from Affinity Biosciences (Cincinnati, OH, USA). Anti-GR (cat. no. ab3578) was purchased from Abcam.

**2.8. Statistical Analysis.** All statistical analyses were performed using SPSS version 23.0 (IBM Corp., Armonk, NY, USA). Descriptive statistics were calculated for each group. One-way analyses of variance (ANOVA) was used

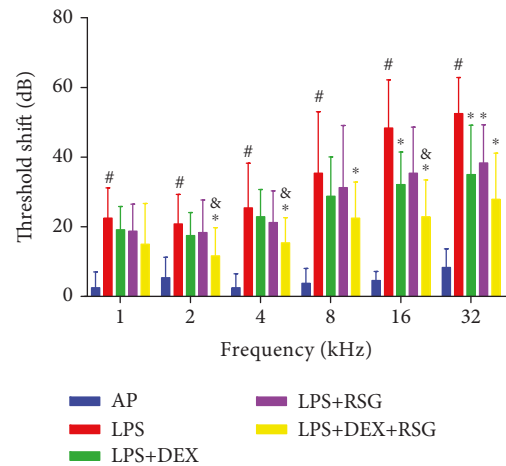


FIGURE 1: Hearing threshold shifts in each group were measured using the ABR tests before and 48 h after surgery at different frequencies. # $p < 0.05$  vs. AP group; \* $p < 0.05$  vs. LPS group; and  $p < 0.05$  vs. LPS+DEX group.

to assess the differences between groups. The significance level was set at  $p < 0.05$ .

### 3. Results

**3.1. Evaluation of Hearing Function in Each Group.** The hearing threshold shift in each group was measured using the ABR tests before and 48 h after surgery at different frequencies (Figure 1). The average threshold shift at each frequency (1, 2, 4, 8, 16, and 32 kHz) in the AP group was less than 10 dB, indicating the surgery had no effect on hearing function. The threshold shift in the LPS group was significantly higher than that in the AP group ( $p < 0.05$ ). Also, the extent of hearing impairment increased with frequency. The threshold shift in the LPS+DEX group decreased compared to that in the LPS group; however, significant differences were observed only at 16 and 32 kHz. This suggests that DEX has only a partial effect on LPS-induced hearing loss and glucocorticoid resistance. The threshold shift in the LPS+RSG group decreased partially, but there was no significant difference when compared with that of the LPS group, except at 32 kHz. The LPS+DEX+RSG group possessed a significant hearing protection. The threshold shift decreased significantly compared to that in the LPS group at 2, 4, 8, 16, and 32 kHz. Moreover, the threshold shift decreased significantly at 2, 4, and 16 kHz for the LPS+DEX+RSG and LPS+DEX groups. These findings show that LPS causes a significant hearing loss in the inner ear, and the combination of RSG and DEX substantially protects against hearing loss.

**3.2. Immunostaining of MKP-1 in the Basilar Membrane and Spiral Ganglion.** As shown in Figure 2, MKP-1 immunofluorescence staining of cochlear basilar membranes in the AP group showed MKP-1 is located in the hair cell nucleus and cytoplasm. Also, Figure 3 shows the localization of MKP-1 in the spiral ganglion of pigs in the AP group. However, MKP-1 is abundant in the cytoplasm of neurons than in hair cells. There was no significant difference in the location of

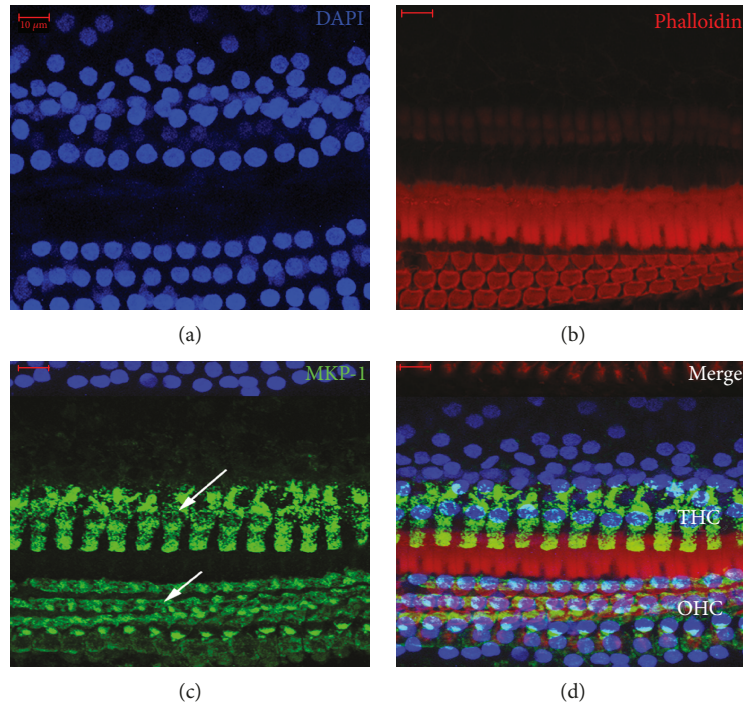


FIGURE 2: MKP-1 immunofluorescence staining of cochlear basilar membranes of pigs in the AP group. MKP-1 stained in the spiral ganglion cell (white arrows). Blue: nuclei stained with DAPI; red: stereocilia stained with FITC-phalloidin; green: MKP-1 stained in inner hair cell (IHC) and outer hair cell (OHC). Scale bars = 10  $\mu\text{m}$ .

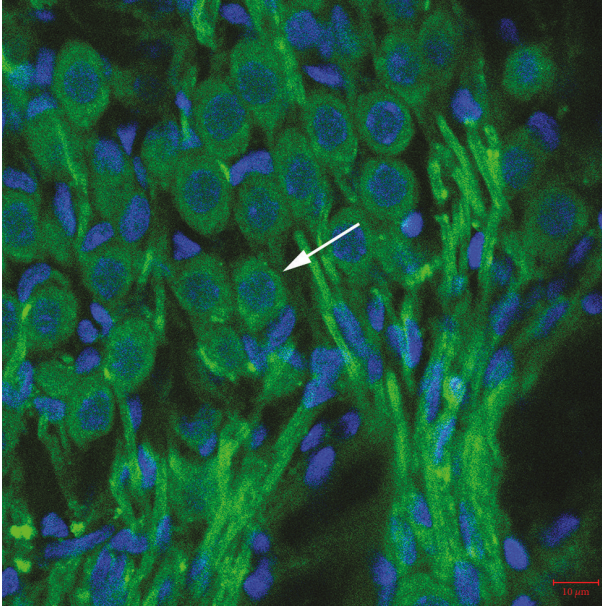


FIGURE 3: MKP-1 immunofluorescence staining of cochlear spiral ganglion of pigs in the AP group. MKP-1 stained in the spiral ganglion cell (white arrows). Blue: nuclei stained with DAPI; green: MKP-1 stained in inner hair cell (IHC) and outer hair cell (OHC). Scale bars = 10  $\mu\text{m}$ . The red marker is the stereocilia of hair cells, and the blue marker is the cell nucleus.

MKP-1 among different groups. Figure 4 shows the immunostaining of complete basilar membranes in the AP and LPS groups. Compared to the AP group, the LPS group showed

no obvious loss of inner or outer hair cells, and the structure of stereocilia was normal.

**3.3. Histological Examination of the Cochlea.** The pathological observation of the cochlea in each group is shown in Figure 5. The HE stain uniformly stained the spiral ligaments in the AP group, and there was no gap within the cochlear lateral wall. The stria vascularis was normal in shape, with no rupture or erythrocyte exudation. The spiral ganglions were well arranged, and the nuclear/plasma ration was normal. In the LPS group, spiral ligaments were sparse and their structure was disordered. The spiral ganglion showed vacuolar degeneration and decreased nuclear/plasma ratio. These observations indicate that LPS destroys the inner ear morphology. However, the morphological damage was slightly decreased in the LPS+DEX and LPS+RSG groups, but some changes such as loosened spiral ligament and decreased nuclear/plasma ratio were still observed. The morphological recovery in the LPS+DEX+RSG group was the most obvious. The morphology of the stria vascularis and spiral ligament was normal, and there was no obvious gap between them and the lateral wall of the cochlea. The spiral ganglion/nucleoplast ration was also improved. The density of spiral ganglion cells in the LPS group was significantly lower than that in the AP group ( $p < 0.01$ ). The LPS+DEX and LPS+RSG groups had no significant increase compared to the LPS group ( $p > 0.05$ ), but the LPS+DEX+RSG group showed a significant increase compared to the LPS group ( $p < 0.01$ ). Although the density of spiral ganglion cells in the LPS+DEX+RSG group was significantly lower than that in the AP group ( $p < 0.05$ ), it was significantly higher than that

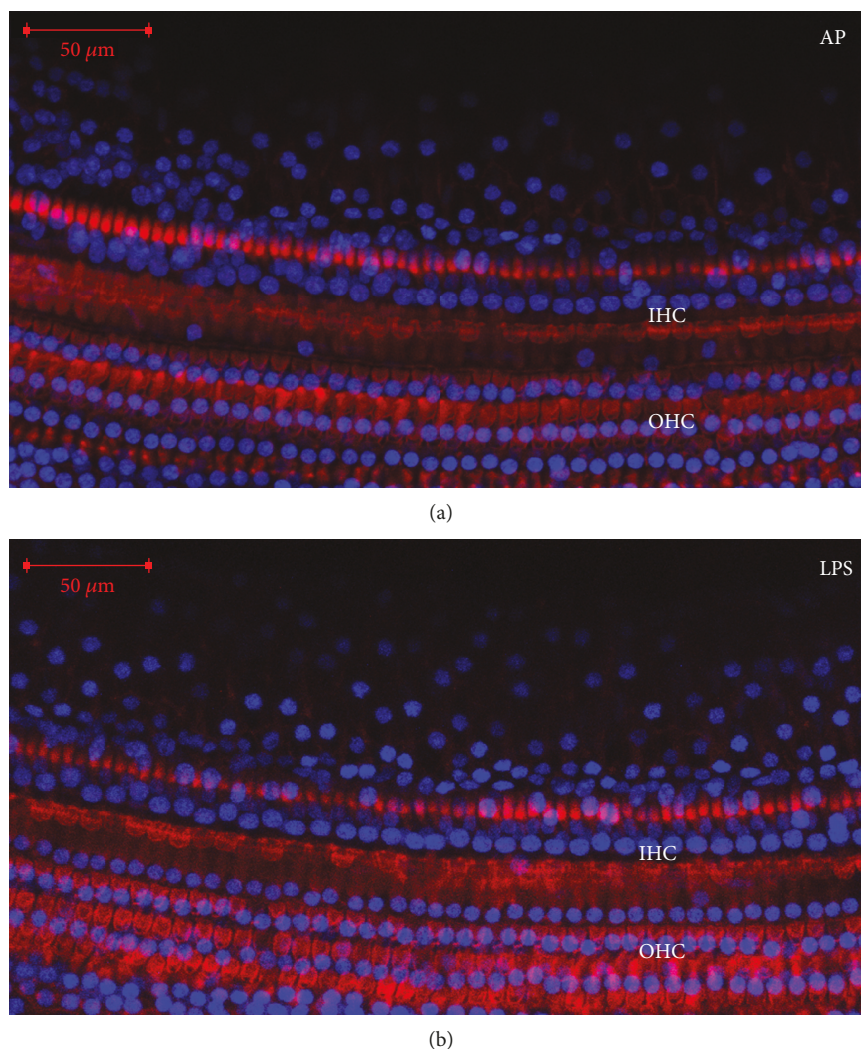


FIGURE 4: The immunostaining of basilar membranes of pigs in the AP and LPS groups. Blue: nuclei stained with DAPI; red: stereocilia stained with FITC-phalloidin. Scale bars = 50  $\mu\text{m}$ . Compared to the AP group, the LPS group showed no obvious loss of inner and outer hair cells, and the structure of stereocilia was normal.

in the LPS+DEX group or LPS+RSG group ( $p < 0.05$ ). This indicates a combination of DEX, and RSG has a stronger protective effect than each alone.

#### 3.4. Western Blot Analysis of MKP-1 and Related Proteins.

The expression of MKP-1, GR, p38, p-p38, NF- $\kappa\text{B}$  p65, and p-NF- $\kappa\text{B}$  p65 was determined by western blot analysis (Figure 6). The expression of MKP-1 in the LPS group was significantly lower than that in the AP group ( $p < 0.01$ ). MKP-1 expression was not significantly higher in the LPS+DEX or LPS+RSG group compared to the LPS group ( $p > 0.05$ ) but was significantly higher in the LPS+DEX+RSG group than in the LPS+DEX group ( $p < 0.01$ ). Also, GR expression in the LPS group was significantly higher than that in the AP group ( $p < 0.05$ ) and also significantly higher in the LPS+DEX+RSG group than the LPS+DEX group ( $p < 0.05$ ). Additionally, the expression of p-p38/p-NF- $\kappa\text{B}$  p65 in the LPS group was significantly higher than that in the AP group ( $p < 0.05$ ), while it was significantly lower in the LPS+DEX group ( $p < 0.05$ )

compared to the LPS+DEX+RSG group. In addition, there was no significant decrease in the LPS+DEX and LPS+RSG groups when compared to the LPS group ( $p > 0.05$ ). These results suggest that a combination of DEX and RSG can significantly increase the expression of MKP-1 and GR. Moreover, lesions induced by LPS can be alleviated by inhibiting the activation of p38/p-NF- $\kappa\text{B}$ .

## 4. Discussion

In this study, we investigated the role of MKP-1 and RSG in glucocorticoid resistance using a guinea pig model of LPS-induced SSSL. We demonstrated for the first time that MKP-1 protects inner ear tissues from inflammation-induced morphological damage and dysfunction by inhibiting the activation of p38 MAPK and NF- $\kappa\text{B}$ . Our results also show that the synergy between RSG and DEX can increase the MKP-1 expression and reduce glucocorticoid resistance.

Although glucocorticoids are widely clinically used, a considerable number of patients show resistance to

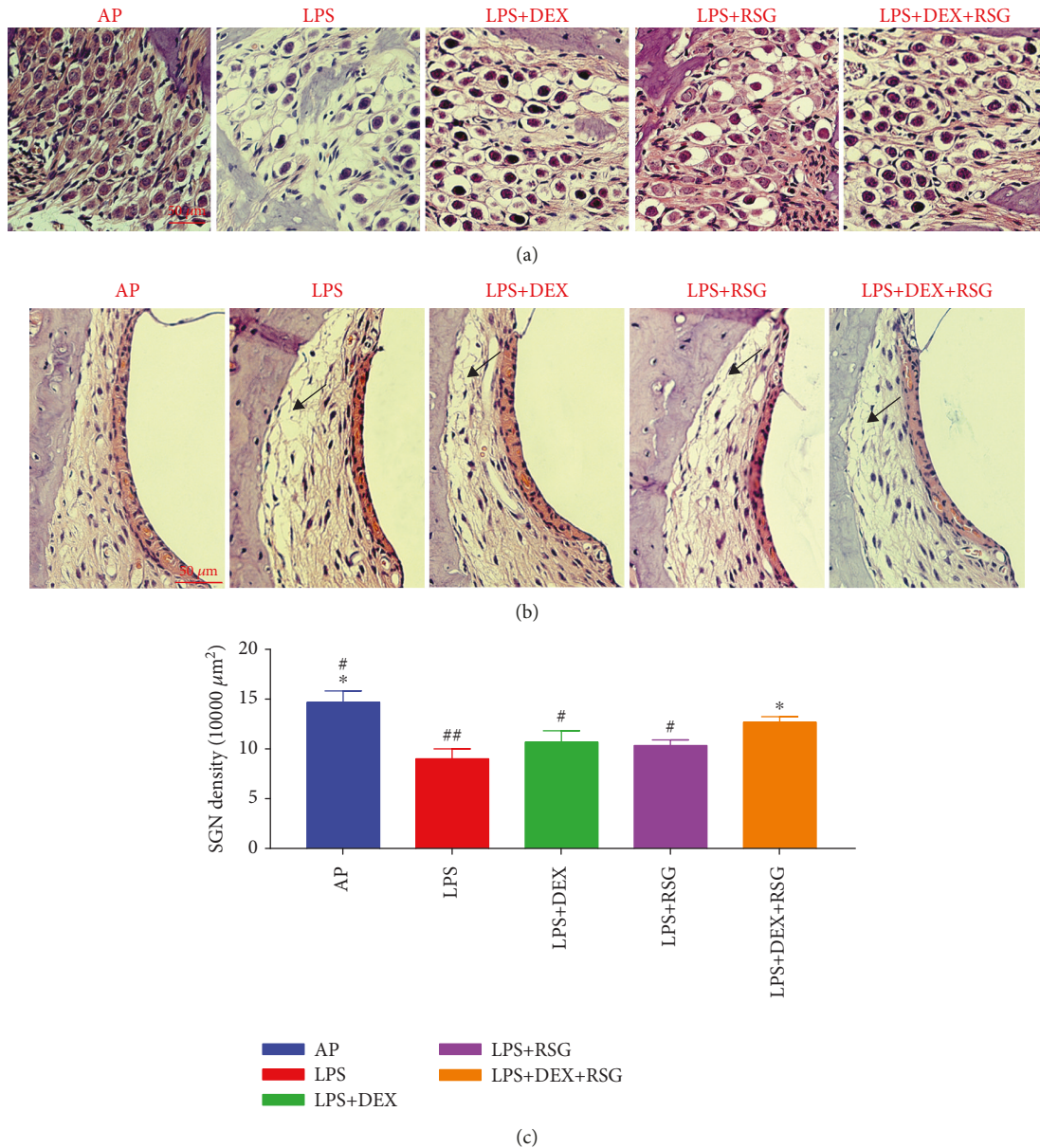
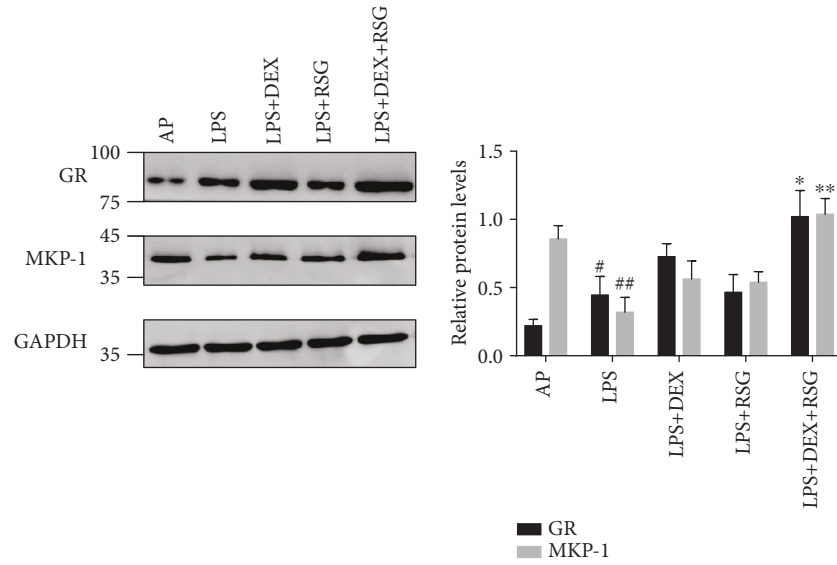


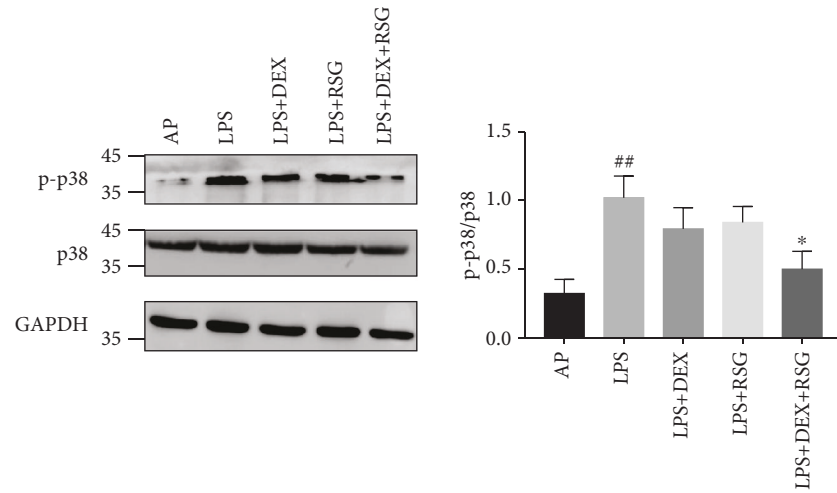
FIGURE 5: (a) Pathological observation of the spiral ganglion of pigs in each group. Scale bars = 50  $\mu\text{m}$ ; (b) pathological observation of the stria vascularis in each group. Spiral ligament was sparse and disordered (black arrows). Scale bars = 50  $\mu\text{m}$ ; (c) the bar graphs show the density of spiral ganglion cells in each group. Data are shown as means  $\pm$  SD from different experiments, #  $p < 0.05$  vs. LPS+DEX+RSG group; ##  $p < 0.01$  vs. LPS+DEX+RSG group; \*  $p < 0.01$  vs. LPS group.

glucocorticoid therapy. These patients often have a high risk of poor prognosis not only due to the primary disease itself but also the adverse reactions resulting from the long-term use of glucocorticoids. Their visit and hospitalization rates are often far higher than those of other patients, thus increasing the economic burden of these individuals and the society. When glucocorticoids enter the plasmalemma and combine with GR, they can induce the rearrangement of the GR complex to facilitate its entry into the nucleus, for positive or negative regulation of gene transcription [21]. Multiple factors are involved in the molecular mechanism of glucocorticoid resistance [22, 23]. In recent years, it has been found that polymorphisms of the GR reduces its affinity to ligands,

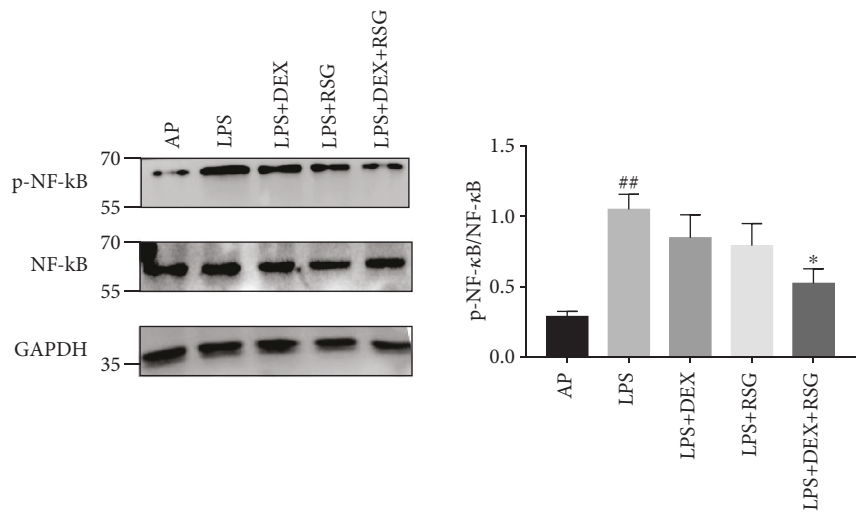
leading to glucocorticoid resistance [24]. Another study reported that glucocorticoid resistance is related to defects in GR expression and elevated expression of proinflammatory transcription factors [25]. Kojika et al. found that changes in HSP90 and HSP70 may be related to decreased glucocorticoid sensitivity. Abnormal HSP90 and HSP70 protein levels were successfully detected in two glucocorticoid-resistant human leukemia cell lines [26]. The increased expression of NF- $\kappa$ B in the peripheral blood mononuclear cells of asthmatic patients was found to be negatively correlated with glucocorticoid responsiveness. The possible underlying mechanism is antagonism between NF- $\kappa$ B and GR, which reduces glucocorticoid sensitivity [27].



(a)



(b)



(c)

FIGURE 6: The protein expression of (a) MKP-1 and GR, (b) p38 and p-p38, and (c) NF-κB and p-NF-κB p65 was determined by western blot analysis. Bar graphs show the quantification of the indicated proteins. Data are shown as means ± SD from at least three independent experiments, <sup>#</sup>*p* < 0.05 vs. AP group; <sup>##</sup>*p* < 0.01 vs. AP group; <sup>\*</sup>*p* < 0.05 vs. LPS+DEX group; <sup>\*\*</sup>*p* < 0.01 vs. LPS+DEX group.

Recently, Irusen et al. found that p38 MAPK activation can induce GR phosphorylation and function impairment [28]. In addition, p38 MAPK activation can increase the phosphorylation of the NF- $\kappa$ B p65 subunit [29]. MKP-1 serves as an important regulator of the innate immune response by deactivating MAP kinases and NF- $\kappa$ B [9–13]. Goleva et al. found that glucocorticoid resistance is associated with reduced induction of MKP-1, resulting in persistent p38 MAPK activation in peripheral blood mononuclear cells. Also, Bhavsar et al. reported that DEX could not induce the expression of MKP-1 in patients with severe (steroid-resistant) asthma [15]. Under the influence of inflammatory factors, MKP-1 knockout mice experienced increased levels of cytokines and chemical factors, increased neutrophil infiltration, and more severe organ damage than wild-type mice [30]. In addition, inflammation and oxidative stress also lead to SSHL. In the present study, we found that MKP-1 is expressed in inner and outer hair cells, supporting cells, and spiral ganglion cells in the cochlea. This was mainly observed in the cytoplasm and to some extent in the nucleus.

RSG is mainly used as an insulin sensitizer for the treatment of diabetes. Recent studies on peroxisome proliferative-activated receptor (PPAR) gamma have shown that RSG has anti-inflammatory and antioxidative effects [31–33]. Also, Tai et al. found that RSG could inhibit the proliferation and metastasis of non-small-cell lung cancer *in vivo* and *in vitro* via induction of MKP-1 [16]. RSG can also increase MKP-1 expression, which inhibits cell invasion in human glioma cells [34].

The anti-inflammatory effect of glucocorticoids after binding with GR is mainly achieved by enhancing the transcription of anti-inflammatory or inflammatory genes. MKP-1 is an important anti-inflammatory protein transcribed by glucocorticoids [35]. In this, as in a previous study, we found that the hearing function of guinea pigs with SSHL did not significantly improve after glucocorticoid treatment, which indicates glucocorticoid resistance or insensitivity [5]. Also, the threshold shift in the LPS+DEX+RSG group was the lowest, indicating MKP-1 could achieve its anti-inflammatory effect by inhibiting the activity of p38 MAPK in the inner ear. Further, the MKP-1 expression in the LPS+DEX+RSG group was higher than that in the LPS+DEX and LPS+RSG groups. DEX alone could not effectively increase the expression of MKP-1 in SSHL, which resulted in uncontrollable inflammation. Additionally, during LPS stimulation, GR expression was upregulated as a feedback effector, but its upregulation was more significant in the LPS+DEX+RSG group than in the LPS+DEX group. The LPS+DEX+RSG group had the best anti-inflammatory effect. Further, RSG exhibited anti-inflammatory effects, resulting in the restoration of decreased GR levels and impaired function caused by inflammation. Thus, when RSG is combined with DEX, the expression of MKP-1 can be enhanced. Therefore, RSG may play an important role in improving glucocorticoid resistance in SSHL and other inner ear disorders, owing to its ability of lower blood glucose levels, control inflammation, and eliminate toxins and side effects. It is therefore a potential new treatment option for such diseases.

There are certain limitations to our study. First, the guinea pig model of LPS-induced SSHL does not completely represent the clinical pathogenesis of SSHL. Further research should be performed using animal models more suitable for SSHL studies and clinical trials. Secondly, this is the first study to use the PPAR- $\gamma$  agonist RSG for the treatment of an inner ear disease, the structure and function of PPAR- $\gamma$  are very complex, and there are many unknown aspects to be explored.

We will investigate the route and administration time of RSG in future experiments.

## 5. Conclusion

In summary, MKP-1 is a key factor for the anti-inflammatory effect of hormones in inner ear tissues. The mechanism of glucocorticoid resistance in the guinea pig model of LPS-induced SSHL may be associated with reduced levels of MKP-1 induction, resulting in persistent MAPK activation in the inner ear. The combined use of RSG and glucocorticoids provides a new treatment option for glucocorticoid resistance in SSHL.

## Data Availability

To anyone who needs dates, please contact the corresponding authors.

## Conflicts of Interest

The authors declare that there is no competing interest relevant to the publication of this paper.

## Authors' Contributions

Liang Xia and Jingjing Liu contributed equally to this paper.

## Acknowledgments

This study was supported by grants from the National Natural Science Foundation of China (No. 81771015 and No. 81670937), the Three-Year Action Program on the Promotion of Clinical Skills/Clinical Innovation for Municipal Hospitals (No. 16CR4027A), and the Shanghai Municipal Education Commission/Gaofeng Clinical Medicine Grant Support (No. 20152526).

## References

- [1] J. Y. Um, C. H. Jang, H. L. Kim et al., "Proinflammatory cytokine IL-1  $\beta$  polymorphisms in sudden sensorineural hearing loss," *Immunopharmacology and Immunotoxicology*, vol. 35, no. 1, pp. 52–56, 2013.
- [2] G. Cadoni, E. Gaetani, P. M. Picciotti et al., "A case-control study on proinflammatory genetic polymorphisms on sudden sensorineural hearing loss," *The Laryngoscope*, vol. 125, no. 1, pp. E28–E32, 2015.
- [3] M. Masuda, S. Kanzaki, S. Minami et al., "Correlations of inflammatory biomarkers with the onset and prognosis of

- idiopathic sudden sensorineural hearing loss," *Otology & Neurotology*, vol. 33, no. 7, pp. 1142–1150, 2012.
- [4] Z. Jiang and L. Zhu, "Update on molecular mechanisms of corticosteroid resistance in chronic obstructive pulmonary disease," *Pulmonary Pharmacology & Therapeutics*, vol. 37, pp. 1–8, 2016.
- [5] Q. Q. Zhou, Y. H. Dai, X. P. du, J. Hou, H. Qi, and W. D. She, "Aminophylline restores glucocorticoid sensitivity in a guinea pig model of sudden sensorineural hearing loss induced by lipopolysaccharide," *Scientific Reports*, vol. 7, no. 1, article 2736, 2017.
- [6] S. M. Moosavi, P. Prabhala, and A. J. Ammit, "Role and regulation of MKP-1 in airway inflammation," *Respiratory Research*, vol. 18, no. 1, p. 154, 2017.
- [7] M. Camps, A. Nichols, and S. Arkininstall, "Dual specificity phosphatases: a gene family for control of MAP kinase function," *The FASEB Journal*, vol. 14, no. 1, pp. 6–16, 2000.
- [8] K. Kondoh and E. Nishida, "Regulation of MAP kinases by MAP kinase phosphatases," *Biochimica et Biophysica Acta (BBA) - Molecular Cell Research*, vol. 1773, no. 8, pp. 1227–1237, 2007.
- [9] C. Y. Huang and T. H. Tan, "DUSPs, to MAP kinases and beyond," *Cell & Bioscience*, vol. 2, no. 1, p. 24, 2012.
- [10] G. L. Johnson and R. Lapadat, "Mitogen-activated protein kinase pathways mediated by ERK, JNK, and p38 protein kinases," *Science*, vol. 298, no. 5600, pp. 1911–1912, 2002.
- [11] K. F. Chung, "p38 mitogen-activated protein kinase pathways in asthma and COPD," *Chest*, vol. 139, no. 6, pp. 1470–1479, 2011.
- [12] Y. Pan, Y. Liu, L. Wang et al., "MKP-1 attenuates LPS-induced blood-testis barrier dysfunction and inflammatory response through p38 and I $\kappa$ B $\alpha$  pathways," *Oncotarget*, vol. 7, no. 51, pp. 84907–84923, 2016.
- [13] Y. Liu, M. Gorospe, C. Yang, and N. J. Holbrook, "Role of mitogen-activated protein kinase phosphatase during the cellular response to genotoxic stress. Inhibition of c-Jun N-terminal kinase activity and AP-1-dependent gene activation," *Journal of Biological Chemistry*, vol. 270, no. 15, pp. 8377–8380, 1995.
- [14] J. Raugeaud, S. Gupta, J. S. Rogers et al., "Pro-inflammatory cytokines and environmental stress cause p38 mitogen-activated protein kinase activation by dual phosphorylation on tyrosine and threonine," *Journal of Biological Chemistry*, vol. 270, no. 13, pp. 7420–7426, 1995.
- [15] P. Bhavsar, M. Hew, N. Khorasani et al., "Relative corticosteroid insensitivity of alveolar macrophages in severe asthma compared with non-severe asthma," *Thorax*, vol. 63, no. 9, pp. 784–790, 2008.
- [16] C. J. Tai, A. T. H. Wu, J. F. Chiou et al., "The investigation of mitogen-activated protein kinase phosphatase-1 as a potential pharmacological target in non-small cell lung carcinomas, assisted by non-invasive molecular imaging," *BMC Cancer*, vol. 10, no. 1, p. 95, 2010.
- [17] W. Chen, Y. J. Lin, X. Y. Zhou, H. Chen, and Y. Jin, "Rosiglitazone protects rat liver against acute liver injury associated with the NF- $\kappa$ B signaling pathway," *Canadian Journal of Physiology and Pharmacology*, vol. 94, no. 1, pp. 28–34, 2016.
- [18] M. J. Tarlow, S. D. Comis, and M. P. Osborne, "Endotoxin induced damage to the cochlea in guinea pigs," *Archives of Disease in Childhood*, vol. 66, no. 2, pp. 181–184, 1991.
- [19] D. H. Darrow, E. M. Keithley, and J. P. Harris, "Effects of bacterial endotoxin applied to the guinea pig cochlea," *Laryngoscope*, vol. 102, no. 6, pp. 683–688, 1992.
- [20] J. Liu, C. Jiang, X. Ma, and J. Wang, "Notoginsenoside Fc attenuates high glucose-induced vascular endothelial cell injury via upregulation of PPAR- $\gamma$  in diabetic Sprague-Dawley rats," *Vascular Pharmacology*, vol. 109, pp. 27–35, 2018.
- [21] S. C. Biddie, B. L. Conway-Campbell, and S. L. Lightman, "Dynamic regulation of glucocorticoid signalling in health and disease," *Rheumatology*, vol. 51, no. 3, pp. 403–412, 2012.
- [22] C. R. Keenan, D. Radojicic, M. Li, A. Radwan, and A. G. Stewart, "Heterogeneity in mechanisms influencing glucocorticoid sensitivity: the need for a systems biology approach to treatment of glucocorticoid-resistant inflammation," *Pharmacology & Therapeutics*, vol. 150, pp. 81–93, 2015.
- [23] W. Wang, J. Jing Li, P. S. Foster, P. M. Hansbro, and M. Yang, "Potential therapeutic targets for steroid-resistant asthma," *Current Drug Targets*, vol. 11, no. 8, pp. 957–970, 2010.
- [24] A. Vazquez-Tello, A. Semlali, J. Chakir et al., "Induction of glucocorticoid receptor- $\beta$  expression in epithelial cells of asthmatic airways by T-helper type 17 cytokines," *Clinical & Experimental Allergy*, vol. 40, no. 9, pp. 1312–1322, 2010.
- [25] K. F. Chung, S. E. Wenzel, J. L. Brozek et al., "International ERS/ATS guidelines on definition, evaluation and treatment of severe asthma," *European Respiratory Journal*, vol. 43, no. 2, pp. 343–373, 2014.
- [26] S. Kojika, K. Sugita, T. Inukai et al., "Mechanisms of glucocorticoid resistance in human leukemic cells: implication of abnormal 90 and 70 kDa heat shock proteins," *Leukemia*, vol. 10, no. 6, pp. 994–999, 1996.
- [27] B. Vrugt, S. Wilson, A. Bron et al., "Low-dose methotrexate treatment in severe glucocorticoid-dependent asthma: effect on mucosal inflammation and in vitro sensitivity to glucocorticoids of mitogen-induced T-cell proliferation," *European Respiratory Journal*, vol. 15, no. 3, pp. 478–485, 2000.
- [28] E. Irusen, J. G. Matthews, A. Takahashi, P. J. Barnes, K. F. Chung, and I. M. Adcock, "p38 Mitogen-activated protein kinase-induced glucocorticoid receptor phosphorylation reduces its activity: role in steroid-insensitive asthma," *Journal of Allergy and Clinical Immunology*, vol. 109, no. 4, pp. 649–657, 2002.
- [29] J. M. O'Shea and N. D. Perkins, "Regulation of the RelA (p65) transactivation domain," *Biochemical Society Transactions*, vol. 36, no. 4, pp. 603–608, 2008.
- [30] X. Wang, X. Meng, J. R. Kuhlman et al., "Knockout of *Mkp-1* enhances the host inflammatory responses to gram-positive bacteria," *The Journal of Immunology*, vol. 178, no. 8, pp. 5312–5320, 2007.
- [31] J. H. Yi, S. W. Park, N. Brooks, B. T. Lang, and R. Vemuganti, "PPAR $\gamma$  agonist rosiglitazone is neuroprotective after traumatic brain injury via anti-inflammatory and anti-oxidative mechanisms," *Brain Research*, vol. 1244, pp. 164–172, 2008.
- [32] S. Kavak, L. Ayaz, M. Emre, T. Inal, L. Tamer, and I. Günay, "The effects of rosiglitazone on oxidative stress and lipid profile in left ventricular muscles of diabetic rats," *Cell Biochemistry and Function*, vol. 26, no. 4, pp. 478–485, 2008.
- [33] D. Mingfeng, M. Xiaodong, L. Yue, P. Taikui, X. Lei, and L. Ming, "Effects of PPAR- $\gamma$  agonist treatment on LPS-induced mastitis in rats," *Inflammation*, vol. 37, no. 6, pp. 1919–1924, 2014.

- [34] H. J. Jan, C. C. Lee, Y. M. Lin, J. H. Lai, H. W. Wei, and H. M. Lee, "Rosiglitazone reduces cell invasiveness by inducing MKP-1 in human U87MG glioma cells," *Cancer Letters*, vol. 277, no. 2, pp. 141-148, 2009.
- [35] P. J. Barnes, "Molecular mechanisms and cellular effects of glucocorticosteroids," *Immunology and Allergy Clinics of North America*, vol. 25, no. 3, pp. 451-468, 2005.

## Research Article

# Dendritic Cells in Subcutaneous and Epicardial Adipose Tissue of Subjects with Type 2 Diabetes, Obesity, and Coronary Artery Disease

Miloš Mráz,<sup>1,2</sup> Anna Cinkajzlová,<sup>2,3</sup> Jana Kloučková,<sup>2,3</sup> Zdeňka Lacinová,<sup>2,3</sup>  
Helena Kratochvílová,<sup>2,3</sup> Michal Lipš,<sup>4</sup> Michal Pořízka,<sup>4</sup> Petr Kopecký,<sup>4</sup> Jaroslav Lindner,<sup>5</sup>  
Tomáš Kotulák ,<sup>6</sup> Ivan Netuka,<sup>7</sup> and Martin Haluzík <sup>1,2,3</sup>

<sup>1</sup>Department of Diabetes, Diabetes Centre, Institute for Clinical and Experimental Medicine, Prague, Czech Republic

<sup>2</sup>Department of Medical Biochemistry and Laboratory Diagnostics, First Faculty of Medicine, Charles University and General University Hospital, Prague, Czech Republic

<sup>3</sup>Centre for Experimental Medicine, Institute for Clinical and Experimental Medicine, Prague, Czech Republic

<sup>4</sup>Department of Anaesthesiology, Resuscitation and Intensive Medicine, First Faculty of Medicine, Charles University and General University Hospital, Prague, Czech Republic

<sup>5</sup>2nd Department of Surgery-Department of Cardiovascular Surgery, Charles University and General University Hospital, Prague, Czech Republic

<sup>6</sup>Anesthesiology Department, Cardiac Centre, Institute for Clinical and Experimental Medicine, Prague, Czech Republic

<sup>7</sup>Cardiovascular Surgery Department, Cardiac Centre, Institute for Clinical and Experimental Medicine, Prague, Czech Republic

Correspondence should be addressed to Martin Haluzík; [mhalu@lf1.cuni.cz](mailto:mhalu@lf1.cuni.cz)

Received 26 November 2018; Revised 29 January 2019; Accepted 21 February 2019; Published 9 May 2019

Guest Editor: Qingdong Guan

Copyright © 2019 Miloš Mráz et al. This is an open access article distributed under the Creative Commons Attribution License, which permits unrestricted use, distribution, and reproduction in any medium, provided the original work is properly cited.

Dendritic cells (DCs) are professional antigen-presenting cells contributing to regulation of lymphocyte immune response. DCs are divided into two subtypes: CD11c-positive conventional or myeloid (cDCs) and CD123-positive plasmacytoid (pDCs) DCs. The aim of the study was to assess DCs (HLA-DR+ lineage-) and their subtypes by flow cytometry in peripheral blood and subcutaneous (SAT) and epicardial (EAT) adipose tissue in subjects with (T2DM,  $n = 12$ ) and without (non-T2DM,  $n = 17$ ) type 2 diabetes mellitus undergoing elective cardiac surgery. Subjects with T2DM had higher fasting glycemia ( $8.6 \pm 0.7$  vs.  $5.8 \pm 0.2$  mmol/l,  $p < 0.001$ ) and glycated hemoglobin ( $52.0 \pm 3.4$  vs.  $36.9 \pm 1.0$  mmol/mol,  $p < 0.001$ ) and tended to have more pronounced inflammation (hsCRP:  $9.8 \pm 3.1$  vs.  $5.1 \pm 1.9$  mg/ml,  $p = 0.177$ ) compared with subjects without T2DM. T2DM was associated with reduced total DCs in SAT ( $1.57 \pm 0.65$  vs.  $4.45 \pm 1.56\%$  for T2DM vs. non-T2DM,  $p = 0.041$ ) with a similar, albeit insignificant, trend in EAT ( $0.996 \pm 0.33$  vs.  $2.46 \pm 0.78\%$  for T2DM vs. non-T2DM,  $p = 0.171$ ). When analyzing DC subsets, no difference in cDCs was seen between any of the studied groups or adipose tissue pools. In contrast, pDCs were increased in both SAT ( $13.5 \pm 2.0$  vs.  $4.6 \pm 1.9\%$  of DC cells,  $p = 0.005$ ) and EAT ( $29.1 \pm 8.7$  vs.  $8.4 \pm 2.4\%$  of DC,  $p = 0.045$ ) of T2DM relative to non-T2DM subjects as well as in EAT of the T2DM group compared with corresponding SAT ( $29.1 \pm 8.7$  vs.  $13.5 \pm 2.0\%$  of DC,  $p = 0.020$ ). Neither obesity nor coronary artery disease (CAD) significantly influenced the number of total, cDC, or pDC in SAT or EAT according to multiple regression analysis. In summary, T2DM decreased the amount of total dendritic cells in subcutaneous adipose tissue and increased plasmacytoid dendritic cells in subcutaneous and even more in epicardial adipose tissue. These findings suggest a potential role of pDCs in the development of T2DM-associated adipose tissue low-grade inflammation.

## 1. Introduction

Dendritic cells (DCs) are professional antigen-presenting cells with the ability to suppress or instigate immune responses and to bridge innate and adaptive immunity [1]. Upon activation by damage- or pathogen-associated signals, immature DCs undergo a maturation process characterized by expression of surface antigens and cytokines important for priming and activation of naïve T cells and initiation of adaptive immune responses [2]. In addition, DCs also play an important role in maintaining immunological tolerance [3]. Two major subtypes of DCs are recognized according to morphology and cell marker expression: CD11c-positive conventional or myeloid DCs (cDCs) involved in the differentiation of CD4+ T helper (Th) cells and CD123-positive plasmacytoid DCs (pDCs) characterized by production of type I interferon, activation of macrophages, and antiviral defense [2, 4, 5]. Except the typical lymphoid organs such as the spleen and lymph nodes, both types are routinely found in a broad spectrum of nonlymphoid tissues including adipose tissue (AT), where they have recently been implied in the development of metabolic inflammation [2, 6, 7].

Chronic low-grade inflammation characterized by increased accumulation of immune cells, especially macrophages and T lymphocytes, in adipose tissue is one of the main mechanisms associating obesity with insulin resistance, type 2 diabetes mellitus (T2DM), and atherosclerosis [8]. DCs with their capability to influence both T cells and macrophages have been suggested as potential initiators of other immune cell recruitment; however, their role in regulating AT inflammation seems dependent on the actual adipose tissue metabolic state. In lean animals, cDCs were shown to promote an anti-inflammatory state and delay the onset of obesity-induced chronic inflammation and insulin resistance [9]. In contrast, long-term overnutrition induced a proinflammatory switch in their phenotype resulting in activation of Th1 and Th17 responses [10, 11]. The presence of DCs was also essential for AT macrophage recruitment and activation, and high-fat diet increased local AT DC content in murine models [12, 13]. Similarly, in humans, DCs were shown to correlate positively with BMI in subcutaneous adipose tissue (SAT) [10].

Despite the emerging data on adipose tissue DCs, little is known about the presence of DCs in other than subcutaneous and abdominal visceral adipose tissue depots. Epicardial adipose tissue (EAT) with its close proximity to coronary arteries has recently been highlighted as an important player in the development of coronary artery disease [14]. To date, only one experimental study on a murine model of acute coronary syndrome has assessed the presence of DCs in EAT, with no data available in humans [15]. Moreover, the influence of fully developed diabetes mellitus on adipose tissue DC count and phenotype has thus far not been addressed. To this end, we performed a flow cytometry analysis of DCs and their subtypes in peripheral blood and subcutaneous and epicardial adipose tissue of subjects with and without type 2 diabetes mellitus undergoing elective cardiac surgery.

## 2. Methods

**2.1. Study Subjects.** Seventeen subjects without T2DM and 12 subjects with T2DM, all undergoing elective cardiac surgery (coronary artery bypass graft implantation and/or valvular surgery), were included into the study. The diagnosis of coronary artery disease was established by presurgical coronarography. T2DM treatment included metformin (9 subjects), dipeptidylpeptidase-4 inhibitors (3 subjects), sulfonylurea derivatives (2 subjects), and insulin therapy with multiple daily injections (1 subject). Written informed consent was signed by each subject prior to inclusion, and the study was approved by the Human Ethics Review Board, First Faculty of Medicine and General University Hospital, Prague, Czech Republic. The study was performed in accordance with the principles of the Declaration of Helsinki as revised in 2008.

**2.2. Blood and Adipose Tissue Sampling.** Blood samples were taken at the beginning of surgery after overnight fasting. Samples were centrifuged for 10 min at 1000x g within 30 min after withdrawal. Serum or plasma aliquots were subsequently stored at -80 °C.

Analogously, 1-2 g of SAT and EAT was obtained at the beginning of surgery immediately after sternotomy. EAT was taken from the anterior interventricular sulcus or the right margin of the heart, and SAT was obtained from the sternotomy site. Freshly collected specimens in PBS buffer (0.01 M PBS, pH 7.4) were used for flow cytometry, and aliquots in RNAlater® solution (Ambion®- Invitrogen, Carlsbad, California, USA) were stored at -80 °C and subsequently used for determination of mRNA expression. Samples for immunohistochemistry were immediately fixed in 4% formaldehyde and processed further.

**2.3. Hormonal and Biochemical Assays.** Serum levels of cytokines were measured by the multiplex assay MILLIPLEX® MAP Human Cytokine/Chemokine Magnetic Bead Panel (Merck KGaA, Darmstadt, Germany). Sensitivity for IFN- $\gamma$  was 0.8 pg/ml, for IL-6 0.9 pg/ml, for IL-8 0.4 pg/ml, and for TNF- $\alpha$  0.7 pg/ml. The intra- and interassay variabilities for all analytes were between 5.0 and 15.0%. Serum high-sensitivity C-reactive protein (hsCRP) levels were measured by high-sensitivity ELISA kit (Bender MedSystems, Vienna, Austria) with a sensitivity of 3 pg/ml. Insulin levels were measured by RIA kit (CIS Bio International, Gif-sur-Yvette, France). Sensitivity was 2.0  $\mu$ IU/ml. The intra- and interassay variabilities for all assays were between 5.0 and 10.0%.

Biochemical parameters were measured, and LDL cholesterol was calculated at the Department of Medical Biochemistry and Laboratory Diagnostics, General University Hospital, Prague, Czech Republic, by standard laboratory methods.

**2.4. Isolation of Stromal Vascular Fraction from Adipose Tissue and Flow Cytometry.** Standard 0.5-1.0 g amount of adipose tissue was minced with sterile scissors, and visible blood vessels were removed. Samples were washed with PBS, digested by 0.01% collagenase (Collagenase from *Clostridium histolyticum*, St. Louis, MO, USA) for 30 min at 37 °C, and centrifuged for 12 min at 1200x g. Visible

adipocytes were then manually collected from surface via a pipette with subsequent repeated washings and removal of remaining adipocytes from the supernatant. Finally, samples were filtered through Falcon® 40 µm Cell Strainer (Becton, Dickinson and Company, Franklin Lakes, USA) to eliminate any remnant adipocytes. Flow cytometry was performed using freshly isolated and filtered stromal vascular fraction or EDTA whole blood. A total amount of 100 µl of cell suspension with average 10<sup>6</sup> cell content was labeled by monoclonal antibodies conjugated with FITC (fluorescein isothiocyanate), PE (phycoerythrin), PerCP (peridinin-chlorophyll protein complex), and APC (allophycocyanin). For labelling a commercial lineage cocktail (CD3/CD14/CD16/CD19/CD20/CD56) FITC and single-labelled antibodies CD11c PE, HLA-DR PerCP, and CD123 APC (Exbio Prague, a.s., Vestec, Czech Republic) were used. The samples were labeled in the dark for 30 min at 2–8 °C, and then red cells were lysed using Excellyse I (Exbio Prague, a.s., Vestec, Czech Republic) according to the manufacturer's instructions. Finally, labelled cells were analyzed on BD Accuri™ C6 (Becton, Dickinson and Company, Franklin Lakes, NJ, USA). Data analysis was performed using FlowJo X 10.0.7r2 software (FlowJo, LCC, Ashland, OR, USA). Gating strategy was as follows: doublets were excluded, dendritic cells were gated according to HLA-DR positivity and lineage cocktail negativity, and then CD11c-positive and CD123-positive cells were assessed (Figure 1). HLA-DR+ lineage DC cells are expressed as percentage of single cells and their subtypes are expressed as percentage of HLA-DR+ lineage- DCs to determine DC composition. Minimal count of acquired events was 100,000.

**2.5. Statistical Analysis.** Statistical analysis was performed and graphs were drawn using SigmaPlot 13.0 (SPSS Inc., Chicago, IL, USA). Results are expressed as mean ± standard error of the mean (SEM). The unpaired *t*-test or Mann-Whitney rank sum test and paired *t*-test or Wilcoxon signed-rank test were used for the assessment of intergroup differences, as appropriate. The Spearman or Pearson correlation test was used to assess the association between DCs and other measured parameters. Multiple linear regression was used to assess the influence of T2DM, obesity, and coronary artery disease on the presence of DCs in tissues. Baseline data of all study subjects were used for correlation and regression analyses. Statistical significance was assigned to  $p < 0.05$ .

### 3. Results

**3.1. Anthropometric and Biochemical Parameters.** As expected, subjects with T2DM had higher fasting glucose and glycated hemoglobin levels along with increased BMI (body mass index) relative to non-T2DM individuals. Other anthropometric and biochemical parameters including age, lipid profile, creatinine, and hsCRP were comparable between both groups (Table 1). T2DM subjects showed elevated circulating levels of TNF-α and MCP-1 relative to the non-T2DM group, while no difference was present in other measured cytokines (Table 2).

**3.2. Dendritic Cells in Peripheral Blood, SAT, and EAT.** The total number of circulating DCs and their subtypes showed no differences between both study groups (Figure 2). T2DM subjects had reduced total DCs in SAT ( $1.57 \pm 0.65$  vs.  $4.45 \pm 1.56\%$  for T2DM vs. non-T2DM,  $p = 0.041$ ), while showing a similar, though insignificant, tendency in EAT ( $0.996 \pm 0.33$  vs.  $2.46 \pm 0.78\%$  for T2DM vs. non-T2DM,  $p = 0.171$ ). In either group, the amount of total DCs was comparable between SAT and EAT (Figure 2(a)). When analyzing DC subsets, no difference in the percentage of cDC could be seen between any of the studied groups or adipose tissue pools (SAT:  $15.7 \pm 2.6$  vs.  $11.5 \pm 3.2\%$  for T2DM vs. non-T2DM,  $p = 0.335$ ; EAT:  $16.2 \pm 3.9$  vs.  $16.0 \pm 4.6\%$  for T2DM vs. non-T2DM,  $p = 0.724$ ) (Figure 2(b)). In contrast, pDCs were increased in both SAT ( $13.5 \pm 2.0$  vs.  $4.6 \pm 1.9\%$  of DC cells,  $p = 0.005$ ) and EAT ( $29.1 \pm 8.7$  vs.  $8.4 \pm 2.4\%$  of DC,  $p = 0.045$ ) of T2DM relative to non-T2DM subjects as well as in EAT of the T2DM group compared with corresponding SAT ( $29.1 \pm 8.7$  vs.  $13.5 \pm 2.0\%$  of DC,  $p = 0.020$ ) (Figure 2(c)).

**3.3. Association of Dendritic Cells with Other Measured Parameters.** Total circulating DCs inversely correlated with glycemia ( $R = -0.528$ ,  $p = 0.004$ ) and hsCRP ( $R = -0.399$ ,  $p = 0.048$ ). Multiple linear regression showed glycemia as the only independent predictor ( $p = 0.044$ , Adj Rsqr = 0.129). Circulating cDCs positively correlated with serum IFN-γ ( $R = 0.425$ ,  $p = 0.043$ ) and inversely with C-peptide ( $R = -0.486$ ,  $p = 0.019$ ) and hsCRP levels ( $R = -0.434$ ,  $p = 0.030$ ), with only C-peptide exerting an independent association ( $p = 0.012$ , Adj Rsqr = 0.262). No correlation of total DCs, cDCs, or pDCs with any assessed parameters was observed in either SAT or EAT.

Multiple linear regression showed that the prevalence of DCs in EAT was associated with T2DM ( $p = 0.015$ ), but not with obesity ( $p = 0.051$ ) or coronary artery disease ( $p = 0.091$ ), the Adj Rsqr = 0.424. Similarly, T2DM was the sole positive predictor of pDCs in SAT ( $p = 0.025$ , Adj Rsqr = 0.398) as well as in EAT ( $p = 0.036$  for T2DM, Adj Rsqr = 0.377) with neither obesity nor coronary artery disease showing any association in either adipose tissue depot. In contrast, cDC showed no correlation with either T2DM, obesity, or CAD in any studied compartment.

### 4. Discussion

Dendritic cells are professional antigen-presenting cells responsible for maintaining immunological tolerance and coupling innate and adaptive immunity [7]. Adipose tissue DCs have been suggested to contribute to adipose tissue inflammation by regulating macrophage and T cell accumulation and activation [2]. Here, we show that in subjects with T2DM, total DCs are decreased in subcutaneous adipose tissue compared with nondiabetic individuals, while the subset of plasmacytoid DCs is increased both in SAT and EAT as well as in EAT relative to SAT.

Compared with the evidence of positive association between obesity and high-fat feeding and increased number of AT DCs, data on the relationship between AT DCs and

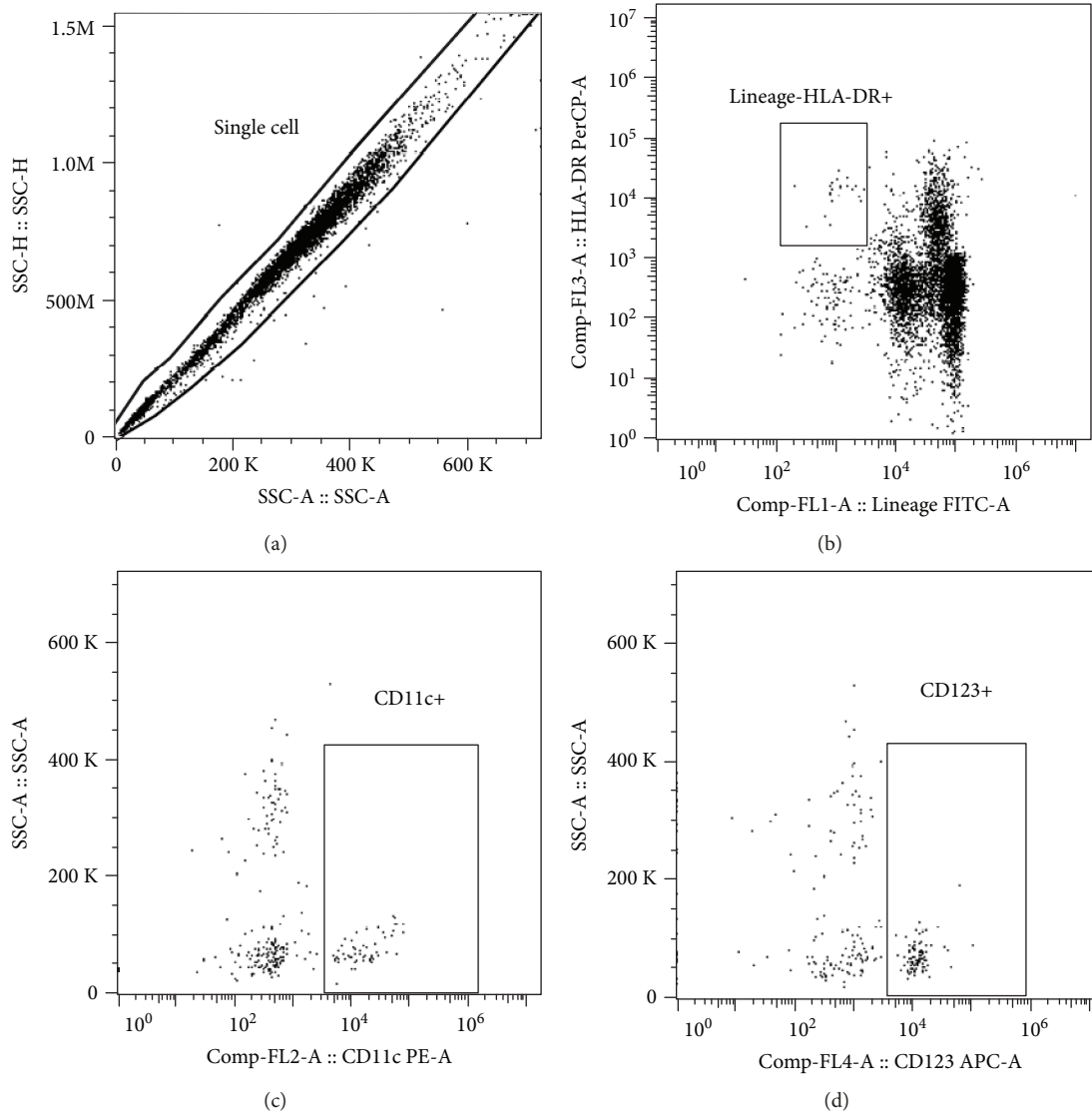


FIGURE 1: Flow cytometry gating strategy. Gating strategy was as follows: (a) single cells were gated, (b) total dendritic cells were assessed, and (c) CD11c+ conventional dendritic cells or (d) CD123+ plasmacytoid dendritic cells were gated.

insulin resistance or type 2 diabetes mellitus are much scarcer. Bertola et al. [10] showed positive correlation between DC marker CD1c and HOMA index of insulin resistance in SAT of subjects with and without T2DM and obesity. In a murine model, Cho et al. [13] demonstrated that the absence of the chemokine receptor CCR7, which is necessary for the high-fat diet-induced accumulation of DCs in adipose tissue, was associated with lower fasting glucose and insulin levels. In another experimental study, mice completely lacking DCs were protected against diet-induced obesity and insulin resistance; however, in this model, DCs were absent not only from adipose tissue but also from all other organs including the liver, which may have also contributed to the outcomes [12]. Here, we have rather surprisingly found reduced numbers of total DCs in SAT of T2DM subjects with a similar trend observed also in EAT despite increased fasting glucose and higher BMI in the diabetic group. On the other hand, higher prevalence of total

DCs in SAT relative to EAT in both groups corresponds well with the findings of Cho et al. [13], who reported increased numbers of DCs in SAT compared with omental adipose tissue in obese humans undergoing bariatric surgery. The partial discrepancies with previous results are not easily explained; however, as this is the first human study to directly assess the number of DCs in diabetic vs. nondiabetic subjects, no directly comparable data to verify these findings are available to date. Nevertheless, differences in DC assessment methodology and limited transferability of animal data to humans might have contributed to these outcomes. Clearly, other studies on larger patient populations are needed to clarify this issue.

Interestingly, while conventional DCs did not differ between both groups, plasmacytoid DCs were increased in diabetic subjects in both SAT and EAT in a manner completely opposite to total DCs. These findings are in line with the data of Ghosh et al. [16] who showed a positive

TABLE 1: Baseline characteristics of study subjects.

	Non-T2DM	T2DM
Number of subjects (males/females)	17 (14/3)	12 (9/3)
Age (year)	65.9 ± 3.3	66.2 ± 2.2
BMI (kg/m <sup>2</sup> )	27.4 ± 1.0	32.6 ± 1.2 <sup>x</sup>
Fasting glycemia (mmol/l)	5.81 ± 0.24	8.55 ± 0.74 <sup>x</sup>
HbA <sub>1c</sub> (mmol/mol)	36.9 ± 1.0	52.0 ± 3.4 <sup>x</sup>
Total cholesterol (mmol/l)	3.85 ± 0.25	4.39 ± 0.24
HDL cholesterol (mmol/l)	1.11 ± 0.07	1.33 ± 0.17
LDL cholesterol (mmol/l)	2.22 ± 0.21	2.34 ± 0.16
Triglycerides (mmol/l)	1.24 ± 0.13	1.79 ± 0.36
hs C-reactive protein (mg/ml)	5.06 ± 1.89	9.83 ± 3.08
Creatinine (μmol/l)	81.2 ± 5.4	82.8 ± 4.8
Arterial hypertension (n, %)	14 (82.4%)	12 (100%)
LVEF (%)	56.6 ± 3.9	50.6 ± 5.7
Coronary artery disease (n, %)	9 (52.9%)	9 (75.0%)

Data are presented as mean ± SEM. <sup>x</sup> $p < 0.05$  vs. non-DM. LVEF: left ventricular ejection fraction; CABG: coronary artery bypass graft.

TABLE 2: The influence of T2DM on circulating cytokine levels.

	Non-T2DM (n = 17)	T2DM (n = 12)
TNF- $\alpha$ (pg/ml)	4.224 ± 0.443	8.285 ± 1.439 <sup>x</sup>
IFN- $\gamma$ (pg/ml)	6.737 ± 2.232	5.599 ± 1.813
IL-6 (pg/ml)	2.586 ± 1.914	2.663 ± 1.062
IL-8 (pg/ml)	1.732 ± 0.385	3.168 ± 0.758
IL-23 (pg/ml)	453.7 ± 87.3	264.3 ± 67.5
MCP-1 (pg/ml)	121.5 ± 8.6	148.3 ± 26.6

Data are presented as mean ± SEM. <sup>x</sup> $p < 0.05$  vs. without T2DM.

correlation between the expression of pDC-specific transcripts (CLEC4C, INF signature genes) and HOMA index of insulin resistance in visceral adipose tissue of obese diabetic subjects. They also confirm the results of a murine model deficient in pDCs, in which the animals were protected from diet-induced obesity and insulin resistance [17]. Our findings thus suggest that in human adipose tissue, pDCs might be more important for the development of insulin resistance and T2DM than total or conventional DCs.

Epicardial adipose tissue, localized predominantly in the atrioventricular and interventricular grooves and free wall of the right ventricle, has been shown to be more proinflammatory than SAT and, due to its proximity to coronary arteries and the absence of a dividing fascia, has been suggested to directly contribute to the development of coronary artery disease [18–21]. Even though human data are rather limited, especially compared with SAT and abdominal VAT, EAT was reported to harbor most types of immune cells including macrophages, different subsets of T lymphocytes, and natural killer (NK) cells and B lymphocytes [15, 22, 23]. However, to date, only minimal information on DCs in animal EAT has been available, while no data exist for humans. In a model

of acute coronary syndrome, Horckmans et al. [15] showed that acute ligation of coronary arteries was associated with increased amount of DCs in EAT due to their migration from the infarct site in the myocardium. This process was reversed by B lymphocyte depletion or neutralization of granulocyte-macrophage colony-stimulating factor (GM-CSF). Similarly, in obese diabetic db/db mice, DCs accumulated predominantly in perivascular adipose tissue as compared with vessel wall and total depletion of DCs improved vasorelaxation in mesenteric arteries [24]. Here, we for the first time in humans identify total as well as conventional and plasmacytoid DCs in EAT. Strikingly, while total DCs tended to be lower in EAT relative to corresponding SAT regardless of the presence of T2DM as well as in EAT of diabetic compared with nondiabetic subjects and cDCs did not show any meaningful difference between both groups and adipose tissue pools, pDCs were significantly increased in EAT of T2DM individuals relative to both corresponding SAT and EAT of nondiabetics. This was corroborated by positive association between EAT pDCs and the presence of T2DM in multiple regression analysis. Interestingly, no independent relationship between EAT pDCs and obesity or coronary artery disease could be established in either group. As already mentioned, pDCs might contribute to adipose tissue inflammation by a number of mechanisms including macrophage recruitment and M1 polarization, maturation of conventional DCs, activation of B and T cells, or altered immune-metabolic interplay resulting from increased type I IFN production [9, 12, 16, 25–28]. Collectively, these data suggest a specific proinflammatory phenotype of EAT mediated by plasmacytoid DCs that is further augmented by the presence of type 2 diabetes mellitus. This hypothesis is supported by a recent transcriptomic analysis showing increased expression of a number of proinflammatory genes involved in TNF- $\alpha$ , NF- $\kappa$ B, and other inflammatory pathways in EAT from diabetic relative to nondiabetic individuals [29]. The cross-sectional nature of our study does not enable us to dissect cause from consequence; however, our data warrant further research into the function of pDCs in EAT, as these cells might comprise a potentially interesting target for therapeutic interventions.

The main limitations of our study include the relatively low sample size and preexisting differences, albeit mostly insignificant, in several baseline characteristics between both groups including BMI and the prevalence of coronary artery disease and arterial hypertension, even though multiple regression analysis was performed to account for most of the differences. Two different EAT sampling sites—anterior interventricular sulcus and right cardiac margin—could have also influenced the results as the periventricular and pericoronary location of EAT was recently shown to have different transcriptomic signatures [30]; however, sampling location in our study was guided primarily by the availability of EAT and thus could not be kept absolutely uniform in all participants.

## 5. Conclusions

Taken together, our study demonstrated for the first time in humans the presence of dendritic cells and their both

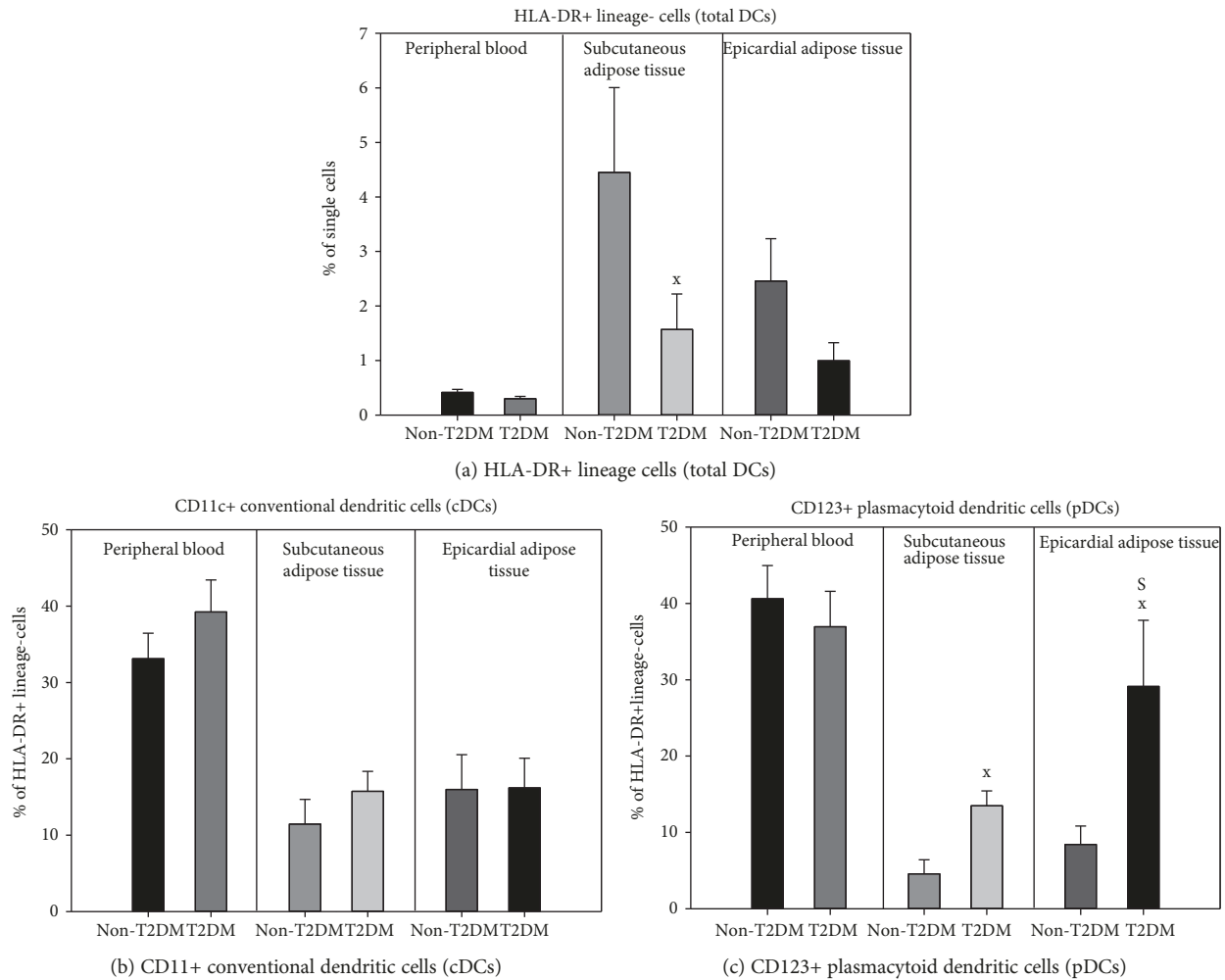


FIGURE 2: Dendritic cell populations in peripheral blood and subcutaneous and epicardial adipose tissue in subjects with and without type 2 diabetes mellitus. T2DM: type 2 diabetes mellitus; DCs: dendritic cells. Total DCs are gated as percentage of single cells, and other populations are gated as percentage of total DCs. <sup>x</sup> $p < 0.05$  T2DM vs. non-T2DM; <sup>S</sup> $p < 0.05$  subcutaneous vs. epicardial adipose tissue.

subtypes (conventional and plasmacytoid) in epicardial adipose tissue. It further showed that type 2 diabetes mellitus is associated with the reduction of total DCs in subcutaneous adipose tissue, while pDCs are conversely increased in subcutaneous and even more in epicardial adipose tissue. These findings suggest a potential role of pDCs in the development of T2DM and as a future therapeutic target.

### Data Availability

The data used to support the findings of this study are available from the corresponding author upon request.

### Conflicts of Interest

The authors declare that they have no conflict of interest.

### Acknowledgments

This work was supported by the Ministry of Health of the Czech Republic (grant number 15-26854A) and the

Ministry of Health of the Czech Republic Conceptual Development of Research Organization (“Institute for Clinical and Experimental Medicine” (IKEM), IN00023001 and RVO-VFN 64165).

### References

- [1] M. Collin and V. Bigley, “Human dendritic cell subsets: an update,” *Immunology*, vol. 154, no. 1, pp. 3–20, 2018.
- [2] S. Sundara Rajan and M. P. Longhi, “Dendritic cells and adipose tissue,” *Immunology*, vol. 149, no. 4, pp. 353–361, 2016.
- [3] N. Cools, P. Ponsaerts, V. F. I. van Tendeloo, and Z. N. Berneman, “Balancing between immunity and tolerance: an interplay between dendritic cells, regulatory T cells, and effector T cells,” *Journal of Leukocyte Biology*, vol. 82, no. 6, pp. 1365–1374, 2007.
- [4] T. Tamura, P. Taylor, K. Yamaoka et al., “IFN regulatory factor-4 and -8 govern dendritic cell subset development and their functional diversity,” *Journal of Immunology*, vol. 174, no. 5, pp. 2573–2581, 2005.

- [5] M. Gilliet, W. Cao, and Y. J. Liu, "Plasmacytoid dendritic cells: sensing nucleic acids in viral infection and autoimmune diseases," *Nature Reviews Immunology*, vol. 8, no. 8, pp. 594–606, 2008.
- [6] M. Merad, P. Sathe, J. Helft, J. Miller, and A. Mortha, "The dendritic cell lineage: ontogeny and function of dendritic cells and their subsets in the steady state and the inflamed setting," *Annual Review of Immunology*, vol. 31, no. 1, pp. 563–604, 2013.
- [7] C. Y. J. Chung, D. Ysebaert, Z. N. Berneman, and N. Cools, "Dendritic cells: cellular mediators for immunological tolerance," *Clinical & Developmental Immunology*, vol. 2013, article 972865, 8 pages, 2013.
- [8] G. Murdolo and U. Smith, "The dysregulated adipose tissue: a connecting link between insulin resistance, type 2 diabetes mellitus and atherosclerosis," *Nutrition, Metabolism, and Cardiovascular Diseases*, vol. 16, Supplement 1, pp. S35–S38, 2006.
- [9] C. E. Macdougall, E. G. Wood, J. Loschko et al., "Visceral adipose tissue immune homeostasis is regulated by the crosstalk between adipocytes and dendritic cell subsets," *Cell Metabolism*, vol. 27, no. 3, pp. 588–601.e4, 2018.
- [10] A. Bertola, T. Ciucci, D. Rousseau et al., "Identification of adipose tissue dendritic cells correlated with obesity-associated insulin-resistance and inducing Th17 responses in mice and patients," *Diabetes*, vol. 61, no. 9, pp. 2238–2247, 2012.
- [11] Y. Chen, J. Tian, X. Tian et al., "Adipose tissue dendritic cells enhances inflammation by prompting the generation of Th17 cells," *PLoS One*, vol. 9, no. 3, article e92450, 2014.
- [12] M. Stefanovic-Racic, X. Yang, M. S. Turner et al., "Dendritic cells promote macrophage infiltration and comprise a substantial proportion of obesity-associated increases in CD11c<sup>+</sup> cells in adipose tissue and liver," *Diabetes*, vol. 61, no. 9, pp. 2330–2339, 2012.
- [13] K. W. Cho, B. F. Zamarron, L. A. Muir et al., "Adipose tissue dendritic cells are independent contributors to obesity-induced inflammation and insulin resistance," *Journal of Immunology*, vol. 197, no. 9, pp. 3650–3661, 2016.
- [14] J. Salazar, E. Luzardo, J. C. Mejías et al., "Epicardial fat: physiological, pathological, and therapeutic implications," *Cardiology Research and Practice*, vol. 2016, Article ID 1291537, 15 pages, 2016.
- [15] M. Horckmans, M. Bianchini, D. Santovito et al., "Pericardial adipose tissue regulates granulopoiesis, fibrosis, and cardiac function after myocardial infarction," *Circulation*, vol. 137, no. 9, pp. 948–960, 2018.
- [16] A. R. Ghosh, R. Bhattacharya, S. Bhattacharya et al., "Adipose recruitment and activation of plasmacytoid dendritic cells fuel metaflammation," *Diabetes*, vol. 65, no. 11, pp. 3440–3452, 2016.
- [17] T. D. Hannibal, A. Schmidt-Christensen, J. Nilsson, N. Fransén-Petersson, L. Hansen, and D. Holmberg, "Deficiency in plasmacytoid dendritic cells and type I interferon signalling prevents diet-induced obesity and insulin resistance in mice," *Diabetologia*, vol. 60, no. 10, pp. 2033–2041, 2017.
- [18] E. Henrichot, C. E. Juge-Aubry, A. Pernin et al., "Production of chemokines by perivascular adipose tissue: a role in the pathogenesis of atherosclerosis?," *Arteriosclerosis, Thrombosis, and Vascular Biology*, vol. 25, no. 12, pp. 2594–2599, 2005.
- [19] G. Iacobellis, D. Corradi, and A. M. Sharma, "Epicardial adipose tissue: anatomic, biomolecular and clinical relationships with the heart," *Nature Clinical Practice Cardiovascular Medicine*, vol. 2, no. 10, pp. 536–543, 2005.
- [20] Y. Hirata, H. Kurobe, M. Akaike et al., "Enhanced inflammation in epicardial fat in patients with coronary artery disease," *International Heart Journal*, vol. 52, no. 3, pp. 139–142, 2011.
- [21] E. A. McAninch, T. L. Fonseca, R. Poggioli et al., "Epicardial adipose tissue has a unique transcriptome modified in severe coronary artery disease," *Obesity*, vol. 23, no. 6, pp. 1267–1278, 2015.
- [22] E. Vianello, E. Dozio, F. Arnaboldi et al., "Epicardial adipocyte hypertrophy: association with M1-polarization and toll-like receptor pathways in coronary artery disease patients," *Nutrition, Metabolism, and Cardiovascular Diseases*, vol. 26, no. 3, pp. 246–253, 2016.
- [23] T. Mazurek, L. F. Zhang, A. Zalewski et al., "Human epicardial adipose tissue is a source of inflammatory mediators," *Circulation*, vol. 108, no. 20, pp. 2460–2466, 2003.
- [24] T. Qiu, M. Li, M. A. Tanner et al., "Depletion of dendritic cells in perivascular adipose tissue improves arterial relaxation responses in type 2 diabetic mice," *Metabolism*, vol. 85, pp. 76–89, 2018.
- [25] V. A. Koivisto, R. Pelkonen, and K. Cantell, "Effect of interferon on glucose tolerance and insulin sensitivity," *Diabetes*, vol. 38, no. 5, pp. 641–647, 1989.
- [26] D. Braun, I. Caramalho, and J. Demengeot, "IFN- $\alpha/\beta$  enhances BCR-dependent B cell responses," *International Immunology*, vol. 14, no. 4, pp. 411–419, 2002.
- [27] K. Bratke, C. Klein, M. Kuepper, M. Lommatzsch, and J. C. Virchow, "Differential development of plasmacytoid dendritic cells in Th1- and Th2-like cytokine milieus," *Allergy*, vol. 66, no. 3, pp. 386–395, 2011.
- [28] M. Alsharifi, M. Lobigs, M. Regner, E. Lee, A. Koskinen, and A. Mullbacher, "Type I interferons trigger systemic, partial lymphocyte activation in response to viral infection," *Journal of Immunology*, vol. 175, no. 7, pp. 4635–4640, 2005.
- [29] V. Camarena, D. Sant, M. Mohseni et al., "Novel atherogenic pathways from the differential transcriptome analysis of diabetic epicardial adipose tissue," *Nutrition, Metabolism and Cardiovascular Diseases*, vol. 27, no. 8, pp. 739–750, 2017.
- [30] B. Gaborit, N. Venteclef, P. Ancel et al., "Human epicardial adipose tissue has a specific transcriptomic signature depending on its anatomical peri-atrial, peri-ventricular, or pericoronary location," *Cardiovascular Research*, vol. 108, no. 1, pp. 62–73, 2015.

## Research Article

# Epigenetic Regulation of IL-17-Induced Chemokines in Lung Epithelial Cells

Jiadi Luo <sup>1,2</sup>, Xiaojing An,<sup>2</sup> Yong Yao,<sup>2</sup> Carla Erb,<sup>2</sup> Annabel Ferguson,<sup>2</sup> Jay K. Kolls,<sup>3</sup> Songqing Fan,<sup>1</sup> and Kong Chen <sup>2</sup>

<sup>1</sup>Department of Pathology, The Second Xiangya Hospital, Central South University, Changsha, Hunan, China

<sup>2</sup>Division of Pulmonary Medicine, Allergy, and Critical Care Medicine, University of Pittsburgh Medical Center, Pittsburgh, PA, USA

<sup>3</sup>Department of Medicine, Tulane School of Medicine, New Orleans, LA, USA

Correspondence should be addressed to Kong Chen; koc5@pitt.edu

Received 11 November 2018; Accepted 18 December 2018; Published 17 March 2019

Guest Editor: Minggang Zhang

Copyright © 2019 Jiadi Luo et al. This is an open access article distributed under the Creative Commons Attribution License, which permits unrestricted use, distribution, and reproduction in any medium, provided the original work is properly cited.

Epithelial cells are known to have barrier functions in multiple organs and regulate innate immune responses. Airway epithelial cells respond to IL-17 by altering their transcriptional profiles and producing antimicrobial proteins and neutrophil chemoattractants. Although IL-17 has been shown to promote inflammation through stabilizing mRNA of CXCR2 ligands, how IL-17 exerts its downstream effects on its target cells through epigenetic mechanisms is largely unknown. Using primary human bronchial epithelial cells and immortalized epithelial cell line from both human and mouse, we demonstrated that IL-17-induced CXCR2 ligand production is dependent on histone acetylation specifically through repressing HDAC5. Furthermore, the chemokine production induced by IL-17 is strictly dependent on the bromodomain and extraterminal domain (BET) family as BET inhibition abolished the IL-17A-induced proinflammatory chemokine production, indicating a pivotal role of the recognition of acetylated histones. In combination with single-cell RNA-seq analysis, we revealed that the cell lines we employed represent specific lineages and their IL-17 responses were regulated differently by the DNA methylation mechanisms. Taken together, our data strongly support that IL-17 sustains epithelial CXCR2 ligand production through epigenetic regulation and the therapeutic potential of interrupting histone modification as well as the recognition of modified histones could be evaluated in neutrophilic lung diseases.

## 1. Introduction

The IL-17 cytokine family includes 6 members, which are produced by multiple cell types [1] and signal through the IL-17 receptor family [2]. IL-17RA is shared among many IL-17 family members, while IL-17RC is the unique receptor for IL-17 and IL-17F. IL-17 and IL-17F have been demonstrated to be critical players in host defense and inflammatory diseases [3–5]. Airway epithelial cells respond to IL-17 through producing antimicrobial proteins and neutrophil chemoattractants, promoting to eradicate extracellular pathogens such as *K. pneumoniae* in the setting of host defense [6] while contributing to tissue damage and lung pathology in chronic inflammatory diseases [7].

The chemokine superfamily has expanded rapidly, since the identification of CXCL8 (IL-8) and CCL2 (MCP-1) in the late 1980s [8]. CXCR2 is mainly expressed on neutrophils and mediates neutrophil migration to sites of inflammation [9]. Several studies, including our previous work, have shown that IL-17 is a key driver for the production of these CXCR2 ligands both in vitro and in vivo [10–12]. IL-17 can promote chemokine production through mRNA stabilization and prolongation of chemokine half-life [12–15]. However, this mechanism does not explain why primary cells derived from patients with chronic inflammatory diseases spontaneously produce CXCR2 ligands without any further ex vivo stimulation [16–18]. This leads us to hypothesize that the chromatin state of these loci has been modulated to become

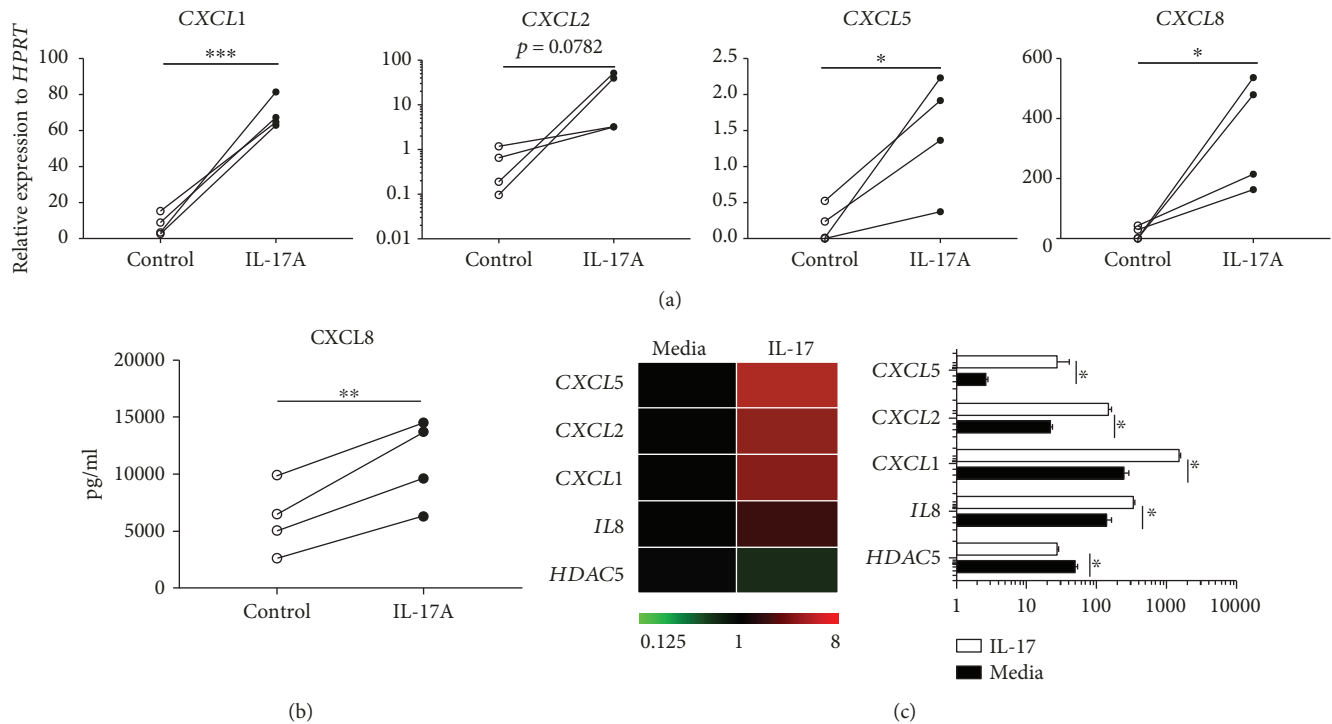


FIGURE 1: IL-17A induces proinflammatory chemokine production in primary human airway epithelial cells. (a) NHBE cells from 4 donors (derived from CORE donors) were established in the air-liquid interphase culture and treated with human recombinant IL-17A protein 100 ng/ml or control medium for 48 h. RT-PCR was performed to detect chemokine mRNA level. (b) Supernatant at 48 h was collected to measure the CXCL8 protein level by ELISA. (c) Heat map of the expression of multiple CXCR2 ligands and *HDAC5* expression in normal HBE cell cultured in air-liquid interphase in the presence or absence of 100 ng/ml IL-17 in basal media for 48 h. \* $p < 0.05$ ; \*\* $p < 0.01$ ; \*\*\* $p < 0.001$ ; by paired *t*-test, one-tailed.

constitutively active and this active chromatin state leads to enhanced chemokine production in these diseased settings. Indeed, such permissive chromatin structural changes in CXCR2 ligands have been observed in both skin infection [19] and lung cancer [20].

To determine if there is any epigenetic regulation in IL-17-mediated chemokine production in the lung epithelium, we took advantage of several unique inhibitors targeting various epigenetic pathways including DNA methylation and acetylated histone recognition. Our study provides novel findings on epigenetic regulation of IL-17 signaling in the lung epithelial cells and suggests an alternative epigenetic pathway to target the treatment and diagnosis of chronic inflammatory diseases.

## 2. Results

The synergistic effects of IL-17 and TNF- $\alpha$  on the expression of IL-17-induced responses are well established [2]. To determine if IL-17 alone can induce proinflammatory chemokine production, we treated primary normal human bronchial epithelial (NHBE) cells and examined the induction of CXCR2 ligands. The data by RT-PCR and ELISA both suggested that the induction was robust and consistent among 4 different donors (Figures 1(a) and 1(b)). Since we are particularly interested in the epigenetic regulation of this induction, we mined RNA-seq data published earlier on IL-17-stimulated primary NHBE cells with the focus on these

chemokines and genes that are involved in DNA methylation and histone modification. We found histone acetyltransferase (HAT) expressions were unaltered while one of the histone deacetylases, e.g., *HDAC5*, is significantly downregulated (Figure 1(c), Figure S1), suggesting that IL-17 could enhance these CXCR2 ligands through histone deacetylation. HDACs have the ability to dynamically regulate gene expression through the removal of acetyl groups from lysine residues. This process subsequently changes the chromatin accessibility and has major impacts on transcription.

Primary NHBE cells contain a heterogeneous population (e.g., ciliated, secretory, and basal) and could have variability in a number of responses. Therefore, to examine the underlying mechanisms by IL-17, we chose an epithelial cell line derived from a normal donor [21]. RNA-seq analysis on IL-17-treated HBE1 cells demonstrated that the gene expression profile is similar between primary NHBE cells and HBE1 cell line (Figure 2), especially in terms of the CXCR2 ligand induction including *CXCL1*, *CXCL2*, and *CXCL8*. *CXCL5* expression was extremely low in these cells, and we were unable to detect its expression by PCR (data not shown). According to our single-cell RNA-seq analysis in the normal human lung mononuclear cells, these cells had a similar gene expression profile to bronchial epithelial cells which highly express *SCGB1A1* (Figure 3). In contrast, the more type II cell-like population (marked by more *SFTPC*) seemed to be the *CXCL5* producers while both populations seemed to produce other CXCR2 ligands to the same degree (Figure 3).

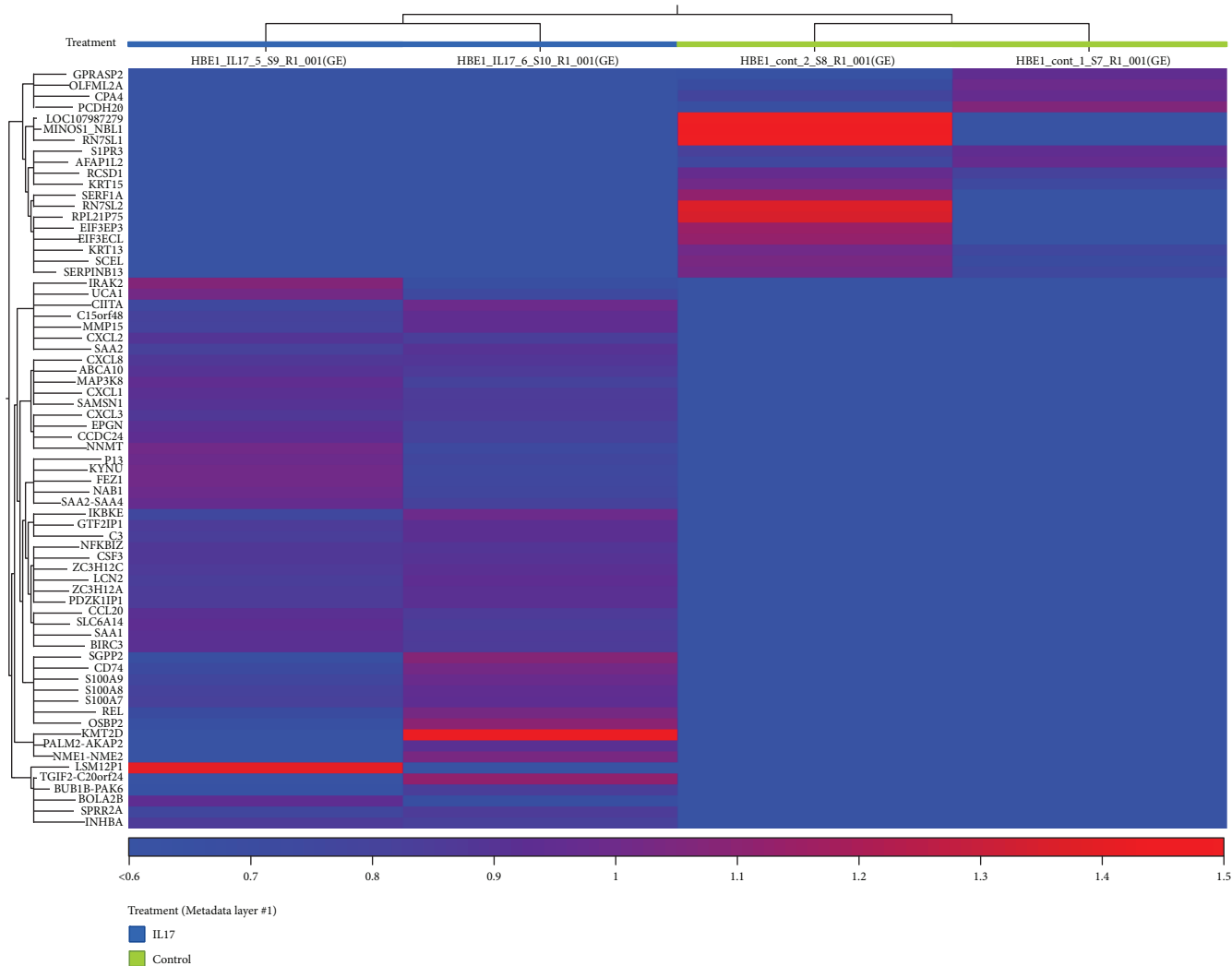


FIGURE 2: Heat map of genes regulated by IL-17A in HBE1 cells. Cells from the left two columns (under the blue bar) were treated with 100 ng/ml h-IL-17A protein for 24 h while the right two columns (under the green bar) were treated with the control medium for 24 h.

Ingenuity Pathway Analysis (IPA) identified several top canonical pathways that were related to IL-17 signaling in a variety of cell types including the role of IL-17A in psoriasis, IL-17A signaling in fibroblasts, and differential regulation of cytokine production in intestinal epithelial cells by IL-17A and IL-17F (Figure S2A), suggesting HBE1 cells were IL-17 responsive and could be used to study signaling pathways mediated by IL-17. With the same dataset and the same upstream regulator analytic setting from the IPA software, several signaling pathways associated with innate immunity (lipopolysaccharide, TLR4) and inflammation (TNF, IL1A, and IL17C) (Figure S2B) were identified, similar to an analysis on the bronchial epithelium carried out earlier using an in vivo model [6], further proved that the HBE1 cell lines could serve as a tool for investigating the role of IL-17 in the lung epithelial cells.

Histone acetylation usually increases chromatin accessibility and based on the RNA-seq data from primary NHBE cells (Figure 1(c)), we decided to test if histone deacetylation would affect the IL-17 signaling by overexpressing HDAC5 using adenoviral transduction. HDAC5 overexpression was

successfully achieved as assessed by PCR (Figure 4(a)) and Western blotting (Figure 4(b)). More importantly, CXCR2 ligand gene expression including *CXCL1*, *CXCL2*, and *CXCL8* was substantially repressed (Figure 4(c)), and this was also confirmed at *CXCL8* protein level (Figure 4(d)).

Chromatin remodeling is well known accomplished through two main mechanisms: histone modification and DNA methylation. To explore the potential regulatory mechanism in IL-17-induced chemokine production in lung epithelial cells, we treated IL-17-stimulated HBE1 cells with 5-azacytidine (5AZ), a DNA methyltransferase inhibitor. However, inhibition DNA methyltransferase activity did not cause significant CXCR2 ligand induction or reduction in these cells, compared to single IL-17-stimulated HBE1 cells (Figure 5), suggesting that histone acetylation rather than DNA methylation is a key regulator in these cells. In contrast, when these cells were treated with a small molecule inhibitor (CPI) which blocks BET bromodomain binding, IL-17-induced CXCR2 ligand production was substantially reduced (Figure 6), suggesting an essential role of the recognition of acetylated histones in this pathway. To further

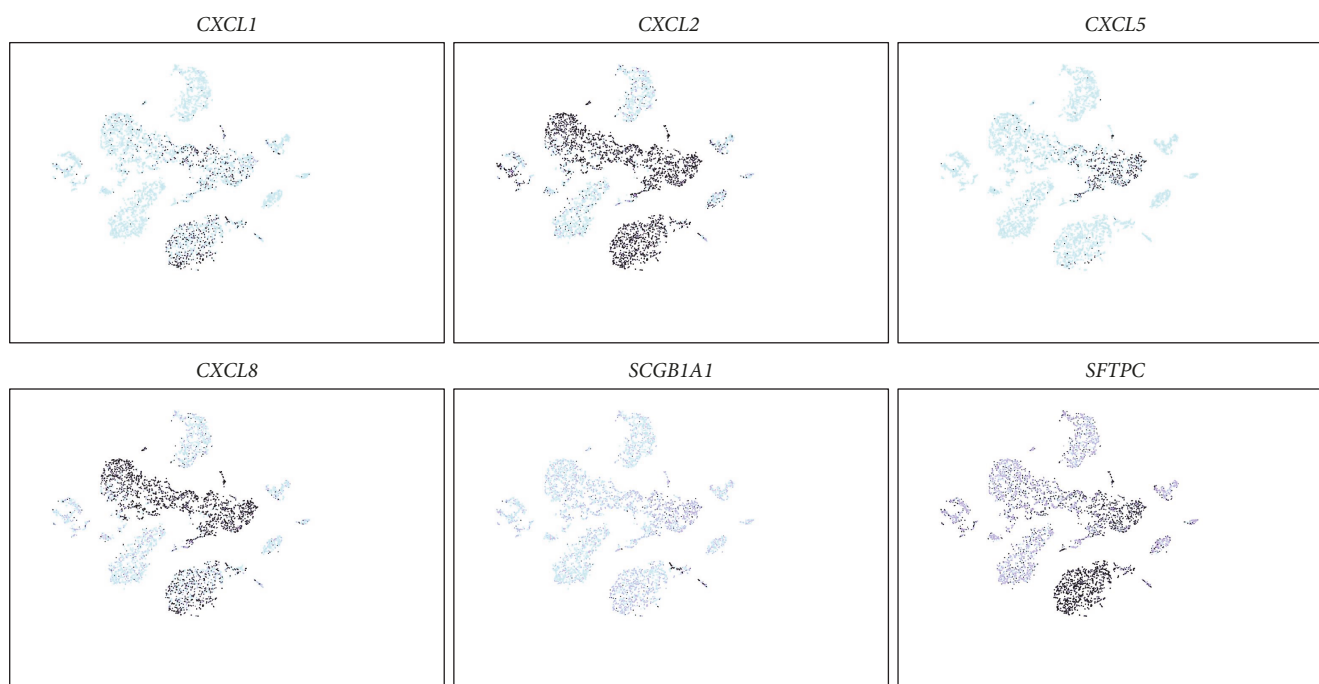


FIGURE 3: Human lung scRNA-seq. Cells were grouped into several clusters. The classification of specific cell types was inferred from the annotation of cluster-specific genes and based on expression of some well-known markers of certain cell types. *CXCL1*, *CXCL2*, *CXCL5*, *CXCL8*, *SCGB1A1*, and *SFTPC* expression cells were displayed in the cell population separately. The darker the color the cell was labelled, the higher mRNA level of target gene the cell had (the light green cells were the ones without the target gene expression).

investigate whether this epigenetic regulation is specific to human cells, we treated the mouse lung epithelial cell line, MLE12, with IL-17 in the presence or absence of 5AZ or CPI (Figure 7). Interestingly, *CXCL1* induction was further enhanced by the inhibition of DNA methylation, suggesting that these murine cells or type II-like cells [22] can be regulated at DNA methylation level. However, BET inhibition again substantially reduced the *CXCL1* expression, indicating that BET binding is essential for the induction of IL-17 downstream chemokines and this regulation is conserved in mammals. We also conducted RNA-seq analysis on IL-17-treated MLE12 cells and confirmed *CXCL1* as one of the top induced genes (Figure 8) and IPA analysis also suggested enrichment of the IL-17A and NF- $\kappa$ B signaling pathways (Figure S3).

### 3. Discussion

IL-17 has been implicated to play essential roles in many proinflammatory lung diseases including asthma and cystic fibrosis (CF). In CF patients, chronic *Pseudomonas aeruginosa* (PA) infection leads to increased mortality by promoting irritated airway inflammation and cumulative lung damage in CF patients [23]. IL-17 levels elevated in the sputum during CF exacerbations [24], and CD4<sup>+</sup> Th17 cells are identified as a critical source of IL-17 in the CF lung [25]. Indeed, PA-specific Th17 responses have been observed in the lymph nodes from patients with CF [25]. Although IL-17-mediated inflammation is essential for the clearance of extracellular pathogens such as *K. pneumoniae* and *C. albicans* [3] in several acute infection models, recent studies also

suggested a possible detrimental role of the IL-17 downstream signaling in a chronic PA lung infection model through recruitment of neutrophils [26, 27]. Furthermore, HCO<sub>3</sub><sup>-</sup> is indispensable for the antimicrobial function of the CF airway [28], and HCO<sub>3</sub><sup>-</sup> transport can be regulated in normal human bronchial epithelial cells, however, in a cystic fibrosis transmembrane conductance regulator- (CFTR-) dependent fashion [29]. Thus, in the absence of functional CFTR, IL-17 likely contributes to pathological inflammation [3], and IL-17 itself or its downstream signaling may represent a novel target to manage the neutrophilic lung inflammation in CF. In this study, normal human and mouse cell lines were used to identify key epigenetic mechanisms of chemokine production induced by IL-17, suggesting these pathways are not unique to CF and these implications can be adapted to other lung diseases such as asthma and chronic obstructive pulmonary disease (COPD).

Epigenetic marks on histones are related to transcriptional processes. For example, trimethylated histone H3K4 is enriched at promoters [30], while monomethylated H3K4 and acetylated H3Lys27 (H3K27ac) are enriched at active enhancers [31, 32]. The bromodomain and extraterminal domain (BET) family proteins, including BRD2, BRD3, BRD4, and BRDT, contain two bromodomains, which recognize and interact with acetylated histones and other acetylated proteins with varying degrees of affinity. Small-molecule BET inhibitors mimic the acetyl moiety and insert into the bromodomain acetyl-lysine-binding pocket, which is unique to the BET family proteins. It has been shown that BRD4 plays a critical role in IL-1 $\beta$ -induced inflammation in human airway epithelial cells [33], and we have confirmed

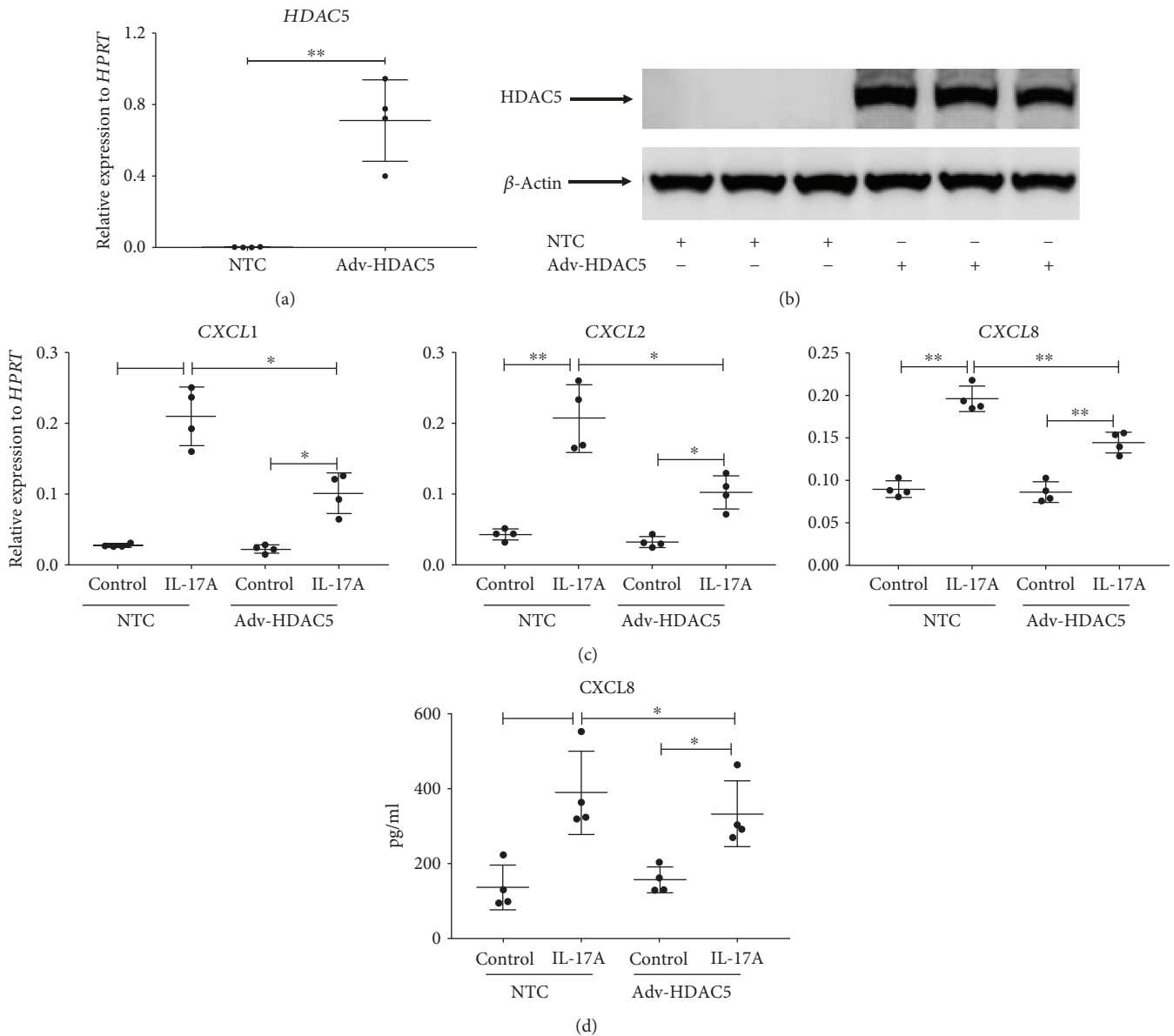


FIGURE 4: Induction of proinflammatory chemokines mediated by IL-17A can be suppressed by overexpressing HDAC5. HBE1 cells were plated 0.08-0.15 million cells per well in a 12-well plate. When 70-80% confluent, cells were transfected with 0.1 moi human HDAC5 adenovirus and nontarget adenovirus in 300  $\mu$ l medium, respectively, for one hour, and then we added 100 ng/ml h-IL-17A protein or 700  $\mu$ l control medium directly into each corresponding well in both adenovirus-infected groups. 24 h after transfection, (a) *HDAC5*, (c) *CXCL1*, *CXCL2*, and *CXCL8* mRNA levels were determined by RT-PCR. (d) 48 h supernatant after transfection was collected. *CXCL8* protein level was achieved by ELISA. \* $p < 0.05$ ; \*\* $p < 0.01$ ; by paired  $t$ -test, two-tailed. (b) *HDAC5* protein level of cells with adenovirus transfection for 24 h was detected by Western blotting ( $\beta$ -actin as reference). This experiment has been repeated.

high levels of expression of BRD2, BRD3, and BRD4 in primary HBE cells as well as bronchial brushings obtained by clinical bronchoscopy [34], making BET inhibitors ideal candidates for blocking the constitutively active loci that have active histone marks. BET inhibition has been shown to reduce naive T cells differentiate into Th17 cells [35], consistent with the data showing that suppression of IL-17 produced by T cells isolated from CF lungs following BET inhibition. We believe that the optimal suppression of airway inflammation will be achieved by targeting both the production of IL-17 and the downstream chemokine

expression. This may be critically true for chronic diseases where the genomic landscape of CXCR2 ligands is altered in the lung epithelium. Indeed, we found CXCR2 ligand production in epithelial cells can be inhibited by a BET inhibitor. However, the exact mechanism as to which histone modification yielded the inhibition needs further definition by the chromatin immunoprecipitation assay.

Primary HBE cells are heterogeneous and can be difficult to manipulate in knockdown and overexpression experiments. Thus, we used the cell lines, HBE1 and MLE12. Histone acetylation is regulated by both histone acetyltransferases (HATs)

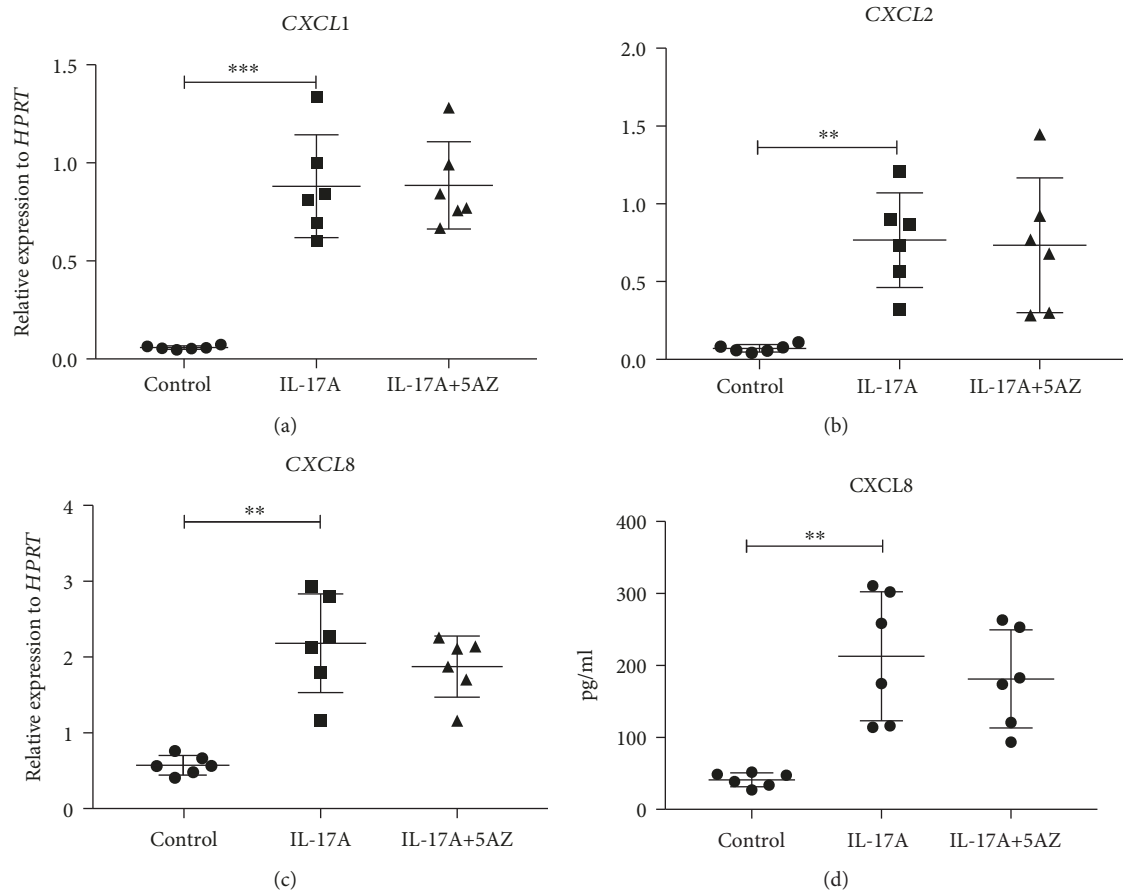


FIGURE 5: DNA methyltransferase inhibition in HBE1 cells. HBE1 cells were plated 0.08-0.15 million cells per well in a 12-well plate. After incubating with BronchiaLife™ Epithelial Airway Medium overnight, cells were treated with control medium, 100 ng/ml h-IL-17A protein, 1  $\mu$ M 5-azacytidine, and 100 ng/ml h-IL-17A plus 1  $\mu$ M 5-azacytidine, respectively. 6 h after stimulation, chemokine production (a) CXCL1, (b) CXCL2, and (c) CXCL8 was determined by RT-PCR. (d) 24 h supernatant was collected, and CXCL8 protein level was obtained by ELISA. \* $p < 0.05$ ; \*\* $p < 0.01$ ; \*\*\* $p < 0.001$ ; by paired  $t$ -test, two-tailed. This experiment has been repeated.

and HDAC enzymes. We did not hypothesize a regulatory mechanism by HAT as our RNA-seq data showed that HAT expression was not affected by IL-17 stimulation. However, in the experiments with HDAC overexpression, HAT can play a role to compromise the effect of altered HDAC5 expression, which may explain why we observed a modest effect using adenovirus overexpressing HDAC5 (Figure 4). Thus, the expression of HATs will be further examined by RNA-seq. HDAC5 phosphorylation and subcellular distribution have been implicated in regulating gene expression [36, 37] and could be carefully determined by Western blot in the future.

In this study, we observed major differences in DNA methylation regulation in human cells (Figure 5) vs. mouse cells (Figure 7). As to a certain gene expression, different organisms/tissues use different epigenetic machinery, so do different species. We found differential expression of Human antigen R (HuR), encoded by *ELAVL1*, in HBE1 and MLE12 cells (Figure S4). The ubiquitously expressed HuR protein was recently shown to regulate the expression of DNA methyltransferases posttranscriptionally [38]. Therefore, the lower expression of *ELAVL1* may explain why HBE1 cells are less sensitive to DNA methyltransferase inhibition, indicating that a tissue-specific targeting of epigenetic regulation should

be considered in future drug development. The observed differences are also likely due to sequence differences in the mouse and human genome, for example, differences in CpG island distribution near the promoter regions could lead to the loci to be more resistant to DNA methylation.

Taken together, our data support IL-17 enhances chemokine production in lung epithelial cells through histone modification and recognition and the therapeutic potential of interrupting this pathway could be evaluated in IL-17-mediated diseases.

## 4. Materials and Methods

**4.1. Primary Cell Culture and Stimulation.** Human lung parenchyma tissue was processed to isolate mononuclear cells, as we previously described [34]. Cells were used for single-cell RNA sequencing (scRNA-seq) analysis.

Normal human bronchial epithelial cells (NHBE cells) obtained from the University of Pittsburgh tissue and cell core lab were prepared according to the previously described methods approved by the University of Pittsburgh IRB [39]. Cells established in the air-liquid interphase culture were exposed to 100 ng/ml human recombinant IL-17A protein

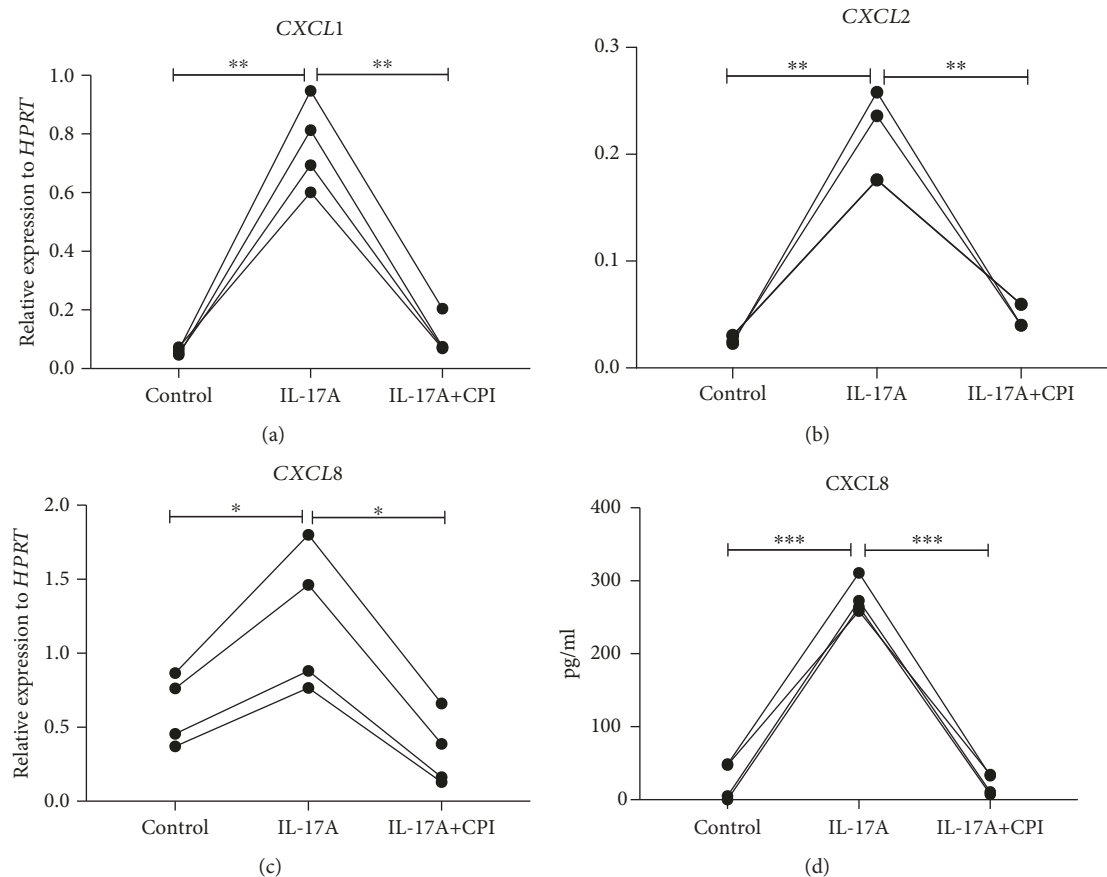


FIGURE 6: Induction of proinflammatory chemokines is dependent on BET. Human bronchial epithelial cell line HBE1 cells were plated 0.08-0.15 million cells per well in a 12-well plate. After incubating with BronchiaLife™ Epithelial Airway Medium overnight, cells were treated with control medium, 100 ng/ml h-IL-17A protein, 200 nM CPI, and 100 ng/ml h-IL-17A plus 200 nM CPI, respectively. 6 h after stimulation, (a) *CXCL1*, (b) *CXCL2*, and (c) *CXCL8* mRNA levels were determined by RT-PCR. (d) 24 h after stimulation, supernatant was collected and CXCL8 protein level was measured by ELISA. \* $p < 0.05$ ; \*\* $p < 0.01$ ; \*\*\* $p < 0.001$ ; by a one-way ANOVA test. It is the representative figure from 4 experiments.

(BioLegend, Cat# 570506) or control medium for 48 h. Cells were harvested in a QIAGEN RLT buffer for further gene expression detection.

**4.2. Cell Line Culture and Stimulation.** Human bronchial epithelial cell line HBE1 cells [21] were cultured in complete a bronchial epithelial airway medium (BronchiaLife™ Epithelial Airway Medium Complete Kit, Lifeline, LL-0023). Cells were plated 0.08-0.15 million cells in 1 ml medium per well in a 12-well plate. Around 80% of confluence, cells were then treated with control medium, 100 ng/ml h-IL-17A protein, 1  $\mu$ M 5-azacytidine (Sigma, Cat# A2385), 200 nM CPI (Cayman, Cat# 15479), 100 ng/ml h-IL-17A plus 1  $\mu$ M 5-azacytidine, and 100 ng/ml h-IL-17A plus 200 nM CPI, respectively, for 6 h or 24 h. At 6 h time point, cells were lysed in a RLT buffer with 2-mercaptoethanol for RNA extraction and later gene expression; at 24 h time point, supernatant was collected for ELISA. Cells stimulated with or without 100 ng/ml h-IL-17A medium for 24 h were harvested for mRNA-seq.

Murine lung epithelial cell line MLE12 cells [22] were cultured with HITES (DMEM/F12 with hydrocortisone, insulin, transferrin, estradiol, and selenium) medium

containing 10% fetal bovine serum (FBS) and antibiotics at 37°C in an incubator containing 5% CO<sub>2</sub>. Similar to HBE1 cells, MLE12 cells were stimulated with a control medium, 50 ng/ml m-IL-17A protein (BioLegend, Cat# 576004), 1  $\mu$ M 5-azacytidine, 200 nM CPI, 50 ng/ml h-IL-17A plus 1  $\mu$ M 5-azacytidine, and 50 ng/ml h-IL-17A plus 200 nM CPI, respectively, for 6 h or 24 h. 6 h after stimulation, cells were obtained for further RNA extraction and mRNA-seq; 24 h after stimulation, supernatant was collected for protein measurement.

**4.3. HDAC5 Overexpression.** HBE1 cells were plated 0.08-0.15 million cells per well in a 12-well plate. When 70-80% confluent, cells were transfected with 0.1 moi human HDAC5 adenovirus (a.b.m., Cat# 096660A) and nontarget adenovirus (a.b.m., Cat# 000541A) in 300  $\mu$ l medium, respectively, for one hour, and then we added 100 ng/ml h-IL-17A protein or 700  $\mu$ l control medium directly into each corresponding well in both adenovirus-infected groups. 24 h after transfection, cells were harvested for protein and gene expression measurement; 48 h after transfection, supernatant was obtained for protein detection.

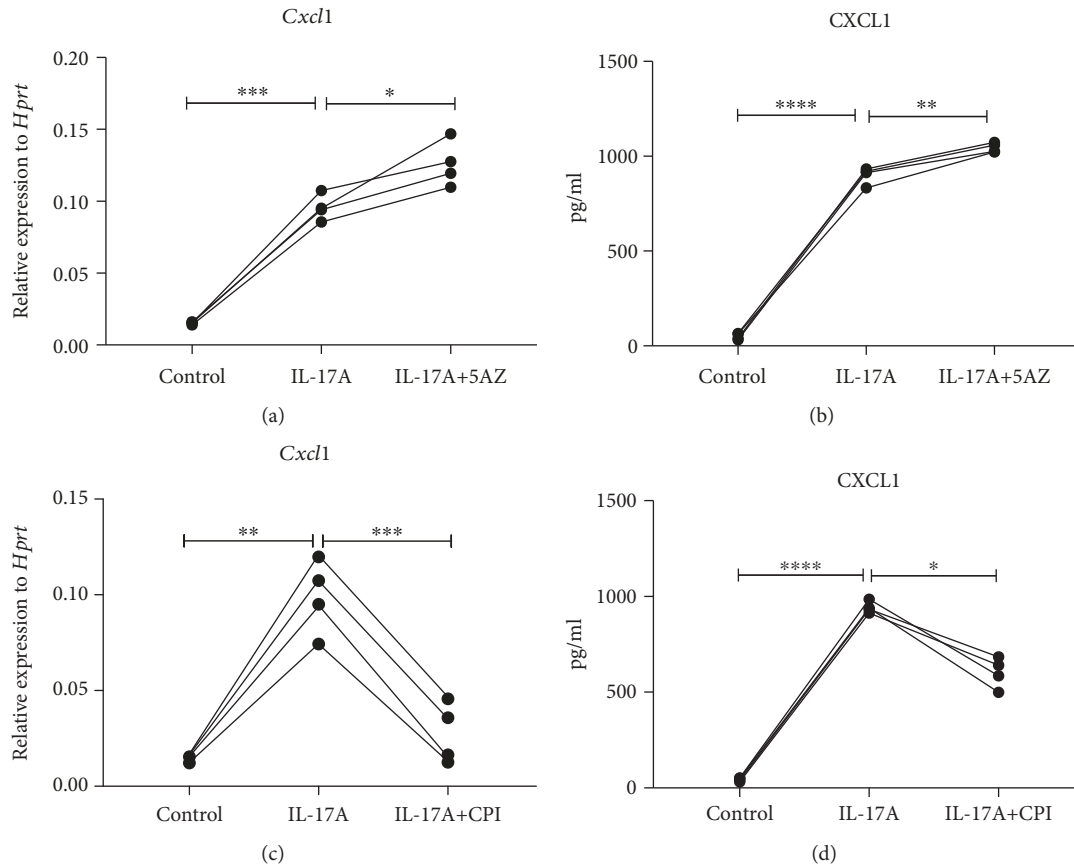


FIGURE 7: Epigenetic regulation of IL-17 pathway in mouse airway epithelial cells. Murine lung epithelial (MLE12) cells were cultured with HITES (hydrocortisone, insulin, transferrin, estradiol, and selenium) medium containing 10% fetal bovine serum (FBS) and antibiotics at 37°C in an incubator containing 5% CO<sub>2</sub>. Cells were treated with control medium, 50 ng/ml m-IL-17A protein, 1 μM 5-azacytidine, 200 nM CPI, 50 ng/ml h-IL-17A plus 1 μM 5-azacytidine and 50 ng/ml h-IL-17A plus 200 nM CPI, respectively. 6 h qPCR was performed for *Cxcl1* mRNA production with (a) IL-17A/5-azacytidine and (c) IL-17A/CPI-treated cells. 24 h supernatant was collected to reach CXCL1 protein level by ELISA for (b) IL-17A/5-azacytidine and (d) IL-17A/CPI-treated cells. \* $p < 0.05$ ; \*\* $p < 0.01$ ; \*\*\* $p < 0.001$ ; \*\*\*\* $p < 0.0001$ ; by a one-way ANOVA test. It is the representative figure from 4 experiments.

**4.4. RNA Extraction and cDNA Synthesis.** RNA was extracted from cell samples with RNeasy Miniprep Kit (QIAGEN, Cat# 74136; Zymo Research, Cat# R1055), according to the manufacturer's instructions. Further cDNA was constructed with qScript™ cDNA Synthesis Kits (Quantabio, Cat# 95047-100).

**4.5. Real-Time PCR.** Real-time PCR was conducted with the Bio-Rad CFX96 system employing TaqMan PCR Master Mix (Bio-Rad, Cat# 1725284) and pre-mixed primers/probe sets (mouse: CXCL1 (Mm04207460\_m1) and Hprt (Mm03024075\_m1); human: CXCL1 (Hs00236937\_m1), CXCL2 (Hs00601975\_m1), CXCL5 (Hs01099660\_g1), CXCL8 (Hs00174103\_m1), HDAC5 (Hs00608351\_m1), and HPRT (Hs02800695\_m1)) from Thermo Fisher Scientific.

**4.6. ELISA.** ELISA kits were used for detecting human CXCL8 (BioLegend, Cat# 431505) and mouse CXCL1 (R&D Systems, Cat# DY453). The procedures were performed in strict accordance with the manufacturer's protocol.

**4.7. Western Blotting.** Equal amount of protein (30 μg) was separated by Bolt™ 4-12% Bis-Tris Plus Gels (Thermo Fisher,

Cat# NW04122BOX) and then electrophoretically transferred onto nitrocellulose membranes. The membranes were then blocked for 1 hour with 5% skim milk in Tris-buffered saline (TBS) Tween 20 and probed with specific primary antibodies (HDAC5: Abcam, Cat# ab55403; β-actin: Abcam, Cat# ab8226) at 4°C overnight. After washing the primary antibodies with TBS Tween 20, the blots were incubated with appropriate horseradish peroxidase-conjugated secondary antibodies for 2 hours at room temperature. Images were captured by ChemiDoc™ MP Imaging System (Bio-Rad, Cat# 12003154).

**4.8. ScRNA-seq and mRNA-seq.** ScRNA-seq libraries were constructed according to the "Single Cell 3' Reagent Kits v2 User Guide" (10X Genomics). Generally, single-cell population was barcoded, and barcoded cDNA was prepared inside each cell by reverse transcription. Cell lysis followed, and then cDNA library was achieved through a released barcoded cDNA amplification. Following fragmentation, end repair, and addition of a single A base, double-sided size selection was used to isolate cDNA around 200 bp. Further adaptor ligation, sample index PCR amplification, and

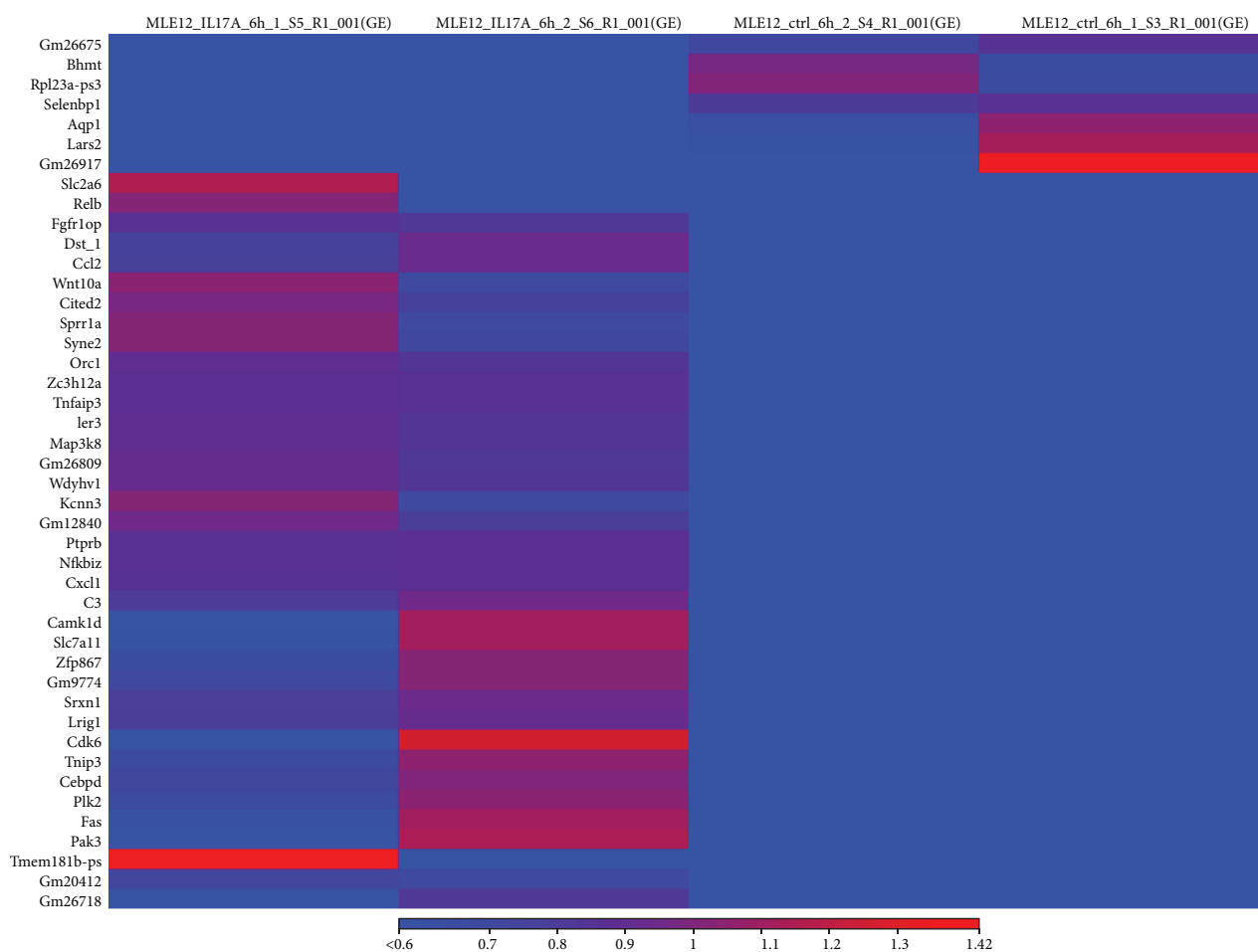


FIGURE 8: Heat map of genes regulated by IL-17A (50 ng/ml for 6 h) in MLE12 cells. The left two columns shown on the map were the two samples of m-IL-17A-treated group, and the right two columns were the control group samples.

another double-sided size selection, the final 300~600 bp DNA sequencing library was constructed and sequenced on Illumina HiSeq by Novogene (Chula Vista, CA). The RNA-seq analysis methodology was published previously [40]. Heat maps were generated by CLC Genomics Workbench (QIAGEN Inc.).

**4.9. Statistics.** All data analyses were performed with Prism 7.0 (GraphPad). The one-way ANOVA test was used for the comparison of gene expression among the three groups. For other comparisons between the paired two groups, paired Student's *t*-test was performed.

### Data Availability

The RNA-seq data used to support the findings of this study are available from the corresponding author upon request.

### Ethical Approval

Human samples collected were approved by the University of Pittsburgh IRB.

### Conflicts of Interest

The authors declare no conflict of interest.

### Authors' Contributions

JL and KC designed the experiments and wrote the paper. JL performed most of the experiment and analyzed the PCR data. XA and YY performed the Western blotting and constructed RNA-seq libraries. CE and AF did single-cell RNA-seq analysis. JKK, SF, and KC wrote and revised the manuscript.

### Acknowledgments

This study is supported by the NIH (R01HL137709) and the CFF (KOLLS16I0).

### Supplementary Materials

*Supplementary 1.* Figure S1: heat map of the expression of multiple HDAC expression in normal HBE cell cultured in air-liquid interphase in the presence or absence of 100 ng/ml IL-17 in basal media for 48 h.

**Supplementary 2.** Figure S2: IPA analysis for gene expression in human bronchial epithelial cells (HBE1) cultured in BronchiaLife™ Epithelial Airway Medium, stimulated with or without 100 ng/ml IL-17A for 24 h.

**Supplementary 3.** Figure S3: IPA analysis for gene expression in murine lung epithelial (MLE12) cells treated with 50 ng/ml IL-17A or control medium for 6 h.

**Supplementary 4.** Figure S4: baseline HuR expression level in both human HBE1 and mouse airway epithelial cell line MLE12 cells. Total transcript counts of HuR from mRNA sequencing data of HBE1 and MLE12 cells without any stimulation.

**Supplementary 5.** Figure S5: original Western blotting membrane scan pictures. The membrane was cut into 2 parts. Two different protein markers were loaded to show the protein size (ladder labelled on the left side: ExcelBand™ 3-color Pre-Stained Protein Ladder, PM5200, SMOBIO; ladder labelled on the right side: MagicMark™ XP Western Protein Standard, LC5602, Invitrogen). Sample conditions were also listed.

## References

- [1] R. Pappu, V. Ramirez-Carrozzi, and A. Sambandam, "The interleukin-17 cytokine family: critical players in host defence and inflammatory diseases," *Immunology*, vol. 134, no. 1, pp. 8–16, 2011.
- [2] S. L. Gaffen, "Structure and signalling in the IL-17 receptor family," *Nature Reviews Immunology*, vol. 9, no. 8, pp. 556–567, 2009.
- [3] K. Chen and J. K. Kolls, "T cell-mediated host immune defenses in the lung," *Annual Review of Immunology*, vol. 31, no. 1, pp. 605–633, 2013.
- [4] E. E. Way, K. Chen, and J. K. Kolls, "Dysregulation in lung immunity - the protective and pathologic Th17 response in infection," *European Journal of Immunology*, vol. 43, no. 12, pp. 3116–3124, 2013.
- [5] P. Kumar and G. Subramaniam, "Molecular underpinnings of Th17 immune-regulation and their implications in autoimmune diabetes," *Cytokine*, vol. 71, no. 2, pp. 366–376, 2015.
- [6] K. Chen, T. Eddens, G. Trevejo-Nunez et al., "IL-17 receptor signaling in the lung epithelium is required for mucosal chemokine gradients and pulmonary host defense against *K. pneumoniae*," *Cell Host & Microbe*, vol. 20, no. 5, pp. 596–605, 2016.
- [7] K. Chen, D. A. Pociask, J. P. McAleer et al., "IL-17RA is required for CCL2 expression, macrophage recruitment, and emphysema in response to cigarette smoke," *PLoS One*, vol. 6, no. 5, article e20333, 2011.
- [8] A. Zlotnik and O. Yoshie, "The chemokine superfamily revisited," *Immunity*, vol. 36, no. 5, pp. 705–716, 2012.
- [9] Y. Kobayashi, "Neutrophil infiltration and chemokines," *Critical Reviews in Immunology*, vol. 26, no. 4, pp. 307–316, 2006.
- [10] P. Ye, F. H. Rodriguez, S. Kanaly et al., "Requirement of interleukin 17 receptor signaling for lung CXC chemokine and granulocyte colony-stimulating factor expression, neutrophil recruitment, and host defense," *The Journal of Experimental Medicine*, vol. 194, no. 4, pp. 519–528, 2001.
- [11] S. Cai, S. Batra, S. A. Lira, J. K. Kolls, and S. Jeyaseelan, "CXCL1 regulates pulmonary host defense to *Klebsiella* infection via CXCL2, CXCL5, NF- $\kappa$ B, and MAPKs," *Journal of Immunology*, vol. 185, no. 10, pp. 6214–6225, 2010.
- [12] T. Herjan, P. Yao, W. Qian et al., "HuR is required for IL-17-induced Act1-mediated CXCL1 and CXCL5 mRNA stabilization," *Journal of Immunology*, vol. 191, no. 2, pp. 640–649, 2013.
- [13] S. Datta, M. Novotny, P. G. Pavicic et al., "IL-17 regulates CXCL1 mRNA stability via an AUUUA/tristetraprolin-independent sequence," *The Journal of Immunology*, vol. 184, no. 3, pp. 1484–1491, 2010.
- [14] D. Sun, M. Novotny, K. Bulek, C. Liu, X. Li, and T. Hamilton, "Treatment with IL-17 prolongs the half-life of chemokine CXCL1 mRNA via the adaptor TRAF5 and the splicing-regulatory factor SF2 (ASF)," *Nature Immunology*, vol. 12, no. 9, pp. 853–860, 2011.
- [15] J. Hartupee, C. Liu, M. Novotny, X. Li, and T. Hamilton, "IL-17 enhances chemokine gene expression through mRNA stabilization," *Journal of Immunology*, vol. 179, no. 6, pp. 4135–4141, 2007.
- [16] I. Striz, T. Mio, Y. Adachi, R. A. Robbins, D. J. Romberger, and S. I. Rennard, "IL-4 and IL-13 stimulate human bronchial epithelial cells to release IL-8," *Inflammation*, vol. 23, no. 6, pp. 545–555, 1999.
- [17] F. Gormand, S. Cheria-Sammari, R. Aloui et al., "Granulocyte-macrophage colony stimulating factors (GM-CSF) and interleukin 8 (IL-8) production by human bronchial epithelial cells (HBEC) in asthmatics and controls. Lack of in vitro effect of salbutamol compared to sodium nedocromil," *Pulmonary Pharmacology*, vol. 8, no. 2-3, pp. 107–113, 1995.
- [18] H. Takizawa, M. Desaki, T. Ohtoshi et al., "Erythromycin modulates IL-8 expression in normal and inflamed human bronchial epithelial cells," *American Journal of Respiratory and Critical Care Medicine*, vol. 156, no. 1, pp. 266–271, 1997.
- [19] T. Angrisano, R. Pero, I. Paoletti et al., "Epigenetic regulation of IL-8 and  $\beta$ -defensin genes in human keratinocytes in response to *Malassezia furfur*," *The Journal of Investigative Dermatology*, vol. 133, no. 8, pp. 2101–2104, 2013.
- [20] A. M. Baird, S. G. Gray, and K. J. O'Byrne, "Epigenetics underpinning the regulation of the CXC (ELR+) chemokines in non-small cell lung cancer," *PLoS One*, vol. 6, no. 1, article e14593, 2011.
- [21] J. R. Yankaskas, J. E. Haizlip, M. Conrad et al., "Papilloma virus immortalized tracheal epithelial cells retain a well-differentiated phenotype," *American Journal of Physiology-Cell Physiology*, vol. 264, no. 5, pp. C1219–C1230, 1993.
- [22] Q. Zhou, X. Ye, R. Sun et al., "Differentiation of mouse induced pluripotent stem cells into alveolar epithelial cells in vitro for use in vivo," *Stem Cells Translational Medicine*, vol. 3, no. 6, pp. 675–685, 2014.
- [23] A. Y. Guh, B. M. Limbago, and A. J. Kallen, "Epidemiology and prevention of carbapenem-resistant Enterobacteriaceae in the United States," *Expert Review of Anti-Infective Therapy*, vol. 12, no. 5, pp. 565–580, 2014.
- [24] F. McAllister, A. Henry, J. L. Kreindler et al., "Role of IL-17A, IL-17F, and the IL-17 receptor in regulating growth-related oncogene-alpha and granulocyte colony-stimulating factor in bronchial epithelium: implications for airway inflammation in cystic fibrosis," *Journal of Immunology*, vol. 175, no. 1, pp. 404–412, 2005.

- [25] Y. R. Chan, K. Chen, S. R. Duncan et al., "Patients with cystic fibrosis have inducible IL-17+IL-22+ memory cells in lung draining lymph nodes," *The Journal of Allergy and Clinical Immunology*, vol. 131, no. 4, pp. 1117–1129.e5, 2013.
- [26] P. J. Dubin and J. K. Kolls, "IL-23 mediates inflammatory responses to mucoid *Pseudomonas aeruginosa* lung infection in mice," *American Journal of Physiology-Lung Cellular and Molecular Physiology*, vol. 292, no. 2, pp. L519–L528, 2007.
- [27] P. J. Dubin, A. Martz, J. R. Eisenstatt, M. D. Fox, A. Logar, and J. K. Kolls, "Interleukin-23-mediated inflammation in *Pseudomonas aeruginosa* pulmonary infection," *Infection and Immunity*, vol. 80, no. 1, pp. 398–409, 2011.
- [28] A. A. Pezzulo, X. X. Tang, M. J. Hoegger et al., "Reduced airway surface pH impairs bacterial killing in the porcine cystic fibrosis lung," *Nature*, vol. 487, no. 7405, pp. 109–113, 2012.
- [29] J. L. Kreindler, C. A. Bertrand, R. J. Lee et al., "Interleukin-17A induces bicarbonate secretion in normal human bronchial epithelial cells," *American Journal of Physiology-Lung Cellular and Molecular Physiology*, vol. 296, no. 2, pp. L257–L266, 2009.
- [30] Z. Wang, C. Zang, J. A. Rosenfeld et al., "Combinatorial patterns of histone acetylations and methylations in the human genome," *Nature Genetics*, vol. 40, no. 7, pp. 897–903, 2008.
- [31] A. Rada-Iglesias, R. Bajpai, T. Swigut, S. A. Brugmann, R. A. Flynn, and J. Wysocka, "A unique chromatin signature uncovers early developmental enhancers in humans," *Nature*, vol. 470, no. 7333, pp. 279–283, 2011.
- [32] Y. Shen, F. Yue, D. F. McCleary et al., "A map of the cis-regulatory sequences in the mouse genome," *Nature*, vol. 488, no. 7409, pp. 116–120, 2012.
- [33] Y. M. Khan, P. Kirkham, P. J. Barnes, and I. M. Adcock, "Brd4 is essential for IL-1 $\beta$ -induced inflammation in human airway epithelial cells," *PLoS One*, vol. 9, no. 4, article e95051, 2014.
- [34] K. Chen, B. T. Campfield, S. E. Wenzel et al., "Antiinflammatory effects of bromodomain and extraterminal domain inhibition in cystic fibrosis lung inflammation," *JCI Insight*, vol. 1, no. 11, 2016.
- [35] D. A. Mele, A. Salmeron, S. Ghosh, H. R. Huang, B. M. Bryant, and J. M. Lora, "BET bromodomain inhibition suppresses TH17-mediated pathology," *The Journal of Experimental Medicine*, vol. 210, no. 11, pp. 2181–2190, 2013.
- [36] W. Wang, C. H. Ha, B. S. Jhun, C. Wong, M. K. Jain, and Z. G. Jin, "Fluid shear stress stimulates phosphorylation-dependent nuclear export of HDAC5 and mediates expression of KLF2 and eNOS," *Blood*, vol. 115, no. 14, pp. 2971–2979, 2010.
- [37] J. Pang, C. Yan, K. Natarajan et al., "GIT1 mediates HDAC5 activation by angiotensin II in vascular smooth muscle cells," *Arteriosclerosis, Thrombosis, and Vascular Biology*, vol. 28, no. 5, pp. 892–898, 2008.
- [38] H. Denis, M. N. Ndlovu, and F. Fuks, "Regulation of mammalian DNA methyltransferases: a route to new mechanisms," *EMBO Reports*, vol. 12, no. 7, pp. 647–656, 2011.
- [39] M. M. Myerburg, P. R. Harvey, E. M. Heidrich, J. M. Pilewski, and M. B. Butterworth, "Acute regulation of the epithelial sodium channel in airway epithelia by proteases and trafficking," *American Journal of Respiratory Cell and Molecular Biology*, vol. 43, no. 6, pp. 712–719, 2010.
- [40] M. Ray, W. Horne, J. P. McAleer et al., "RNA-seq in pulmonary medicine: how much is enough?," *American Journal of Respiratory and Critical Care Medicine*, vol. 192, no. 3, pp. 389–391, 2015.

## Research Article

# The Effect of Taxifolin on Cisplatin-Induced Pulmonary Damage in Rats: A Biochemical and Histopathological Evaluation

Edhem Unver <sup>1</sup>, Mustafa Tosun,<sup>1</sup> Hasan Olmez,<sup>1</sup> Mehmet Kuzucu,<sup>2</sup> Ferda Keskin Cimen,<sup>3</sup> and Zeynep Suleyman<sup>4</sup>

<sup>1</sup>Department of Chest Diseases, Faculty of Medicine, Erzincan Binali Yildirim University, Erzincan, Turkey

<sup>2</sup>Department of Biology, Faculty of Arts and Sciences, Erzincan Binali Yildirim University, Erzincan, Turkey

<sup>3</sup>Department of Pathology, Faculty of Medicine, Erzincan Binali Yildirim University, Erzincan, Turkey

<sup>4</sup>Department of Nursing, Faculty of Health Sciences, Erzincan Binali Yildirim University, Erzincan, Turkey

Correspondence should be addressed to Edhem Unver; [ethemunver@hotmail.com](mailto:ethemunver@hotmail.com)

Received 20 October 2018; Revised 21 December 2018; Accepted 1 January 2019; Published 12 March 2019

Guest Editor: Cheng Xiao

Copyright © 2019 Edhem Unver et al. This is an open access article distributed under the Creative Commons Attribution License, which permits unrestricted use, distribution, and reproduction in any medium, provided the original work is properly cited.

The effect of taxifolin on cisplatin-induced oxidative pulmonary damage was investigated biochemically and histopathologically in male albino Wistar rats. There were four groups, with six animals in each group: 50 mg/kg of taxifolin plus 2.5 mg/kg of cisplatin (TC) group, 2.5 mg/kg of cisplatin only (CIS) group, 50 mg/kg of taxifolin only (TG) group, and a healthy control group (HG). In terms of the experimental procedure, the animals in the TC and TG groups were first treated via oral gavage. The CIS and HG groups received distilled water as solvent, respectively. One hour later, the TC and CIS groups received cisplatin at a dose of 2.5 mg/kg (injected intraperitoneally). Taxifolin, cisplatin, and the distilled water were administered at the indicated dose and volume, using the same method daily for 14 d. At the end of this period, the animals were killed with a high dosage of thiopental anaesthesia (50 mg/kg). Blood and lung tissue samples were taken for biochemical (malondialdehyde (MDA), myeloperoxidase (MPO), total glutathione (tGSH), and 8-hydroxy-2 deoxyguanosine (8-OHdG)) analyses and histopathological examinations. The biochemical and histopathological results in the TC and HG groups were then compared with those in the CIS group. Cisplatin increased the levels of MDA, myeloperoxidase, and 8-OHdG, a marker of oxidative DNA damage, and reduced the amount of tGSH in the lung tissue. Moreover, severe alveolar damage, including oedema and extensive alveolar septal fibrosis, in addition to infiltration of polymorphic nuclear leucocytes and haemorrhagic foci, was observed in the CIS group. These histopathological findings demonstrate that taxifolin provides protection against pulmonary oxidative stress by preventing increases in oxidant parameters and decreases in antioxidants.

## 1. Introduction

Cisplatin (cis-dichlorodiammine platinum II) is a platinum compound and antineoplastic drug, with broad-spectrum activity against various solid cancers [1, 2]. The anticancer activity of cisplatin increases in accordance with dose augmentation, but increased cisplatin doses cause severe side effects [3]. The reported side effects include oxidative stress, which affects the lungs and various other tissues and organs [4]. Interstitial inflammation, fibrosis, structural pulmonary damage, and other severe complications have also been reported during cisplatin chemotherapy [5]. These adverse effects of cisplatin-induced pulmonary damage have been

attributed to increased lipid peroxidation caused by free oxygen radicals and decreases in antioxidant parameters [6]. Previous research showed that cisplatin increased the amount of malondialdehyde (MDA) in animal lungs, reduced enzymatic and nonenzymatic antioxidant levels, and caused severe DNA damage [7]. In another study, the authors reported oxidative DNA damage in the lung tissue of a cisplatin-treated group [8]. In this group, the levels of total oxidants were high, whereas those of antioxidants were low [8].

Based on the literature, both oxidative stress and DNA damage appear to be important in the pathogenesis of cisplatin tissue and organ toxicity. Thus, a drug that did not

induce oxidative stress and exhibited anticancer activity would reduce cisplatin-related pulmonary toxicity. Taxifolin (3,3',4',5,7-pentahydroxyflavanon), a flavanone found in onions, milk thistle, French maritime, and Douglas fir bark, has a known antioxidant activity [9, 10]. Furthermore, previous studies suggested that taxifolin was effective against various types of cancer [11, 12]. Thus, the literature suggests that taxifolin may reduce lung toxicity without suppressing the anticancer effects of cisplatin, possibly potentiating its anticancer activity. No previous studies have investigated the effect of taxifolin on cisplatin-induced lung toxicity. Therefore, the aim of this study was to examine the protective effect of taxifolin against cisplatin-induced oxidative pulmonary damage in rats via biochemical and histopathological analyses.

## 2. Material and Methods

**2.1. Animals.** Experimental animals were obtained from Ataturk University Medical Experimental Application and Research Centre. In total, 18 male albino Wistar rats (weight: 255–265 g) were used in the experiment. Prior to the experiment, the animals were housed in groups in a normal laboratory environment (22°C). The animal experiments were performed in accordance with the National Guidelines for the Use and Care of Laboratory Animals and were approved by the local animal ethics committee of Ataturk University (AUHADYEK), Erzurum, Turkey (decision date: 27.04.2018; no. 119).

**2.2. Chemicals.** Thiopental sodium used in the experiment was supplied by IE Ulagay (Turkey), cisplatin (Ebewa) was supplied by Liba (Turkey), and taxifolin was supplied by Evalar, (Russia).

**2.3. Experimental Groups.** The animals were divided into four groups, with six animals in each group: 50 mg/kg of taxifolin plus 2.5 mg/kg cisplatin (TC) group, 2.5 mg/kg cisplatin only (CIS) group, 50 mg/kg of taxifolin only (TG) group, and a healthy control group (HG).

**2.4. Experimental Procedure.** A 50 mg/kg dose of taxifolin was administered via oral gavage to the TC and TG groups. Distilled water as solvent was administered to the CIS and HG groups. In accordance with previous research that examined the protective effects of drugs against cisplatin toxicity [13], 1 h after the application of taxifolin and distilled water, cisplatin at a dose of 2.5 mg/kg was injected intraperitoneally in the TC and CIS groups. Taxifolin, cisplatin, and distilled water at the indicated dose and volume were administered daily for 14 d using the same method.

At the end of the 14 d period, blood samples were taken from the tail veins of the animals. The animals were then killed with a high dosage of thiopental anaesthesia (50 mg/kg), and lung tissues were removed. Malondialdehyde (MDA), myeloperoxidase (MPO), and total glutathione (tGSH) levels in the blood and lung tissue samples were measured. In addition, 8-hydroxy-2 deoxyguanosine (8-OHdG), a marker of DNA oxidative damage in the lung tissue, was measured, and histopathological examinations were carried

out. The biochemical and histopathological results obtained in the TC, TG, and HG groups were compared with those in the CIS group.

### 2.5. Biochemical Analyses

**2.5.1. Sample Preparation.** The blood samples from the tail veins were collected in separation gel Vacutainer serum tubes. The blood samples were incubated for 15 min at room temperature, and the serum was separated by centrifugation at 1,500×g for 15 min. The serum samples were stored at -80°C until used in the biochemical analysis. Prior to lung dissection, the tissue was rinsed with phosphate-buffered saline. The lung tissues were homogenized in ice-cold phosphate buffers (50 mM, pH 7.4) appropriate for the measured parameter. The tissue homogenates were centrifuged at 5,000 rpm for 20 min at 4°C, and the supernatants were extracted to analyse the tGSH, MDA, and MPO levels and protein concentrations. The protein concentration of the supernatant was measured using the Bradford method and expressed by dividing to grams of protein [14].

**2.5.2. MDA Levels in Serum and Tissue Samples.** The measurement of MDA was based on the method of Ohkawa et al. [15], with spectrophotometric measurements of the absorbance of the pink-coloured complex formed by thiobarbituric acid and MDA. The serum/tissue homogenate sample (0.1 ml) was added to a solution containing 0.2 ml of 80 g/l of sodium dodecyl sulphate, 1.5 ml of 200 g/l of acetic acid, 1.5 ml of 8 g/l 2-thiobarbiturate, and 0.3 ml of distilled water. The mixture was then incubated at 95°C for 1 h. Upon cooling, 5 ml of n-butanol:pyridine (15:1) was added. The mixture was vortexed for 1 min and centrifuged for 30 min at 4,000 rpm. The absorbance of the supernatant was measured at 532 nm. A standard curve was obtained using 1,1,3,3-tetra-methoxypropane [15].

**2.5.3. MPO Activity in Serum and Tissue Samples.** The method of Bradley et al. [16] was used to determine MPO activity in serum and tissue homogenates. Hydrogen peroxide (H<sub>2</sub>O<sub>2</sub>) in phosphate buffer (50 mM, pH 6) was used as substrate. Serum/tissue homogenate (20 µl) was added to 280 µl of assay buffer (7.0 mg of O-dianisidine HCl and 5 ml of 0.0005% H<sub>2</sub>O<sub>2</sub> in 40 ml of phosphate buffer). The MPO activity was kinetically measured at 460 nm for 5 min [16].

**2.5.4. tGSH Level in Serum and Tissue Samples.** The method of Sedlak and Lindsay [17] was used to measure tGSH. A cocktail solution (5.85 ml of 100 mM sodium phosphate buffer, 2.8 ml of 1 mM 5,5'-dithiobis(2-nitrobenzoic acid) (DTNB), 3.75 ml of 1 mM NADPH, and 80 µl of 625 U/l glutathione reductase) was prepared. DTNB disulphide is chromogenic in medium. It is reduced by sulfhydryl groups and produces a yellow colour, which is measured by spectrophotometry at 412 nm. Before the measurement of tGSH, 0.1 ml of metaphosphoric acid was added to 0.1 ml of the serum/tissue homogenate and centrifuged for 2 min at 2,000 rpm for deproteinization. This cocktail solution (0.15 ml) was then added to 50 µl of the supernatant. A standard curve was obtained using GSSG [17].

**2.6. DNA Oxidation Analysis.** The levels of 8-OHdG and deoxyguanosine (dG) were measured in predefined systems at various wavelengths using HPLC with HPLC-UV and HPLC-ECD electrochemical detectors. Before the HPLC analysis, the hydrolysed DNA samples were redissolved with HPLC eluent to produce a final volume of 1 ml consisting of 20 ml of the final hydrolysate. HPLC-ECD (HP, HP 1049A ECD detector, Agilent 1100 modular systems HP 1049A ECD detector, Germany) reverse-phase C18 column (250 mm × 4.6 mm × 4.0 μm, Phenomenex, Torrance, CA) and a 0.05 M potassium phosphate (pH = 5.5) tampon contained acetonitrile (97:3, v/v), with 1 ml flow velocity per minute as the mobile phase. The dG concentration was quantified by measuring the absorbance at 245 nm, and 8-OHdG was observed with electrochemical readings (600 mV). The amounts of dG and 8-OHdG were identified using dG and 8-OHdG standards (Sigma, St. Louis, MO). 8-OHdG/10<sup>5</sup> was used as a marker of DNA damage.

**2.7. Histopathological Examination.** The dissected tissues were fixed in 10% formalin solution for 24 h. 4 μm thick sections were obtained from paraffin blocks following routine tissue monitoring and stained with haematoxylin and eosin (H&E). The sections were evaluated under light microscopy (Olympus BX 52; Tokyo, Japan) by a pathologist who was blinded to the treatment protocols.

**2.8. Statistical Analysis.** The data were analysed using Microsoft Excel and MedCal (Ostend, Belgium). Descriptive statistics were generated for each group. Outlier analysis was performed using Tukey's test. Differences between groups were compared by a one-way analysis of variance.

### 3. Results

**3.1. Blood Serum and Lung Tissue MDA, MPO, and tGSH Levels.** As shown in Figure 1, the levels of MDA and MPO in the blood serum of the cisplatin (CIS) group increased significantly as compared with those in the HG, TG, and TC groups ( $P < 0.0001$ ). The difference between the MDA and MPO values in the HG, TG, and TC groups was statistically insignificant ( $P > 0.05$ ). In the blood serum samples of the CIS group, the tGSH level significantly decreased as compared with that of the HG, TG, and TC groups ( $P < 0.0001$ ). The difference between the levels of tGSH in the TG, TC, and HG groups was statistically insignificant ( $P > 0.05$ ).

In the CIS group, the lung tissue levels of MDA and MPO significantly increased ( $P < 0.0001$ ), whereas those of tGSH significantly decreased ( $P < 0.0001$ ) as compared with the levels in the HG, TG, and TC groups. The lung tissue MDA, MPO, and tGSH levels were very close to those found in the HG, TG, and TC groups (Figure 2).

**3.2. Lung Tissue Levels of 8-OHdG.** In the CIS group, the lung tissue levels of 8-OHdG increased as compared with those in the HG, TG, and TC group (Figure 3). The difference between the 8-OHdG levels in the CIS, HG, TG, and TC groups was statistically significant ( $P < 0.0001$ ). In contrast, the difference between the 8-OHdG levels in the HG, TG, and TC groups was statistically insignificant ( $P > 0.05$ ).

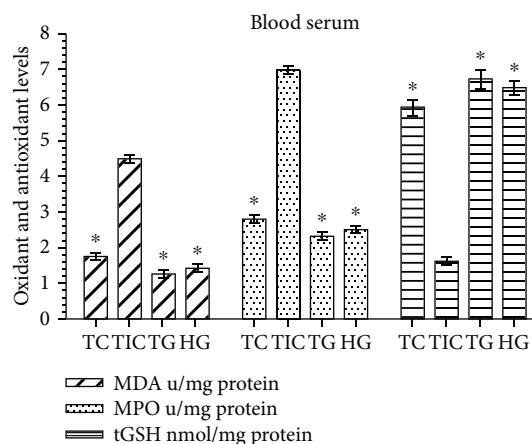


FIGURE 1: MDA, MPO, and tGSH levels in blood serum of the study groups. TC, TG, and HG groups were compared with the CIS group ( $n = 6$ ,  $*P < 0.0001$ ).

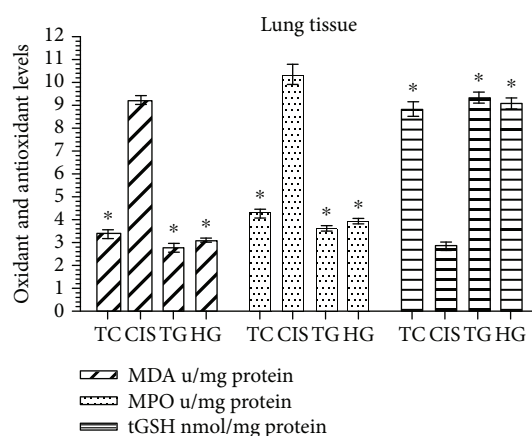


FIGURE 2: MDA, MPO and tGSH values in lung tissues of the study groups. TC, TG and HG groups were compared with the CIS group ( $n = 6$ ,  $*P < 0.0001$ ).

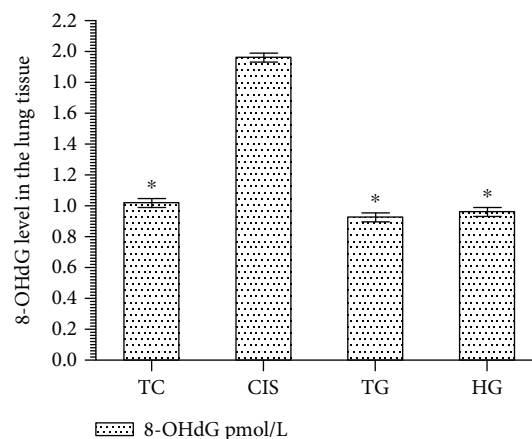


FIGURE 3: 8-OHdG level in lung tissues of the study groups. TC, TG, and HG groups were compared with the CIS group ( $n = 6$ ,  $*P < 0.0001$ ).

**3.3. Histopathological Findings.** As shown in Figure 4, no histopathological evidence of lung damage was observed in the TC group, other than slight pulmonary oedema and congestion. However, extensive alveolar oedema and severe alveolar damage were observed in the lung tissue of the CIS group (Figure 5), with extensive alveolar septal fibrosis, infiltration of polymorphic nuclear leucocytes, and haemorrhagic foci observed (Figure 6). The pleural mesothelium, pulmonary arterioles, structure of the bronchioles, and alveolar structure were all healthy in the HG (Figure 7). As observed under a microscope, the histological structure of the alveolar channels in the lung tissue of the HG was also normal (Figure 7). In the TG, lung tissue congestion and microscopic histopathological findings were absent (Figure 8).

## 4. Discussion

In this study, the effect of taxifolin on cisplatin-induced lung damage in rats was investigated biochemically and histopathologically. The results of the biochemical tests revealed significantly increased levels of MDA, MPO, and 8-OHdG and significant decreases in tGSH levels in the lung tissues of the CIS group as compared with those in the HG, TG, and TC groups.

Previous research demonstrated that various parameters, including MDA, MPO, and 8-OHdG, can be used to determine oxidative stress [18]. Free oxygen radicals give rise to oxidative stress, which oxidizes cell membrane lipids. These then form toxic products (e.g. MDA) that further increase cell damage [19]. Hypochlorous acid (HOCl), a toxic oxidant/free oxygen radical, is produced by MPO and causes lipid peroxidation [20]. MPO oxidizes  $H_2O_2$  to chloride ions and leads to the formation of HOCl [19]. HOCl reacts with proteins, amino acids, lipids, and nucleic acids, causing tissue damage [21]. The release of HOCl from PNLs is upregulated in damaged tissues. Reactive oxygen species react with DNA and cause oxidative DNA damage. As a result of free radical reactions, cation exchanges in nucleic acids and chain breaks in DNA occur. If such changes cannot be repaired, DNA is mutated. 8-hydroxyguanine is considered a mutagenic form of DNA [22].

The therapeutic use of cisplatin causes oxidative stress and DNA damage in noncancerous tissues (e.g. kidney, liver, testicular, brain, and lung) [4]. According to previous research, tissue damage may be associated with a decrease in antioxidant defence mechanisms in the pathogenesis of cisplatin-induced oxidative damage [6]. In the present study, lung tissue levels of tGSH, an endogenous antioxidant molecule, significantly decreased in the CIS group as compared with those in the HG and TG groups. These findings in accordance with those of Afsar et al. [7] reported that MDA and  $H_2O_2$  levels increased in the presence of cisplatin-induced lung damage, whereas the levels of GSH and other enzymatic antioxidants decreased significantly.

Taxifolin is a flavanone and a powerful antioxidant agent [23]. Flavonoids exhibit their antioxidant activity by different mechanisms, for example, by scavenging radicals [24]. These induce lipid peroxide radicals and lipid peroxidation by binding metal ions and inhibiting enzymatic reactions responsible

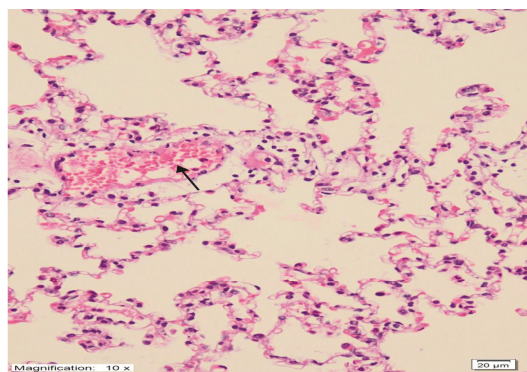


FIGURE 4: Histopathological findings (TAF) in the TC group. There were no histopathological findings, except for slight oedema and lung congestion (H&E  $\times 200$ ).

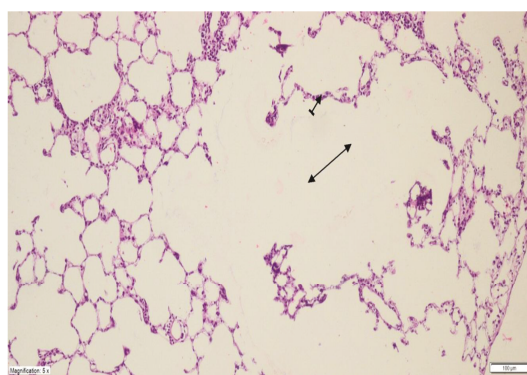


FIGURE 5: Extensive alveolar oedema (double-sided arrow) and severe alveolar damage (dashed arrow) in the lung tissue of the CIS group (H&E  $\times 100$ ).

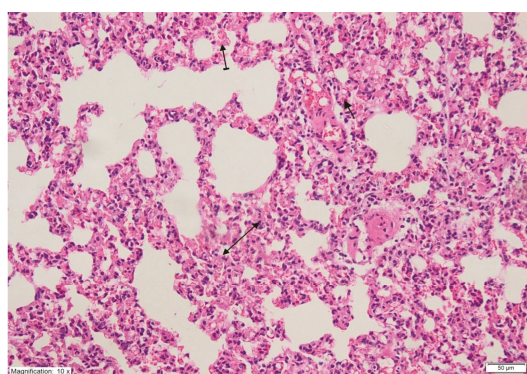


FIGURE 6: Extensive alveolar septal fibrosis (double-sided arrow), infiltration of polymorphic nuclear leucocytes (straight arrow), and haemorrhagic foci (dashed arrow) in the lung tissue of the CIS group (H&E  $\times 200$ ).

for the formation of free radicals [24]. In previous research, taxifolin suppressed the development of oxidative stress in the lung tissue of cisplatin-treated animals. Studies also reported that taxifolin suppressed MDA production in a PC12 cell line [25] and that it provided protection against inflammatory-induced damage in the lung tissue in an experimental study by suppressing MPO activity [26]. No previous

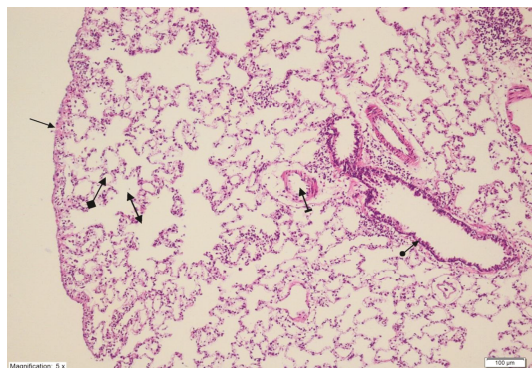


FIGURE 7: Healthy pleural mesothelium (straight arrow), healthy pulmonary arterioles (dashed arrow), normal bronchiole (round arrow) structure and alveolar structure (squared arrow), and normal histological structure of the alveolar channels (double arrow) in the lung tissue of the HG group (H&E  $\times 100$ ).

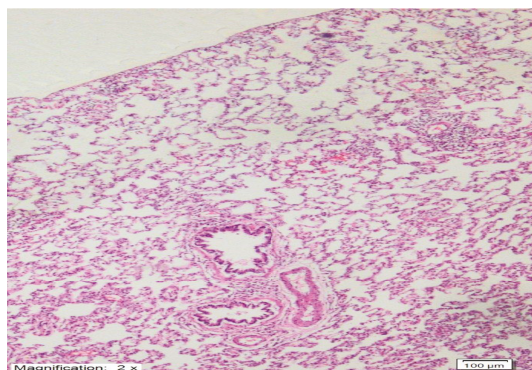


FIGURE 8: Lung tissue congestion and microscopic histopathological findings were absent in the TG group (H&E  $\times 100$ ).

studies have investigated the effect of taxifolin on tGSH in the lung tissue or its effect on DNA oxidative damage. One study reported that GSH protected the liver tissue against ethanol-induced oxidative damage by preventing its reduction [27]. The results of the present study showed that taxifolin protected DNA from oxidative damage.

In the current study, the cisplatin group, which had high levels of oxidants and low levels of antioxidants, was characterized by extensive alveolar oedema and alveolar septal fibrosis, severe alveolar damage, infiltration of polymorphic nuclear leucocytes, and haemorrhagic foci in the lung tissue. The lung tissue of the TG group was histopathologically similar to that observed in the HG group. The presence of only slight oedema and congestion in the lung tissue of the TC group indicated that the biochemical results overlapped with the histopathological findings. Leo et al. also reported that cisplatin chemotherapy induced structural pulmonary damage associated with interstitial inflammation, fibrosis, and obliterative bronchiolitis [5].

In the clinic, cytotoxic drugs have been reported to cause pulmonary inflammation and fibrosis [28]. Antioxidants are used in the treatment of various lung diseases. Previous research reported that herbal antioxidant-based products increased the effectiveness of anticancer drugs and that they

could reduce the harmful effects of these drugs [29, 30]. Impellizzeri et al. experimentally demonstrated that taxifolin inhibited lung inflammation and fibrosis by inducing anti-inflammatory activity [26].

In conclusion, cisplatin caused pulmonary oxidative stress by raising levels of oxidant and proinflammatory markers and lowering antioxidant levels. Cisplatin also caused extensive alveolar septal fibrosis. As shown by the biochemical and histopathological findings, oxidative pulmonary damage was absent in the TC group. Biochemical and histopathological manifestations of oxidative damage were not observed in the blood and lung tissues of the TG group. These findings indicate that taxifolin protected the lung tissue from the toxic effects of cisplatin. Taxifolin may be clinically effective against cisplatin-associated lung toxicity.

## Data Availability

No data were used to support this study.

## Conflicts of Interest

The authors report no conflicts of interest in this work.

## Acknowledgments

We would like to thank Ataturk University Medical Experimental Application and Research Centre.

## References

- [1] C. A. Rabik and M. E. Dolan, "Molecular mechanisms of resistance and toxicity associated with platinating agents," *Cancer Treatment Reviews*, vol. 33, no. 1, pp. 9–23, 2007.
- [2] S. H. Choi, J. Leem, and I. K. Lee, "Protective effects of gemigliptin, a dipeptidyl peptidase-4 inhibitor, against cisplatin-induced nephrotoxicity in mice," *Mediators of Inflammation*, vol. 2017, Article ID 4139439, 9 pages, 2017.
- [3] R. Khan, A. Q. Khan, W. Qamar et al., "Chrysin abrogates cisplatin-induced oxidative stress, p53 expression, goblet cell disintegration and apoptotic responses in the jejunum of Wistar rats," *The British Journal of Nutrition*, vol. 108, no. 09, pp. 1574–1585, 2012.
- [4] Y. Chen, P. Jungsuwadee, M. Vore, D. A. Butterfield, and D. K. St Clair, "Collateral damage in cancer chemotherapy: oxidative stress in nontargeted tissues," *Molecular Interventions*, vol. 7, no. 3, pp. 147–156, 2007.
- [5] F. Leo, G. Pelosi, A. Sonzogni, M. Chilosi, G. Bonomo, and L. Spaggiari, "Structural lung damage after chemotherapy: fact or fiction?," *Lung Cancer*, vol. 67, no. 3, pp. 306–310, 2010.
- [6] R. Pratibha, R. Sameer, P. V. Rataboli, D. A. Bhiwgade, and C. Y. Dhume, "Enzymatic studies of cisplatin induced oxidative stress in hepatic tissue of rats," *European Journal of Pharmacology*, vol. 532, no. 3, pp. 290–293, 2006.
- [7] T. Afsar, S. Razak, A. Almajwal, and M. R. Khan, "Acacia hydasppica R. Parker ameliorates cisplatin induced oxidative stress, DNA damage and morphological alterations in rat pulmonary tissue," *BMC Complementary and Alternative Medicine*, vol. 18, no. 1, article 49, 2018.
- [8] F. Geyikoglu, H. Isikgoz, H. Onalan et al., "Impact of high-dose oleuropein on cisplatin-induced oxidative stress,

- genotoxicity and pathological changes in rat stomach and lung," *Journal of Asian Natural Products Research*, vol. 19, no. 12, pp. 1214–1231, 2017.
- [9] Q. Wang, L. Wang, G. Li, and B. Ye, "A simple and sensitive method for determination of taxifolin on palladium nanoparticles supported poly (diallyldimethylammonium chloride) functionalized graphene modified electrode," *Talanta*, vol. 164, pp. 323–329, 2017.
- [10] F. Topal, M. Nar, H. Gocer et al., "Antioxidant activity of taxifolin: an activity-structure relationship," *Journal of Enzyme Inhibition and Medicinal Chemistry*, vol. 31, no. 4, pp. 674–683, 2016.
- [11] M. W. Haque and S. P. Pattanayak, "Taxifolin inhibits 7, 12-dimethylbenz (a)anthracene-induced breast carcinogenesis by regulating AhR/CYP1A1 signaling pathway," *Pharmacognosy Magazine*, vol. 13, Supplement 4, pp. S749–S755, 2018.
- [12] X. Chen, N. Gu, C. Xue, and B.-R. Li, "Plant flavonoid taxifolin inhibits the growth, migration and invasion of human osteosarcoma cells," *Molecular Medicine Reports*, vol. 17, pp. 3239–3245, 2018.
- [13] R. Coskun, M. I. Turan, I. S. Turan, and M. Gulapoglu, "The protective effect of thiamine pyrophosphate, but not thiamine, against cardiotoxicity induced with cisplatin in rats," *Drug and Chemical Toxicology*, vol. 37, no. 3, pp. 290–294, 2014.
- [14] M. M. Bradford, "A rapid and sensitive method for the quantitation of microgram quantities of protein utilizing the principle of protein-dye binding," *Analytical Biochemistry*, vol. 72, no. 1–2, pp. 248–254, 1976, 942051.
- [15] H. Ohkawa, N. Ohishi, and K. Yagi, "Assay for lipid peroxides in animal tissues by thiobarbituric acid reaction," *Analytical Biochemistry*, vol. 95, no. 2, pp. 351–358, 1979.
- [16] P. P. Bradley, D. A. Priebat, R. D. Christensen, and G. Rothstein, "Measurement of cutaneous inflammation: estimation of neutrophil content with an enzyme marker," *The Journal of Investigative Dermatology*, vol. 78, no. 3, pp. 206–209, 1982.
- [17] J. Sedlak and R. H. Lindsay, "Estimation of total, protein-bound, and nonprotein sulfhydryl groups in tissue with Ellman's reagent," *Analytical Biochemistry*, vol. 25, pp. 192–205, 1968.
- [18] A. Kisaoglu, B. Borekci, O. E. Yapca, H. Bilen, and H. Suleyman, "Tissue damage and oxidant/antioxidant balance," *The Eurasian Journal of Medicine*, vol. 45, no. 1, pp. 47–49, 2013.
- [19] R. F. Del Maestro, "An approach to free radicals in medicine and biology," *Acta Physiologica Scandinavica. Supplementum*, vol. 492, pp. 153–168, 1980.
- [20] J. M. McCord, "Oxygen-derived free radicals in postischemic tissue injury," *The New England Journal of Medicine*, vol. 312, no. 3, pp. 159–163, 1985.
- [21] C. Bergt, G. Marsche, U. Panzenboeck, J. W. Heinecke, E. Malle, and W. Sattler, "Human neutrophils employ the myeloperoxidase/hydrogen peroxide/chloride system to oxidatively damage apolipoprotein A-I," *European Journal of Biochemistry*, vol. 268, no. 12, pp. 3523–3531, 2001.
- [22] O. E. Yapca, B. Borekci, and H. Suleyman, "Ischemia-reperfusion damage," *The Eurasian Journal of Medicine*, vol. 45, no. 2, pp. 126–127, 2013.
- [23] C. A. Rice-Evans, N. J. Miller, and G. Paganga, "Structure-antioxidant activity relationships of flavonoids and phenolic acids," *Free Radical Biology & Medicine*, vol. 20, no. 7, pp. 933–956, 1996.
- [24] N. Cotelle, "Role of flavonoids in oxidative stress," *Current Topics in Medicinal Chemistry*, vol. 1, no. 6, pp. 569–590, 2001.
- [25] Y. J. Nam, D. H. Lee, Y. K. Shin, D. S. Sohn, and C. S. Lee, "Flavanonol taxifolin attenuates proteasome inhibition-induced apoptosis in differentiated PC12 cells by suppressing cell death process," *Neurochemical Research*, vol. 40, no. 3, pp. 480–491, 2015.
- [26] D. Impellizzeri, E. Talero, R. Siracusa et al., "Protective effect of polyphenols in an inflammatory process associated with experimental pulmonary fibrosis in mice," *The British Journal of Nutrition*, vol. 114, no. 06, pp. 853–865, 2015.
- [27] J. W. Kim, T. B. Kim, H. W. Kim, S. W. Park, H. P. Kim, and S. H. Sung, "Hepatoprotective flavonoids in *Opuntia ficus-indica* fruits by reducing oxidative stress in primary rat hepatocytes," *Pharmacognosy Magazine*, vol. 13, no. 51, pp. 472–476, 2017.
- [28] J. A. Cooper Jr., D. A. White, and R. A. Matthay, "Drug-induced pulmonary disease. Part 1: cytotoxic drugs," *The American Review of Respiratory Disease*, vol. 133, no. 2, pp. 321–340, 1986.
- [29] K. Sak, "Chemotherapy and dietary phytochemical agents," *Chemotherapy Research and Practice*, vol. 2012, Article ID 282570, 11 pages, 2012.
- [30] İ. Topal, A. Özbek Bilgin, F. Keskin Çimen et al., "The effect of rutin on cisplatin-induced oxidative cardiac damage in rats," *The Anatolian Journal of Cardiology*, vol. 20, pp. 136–142, 2018.

## Research Article

# Leukotriene Involvement in the Insulin Receptor Pathway and Macrophage Profiles in Muscles from Type 1 Diabetic Mice

João Pedro Tôrres Guimarães <sup>1,2</sup>, Luciano Ribeiro Filgueiras,<sup>1</sup> Joilson Oliveira Martins <sup>2</sup>, and Sonia Jancar <sup>1</sup>

<sup>1</sup>Laboratory of Immunopharmacology, Department of Immunology, Institute of Biomedical Sciences, University of São Paulo (ICB/USP), São Paulo, Brazil

<sup>2</sup>Laboratory of Immunoendocrinology, Department of Clinical and Toxicological Analyses, School of Pharmaceutical Sciences of University São Paulo (FCF/USP), São Paulo, Brazil

Correspondence should be addressed to Joilson Oliveira Martins; [martinsj@usp.br](mailto:martinsj@usp.br) and Sonia Jancar; [sojancar@icb.usp.br](mailto:sojancar@icb.usp.br)

Received 5 November 2018; Accepted 15 January 2019; Published 28 January 2019

Guest Editor: Qingdong Guan

Copyright © 2019 João Pedro Tôrres Guimarães et al. This is an open access article distributed under the Creative Commons Attribution License, which permits unrestricted use, distribution, and reproduction in any medium, provided the original work is properly cited.

Type 1 diabetes (T1D) is a metabolic disease associated with systemic low-grade inflammation and macrophage reprogramming. There is evidence that this inflammation depends on the increased systemic levels of leukotriene (LT) B<sub>4</sub> found in T1D mice, which shifts macrophages towards the proinflammatory (M1) phenotype. Although T1D can be corrected by insulin administration, over time T1D patients can develop insulin resistance that hinders glycemic control. Here, we sought to investigate the role of leukotrienes (LTs) in a metabolically active tissue such as muscle, focusing on the insulin signaling pathway and muscle-associated macrophage profiles. Type 1 diabetes was induced in the 129/SvE mouse strain by streptozotocin (STZ) in mice deficient in the enzyme responsible for LT synthesis (5LO<sup>-/-</sup>) and the LT-sufficient wild type (WT). The response to insulin was evaluated by the insulin tolerance test (ITT), insulin concentration by ELISA, and Akt phosphorylation by western blotting. The gene expression levels of the insulin receptor and macrophage markers Stat1, MCP-1, Ym1, Arg1, and IL-6 were evaluated by qPCR, and that of IL-10 by ELISA. We observed that after administration of a single dose of insulin to diabetic mice, the reduction in glycemia was more pronounced in 5LO<sup>-/-</sup> than in WT mice. When muscle homogenates were analyzed, diabetic 5LO<sup>-/-</sup> mice showed a higher expression of the insulin receptor gene and higher Akt phosphorylation. Moreover, in muscle homogenates from diabetic 5LO<sup>-/-</sup> mice, the expression of anti-inflammatory macrophage markers *Ym1*, *Arg1*, and IL-10 was increased, and the relative expression of the proinflammatory cytokine *IL-6* was reduced compared with WT diabetic mice. These results suggest that LTs have an impact on the insulin receptor signaling pathway and modulate the inflammatory profile of muscle-resident macrophages from T1D mice.

## 1. Introduction

The incidence of metabolic disorders is increasing dramatically and is now widely considered a serious threat to public health. In diseases such as diabetes, obesity, atherosclerosis, and gout, metabolic imbalance is associated with the establishment of low-grade systemic inflammation, which in turn is a determining factor in the pathophysiology of these diseases. This happens as a consequence of the accumulation of certain metabolic products, such as glucose, fatty acids, uric acid, and cholesterol, which activate

receptors of innate immunity in leukocytes and induce the chronic production of proinflammatory cytokines and lipid mediators [1–3].

Characterized by chronic hyperglycemia with changes in the metabolism of carbohydrates, lipids, and proteins [4], diabetes is classically divided into two forms. In type 2 diabetes (T2D), hyperglycemia is due to insulin resistance established in the liver, muscle, and adipose tissue, and the main risk factor for this condition is obesity [5]. In T1D, hyperglycemia results from deficient insulin production as a consequence of the destruction of pancreatic  $\beta$  cells by

autoimmune processes. This condition is corrected by insulin administration, but throughout treatment, T1D patients also begin to develop resistance to insulin, and glycemic control becomes increasingly difficult, which impairs the patient's quality of life [6]. It is believed that in both T1D and T2D, insulin resistance is due to a systemic low-grade inflammation; however, the mechanisms involved may be distinct and still need to be elucidated.

In muscles, the accumulation of lipids along with their peroxidation promotes endoplasmic reticulum stress, and muscle-associated macrophages undergo reprogramming to the proinflammatory profile, producing IL-6, IL-1 $\beta$ , TNF- $\alpha$ , and lipid mediators [7–10]. The high level of TNF- $\alpha$  produced by these macrophages stimulates production of the chemokine CCL2, leading to the recruitment of activated monocytes (CD11b + LY6C<sup>high</sup>) to the tissue [11]. By binding to their membrane receptors on muscle cells, the cytokines IL-6, IL-1 $\beta$ , and TNF- $\alpha$  can induce insulin resistance [10, 12].

The lipid mediator leukotriene B4 (LTB4) plays a central role in systemic low-grade inflammation [13–15] and the establishment of insulin resistance in animal models of diabetes [10, 16, 17]. Leukotrienes (LTs) are generated from arachidonic acid (AA) metabolism by 5-lipoxygenase (5LO). Arachidonic acid is esterified in cell membrane phospholipids from where it is released by activated phospholipase PLA2. Together with other enzymes of the 5LO metabolic pathway, macrophages and other inflammatory cells are able to generate high amounts of LTs within a few minutes of stimulation. Together with the accessory protein FLAP (5-lipoxygenase-activating protein), 5LO oxidizes AA, generating the unstable intermediate LTA4, which is rapidly hydrolyzed to generate LTB4 [16]. LTB4 binds to G protein-coupled receptors; BLT1 is the high-affinity receptor and is coupled to Gi protein, thereby resulting in decreased intracellular levels of cyclic AMP.

Activation of the BLT1 receptor in macrophages potentiates phagocytosis, microbicidal activity, and the production of proinflammatory cytokines [2]. This proinflammatory profile of macrophages in T1D mice is associated with increased levels of LTB4 in the blood, systemic inflammation, and insulin resistance. Blocking of LTs shifts macrophages towards an anti-inflammatory profile and reduces systemic inflammation and insulin resistance. When sepsis was induced in these animals, the systemic inflammatory response was more intense, and animal mortality was increased. This was reversed by LT antagonists [17].

Recently, it has been demonstrated that in mice fed a high-fat diet, LTB4 is produced in adipose tissue, muscles, and liver. Adipose tissue macrophages exhibit a proinflammatory profile and insulin resistance. Similarly, in the liver and muscle of obese mice, LTB4 promotes inflammation and insulin resistance [10, 16–20]. Therefore, considering studies involving LTs in inflammation and how they may be involved in the development of metabolic syndromes, in the present study we investigated the participation of LTs in the insulin receptor pathway, an important checkpoint pathway related with insulin resistance, and the macrophage profile, an important cell in inflammatory processes.

## 2. Materials and Methods

**2.1. Animals.** We used 8-week-old, male, pathogen-free 129/SvE wild-type (WT) and 5LO knockout (5LO<sup>-/-</sup>) mice. The animals were maintained in a controlled environment at 22°C under a 12-hour light-dark cycle with free access to water and restricted access to food only before the T1D induction protocol, as described below. This study was carried out in strict accordance with the principles and guidelines adopted by the Brazilian National Council for the Control of Animal Experimentation (CONCEA) and approved by the Ethical Committee on Animal Use (CEUA) of the Institute of Biomedical Sciences (ICB) of the University of São Paulo (USP) (CEUA no. 08/2014). All surgical procedures were performed under ketamine/xylazine hydrochloride anesthesia, and care was taken to minimize animal suffering.

**2.2. Induction of Diabetes Mellitus.** For the induction of T1D, the animals were fasted for 5 hours, followed by an intraperitoneal (i.p.) injection of STZ (ChemCruz® U-9889, lot F1816) (30 mg/kg for WT and 25 mg/kg for KO, in 0.1 M citrate buffer, pH 4.5); after that, the animals were maintained with free access to food. This protocol lasted for a period of 5 consecutive days. Animals with glycemia greater than 300 mg/dL (OneTouch® Select Simple™) 10 days after the last dose were considered diabetic. Mice in the nondiabetic control group received a citrate buffer injection alone. To evaluate variation in body weight, the animals were weighed before and 10 and 17 days after STZ administration. The STZ-induced destruction of pancreatic beta cells is commonly accepted as a model of T1D, has been described by other groups [21, 22], and has also been previously standardized in our laboratory [17, 23].

**2.3. Insulin Tolerance Test (ITT).** After a 6-hour fast, the mice received an i.p. injection of insulin (Novolin®, lot CS6G140, 1.0 IU/kg), and the blood glucose level was determined (OneTouch® Select Simple™) using blood samples collected from the caudal vein every 30 minutes.

**2.4. Insulin-Induced AKT Phosphorylation.** The animals were anaesthetized with ketamine/xylazine (90 mg/kg and 10 mg/kg, respectively) and 5 minutes after the i.p. insulin injection, tissue samples were collected and macerated (Polytron PT 1600E) in RIPA buffer (50 mM Tris, pH 8.0, 150 mM NaCl, 1% Triton X-100, and 0.1% SDS) containing a protease inhibitor (Sigma-Aldrich), orthovanadate, and fluoride and subsequently centrifuged (1500 × g for 5 minutes).

**2.5. Measurement of Serum Insulin Levels.** After the collection of whole blood from T1D and control mice, the samples were centrifuged for 20 minutes at 1600 × g (for serum separation). The serum insulin concentration was determined using an insulin kit (Insulin Mouse ELISA Kit, lot 534070518, Thermo Fisher Scientific). The test is based on the capacity of the insulin in the sample to compete with the acetylcholinesterase-conjugated insulin for specific antibody binding. The reading was performed at 414 nm on a microplate reader (Epoch Microplate Spectrophotometer, BioTek Instruments), and the results are expressed in ng/mL.

**2.6. Western Blotting.** Protein concentration in the samples was determined (BCA Assay Kit, Thermo Fisher Scientific). Equal amounts of protein were separated by electrophoresis (SDS-PAGE) and transferred to a nitrocellulose membrane. After blocking of nonspecific binding (nonfat dried skim milk powder), the membranes were incubated overnight at 4°C under constant stirring with primary antibodies specific for pAkt Ser 473 (1:2000, Cell Signaling Technology, lot 0019) and  $\beta$  actin (1:1000, Cell Signaling Technology, lot 0017). Anti-rabbit IgG (1:3000, Cell Signaling Technology, lot 0025) was used as a secondary antibody. Expression was visualized using SuperSignal® West Pico Chemiluminescent Substrate (lot PD202858, Thermo Fisher Scientific).

**2.7. RNA Purification and Real-Time PCR Analysis.** Total RNA from the tissue homogenates was extracted as previously described [24]. cDNA was synthesized using the RevertAid First Strand cDNA Synthesis Kit (lot 00376305, Thermo Fisher Scientific), and qPCR was performed using primers for *Irs1*, *Insr*, *Il-6*, *Arg1*, *Stat1*, *Ym1*, and *Mcp1* (all from Exxtend®) on the Applied Biosystems StepOnePlus™ Real-Time PCR System (Thermo Fisher Scientific). Relative expression was calculated using the comparative threshold cycle (Ct) and expressed relative to the controls ( $\Delta\Delta Ct$  method).

**2.8. Muscle Homogenates.** Tissue samples were separately collected from the mice and homogenized in RIPA buffer with a tissue homogenizer (Polytron PT 1600E). The supernatants were separated from the cellular debris by centrifugation at  $500 \times g$  for 10 minutes, collected, and stored at  $-80^\circ\text{C}$ . The protein concentration in the homogenates was determined using a commercial kit (Pierce™ BCA Protein Assay Kit, lot PE203766, Thermo Fisher Scientific). The assay was performed according to the manufacturer's manual. Absorbance values at 562 nm were obtained using a microplate reader (SpectraMax 190 Microplate Reader).

**2.9. Cytokine Quantifications.** The concentrations of IL-10 in the supernatants of tissue homogenates were measured using a BD OptEIA™ ELISA Set (BD Biosciences) following the manufacturer's protocol.

**2.10. Data Analysis.** Data were processed and analyzed by analysis of variance (ANOVA) and the Bonferroni posttest or unpaired *t*-tests using GraphPad Prism 6.0 software (La Jolla, CA, USA). Two-tailed *p* values with 95% confidence intervals were acquired. Data are represented as the mean  $\pm$  standard error of the mean (SEM). Values of *p* < 0.05 were considered significant.

### 3. Results

**3.1. Characterization of the T1D Model.** Figure 1 illustrates the experimental protocol employed. In WT and  $5LO^{-/-}$  mice, STZ (60 mg/kg) was administered by i.p. injection in 5 doses over 5 days. Before each dose, the mice were fasted for 5 hours, and for 30 minutes after the injection, they were maintained with free access to food and water (Figure 1(a)). Blood glucose levels were measured three days after the last dose of

STZ, and only mice with glycemia greater than 300 mg/dL were used in the experiments (Figure 1(b)). Body weight loss is one of the symptoms of T1D, and in our study both WT and  $5LO^{-/-}$  diabetic mice showed significant body weight loss compared with healthy mice (Figure 1(c)).

**3.2. Insulin Signaling Pathway in T1D.** Diabetic mice were submitted to the insulin tolerance test. After i.p. injection of insulin (1.0 IU/kg), the blood glucose level was determined every 30 minutes. It was observed that diabetic WT mice presented difficulty controlling glucose levels over time, whereas the  $5LO^{-/-}$  diabetic mice were able to control their blood glucose, suggesting a role for LTs in the insulin pathway (Figure 2(a)). When the production of insulin was evaluated in the serum, it was observed that both groups of diabetic mice ( $5LO^{-/-}$  and WT) presented significantly lower insulin content when compared with the nondiabetic controls (Figure 2(b)).

The gene expression of the insulin receptor in homogenates of the quadriceps and gastrocnemius muscles was not significantly different between WT and  $5LO^{-/-}$  mice. However, in diabetic  $5LO^{-/-}$  mice, the expression of the insulin receptor was significantly higher than in diabetic WT mice (Figures 3(a) and 3(b)). In Figures 3(c) and 3(d), we can see that after insulin administration to diabetic and healthy mice, the muscles from diabetic  $5LO^{-/-}$  have higher levels of pAkt than WT diabetic mice.

**3.3. Muscle-Associated Macrophage Profile in T1D.** To assess inflammation in T1D mouse muscles, we analyzed the expression of some markers of the macrophage profile in quadriceps and gastrocnemius muscles. Homogenates of these tissues were obtained, and the mRNA expression of macrophage markers was measured in the precipitate and that of cytokines in the supernatant. We show in Figure 4 the results obtained in the muscle quadriceps. A similar pattern was observed in the gastrocnemius (data not shown).

The expression of proinflammatory macrophage markers *Stat1* and *Mcp-1* (CCL2) did not vary between the groups. However, the expression of the proinflammatory cytokine *IL-6* was significantly increased in the muscles from diabetic mice but only in those able to produce LTs (Figures 4(a)–4(c)). The expression of the anti-inflammatory macrophage markers *Ym1* and *Arg1* and of the anti-inflammatory IL-10 (Figures 4(d)–4(f)) was higher in diabetic  $5LO^{-/-}$  mice compared to diabetic WT.

### 4. Discussion

The mechanisms involved in insulin resistance have been well described in T2D, but in T1D those mechanisms are less known. In the present study, we investigated the involvement of LTs in the development of insulin resistance in the muscle, a metabolically active tissue. It was found that in diabetic mice, LTs downregulated the insulin signaling pathway in muscles of mice pretreated with insulin. In addition, LTs shifted the muscle-associated macrophages towards the proinflammatory phenotype.

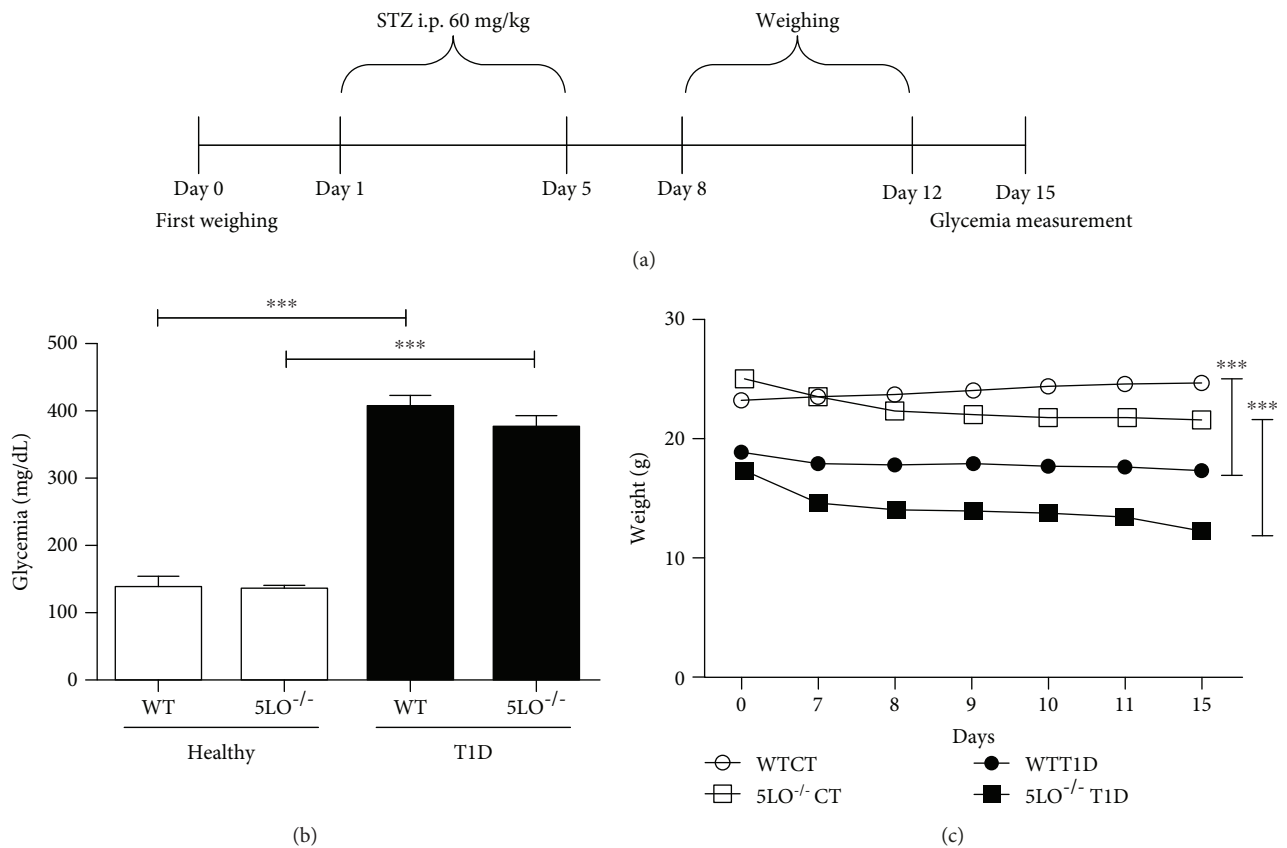


FIGURE 1: Characterization of T1D. (a) T1D induction protocol: 5LO<sup>-/-</sup> and WT mice were fasted for 5 hours before daily injections (i.p.) of streptozotocin (60 mg/kg) for 5 days. Ten days after the last STZ injection, mouse blood glucose levels were measured, and mice with levels higher than 300 mg/dL were considered diabetic. The nondiabetic (healthy) group received the drug diluent, citrate buffer. (b) Blood glucose levels in T1D and healthy groups at day 15. (c) Mice were weighed before streptozotocin administration and 14 days after the last dose.  $n = 4-7$  animals in each group and values are the mean  $\pm$  SEM. \*\*\* $p < 0.001$ .

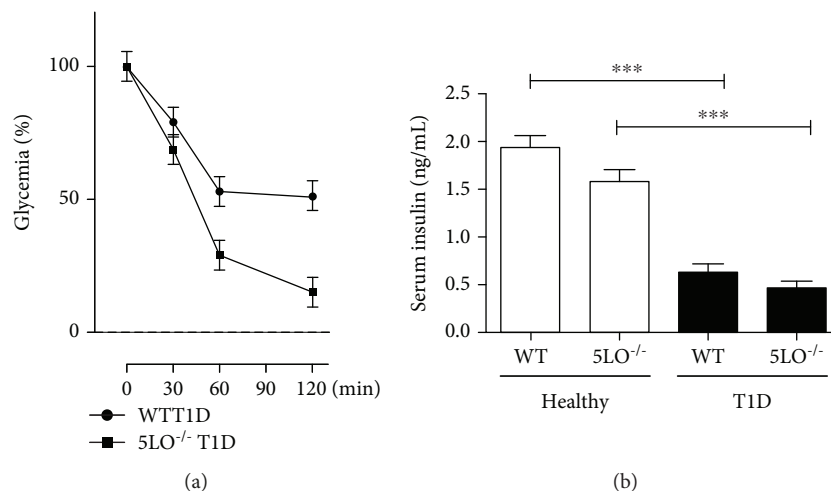


FIGURE 2: Insulin pathway in T1D serum. After insulin (1.0 IU/kg) administration, serum was taken from mice to analyze serum glucose (a) and insulin levels (b).  $n = 4-5$  animals in each group and values are the mean  $\pm$  SEM. \* $p < 0.05$ ; \*\*\* $p < 0.001$ .

T1D was induced chemically using STZ, an antibiotic that kills the insulin-producing beta cells in the pancreas, thus inducing a deficiency in insulin production, insulin

resistance, and chronic inflammation of the pancreatic islets. Because these symptoms resemble those of T1D in humans, the use of STZ has become popular as a model of T1D in rats

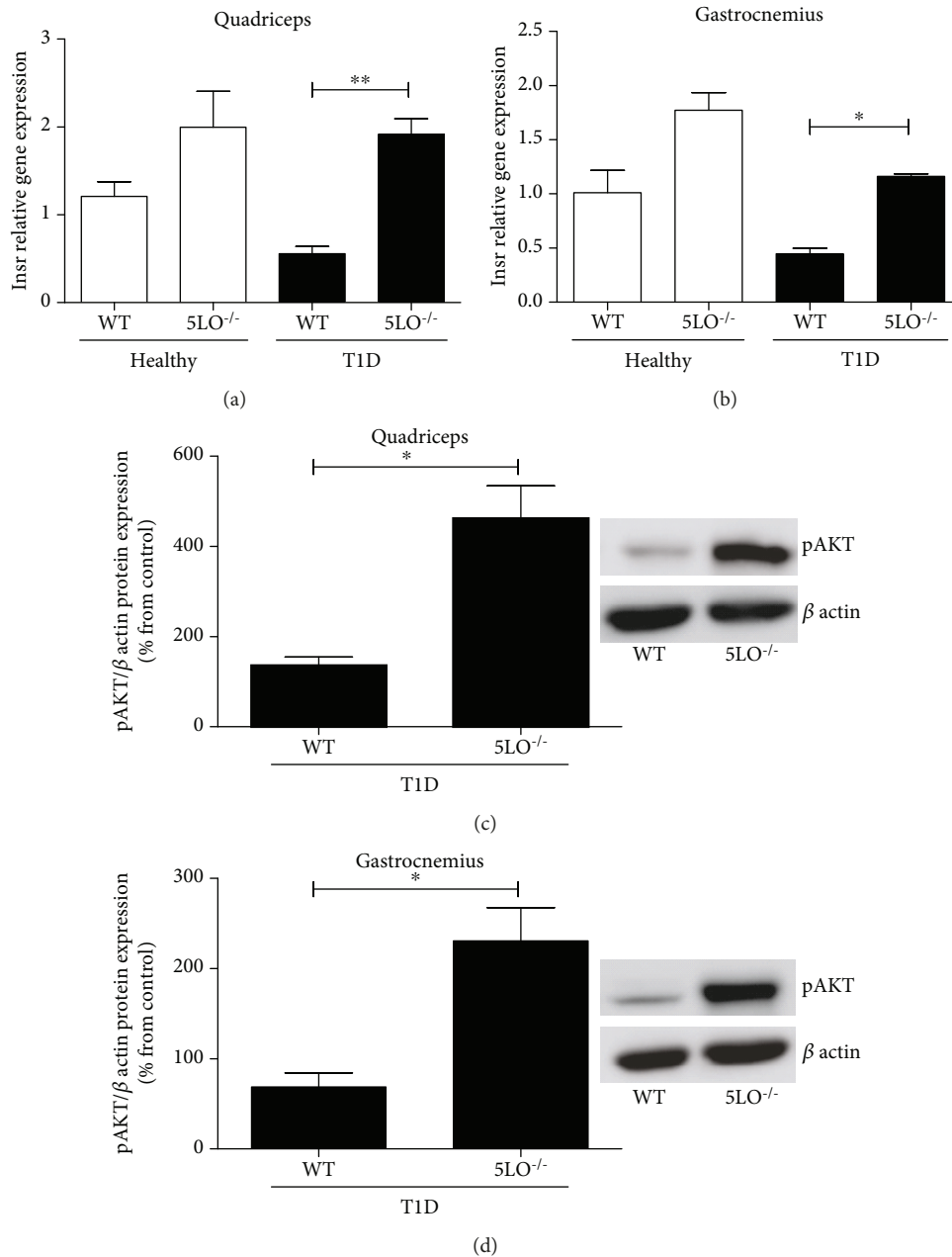


FIGURE 3: Insulin pathway in T1D muscle. The expression of the insulin receptor gene (*Insr*) in muscle homogenates of quadriceps (a) and gastrocnemius (b). Phosphorylation of AKT in quadriceps (c) and gastrocnemius (d).  $n = 4-6$  animals in each group. For western blot,  $n = 3$ . Values are the mean  $\pm$  SEM. \* $p < 0.05$ ; \*\* $p < 0.01$ .

and mice [21]. In 2015, Wu and Liang [22] showed that a single dose of STZ, although not enough to induce insulin resistance, was able to maintain hyperglycemia. We adapted the original model by giving five doses over 1 week, and after the last dose, all mice lost significant weight, exhibited polyuria, and had high blood glucose levels. In addition, we observed the phosphorylation of AKT in the muscle, which is indicative of insulin resistance.

Insulin resistance is a pathological characteristic of numerous metabolic diseases. To confirm that LTs produced during T1D promote insulin resistance, the response of diabetic WT and 5LO<sup>-/-</sup> mice to insulin was initially evaluated.

We observed that after a single dose of insulin, diabetic 5LO<sup>-/-</sup> mice had a greater reduction in glycemia than WT diabetic mice. Li et al. [10] and Spite et al. [18] have shown that in T2D, the activation of the LTB<sub>4</sub> receptor BLT1 leads to the downregulation of the insulin receptor cascade, blocking the action of the insulin receptor substrates and leading to insulin resistance. The same pattern was observed in our study. We observed that even with low levels of serum insulin, diabetic 5LO<sup>-/-</sup> mice exhibited higher insulin receptor gene expression in both muscles tested. After treatment with one dose of insulin, only diabetic 5LO<sup>-/-</sup> mice were able to recover the phosphorylation of AKT, an important molecule

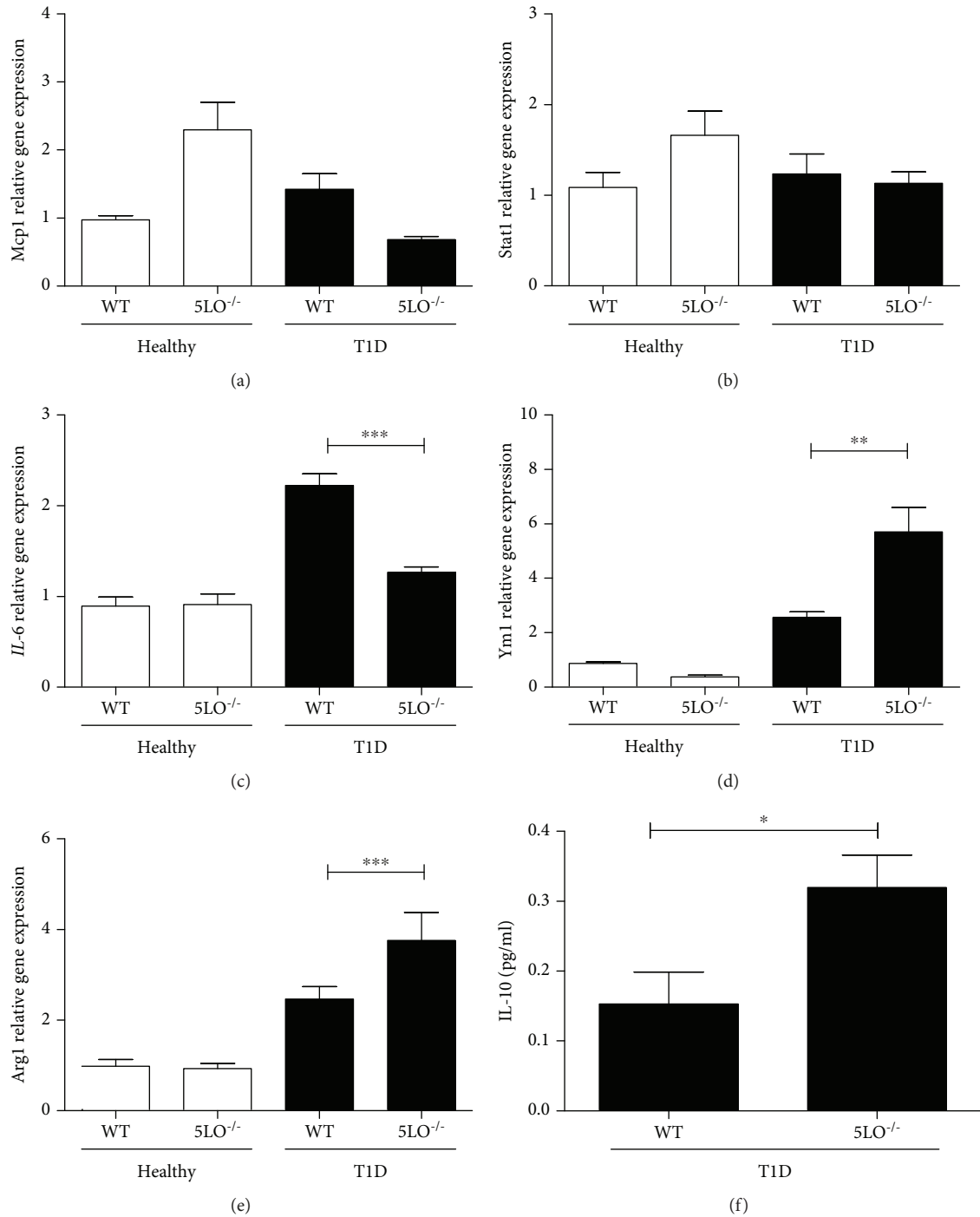


FIGURE 4: Muscle-associated macrophage profile in T1D. Quadriceps homogenates from diabetic mice were analyzed for the expression of anti-inflammatory markers (*Ym1*, *Arg*, and *IL-10*) and proinflammatory markers (*Mcp1*, *Stat1*, and *IL-6*).  $n = 4-5$  animals in each group. Values are the mean  $\pm$  SEM. \*\* $p < 0.01$ ; \*\*\* $p < 0.001$ .

in the insulin signaling pathway. These data suggest that similarly to what happens in T2D, LTs also affect the insulin signaling cascade in T1D.

It has been described that in skeletal striated muscle tissue, including the quadriceps and gastrocnemius, T2D induces the expression of the proinflammatory cytokine *IL-6* and a reduction in *IL-10* levels [25]. Our results show that this also occurs in T1D; in addition, we showed that T1D mice unable to

produce LTs (5LO<sup>-/-</sup>) produced a higher amount of the anti-inflammatory cytokine *IL-10*, which indicates that in diabetic mice, in the absence of LTs, muscle-associated macrophages acquire an anti-inflammatory profile. Kim et al. [26] showed that *IL-6* decreased skeletal muscle insulin action and signaling, which corroborates our results showing that higher *IL-6* expression was correlated with a lower expression of the insulin receptor and AKT phosphorylation

in the muscles of diabetic WT mice. Hong et al. [25] showed, in a model of diet-induced insulin resistance, that treatment with IL-10 prevented insulin resistance and increased AKT phosphorylation. These findings are similar to those found in the muscles of the diabetic 5LO<sup>-/-</sup> mice in the present study, where increased pAKT and IL-10 levels were observed. In addition, in a previous study it was shown that T2D mice have higher systemic levels of LTB4 than healthy mice [20]. Together, these results suggest that in diabetic mice, increased LT levels downregulate the insulin signaling pathway, thereby leading to insulin resistance in muscles. They also help us to understand the mechanisms responsible for the development of insulin resistance in T1D with the involvement of LT.

It has been shown recently that in peritoneal macrophages from T1D 5LO<sup>-/-</sup> mice, the expression of anti-inflammatory macrophage markers (Arg1 and Ym1) was enhanced, whereas the WT macrophages expressed higher levels of proinflammatory markers. Also, systemic inflammation is less intense in T1D 5LO<sup>-/-</sup> mice compared to the WT. This indicates an important role for LTs in the development of systemic inflammation in diabetes and reprogramming of tissue macrophages towards a proinflammatory phenotype [26]. Here, we show that macrophages resident in muscles are similarly reprogrammed by LTs in T1D mice.

## Data Availability

The values behind the means, standard deviations, and other measures reported in the data supporting the findings of this study can be obtained from the corresponding author upon reasonable request (Dr. Joilson de Oliveira Martins, martinsj@usp.br).

## Disclosure

The funders had no participation in the selection of the subject matter or study materials discussed in this manuscript.

## Conflicts of Interest

The authors declare that there is no conflict of interest that would prejudice the impartiality of this scientific work.

## Acknowledgments

The authors would like to sincerely thank Marlise Bonetti Agostinho Montes for expert technical help. The authors are supported by grants 2013/15719-0 and 2017/11540-7 from the São Paulo Research Foundation (FAPESP) and grants 302903/2016-0 and 301617/2016-3 from the National Council of Scientific and Technological Development (CNPq), Coordenação de Aperfeiçoamento de Pessoal de Nível Superior (CAPES), and Pro-Reitoria de Pesquisa, Universidade de São Paulo (PRP/USP), Brazil.

## References

- [1] G. R. Robbins, H. Wen, and J. P. Ting, "Inflammasomes and metabolic disorders: old genes in modern diseases," *Molecular Cell*, vol. 54, no. 2, pp. 297–308, 2014.
- [2] L. R. Filgueiras, C. H. Serezani, and S. Jancar, "Leukotriene B4 as a potential therapeutic target for the treatment of metabolic disorders," *Frontiers in Immunology*, vol. 6, 2015.
- [3] G. Y. Chen and G. Nunez, "Sterile inflammation: sensing and reacting to damage," *Nature Reviews Immunology*, vol. 10, no. 12, pp. 826–837, 2010.
- [4] International Diabetes Foundation, *IDF Diabetes atlas*, International Diabetes Foundation, 8th edition, 2017.
- [5] M. Stumvoll, B. J. Goldstein, and T. W. van Haefen, "Type 2 diabetes: principles of pathogenesis and therapy," *The Lancet*, vol. 365, no. 9467, pp. 1333–1346, 2005.
- [6] D. Daneman, "Type 1 diabetes," *The Lancet*, vol. 367, no. 9513, pp. 847–858, 2006.
- [7] L. J. Dixon, M. Barnes, H. Tang, M. T. Pritchard, and L. E. Nagy, "Kupffer cells in the liver," *Comprehensive Physiology*, vol. 3, pp. 785–797, 2013.
- [8] J. Jager, M. Aparicio-Vergara, and M. Aouadi, "Liver innate immune cells and insulin resistance: the multiple facets of Kupffer cells," *Journal of Internal Medicine*, vol. 280, no. 2, pp. 209–220, 2016.
- [9] G. Kolios, V. Valatas, and E. Kouroumalis, "Role of Kupffer cells in the pathogenesis of liver disease," *World Journal of Gastroenterology*, vol. 12, no. 46, pp. 7413–7420, 2006.
- [10] P. Li, G. Bandyopadhyay, W. S. Lagakos et al., "LTB4 promotes insulin resistance in obese mice by acting on macrophages, hepatocytes and myocytes," *Nature Medicine*, vol. 21, no. 3, pp. 239–247, 2015.
- [11] U. Klueh, C. Czajkowski, I. Ludzinska, Y. Qiao, J. Frailey, and D. L. Kreutzer, "Impact of CCL2 and CCR2 chemokine/receptor deficiencies on macrophage recruitment and continuous glucose monitoring *in vivo*," *Biosensors and Bioelectronics*, vol. 86, pp. 262–269, 2016.
- [12] H. Morinaga, R. Mayoral, J. Heinrichsdorff et al., "Characterization of distinct subpopulations of hepatic macrophages in HFD/obese mice," *Diabetes*, vol. 64, no. 4, pp. 1120–1130, 2015.
- [13] P. Borgeat and B. Samuelsson, "Arachidonic acid metabolism in polymorphonuclear leukocytes: unstable intermediate in formation of dihydroxy acids," *Proceedings of the National Academy of Sciences of the United States of America*, vol. 76, no. 7, pp. 3213–3217, 1979.
- [14] P. Borgeat and B. Samuelsson, "Arachidonic acid metabolism in polymorphonuclear leukocytes: effects of ionophore A23187," *Proceedings of the National Academy of Sciences of the United States of America*, vol. 76, no. 5, pp. 2148–2152, 1979.
- [15] P. Borgeat and P. H. Naccache, "Biosynthesis and biological activity of leukotriene B4," *Clinical Biochemistry*, vol. 23, no. 5, pp. 459–468, 1990.
- [16] M. Peters-Golden and W. R. Henderson Jr., "Leukotrienes," *The New England Journal of Medicine*, vol. 357, no. 18, pp. 1841–1854, 2007.
- [17] L. R. Filgueiras, S. L. Brandt, S. Wang et al., "Leukotriene B4-mediated sterile inflammation promotes susceptibility to sepsis in a mouse model of type 1 diabetes," *Science Signaling*, vol. 8, no. 361, p. ra10, 2015.
- [18] M. Spite, J. Hellmann, Y. Tang et al., "Deficiency of the leukotriene B4 receptor, BLT-1, protects against systemic insulin resistance in diet-induced obesity," *Journal of Immunology*, vol. 187, no. 4, pp. 1942–1949, 2011.
- [19] V. Pardo, A. Gonzalez-Rodriguez, C. Guijas, J. Balsinde, and A. M. Valverde, "Opposite cross-talk by oleate and palmitate

- on insulin signaling in hepatocytes through macrophage activation," *The Journal of Biological Chemistry*, vol. 290, no. 18, pp. 11663–11677, 2015.
- [20] I. Mothe-Satney, C. Filloux, H. Amghar et al., "Adipocytes secrete leukotrienes: contribution to obesity-associated inflammation and insulin resistance in mice," *Diabetes*, vol. 61, no. 9, pp. 2311–2319, 2012.
- [21] B. L. Furman, "Streptozotocin-induced diabetic models in mice and rats," *Current Protocols in Pharmacology*, vol. 70, pp. 5.47.1–5.47.20, 2015.
- [22] J. Wu and J. Y. Liang, "Streptozotocin-induced type 1 diabetes in rodents as a model for studying mitochondrial mechanisms of diabetic  $\beta$  cell glucotoxicity," *Diabetes, Metabolic Syndrome and Obesity: Targets and Therapy*, vol. 2015, pp. 181–188, 2015.
- [23] T. Ramalho, L. Filgueiras, I. A. Silva-Jr, A. F. M. Pessoa, and S. Jancar, "Impaired wound healing in type 1 diabetes is dependent on 5-lipoxygenase products," *Scientific Reports*, vol. 8, no. 1, 2018.
- [24] D. C. Rio, M. Ares Jr., G. J. Hannon, and T. W. Nilsen, "Purification of RNA using TRIzol (TRI reagent)," *Cold Spring Harbor Protocols*, vol. 2010, no. 6, 2010.
- [25] E. G. Hong, H. J. Ko, Y. R. Cho et al., "Interleukin-10 prevents diet-induced insulin resistance by attenuating macrophage and cytokine response in skeletal muscle," *Diabetes*, vol. 58, no. 11, pp. 2525–2535, 2009.
- [26] H. J. Kim, T. Higashimori, S. Y. Park et al., "Differential effects of interleukin-6 and -10 on skeletal muscle and liver insulin action in vivo," *Diabetes*, vol. 53, no. 4, pp. 1060–1067, 2004.

## Review Article

# Innate Lymphoid Cells: A Link between the Nervous System and Microbiota in Intestinal Networks

Lin Han <sup>1</sup>, Xin-miao Wang,<sup>1</sup> Sha Di <sup>1</sup>, Ze-zheng Gao <sup>1,2</sup>, Qing-wei Li <sup>1</sup>,  
Hao-ran Wu <sup>1,2</sup>, Qing Wang,<sup>1,2</sup> Lin-hua Zhao <sup>3</sup>, and Xiao-lin Tong <sup>1</sup>

<sup>1</sup>Department of Endocrinology, Guang'anmen Hospital of China, China Academy of Chinese Medical Sciences, Beijing 100054, China

<sup>2</sup>Laboratory of Molecular and Biology, Guang'anmen Hospital of China, China Academy of Chinese Medical Sciences, Beijing 100053, China

<sup>3</sup>Beijing University of Chinese Medicine, Beijing 100029, China

Correspondence should be addressed to Lin-hua Zhao; melonzhao@163.com and Xiao-lin Tong; tongxiaolin@vip.163.com

Received 30 November 2018; Accepted 1 January 2019; Published 20 January 2019

Guest Editor: Minggang Zhang

Copyright © 2019 Lin Han et al. This is an open access article distributed under the Creative Commons Attribution License, which permits unrestricted use, distribution, and reproduction in any medium, provided the original work is properly cited.

Innate lymphoid cells (ILCs) are a novel family of innate immune cells that act as key coordinators of intestinal mucosal surface immune defense and are essential for maintaining intestinal homeostasis and barrier integrity by responding to locally produced effector cytokines or direct recognition of exogenous or endogenous danger patterns. ILCs are also involved in the pathogenesis of inflammatory bowel disease (IBD). Many studies have demonstrated the occurrence of crosstalk between ILCs and intestinal microbiota, and ILCs have recently been shown to be connected to the enteric nervous system (ENS). Thus, ILCs may act as a key link between the nervous system and microbiota in intestinal networks. In this review, we briefly summarize the role of the ILCs in the intestinal tract (particularly in the context of IBD) and discuss the relationship between ILCs and the microbiota/ENS.

## 1. Introduction

Innate lymphoid cells (ILCs) play an important role in the immune regulatory network, which are not only the effector cells of innate immunity but also mediate acquired immunity-related functions. Recent studies have identified a special subset of lymphocytes in the human and mouse mucosal systems (e.g., the intestines and lungs) and other critical organs (e.g., the liver) that are related to regional immunization. These lymphocytes are derived from a common lymphoid progenitor (CLP), such as T cells and B cells, and depend on the master lymphocyte cytokine receptor interleukin- (IL-) 2 receptor common  $\gamma$  chain and the expression of inhibitor of DNA binding 2 (Id2) [1, 2]. These cells can be distinguished from adaptive lymphocytes by the absence of functionally rearranged antigen-specific receptors that recognize “nonself” structures and participate in the innate immune response. Therefore, these cells have been designated ILCs, including classic cytotoxic natural killer (NK) cells and lymphoid tissue inducer (LTi) cells.

Most CLPs are developed in the bone marrow, whereas mature ILCs are mainly enriched in peripheral tissues such as the gastrointestinal tract, lung, liver, and skin. There are exceptions, for instance, LTi cells are from the fetal liver to the periphery [3]. Recent studies from parabiosis experiments have confirmed that the vast majority of ILCs are tissue-resident [4]. Mature ILCs have been further categorized into three groups based on differences in effector cytokine production [5–7]. Group 1 ILCs (ILC1s), including NK cells, have the capacity to produce the T helper-(Th-) 1 cell signature cytokines interferon- $\gamma$  (IFN- $\gamma$ ) and tumor necrosis factor- $\alpha$  (TNF- $\alpha$ ), and their function is regulated by the transcription factor T-bet or eomesodermin (Eomes) following stimulation with the proinflammatory cytokines IL-12, IL-15, and IL-18 [8–10]. Group 2 ILCs (ILC2s) express and require the transcription factors Gata binding protein 3 (GATA-3) and/or retinoic acid receptor-(RAR-) related orphan receptor- $\alpha$  (ROR $\alpha$ ) and are capable of secreting Th2 cell-type cytokines, such as IL-4, IL-5, IL-9, and IL-13 [11, 12], in response to IL-25, IL-33, or

thymic stromal lymphopoietin [13]. Lastly, group 3 ILCs (ILC3s), including LT $\alpha$  cells, are defined by the expression of the transcription factor ROR $\gamma$ t and have been shown to be associated with the production of IL-17A, IL-17F, IL-22, and colony stimulating factor 2 (CSF2, also known as granulocyte-macrophage CSF) in response to stimulation with IL-23 and IL-1 $\beta$  [13], which are characteristic of Th17/Th22 cells [5, 7, 14]. Different ILC subtypes have different functions, and maintenance of the steady state of the body depends on the coordination of and interactions among the three subtypes.

ILCs are unique in the innate immune system in that they may produce and secrete cytokines that are classically regarded as CD4<sup>+</sup> Th cell products and are considered to be the “mirror image” of CD4<sup>+</sup> Th cells. Compared with adaptive lymphocytes, ILCs are relatively rare in lymphoid tissue and are mainly deposited on barrier surfaces, such as the skin, intestine, lungs, fat, and mucosa-associated lymphoid tissue. Among these tissues, the intestine is a secondary lymphoid organ and the largest immune system-related organ in the body. Notably, the most common intestinal disease is inflammatory bowel disease (IBD), which encompasses Crohn’s disease (CD) and ulcerative colitis (UC). IBD is a chronic, recurrent inflammatory disease of the intestine and strongly impairs the quality of life of patients [13]. Moreover, some studies have shown that IBD may increase the risk of cancer [15, 16]. Currently, the molecular mechanisms mediating IBD remain unclear, and clinical treatments are not satisfactory. However, studies have shown that the pathogenesis of this disease involves genetic, immunologic, infectious, environmental, and mental factors. Additionally, IBD is known to involve impairment of the integrity of the mucosal epithelial barrier. Because ILCs play an important role in mucosal homeostasis and are involved in a critical feedback loop in which damaged epithelium activates ILCs to restore epithelial barrier function [17–19], ILCs may participate in the pathogenesis of IBD.

Many researchers have attempted to elucidate the relationships between ILCs and intestinal microbes, and recent studies have shown that there is a link between ILCs and the enteric nervous system (ENS) [20–22]; however, the details of this connection are still unclear. In this review, we discuss the roles of ILCs in the intestine, particularly in the context of IBD, and trace the connections among ILCs, the intestinal microbiota, and the ENS in intestinal networks.

## 2. Overview of ILCs in the Intestinal Tract

ILCs are important populations of innate immune effectors and are mainly distributed in the intestinal mucosa, including the intraepithelial compartment and lamina propria. ILC1s are the most abundant ILC population in the intraepithelial compartment in both the small and large intestines, whereas ILC2 and ILC3 are the dominant populations in the lamina propria in the large and small intestines, respectively [23]. Moreover, a study considered that ILCs, which are educated in mesenteric lymph node (MLN) and then home to the intestine, have sophisticated migration programs that undergo retinoic acid- (RA-) dependent homing receptor

switching in a shared, yet subset-specific manner. However, the model they used and the data they tested did not directly prove this migration, which needs more evidences [12]. Additionally, another study showed that ILCs in the gut can be locally renewed and expanded in response to acute environmental challenges, such as helminth infection [4]. Although the ILC population in the intestine is only a fraction of the total lymphocytes, ILCs can promote lymphoid tissue genesis, intestinal mucosal barrier protection, gut microbiota and anti-infection immune regulation, tissue repair coordination, and tissue reconstruction, mainly via secretion of effector cytokines and interactions with Leydig cells or other immune cells [5, 24]. Furthermore, ILCs have a certain degree of plasticity, some subgroups will transform into each other when their surrounding microenvironment changes or during the development of certain diseases. The main regulatory mechanisms of ILCs in IBD are shown in Figure 1.

**2.1. Group 1 ILCs.** Group 1 ILCs include cytotoxic conventional (c) NK cells, which were first discovered in 1975 [25], and noncytotoxic ILC1 family. All ILC1s produce IFN- $\gamma$  and TNF- $\alpha$ , and the physiological roles of ILC1s involve immune responses to intracellular pathogens [26] and tumors [13, 27]. cNK cells are effector cells present in the lamina propria and have roles in antitumor responses via secretion of perforin to kill target cells. In addition to direct killing of target cells, cNK cells can produce the proinflammatory factor IFN- $\gamma$  during early inflammation [28]. Some other proinflammatory cytokines, such as IL-15 and IL-21, can induce and activate NK cells to secrete abundant amounts of IFN- $\gamma$  and TNF- $\alpha$  [29]. In comparison with healthy controls, the number of CD16<sup>+</sup> NK cells present in the lamina propria of patients with CD and UC is substantially increased. However, CD161<sup>+</sup> NK cells in the colonic lamina propria have also been shown to have anti-inflammatory roles, and the number of CD161<sup>+</sup> NK cells in patients with UC is obviously decreased [30]. Therefore, further studies are needed to elucidate the regulatory mechanisms mediating these processes.

TNF- $\alpha$  and IFN- $\gamma$  are both characteristic proinflammatory cytokines. TNF- $\alpha$  plays a key role in early rapid immunity via a pathway independent of MHC molecules and antibodies. IFN- $\gamma$  is closely linked to IBD [31]. The number of intraepithelial ILC1s is increased in patients with CD [32] and in mice with anti-CD40-induced colitis [33], thereby contributing to intestinal inflammation via secretion of IFN- $\gamma$  [29, 34] and forming a pathological environment with a high concentration IFN, and this induced inflammation can be ameliorated by depletion of ILC1s [35].

**2.2. Group 2 ILCs.** In the intestinal tract, ILC2s are more homogeneous cells than ILC1s and ILC3s. Group 2 ILCs function to express transcription factor GATA3 and produce type 2 cytokines such as IL-4, IL-5, IL-9, and IL-13. ILC2s are important in the clearance of helminth [36] and viral infections [37] and in the progression of asthma and lung allergies [38, 39]. Studies have indicated that crosstalk occurs between ILC2s and CD4<sup>+</sup> Th2 cells during infection. This

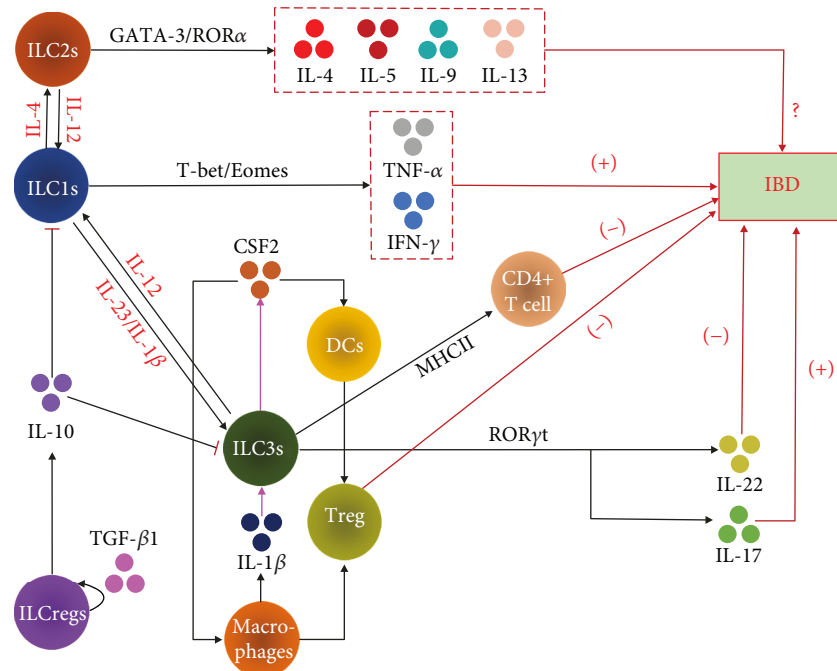


FIGURE 1: The main mechanisms regulating ILCs in IBD. The schematic shows the three ILC subgroup transcription factors and their secretory cytokines, which play proinflammatory (+) or anti-inflammatory (-) roles in IBD, and inhibiting “arrow” means suppression effects on ILCs. Particularly for ILC3s, macrophages secrete IL-1 $\beta$ , which induces ROR $\gamma$ <sup>+</sup> ILC3s to produce colony stimulating factor 2 (CSF2) (shown by purple arrow). CSF2 then acts on dendritic cells (DCs) and macrophages to promote the secretion of regulatory factors and induce the transformation of immature T cells into mature regulatory T cells (Tregs), which are essential for inhibiting inflammation and maintaining intestinal homeostasis. Natural cytotoxicity receptor<sup>-</sup> (NCR<sup>-</sup>) ILC3s express high levels of major histocompatibility complex (MHC) II, which is involved in processing and presenting antigens and can limit the response between CD4<sup>+</sup> T cells and intestinal commensal bacteria, thereby inhibiting inflammation mediated by CD4<sup>+</sup> T cells to prevent IBD. ILCregs can protect against innate intestinal inflammation by secreting IL-10 to suppress the activation of ILC1s, ILC3s, and autocrine TGF- $\beta$ 1 for the expansion and survival of ILCregs during intestinal inflammation. Furthermore, ILCs could mutually transform via induction by specific cytokines (shown by red font).

crosstalk is important for optimizing antihelminthic responses through a transition from innate to adaptive immunological pathways [40], and depletion of ILC2s in mice disrupts Th2 responses [41]. However, in the absence of ILC2s, a normal Th2 response may still occur [42], suggesting that ILC2-derived IL-13 and the underlying antigen-presenting functions of ILC2s may not be essential for enhancing Th2 responses.

The role of ILC2s in IBD is still unclear. The proportion of IL-13-producing ILC2s is increased in the intestinal mucosa of patients with CD, and these cells also produce IFN- $\gamma$  [43]. A study showed that the number of IL-13-producing ILC2s is increased in an oxazolone-induced UC mouse model [44]. Additionally, production of the type 2 cytokines IL-4, IL-5, IL-9, and IL-13 is related to the severity of IBD [45–47], and neutralization of the central cytokines IL-4 and IL-13 has been shown to control experimental intestinal inflammation owing to the involvement of type 2 responses in proinflammatory pathways at the enteric mucosa. Nevertheless, neutralization of human IL-13 had no therapeutic effect in patients with UC. Thus, although ILC2s may be involved in the pathogenesis of IBD, additional studies are needed to elucidate the specific mechanisms.

**2.3. Group 3 ILCs.** Group 3 ILCs include LT $\alpha$ i cells, which were first discovered in 1992 [48], and postnatal ILC3 cells. Compared with the other ILCs, ILC3s are the predominant population in the ileum and colon [49]. LT $\alpha$ i cells are involved in the development of lymphoid organs during embryogenesis by modulating the secretion of lymphotoxin- $\beta$  and TNF- $\alpha$ . In addition, LT $\alpha$ i cells can express IL-17A and IL-22 [13]. Additionally, ILC3s can be subdivided into two subsets according to the expression of natural cytotoxicity receptor (NCR) [5]. NCR<sup>+</sup> ILC3 cells express NK markers (NKp46 in mice and NKp44 in humans) and secrete IL-22 but little IL-17, whereas NCR<sup>-</sup> ILC3 cells produce IL-17 but limited amounts of IL-22 [5, 7]. Notably, the healthy human intestine contains primarily NCR<sup>+</sup> ILC3 [50]. Compared with other ILC subtypes, ILC3s are particularly relevant to the intestinal tract. ILC3s, particularly LT $\alpha$ i cells, contribute to tertiary lymphoid organogenesis [51–53], the containment of commensal bacteria [54], and the clearance of bacterial infections in the gut [55, 56]. Additionally, ILC3s are major regulators of the pathology of IBD [57, 58].

There is a relative decrease in the number of IL-22<sup>+</sup> ILC3s in the intestinal mucosa of IBD animal models or patients with IBD. IL-22 has protective effects on intestinal mucous membranes. NCR<sup>+</sup> ILC3s secrete IL-22 through interactions

with aromatic hydrocarbon receptor (AHR) from gut microbes and food, and IL-22 then acts on nonhematopoietic cells (such as epithelial cells) through interactions with heterodimeric receptors and the signal transducer and activator of transcription 3 (STAT3) pathway, mediating mucosal wound healing responses and promoting the proliferation and fucosylation of epithelial cells to maintain the integrity of the intestinal barrier [13, 59]. IL-22 deficiency causes intestinal mucosal barrier damage, leading to exposure of intestinal tissue to a large number of antigens. Abnormal immune responses are then induced in the host, leading to the development of IBD. Excessive production of IL-22 leads to pathological abnormalities such as tumor growth in a mouse model of colorectal cancer [60].

Inflammatory CD4<sup>+</sup> T cell responses to commensal bacteria are related to the pathogenesis of IBD. NCR<sup>-</sup> ILC3s express high levels of MHC class II gene (MHCII) molecules, which are involved in processing and presenting antigens, thereby limiting the response between CD4<sup>+</sup> T cells and intestinal commensal bacteria and inhibiting inflammation mediated by CD4<sup>+</sup> T cells [61, 62]. Furthermore, MHCII levels are reduced in pediatric patients with IBD [62]. ROR $\gamma$ t<sup>+</sup> ILCs are the primary source of CSF2 in the intestine. IL-1 $\beta$ , which is secreted by macrophages after identifying pathogenic bacteria or symbiotic bacteria, stimulates CSF2 production by ILC3 in the intestinal mucosa. This could in turn act on dendritic cells and macrophages to promote the secretion of regulatory factors, such as RA and IL-10, which induce the transformation of immature T cells into mature regulatory T cells (Tregs), these cells are essential for inhibiting inflammation and maintaining intestinal homeostasis [63]. Recent studies have also shown that IL-10 removes damaged mitochondria by blocking the metabolism of macrophages and promoting mitophagy, thereby suppressing inflammation [64].

Cytokines secreted by ILC3s have different effects in IBD. In addition to playing important roles in limiting chronic intestinal inflammation and maintaining tissue homeostasis, some ILC3s (IL-17-producing NCR<sup>-</sup> ILC3 cells) also have proinflammatory effects in IBD. Researchers have shown that the number of IL-17-producing ILC3s is significantly increased in inflamed intestines in patients with CD but not in patients with UC [58]. NCR<sup>-</sup> ILC3 cells mainly secrete IL-17. Recent evidence has strongly suggested that IL-17-producing ILC3s drive colonic inflammation during *Helicobacter hepaticus* infection, and the number of NCR<sup>-</sup> ILC3s was significantly increased in the intestinal tract of colitis model mice, resulting in activation of mononuclear macrophages via secretion of IL-17 and other cytokines and then inducing a series of mucosal inflammatory responses [65, 66]. Furthermore, IFN- $\gamma$  secreted by ILC3s also has proinflammatory effects, as described below. Excessive production of IL-17A and IFN- $\gamma$  would destroy the intestinal barrier and induce IBD.

**2.4. Other ILCs.** In addition to the three ILC subsets, new cells have been found to be closely associated with ILCs, however, the definitions of these cells remain unclear. Numerous studies have shown that ILCs exhibit plasticity and that plastic

changes among ILCs are likely to cause skewing of the functionally plastic ILC subsets due to the microenvironment, which will also be stated in this part.

iCD8 $\alpha$  cells are innate lymphocytes in the intestinal epithelium. These cells are derived from the lymphatic system and mediate innate immunity; thus, they are easily confused with ILCs. However, the development of iCD8 $\alpha$  cells does not require the transcriptional suppressor Id2, and these cells therefore cannot be classified as ILCs [67], but are instead thought to exist at the edge of the intestinal immune system [68]. Moreover, these cells also participate in the pathogenesis of IBD. In a mouse model of colitis induced by anti-CD40 antibodies, iCD8 $\alpha$  cells secrete abundant granzymes to enhance intestinal inflammation, which may promote infiltration of molecules into the intestinal epithelium [69].

ILCregs, a regulatory subpopulation of ILCs, have been identified in mouse and human intestines and have been shown to be regulated by the translational regulator Id3 [70]. ILCregs have been recently found to contribute protection against innate intestinal inflammation by secreting IL-10 to suppress the activation of ILC1s and ILC3s. In addition, autocrine transforming growth factor- (TGF-)  $\beta$ 1 produced by ILCregs is required for the expansion and survival of ILCregs during intestinal inflammation [70].

Some ILCs are plastic cells that can adopt another ILCs fate depending on environmental cues. Following stimulation with IL-12, some ILC3s have the ability to upregulate T-bet and downregulate ROR $\gamma$ t both in vitro and in vivo [55, 57, 71]. These changes promote the secretion of IFN- $\gamma$  to activate macrophages and other mononuclear phagocytes and induce the development of IBD [72]. IL-7 has also been shown to maintain stable expression of ROR $\gamma$ t and inhibit the transformation of ILC3s into ILC1-like cells, thereby reducing the inflammatory response [73]. The conversion from ILC3 to ILC1 was accompanied via downregulation of AHR [74]. Furthermore, researchers found that differentiation of ILC3s into ILC1s might be reversible. The transformation of CD127<sup>+</sup> ILC1s into ILC3s is induced by IL-23 and IL-1 $\beta$ . This process is dependent on the transcription factor ROR $\gamma$ t and is enhanced by retinoic acid [75]. Accordingly, the subtle balance between ILC1s and ILC3s ensures tissue integrity and maintains intestinal immune defense ability. In addition, plasticity has also been observed in ILC2s, which are modulated by IL-12 and express the Th1 cytokine IFN- $\gamma$  under inflammatory conditions [43], in turn, IL-4 could convert ILC1s into ILC2s [76].

### 3. Crosstalk between ILCs and Gut Microbiota

Many studies have examined the roles of ILCs in the intestinal tract with a focus on their relationships with the intestinal microbiota. The gut microbiota is an essential component of the intestine, and its highly dynamic balance is vital for maintaining intestinal health and preventing chronic inflammation. The ratio of bacteria to human cells is approximately 1:1 based on the recent estimates, most of them are from the intestines, with an amount of about 10<sup>14</sup> bacteria [77]. These bacteria form the gut microbiota [78], which plays an important role in human health and disease [79].

ILCs and the gut microbiota communicate with each other in an indirect manner via cytokine signaling, and these signals also combine with signals from intestinal epithelial cells (IECs) and macrophages. The symbiotic microflora can influence the differentiation of ILCs by inducing the expression of intestinal cytokines. Moreover, ILCs react to the gut microbiota by changing their structure, having protective or destructive effects on gut immunity. Among ILCs, the most important with regard to the gut microbiota are ILC3s. Signals that originate from commensal microorganisms affect the maturation of ILCs and the acquisition of the tissue-specific functions by ILCs. Many studies have shown that the microbiota is indispensable for differentiating ILCs and producing IL-22 [50]. IL-22 production by ILC3s also maintains the balance of the microbiota during early colonization resistance against pathogens [80]. Moreover, ILC3s are known to produce IL-22 to protect the body during *Citrobacter rodentium*-induced colitis [50], and IL-22 drives antimicrobial peptide expression and is required for the prevention of severe intestinal pathology and mortality during *C. rodentium*-induced colitis [81]. Interestingly, even in lymphocyte-replete hosts, mice lacking ROR $\gamma$ t<sup>+</sup> ILCs die from *C. rodentium* infection, although IL-22 can also be produced by Th-17 cells [82].

The gut microbiota can stimulate macrophagocytes to secrete IL- $\beta$ , which can induce ROR $\gamma$ t<sup>+</sup> ILCs to produce IL-22 [83]. Commensal bacteria directly interact with IECs. Additionally, a germ-free mouse experiment showed that the process of IL-7 secretion by IECs depends on the gut microbiota and that IL-7 is indispensable for promoting cytokine secretion from ILC3s [83]. IECs also secrete IL-25 following stimulation by gut microbiota, and IL-25 decreases the production of IL-22 by ILC3s [83]. IL-22 produced by ILC3s can promote the production of antimicrobial peptides (AMPs) secreted by IECs, thereby limiting symbiotic bacteria, and can regulate the anatomic location of lymphoid symbiotic bacteria [81, 84, 85]. Furthermore, IL-22 derived from ILC3s induces fucosylation in IECs, promoting host protection against enteric pathogens [86] and facilitating the establishment of a healthy intestinal microflora by inhibiting the growth of pathogenic bacteria and conditioned pathogens and preventing damage to the gut tissue [87]. In addition, microbial sensing and production of IL-1 $\beta$  by intestinal macrophages drive the secretion of CSF2 by ILC3s, which is needed for macrophage function and the stimulation of oral tolerance [63]. Additionally, the levels of specific *Alcaligenes* IgG in pediatric patients with CD are significantly increased, and the production of IL-22-dependent AMPs inhibits intestinal *Alcaligenes*, indicating that ILC3s play important roles in maintaining intestinal microenvironmental homeostasis [88].

AHR is essential for stimulating innate gut immunity by controlling ROR $\gamma$ t<sup>+</sup> ILCs [89, 90]. ROR $\gamma$ t<sup>+</sup> ILCs increased apoptosis in AHR-deficient mice, together with less production of IL-22 and the mice were particularly prone to infection with *C. rodentium* [89, 91]. Consumption of ILCs leads to infection by commensal bacteria and systemic inflammation, and these events can be suppressed by modulation of IL-22 [88]. Based on these results, ROR $\gamma$ t<sup>+</sup> ILC3s and IL-22

secretion play vital roles in intercommunication among cells [88, 92]. Importantly, ILCs and symbiotic microbes can immediately intercommunicate via Toll-like receptor (TLR) activation. TLR2 expressed on the surface of CD127<sup>+</sup> LTi-like ILCs can identify bacterial signals, permitting direct sensing of microbial cells [93]. ILCs may also interact with bacterial components through NCRs [94]. For example, NKp46 and NKp44 have been shown to immediately bind to epitopes of *Fusobacterium nucleatum* or *Mycobacterium tuberculosis* [95]. The activity of other ILC subsets can also be affected by microbiota. ROR $\gamma$ t<sup>+</sup> ILCs are stimulated by epithelial tuft-cell-derived IL-25 [18] in a microbiota-dependent manner [96]. Furthermore, crosstalk between DCs and ILCs would be important in the regulation of intestinal homeostasis, such as confrontation with *H. typhlonius*-driven inflammation, and T-bet, a T-box family transcription factor, plays a crucial role in regulating this interaction [97].

#### 4. Activation of ILCs by the ENS

ENS, enteric nervous system, is one of the main divisions of the autonomic nervous system and consists of a mesh-like system of neurons that governs the function of the gastrointestinal tract, it also acts a significant role in the activation of ILCs. The ENS includes the myenteric nerve plexuses and submucosal plexuses and can act alone or in combination with exogenous neurons, storing various nerve programs of gastrointestinal behavior patterns, to regulate almost all functions of the intestine, including exercise, nutrient absorption, immune responses, and blood supply. Moreover, the ENS can manipulate the intestinal tract to release various intestinal hormones, thereby affecting all organs within the body. Besides the brain, the ENS is the most complex nervous system and is sometimes called the “intestinal brain”. The interaction between the ENS and immune system has been reported; however, the relationship between the ENS and ILCs is still unclear. Recent studies have indicated that the ENS plays a role in the activation of ILCs, which then produce cytokines to exert their functions.

A novel process that protects the intestinal lining against inflammation and microbial aggression via interactions between enteric glial cells (EGCs) and ILC3s through neurotrophic factor signals has recently been reported. EGCs are the most abundant and widely distributed cells in the ENS and have been shown to support neuron function and to absorb and regulate certain active substances. Indeed, enteric ILC3 subsets express the neuroregulatory receptor tyrosine kinase (RET), which is activated by glial-derived neurotrophic factor (GDNF) family ligands (GFL) derived from EGCs. Activated RET then sends neural regulation signals to induce IL-22 secretion from ILC3s, thereby mediating intestinal repair. Additionally, neurotrophic factors also directly regulate innate IL-22 downstream of the STAT3 activation. These mechanisms then promote efficient gut homeostasis and defense [22]. Thus, the nervous system acts as a surveillance mechanism for the immune system. When nerve cells receive an alert from the gut, specific instructions are passed on to ILCs to produce effectors that can repair intestinal damage.

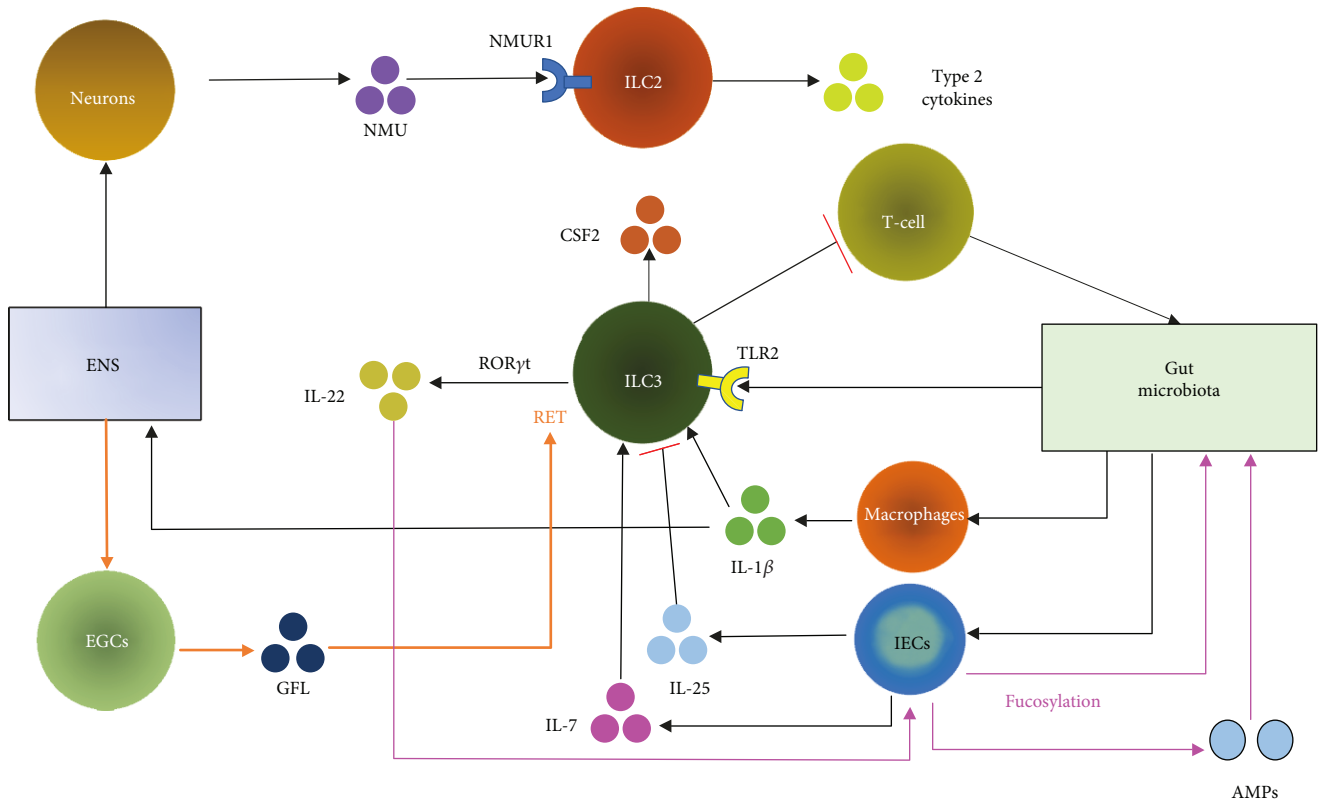


FIGURE 2: The main relationships between ILCs and the gut microbiota and between ILCs and the ENS in IBD. The gut microbiota can stimulate macrophages to secrete IL- $\beta$ , which can induce ROR $\gamma$ t<sup>+</sup> ILCs to produce IL-22. This process is also observed for IL-7, which is secreted by intestinal epithelial cells (IECs). IL-25, which is produced by IECs and stimulated by the gut microbiota, decreases the production of IL-22 by ILC3s. IL-22 can also induce fucosylation, which is required for host protection against enteric pathogens, in IECs. Microbial sensing and production of IL-1 $\beta$  by intestinal macrophages drive CSF2 secretion by ILC3s. Toll-like receptor 2 (TLR2) expressed on the surface of ILC3s can identify bacterial signals. ILC3 subsets express the neuroregulatory receptor tyrosine kinase (RET), which is activated by glial-derived neurotrophic factor family ligands (GFL) derived from enteric glial cells (EGCs), in response to IL-22 secretion. Neuronal messenger neuromedin U (NMU), produced by neurons, binds to NMUR1 on ILC2s, and ILC2s are activated to secrete innate type 2 cytokines. Activation of ILCs via the ENS or induction of cytokines via the gut microbiota can modulate the development or progression of IBD, as detailed in Figure 1. The gut microbiota is also associated with the ENS. Cytokines regulated by gut microbiota could modulate ENS activity directly or indirectly, e.g., IL-1 $\beta$ , which has its receptors on ENS neurons.

In mice, ILC2s, which are essential for immune responses to parasites, have been shown to express a receptor that binds to the neuronal messenger neuromedin U (NMU). Neurons produce large amounts of NMU, and neurons in the intestinal mucosal tissue, as important components of the ENS, rapidly generate NMU following detection of products secreted by helminth, NMU then actively transduces a signal to ILC2s by binding to NMU receptor 1 (NMUR1) on ILC2s. This results in secretion of innate type 2 cytokines to produce a rapid immune response at intestinal mucosal sites [21]. Some other researchers have also found that ILC2s in the intestinal tract of mice colocalize with cholinergic neurons, which produce NMU. In addition to NMUR1, the trigger for this signaling pathway is also dependent on cell-intrinsic expression of G $\alpha$ <sub>q</sub> protein. Furthermore, ILC2s were found to coevolve with the ENS to selectively regulate early sensing and responsiveness to infectious and external stimuli at barrier surfaces [20].

Another study suggested that the ENS maintains intestinal health by regulating the constitution of the gut

microbiota. The experimental results indicated that the number of proinflammatory bacteria increased significantly in the ENS-dysplastic zebrafish intestine, whereas the number of anti-inflammatory bacteria decreased obviously, resulting in increased incidence of IBD [98]. The main relationships between ILCs and the gut microbiota and between ILCs and the ENS in IBD are shown in Figure 2.

## 5. Conclusions and Future Directions

ILCs have been extensively studied in recent years, and there are many conflicting reports on ILC characteristics and functions. ILCs are relatively rare cells in lymphoid tissue, but participate in a variety of biological functions, particularly in the bowel [99]. Moreover, ILCs play pivotal roles in elimination of infectious pathogens, control of inflammation, and induction of sepsis. In addition to maintaining the homeostasis of the intestinal mucosal barrier in the normal intestinal environment, ILCs also participate in the

development and progression of IBD when the intestinal environment changes. Thus, ILCs have dual roles related to anti-inflammatory and proinflammatory responses. Overall, the mechanisms mediating the functions of ILCs are mostly related to the secretion of cytokines and the activities of transcription factors.

The gut microbiota and ENS have important roles in the gut, which are linked through ILCs. Neurons and EGCs (important components of the ENS) can induce ILCs to secrete inflammatory cytokines (such as IL-22). Additionally, the gut microbiota interacts with some cells (such as T cells and IECs), which can induce or inhibit the secretion of inflammatory cytokines by ILCs. The release of these cytokines can also alter the gut microbiota. Several reports have also suggested links between the gut microbiota and ENS, potentially involving ILCs [100, 101].

However, there are still many limitations to studies on ILCs. First, the boundaries between the groups of ILCs are still obscure. Expression profiles of cytokines and transcription factors in some ILC subsets are not stable, and mutual transformation may occur among the groups of ILCs [43]. In addition, there is a close relationship between ILCs and Th cell subsets, which function through the same cytokines, thereby making it difficult to clarify the specific intercellular relationships and to study the functions and mechanisms of each ILC subset separately. Existing data indicate that the nervous system sends out specific instructions to the immune system after nerve cells are stimulated by signals from the intestine. Based on such research, the ENS is known as the “second brain” and exhibits autonomic regulation of intestinal motility and secretion. However, further studies are needed to analyze the relationship between the nervous system and the immune system, including basic research studies on the molecular mechanisms. Neurons secrete NMU, which stimulates ILC2s and induces immune responses within a few minutes. This observation may have practical applications in the clinical setting with regard to the immune responses produced after vaccination, which typically require a few weeks. Moreover, most studies on ILCs have been carried out in mice, e.g., the established developmental hierarchy from a CLP and from more restricted precursors of different ILC lineages in mice, such as NKp, ILC1p, ILC2p, and ILC3p. These topics must also be examined in humans. However, although it is now clear that human CLP-like CD34<sup>+</sup> progenitors from different compartments can give rise to distinct ILC lineages, only NKp and ILC3p have been described in humans. Further in vitro and in vivo studies on human ILCs are needed to elucidate how ILCs operate in the human body. Such research will help us to understand the occurrence and development of IBD and to explore effective treatment strategies to combat related diseases in the future.

## Abbreviations

ILCs:	Innate lymphoid cells
IBD:	Inflammatory bowel disease
ENS:	Enteric nervous system
CLP:	Common lymphoid progenitor
IL:	Interleukin

Id2/3:	Inhibitor of DNA binding 2/3
NK:	Natural killer
LTi:	Lymphoid tissue inducer
Th:	T helper
IFN- $\gamma$ :	Interferon- $\gamma$
TNF- $\alpha$ :	Tumor necrosis factor- $\alpha$
GATA-3:	Gata binding protein 3
RAR:	Retinoic acid receptor
ROR $\alpha$ :	Related orphan receptor- $\alpha$
CSF2:	Colony stimulating factor 2
CD:	Crohn's disease
UC:	Ulcerative colitis
RA:	Retinoic acid
cNK:	Conventional NK
NCR:	Natural cytotoxicity receptor
AHR:	Aromatic hydrocarbon receptor
STAT3:	Signal transducer and activator of transcription 3
MHCII:	MHC class II gene
TGF- $\beta$ :	Transforming growth factor
IECs:	Intestinal epithelial cells
TLR:	Toll-like receptor
EGCs:	Enteric glial cells
RET:	Receptor tyrosine kinase
GFL:	Glial-derived neurotrophic factor family ligands
NMU:	Neuronal messenger neuromedin U
NMUR1:	NMU receptor 1
G $_{\alpha q}$ :	G-protein $\alpha$ -subunit q.

## Disclosure

Dr. Lin-hua Zhao and Dr. Xiao-lin Tong are cocorresponding authors.

## Conflicts of Interest

The authors declare that there are no conflicts of interest associated with the publication of this paper.

## Authors' Contributions

Dr. Lin Han and Dr. Xin-miao Wang contributed equally to this work.

## Acknowledgments

This work was supported by the National Natural Science Foundation of China (81704067 and 81430097), the Strategic Priority Research Program of the Chinese Academy of Sciences (XDA12030202), and Ningxia Key Research and Development Program Grant.

## References

- [1] A. Diefenbach, M. Colonna, and S. Koyasu, “Development, differentiation, and diversity of innate lymphoid cells,” *Immunity*, vol. 41, no. 3, pp. 354–365, 2014.
- [2] G. Eberl, M. Colonna, J. P. di Santo, and A. N. J. McKenzie, “Innate lymphoid cells: a new paradigm in immunology,” *Science*, vol. 348, no. 6237, 2015.

- [3] A. Baerenwaldt, N. von Burg, M. Kreuzaler et al., “Flt3 ligand regulates the development of innate lymphoid cells in fetal and adult mice,” *The Journal of Immunology*, vol. 196, no. 6, pp. 2561–2571, 2016.
- [4] G. Gasteiger, X. Fan, S. Dikiy, S. Y. Lee, and A. Y. Rudensky, “Tissue residency of innate lymphoid cells in lymphoid and nonlymphoid organs,” *Science*, vol. 350, no. 6263, pp. 981–985, 2015.
- [5] D. Artis and H. Spits, “The biology of innate lymphoid cells,” *Nature*, vol. 517, no. 7534, pp. 293–301, 2015.
- [6] T. E. O’Sullivan and J. C. Sun, “Innate lymphoid cell immunometabolism,” *Journal of Molecular Biology*, vol. 429, pp. 3577–3586, 2017.
- [7] V. Konya and J. Mjosberg, “Innate lymphoid cells in graft-versus-host disease,” *American Journal of Transplantation*, vol. 15, no. 11, pp. 2795–2801, 2015.
- [8] K.-A. G. Buela, S. Omenetti, and T. T. Pizarro, “Cross-talk between type 3 innate lymphoid cells and the gut microbiota in inflammatory bowel disease,” *Current Opinion in Gastroenterology*, vol. 31, no. 6, pp. 449–455, 2015.
- [9] D. di Liberto, P. Mansueto, A. D’Alcamo et al., “Predominance of type 1 innate lymphoid cells in the rectal mucosa of patients with non-celiac wheat sensitivity: reversal after a wheat-free diet,” *Clinical and Translational Gastroenterology*, vol. 7, no. 7, article e178, 2016.
- [10] Z. Li, R. J. Jackson, and C. Ransinghe, “Vaccination route can significantly alter the innate lymphoid cell subsets: a feedback between IL-13 and IFN- $\gamma$ ,” *Npj Vaccines*, vol. 3, no. 1, p. 10, 2018.
- [11] S. H. Wong, J. A. Walker, H. E. Jolin et al., “Transcription factor ROR $\alpha$  is critical for nuocyte development,” *Nature Immunology*, vol. 13, no. 3, pp. 229–236, 2012.
- [12] M. H. Kim, E. J. Taparowsky, and C. H. Kim, “Retinoic acid differentially regulates the migration of innate lymphoid cell subsets to the gut,” *Immunity*, vol. 43, no. 1, pp. 107–119, 2015.
- [13] M. Forkel and J. Mjösberg, “Dysregulation of group 3 innate lymphoid cells in the pathogenesis of inflammatory bowel disease,” *Current Allergy and Asthma Reports*, vol. 16, no. 10, p. 73, 2016.
- [14] M. D. Hazenberg and H. Spits, “Human innate lymphoid cells,” *Blood*, vol. 124, no. 5, pp. 700–709, 2014.
- [15] O. Olén, J. Askling, M. C. Sachs et al., “Childhood onset inflammatory bowel disease and risk of cancer: a Swedish nationwide cohort study 1964–2014,” *BMJ*, vol. 358, article j3951, 2017.
- [16] L. Beaugerie and S. H. Itzkowitz, “Cancers complicating inflammatory bowel disease,” *New England Journal of Medicine*, vol. 372, no. 15, pp. 1441–1452, 2015.
- [17] C. A. Lindemans, M. Calafiore, A. M. Mertelsmann et al., “Interleukin-22 promotes intestinal-stem-cell-mediated epithelial regeneration,” *Nature*, vol. 528, no. 7583, pp. 560–564, 2015.
- [18] J. von Moltke, M. Ji, H.-E. Liang, and R. M. Locksley, “Tuft-cell-derived IL-25 regulates an intestinal ILC2–epithelial response circuit,” *Nature*, vol. 529, no. 7585, pp. 221–225, 2016.
- [19] P. Aparicio-Domingo, M. Romera-Hernandez, J. J. Karrich et al., “Type 3 innate lymphoid cells maintain intestinal epithelial stem cells after tissue damage,” *Journal of Experimental Medicine*, vol. 212, no. 11, pp. 1783–1791, 2015.
- [20] C. S. N. Klose, T. Mahlaköiv, J. B. Moeller et al., “The neuropeptide neuromedin U stimulates innate lymphoid cells and type 2 inflammation,” *Nature*, vol. 549, no. 7671, pp. 282–286, 2017.
- [21] V. Cardoso, J. Chesné, H. Ribeiro et al., “Neuronal regulation of type 2 innate lymphoid cells via neuromedin U,” *Nature*, vol. 549, pp. 277–281, 2017.
- [22] S. Ibiza, B. García-Cassani, H. Ribeiro et al., “Glial-cell-derived neuroregulators control type 3 innate lymphoid cells and gut defence,” *Nature*, vol. 535, pp. 440–443, 2016.
- [23] E. van der Gracht, S. Zahner, and M. Kronenberg, “When insult is added to injury: cross talk between ILCs and intestinal epithelium in IBD,” *Mediators of Inflammation*, vol. 2016, Article ID 9765238, 11 pages, 2016.
- [24] Y. Simoni, M. Fehlings, H. N. Kløverpris et al., “Human innate lymphoid cell subsets possess tissue-type based heterogeneity in phenotype and frequency,” *Immunity*, vol. 46, no. 1, pp. 148–161, 2017.
- [25] R. Kiessling, E. Klein, and H. Wigzell, “Natural killer cells in the mouse. I. Cytotoxic cells with specificity for mouse Moloney leukemia cells. Specificity and distribution according to genotype,” *European Journal of Immunology*, vol. 5, no. 2, pp. 112–117, 1975.
- [26] C. S. N. Klose, M. Flach, L. Möhle et al., “Differentiation of type 1 ILCs from a common progenitor to all helper-like innate lymphoid cell lineages,” *Cell*, vol. 157, no. 2, pp. 340–356, 2014.
- [27] C. A. J. Vosshenrich and J. P. Di Santo, “Developmental programming of natural killer and innate lymphoid cells,” *Current Opinion in Immunology*, vol. 25, no. 2, pp. 130–138, 2013.
- [28] E. Vivier, D. H. Raulet, A. Moretta et al., “Innate or adaptive immunity? The example of natural killer cells,” *Science*, vol. 331, no. 6013, pp. 44–49, 2011.
- [29] P. K. Yadav, C. Chen, and Z. Liu, “Potential role of NK cells in the pathogenesis of inflammatory bowel disease,” *BioMed Research International*, vol. 2011, Article ID 348530, 6 pages, 2011.
- [30] M. Janyszek and A. M. Jagodzinski, “Selective decrease in colonic CD56<sup>+</sup> T and CD161<sup>+</sup> T cells in the inflamed mucosa of patients with ulcerative colitis,” *World Journal of Gastroenterology*, vol. 13, no. 45, pp. 5995–6002, 2007.
- [31] G. Bisping, N. Luger, S. Lutke-Brintrup et al., “Patients with inflammatory bowel disease (IBD) reveal increased induction capacity of intracellular interferon-gamma (IFN- $\gamma$ ) in peripheral CD8<sup>+</sup> lymphocytes co-cultured with intestinal epithelial cells,” *Clinical and Experimental Immunology*, vol. 123, no. 1, pp. 15–22, 2001.
- [32] J. W. Bostick and L. Zhou, “Innate lymphoid cells in intestinal immunity and inflammation,” *Cellular and Molecular Life Sciences*, vol. 73, no. 2, pp. 237–252, 2016.
- [33] A. Fuchs, W. Vermi, J. S. Lee et al., “Intraepithelial type 1 innate lymphoid cells are a unique subset of IL-12- and IL-15-responsive IFN- $\gamma$ -producing cells,” *Immunity*, vol. 38, no. 4, pp. 769–781, 2013.
- [34] K. J. Maloy and H. H. Uhlig, “ILC1 populations join the border patrol,” *Immunity*, vol. 38, no. 4, pp. 630–632, 2013.
- [35] S. Sedda, I. Marafini, M. M. Figliuzzi, F. Pallone, and G. Monteleone, “An overview of the role of innate lymphoid cells in gut infections and inflammation,” *Mediators of Inflammation*, vol. 2014, Article ID 235460, 7 pages, 2014.
- [36] D. R. Neill, S. H. Wong, A. Bellosi et al., “Nuocytes represent a new innate effector leukocyte that mediates type-2 immunity,” *Nature*, vol. 464, no. 7293, pp. 1367–1370, 2010.

- [37] L. A. Monticelli, G. F. Sonnenberg, M. C. Abt et al., "Innate lymphoid cells promote lung-tissue homeostasis after infection with influenza virus," *Nature Immunology*, vol. 12, no. 11, pp. 1045–1054, 2011.
- [38] J. C. Nussbaum, S. J. van Dyken, J. von Moltke et al., "Type 2 innate lymphoid cells control eosinophil homeostasis," *Nature*, vol. 502, no. 7470, pp. 245–248, 2013.
- [39] R. G. J. K. Wolterink, A. KleinJan, M. van Nimwegen et al., "Pulmonary innate lymphoid cells are major producers of IL-5 and IL-13 in murine models of allergic asthma," *European Journal of Immunology*, vol. 42, no. 5, pp. 1106–1116, 2012.
- [40] A. S. Mirchandani, A. G. Besnard, E. Yip et al., "Type 2 innate lymphoid cells drive CD4<sup>+</sup> Th2 cell responses," *Journal of Immunology*, vol. 192, no. 5, pp. 2442–2448, 2014.
- [41] C. J. Oliphant, Y. Y. Hwang, J. A. Walker et al., "MHCII-mediated dialog between group 2 innate lymphoid cells and CD4<sup>+</sup> T cells potentiates type 2 immunity and promotes parasitic helminth expulsion," *Immunity*, vol. 41, no. 2, pp. 283–295, 2014.
- [42] S. J. Van Dyken, J. C. Nussbaum, J. Lee et al., "A tissue checkpoint regulates type 2 immunity," *Nature Immunology*, vol. 17, pp. 1381–1387, 2016.
- [43] A. I. Lim, S. Menegatti, J. Bustamante et al., "IL-12 drives functional plasticity of human group 2 innate lymphoid cells," *Journal of Experimental Medicine*, vol. 213, no. 4, pp. 569–583, 2016.
- [44] A. Camelo, J. L. Barlow, L. F. Drynan et al., "Blocking IL-25 signalling protects against gut inflammation in a type-2 model of colitis by suppressing nuocyte and NKT derived IL-13," *Journal of Gastroenterology*, vol. 47, no. 11, pp. 1198–1211, 2012.
- [45] M. S. Shajib, H. Wang, J. J. Kim et al., "Interleukin 13 and serotonin: linking the immune and endocrine systems in murine models of intestinal inflammation," *PLoS One*, vol. 8, no. 8, article e72774, 2013.
- [46] M. N. Ince, D. E. Elliott, T. Setiawan et al., "Role of T cell TGF- $\beta$  signaling in intestinal cytokine responses and helminthic immune modulation," *European Journal of Immunology*, vol. 39, no. 7, pp. 1870–1878, 2009.
- [47] K. Takahashi, H. Imaeda, T. Fujimoto et al., "Regulation of eotaxin-3/CC chemokine ligand 26 expression by T helper type 2 cytokines in human colonic myofibroblasts," *Clinical & Experimental Immunology*, vol. 173, no. 2, pp. 323–331, 2013.
- [48] K. A. Kelly and R. Scollay, "Seeding of neonatal lymph nodes by T cells and identification of a novel population of CD3<sup>+</sup>CD4<sup>+</sup> cells," *European Journal of Immunology*, vol. 22, no. 2, pp. 329–334, 1992.
- [49] B. Krämer, F. Goeser, P. Lutz et al., "Compartment-specific distribution of human intestinal innate lymphoid cells is altered in HIV patients under effective therapy," *PLoS Pathogens*, vol. 13, no. 5, article e1006373, 2017.
- [50] N. Satoh-Takayama, C. A. J. Vosshenrich, S. Lesjean-Pottier et al., "Microbial flora drives interleukin 22 production in intestinal NKp46<sup>+</sup> cells that provide innate mucosal immune defense," *Immunity*, vol. 29, no. 6, pp. 958–970, 2008.
- [51] S. A. van de Pavert and R. E. Mebius, "New insights into the development of lymphoid tissues," *Nature Reviews Immunology*, vol. 10, no. 9, pp. 664–674, 2010.
- [52] E. Scandella, B. Bolinger, E. Lattmann et al., "Restoration of lymphoid organ integrity through the interaction of lymphoid tissue-inducer cells with stroma of the T cell zone," *Nature Immunology*, vol. 9, no. 6, pp. 667–675, 2008.
- [53] M. Y. Kim, "Roles of embryonic and adult lymphoid tissue inducer cells in primary and secondary lymphoid tissues," *Yonsei Medical Journal*, vol. 49, no. 3, pp. 352–356, 2008.
- [54] G. F. Sonnenberg and D. Artis, "Innate lymphoid cell interactions with microbiota: implications for intestinal health and disease," *Immunity*, vol. 37, no. 4, pp. 601–610, 2012.
- [55] C. S. N. Klose, E. A. Kiss, V. Schwierzeck et al., "A T-bet gradient controls the fate and function of CCR6-ROR $\gamma$ t<sup>+</sup> innate lymphoid cells," *Nature*, vol. 494, no. 7436, pp. 261–265, 2013.
- [56] A. Diefenbach, "Innate lymphoid cells in the defense against infections," *European Journal of Microbiology and Immunology*, vol. 3, no. 3, pp. 143–151, 2013.
- [57] J. H. Bernink, C. P. Peters, M. Munneke et al., "Human type 1 innate lymphoid cells accumulate in inflamed mucosal tissues," *Nature Immunology*, vol. 14, no. 3, pp. 221–229, 2013.
- [58] A. Geremia, C. V. Arancibia-Cárcamo, M. P. P. Fleming et al., "IL-23-responsive innate lymphoid cells are increased in inflammatory bowel disease," *Journal of Experimental Medicine*, vol. 208, no. 6, pp. 1127–1133, 2011.
- [59] X. Guo, J. Qiu, T. Tu et al., "Induction of innate lymphoid cell-derived interleukin-22 by the transcription factor STAT3 mediates protection against intestinal infection," *Immunity*, vol. 40, no. 1, pp. 25–39, 2014.
- [60] S. Huber, N. Gagliani, L. A. Zenewicz et al., "IL-22BP is regulated by the inflammasome and modulates tumorigenesis in the intestine," *Nature*, vol. 491, no. 7423, pp. 259–263, 2012.
- [61] M. R. Hepworth, L. A. Monticelli, T. C. Fung et al., "Innate lymphoid cells regulate CD4<sup>+</sup> T cell responses to intestinal commensal bacteria," *Nature*, vol. 498, no. 7452, pp. 113–117, 2013.
- [62] M. R. Hepworth, T. C. Fung, S. H. Masur et al., "Group 3 innate lymphoid cells mediate intestinal selection of commensal bacteria-specific CD4<sup>+</sup> T cells," *Science*, vol. 348, no. 6238, pp. 1031–1035, 2015.
- [63] A. Mortha, A. Chudnovskiy, D. Hashimoto et al., "Microbiota-dependent crosstalk between macrophages and ILC3 promotes intestinal homeostasis," *Science*, vol. 343, no. 6178, p. 1249288, 2014.
- [64] W. K. E. Ip, N. Hoshi, D. S. Shouval, S. Snapper, and R. Medzhitov, "Anti-inflammatory effect of IL-10 mediated by metabolic reprogramming of macrophages," *Science*, vol. 356, no. 6337, pp. 513–519, 2017.
- [65] S. Buonocore, P. P. Ahern, H. H. Uhlig et al., "Innate lymphoid cells drive interleukin-23-dependent innate intestinal pathology," *Nature*, vol. 464, no. 7293, pp. 1371–1375, 2010.
- [66] J. Ermann, T. Staton, J. N. Glickman, R. de Waal Malefyt, and L. H. Glimcher, "Nod/Ripk2 signaling in dendritic cells activates IL-17A-secreting innate lymphoid cells and drives colitis in T-bet<sup>-/-</sup>Rag2<sup>-/-</sup> (TRUC) mice," *Proceedings of the National Academy of Sciences of the United States of America*, vol. 111, no. 25, pp. E2559–E2566, 2014.
- [67] L. van Kaer, H. M. Scott Algood, K. Singh et al., "CD8 $\alpha$ <sup>+</sup> innate-type lymphocytes in the intestinal epithelium mediate

- mucosal immunity,” *Immunity*, vol. 41, no. 3, pp. 451–464, 2014.
- [68] D. Olivares-Villagómez and L. Van Kaer, “iCD8 $\alpha$  cells: living at the edge of the intestinal immune system,” *Oncotarget*, vol. 6, no. 24, pp. 19964–19965, 2015.
- [69] A. A. Kumar, A. G. Delgado, M. B. Piazuelo, L. van Kaer, and D. Olivares-Villagómez, “Innate CD8 $\alpha\alpha^+$  lymphocytes enhance anti-CD40 antibody-mediated colitis in mice,” *Immunity, Inflammation and Disease*, vol. 5, no. 2, pp. 109–123, 2017.
- [70] S. Wang, P. Xia, Y. Chen et al., “Regulatory innate lymphoid cells control innate intestinal inflammation,” *Cell*, vol. 171, no. 1, pp. 201–216.e18, 2017.
- [71] C. Vonarbourg, A. Mortha, V. L. Bui et al., “Progressive loss of ROR $\gamma$ t expression confers distinct functional fates to natural killer cell receptor-expressing ROR $\gamma$ t<sup>+</sup> innate lymphocytes,” *Immunity*, vol. 33, no. 5, pp. 736–751, 2011.
- [72] J. Li, A. L. Doty, A. Iqbal, and S. C. Glover, “The differential frequency of Lineage<sup>−</sup> CRTH2<sup>−</sup> CD45<sup>+</sup> NKp44<sup>−</sup> CD117<sup>−</sup> CD127<sup>+</sup> ILC subset in the inflamed terminal ileum of patients with Crohn’s disease,” *Cellular Immunology*, vol. 304–305, pp. 63–68, 2016.
- [73] C. Vonarbourg, A. Mortha, V. L. Bui et al., “Regulated expression of nuclear receptor ROR $\gamma$ t confers distinct functional fates to NK cell receptor-expressing ROR $\gamma$ t<sup>+</sup> innate lymphocytes,” *Immunity*, vol. 33, no. 5, pp. 736–751, 2010.
- [74] J. Li, A. Doty, and S. C. Glover, “Aryl hydrocarbon receptor signaling involves in the human intestinal ILC3/ILC1 conversion in the inflamed terminal ileum of Crohn’s disease patients,” *Inflamm Cell Signal*, vol. 3, no. 3, article e1404, 2016.
- [75] J. H. Bernink, L. Krabbendam, K. Germar et al., “Interleukin-12 and -23 control plasticity of CD127<sup>+</sup> group 1 and group 3 innate lymphoid cells in the intestinal lamina propria,” *Immunity*, vol. 43, no. 1, pp. 146–160, 2015.
- [76] S. M. Bal, J. H. Bernink, M. Nagasawa et al., “IL-1 $\beta$ , IL-4 and IL-12 control the fate of group 2 innate lymphoid cells in human airway inflammation in the lungs,” *Nature Immunology*, vol. 17, no. 6, pp. 636–645, 2016.
- [77] R. Sender, S. Fuchs, and R. Milo, “Are we really vastly outnumbered? Revisiting the ratio of bacterial to host cells in humans,” *Cell*, vol. 164, no. 3, pp. 337–340, 2016.
- [78] K. Honda and D. R. Littman, “The microbiome in infectious disease and inflammation,” *Annual Review of Immunology*, vol. 30, no. 1, pp. 759–795, 2012.
- [79] Y. W. Min and P. L. Rhee, “The role of microbiota on the gut immunology,” *Clinical Therapeutics*, vol. 37, no. 5, pp. 968–975, 2015.
- [80] X. Guo, Y. Liang, Y. Zhang, A. Lasorella, B. L. Kee, and Y. X. Fu, “Innate lymphoid cells control early colonization resistance against intestinal pathogens through ID2-dependent regulation of the microbiota,” *Immunity*, vol. 42, no. 4, pp. 731–743, 2015.
- [81] Y. Zheng, P. A. Valdez, D. M. Danilenko et al., “Interleukin-22 mediates early host defense against attaching and effacing bacterial pathogens,” *Nature Medicine*, vol. 14, no. 3, pp. 282–289, 2008.
- [82] J. Qiu, X. Guo, Z. M. E. Chen et al., “Group 3 innate lymphoid cells inhibit T-cell-mediated intestinal inflammation through aryl hydrocarbon receptor signaling and regulation of microflora,” *Immunity*, vol. 39, no. 2, pp. 386–399, 2013.
- [83] K. A. G. Buela, S. Omenetti, and T. T. Pizarro, “Crosstalk between type 3 innate lymphoid cells and the gut microbiota in inflammatory bowel disease,” *Current Opinion in Gastroenterology*, vol. 31, no. 6, pp. 449–455, 2015.
- [84] S. Vaishnava, M. Yamamoto, K. M. Severson et al., “The anti-bacterial lectin RegIII $\gamma$  promotes the spatial segregation of microbiota and host in the intestine,” *Science*, vol. 334, no. 6053, pp. 255–258, 2011.
- [85] Y. Goto and I. I. Ivanov, “Intestinal epithelial cells as mediators of the commensal-host immune crosstalk,” *Immunology and Cell Biology*, vol. 91, no. 3, pp. 204–214, 2013.
- [86] Y. Goto, T. Obata, J. Kunisawa et al., “Innate lymphoid cells regulate intestinal epithelial cell glycosylation,” *Science*, vol. 345, no. 6202, article 1254009, 2014.
- [87] J. M. Pickard, C. F. Maurice, M. A. Kinnebrew et al., “Rapid fucosylation of intestinal epithelium sustains host-commensal symbiosis in sickness,” *Nature*, vol. 514, no. 7524, pp. 638–641, 2014.
- [88] G. F. Sonnenberg, L. A. Monticelli, T. Alenghat et al., “Innate lymphoid cells promote anatomical containment of lymphoid-resident commensal bacteria,” *Science*, vol. 336, no. 6086, pp. 1321–1325, 2012.
- [89] E. A. Kiss, C. Vonarbourg, S. Kopfmann et al., “Natural aryl hydrocarbon receptor ligands control organogenesis of intestinal lymphoid follicles,” *Science*, vol. 334, no. 6062, pp. 1561–1565, 2011.
- [90] Y. Li, S. Innocentin, D. R. Withers et al., “Exogenous stimuli maintain intraepithelial lymphocytes via aryl hydrocarbon receptor activation,” *Cell*, vol. 147, no. 3, pp. 629–640, 2011.
- [91] J. Qiu, J. J. Heller, X. Guo et al., “The aryl hydrocarbon receptor regulates gut immunity through modulation of innate lymphoid cells,” *Immunity*, vol. 36, no. 1, pp. 92–104, 2012.
- [92] G. F. Sonnenberg, L. A. Fouser, and D. Artis, “Border patrol: regulation of immunity, inflammation and tissue homeostasis at barrier surfaces by IL-22,” *Nature Immunology*, vol. 12, no. 5, pp. 383–390, 2011.
- [93] N. K. Crellin, S. Trifari, C. D. Kaplan, N. Satoh-Takayama, J. P. di Santo, and H. Spits, “Regulation of cytokine secretion in human CD127<sup>+</sup> LTi-like innate lymphoid cells by toll-like receptor 2,” *Immunity*, vol. 33, no. 5, pp. 752–764, 2010.
- [94] S. Chaushu, A. Wilensky, C. Gur et al., “Direct recognition of fusobacterium nucleatum by the NK cell natural cytotoxicity receptor NKp46 aggravates periodontal disease,” *PLoS Pathogens*, vol. 8, no. 3, article e1002601, 2012.
- [95] P. H. Kruse, J. Matta, S. Ugolini, and E. Vivier, “Natural cytotoxicity receptors and their ligands,” *Immunology & Cell Biology*, vol. 92, no. 3, pp. 221–229, 2014.
- [96] S. Sawa, M. Lochner, N. Satoh-Takayama et al., “ROR $\gamma$ t<sup>+</sup> innate lymphoid cells regulate intestinal homeostasis by integrating negative signals from the symbiotic microbiota,” *Nature Immunology*, vol. 12, no. 4, pp. 320–326, 2011.
- [97] N. Powell, A. W. Walker, E. Stolarczyk et al., “The transcription factor T-bet regulates intestinal inflammation mediated by interleukin-7 receptor<sup>+</sup> innate lymphoid cells,” *Immunity*, vol. 37, no. 4, pp. 674–684, 2012.
- [98] A. S. Rolig, E. K. Mittge, J. Ganz et al., “The enteric nervous system promotes intestinal health by constraining microbiota composition,” *PLoS Biology*, vol. 15, no. 2, article e2000689, 2017.

- [99] H. Spits and J. P. Di Santo, "The expanding family of innate lymphoid cells: regulators and effectors of immunity and tissue remodeling," *Nature Immunology*, vol. 12, pp. 21–27, 2011.
- [100] A. Bessac, P. D. Cani, E. Meunier, G. Dietrich, and C. Knauf, "Inflammation and gut-brain axis during type 2 diabetes: focus on the crosstalk between intestinal immune cells and enteric nervous system," *Frontiers in Neuroscience*, vol. 12, 2018.
- [101] F. de Vadder, E. Grasset, L. M. Holm et al., "Gut microbiota regulates maturation of the adult enteric nervous system via enteric serotonin networks," *Proceedings of the National Academy of Sciences of the United States of America*, vol. 115, no. 25, pp. 6458–6463, 2018.

## Research Article

# Chemokines and Growth Factors Produced by Lymphocytes in the Incompetent Great Saphenous Vein

Ewa Grudzińska <sup>1</sup>, Sławomir Grzegorzczyn,<sup>2</sup> and Zenon P. Czuba <sup>1</sup>

<sup>1</sup>School of Medicine with the Division of Dentistry in Zabrze, Medical University of Silesia in Katowice, Department of Microbiology and Immunology, Jordana 19, 41-808 Zabrze, Poland

<sup>2</sup>School of Medicine with the Division of Dentistry in Zabrze, Medical University of Silesia in Katowice, Department of Biophysics, Jordana 19, 41-808 Zabrze, Poland

Correspondence should be addressed to Ewa Grudzińska; [ewa.grudzinska@med.sum.edu.pl](mailto:ewa.grudzinska@med.sum.edu.pl)

Received 4 October 2018; Revised 20 November 2018; Accepted 28 November 2018; Published 10 January 2019

Guest Editor: Qingdong Guan

Copyright © 2019 Ewa Grudzińska et al. This is an open access article distributed under the Creative Commons Attribution License, which permits unrestricted use, distribution, and reproduction in any medium, provided the original work is properly cited.

The role of cytokines in the pathogenesis of chronic venous disease (CVD) remains obscure. It has been postulated that oscillatory flow present in incompetent veins causes proinflammatory changes. Our earlier study confirmed this hypothesis. This study is aimed at assessing chemokines and growth factors (GFs) released by lymphocytes in patients with great saphenous vein (GSV) incompetence. In 34 patients exhibiting reflux in GSV, blood was derived from the cubital vein and from the incompetent saphenofemoral junction. In 12 healthy controls, blood was derived from the cubital vein. Lymphocyte culture with and without stimulation by phytohemagglutinin (PHA) was performed. Eotaxin, interleukin 8 (IL-8), macrophage inflammatory protein 1 A and 1B (MIP-1A and MIP-1B), interferon gamma-induced protein (IP-10), monocyte chemoattractant protein-1 (MCP-1), interleukin 5 (IL-5), fibroblast growth factor (FGF), granulocyte colony-stimulating factor (G-CSF), granulocyte-macrophage colony-stimulating factor (GM-CSF), platelet-derived growth factor-BB (PDGF-BB), and vascular endothelial growth factor (VEGF) were assessed in culture supernatants by a Bio-Plex assay. Higher concentrations of eotaxin and G-CSF were revealed in the incompetent GSV, compared with the concentrations in the patients' upper limbs. The concentrations of MIP-1A and MIP-1B were higher in the CVD group while the concentration of VEGF was lower. In the stimulated cultures, the concentration of G-CSF proved higher in the incompetent GSV, as compared with the patients' upper limbs. Between the groups, the concentration of eotaxin was higher in the CVD group, while the IL-5 and MCP-1 concentrations were lower. IL-8, IP-10, FGF, GM-CSF, and PDGF-BB did not reveal any significant differences in concentrations between the samples. These observations suggest that the concentrations of chemokines and GFs are different in the blood of CVD patients. The oscillatory flow present in incompetent veins may play a role in these changes. However, the role of cytokines in CVD requires further study.

## 1. Introduction

Chronic venous disease (CVD) affects up to 85% of the population, and more advanced clinical changes (C3–C6 in the Clinical-Etiology-Anatomy-Pathophysiology (CEAP) classification) occur in about 30% of the population [1–4]. Its exact pathogenesis remains unclear. However, the impact of inflammatory processes is considered crucial for venous wall remodeling [5–11]. Reflux in the incompetent veins causes oscillatory flow, with blood moving towards the heart during the contraction of the muscular pump of the calf and

backwards during the relaxation of the calf [12]. It has been demonstrated that these flow changes cause the release of proinflammatory cytokines by endothelial cells and lead to leukocyte-mediated inflammatory reactions [12–16]. Our recent publication demonstrated that proinflammatory cytokines are released by lymphocytes in higher concentrations in the incompetent veins [17].

In order to further investigate the role of cytokines released by lymphocytes in CVD, we studied two other panels: chemotactic cytokines and growth factors (GFs). Both these cytokine groups have previously been described as

released in higher concentrations by endothelium subject to hypoxia [18]. Following our previous findings which confirmed the proinflammatory state in CVD, it seemed probable that the levels of chemotactic cytokines should be elevated in the incompetent vein, recruiting leukocytes and promoting the inflammatory process. The influence of GFs on the histological changes in CVD also seemed possible. The incompetent vein wall is known to be distorted, with a degraded extracellular matrix [19], damaged intima [20–23], and disorganized, hypertrophic media [24, 25]. An imbalance between collagen and elastin has been observed, with lower content of elastin and collagen type III and higher content of collagen type I [26–29]. These changes are linked to a higher metalloproteinase activity [19, 30], dysregulated apoptosis [14, 24, 31], and elevated smooth muscle proliferation [25]. Increased numbers of vasa vasorum in varicose veins have also been observed [23]. The GFs have been demonstrated to play a role in regulating the metalloproteinase activity [32]. Moreover, they take part in neovascularisation. Therefore, their role in CVD progression seems possible.

Few papers describe cytokines in CVD [9], and there are no studies concerning the role of chemokines and GFs released by lymphocytes in this disease. No differences in the lymphocyte percentage were observed in the varicose veins when compared to healthy veins [6, 33], and the lymphocytes were shown to have an important role in venous ulcer development [34].

We expected to find different cytokine production in the incompetent vein with oscillatory flow when compared to the same patients' healthy cubital vein with laminar (unidirectional) flow. The circulating lymphocytes are also subject to contact with turbulent flow and pathologically changed endothelium of the incompetent vein; therefore, differences in cytokine concentrations in the cubital blood from healthy subjects and CVD patients were expected. Finally, the lymphocytes in CVD group may react differently to stimulating agents than the lymphocytes in the healthy group.

## 2. Materials and Methods

The study has been carried out in accordance with the Declaration of Helsinki and approved by the Bioethical Committee of the Medical University of Silesia (KNW/0022/KB1/31/I/12). All participants gave their written informed consent for the study.

The CVD group consisted of 34 primary CVD patients with great saphenous vein (GSV) incompetence confirmed by the Doppler ultrasound examination. The reflux at saphenofemoral junction (reflux time > 0.5 s) was confirmed in all patients in standing position, with blood flow induced by manual squeezing. The control group included 12 volunteers with healthy GSV confirmed by the Doppler ultrasound. The exclusion criteria involved history of venous thrombosis, pregnancy, diabetes, any inflammatory diseases present in the past two weeks, alcohol abuse, smoking, ulceration on the examined limb during the last month, and intake of anti-inflammatory drugs within the past two weeks.

Blood samples were obtained from the cubital vein in both groups, collected to vials containing heparin (10 IU/ml

of blood). Consequently, patients from the CVD group underwent standard surgical procedure of GSV stripping, with femoral nerve block and additional local anaesthesia. The inguinal incision and visualization of the GSV were performed. A blood sample from the GSV directly below the incompetent saphenofemoral junction was collected into a heparinized vial. All samples were immediately transferred to the laboratory, and the temperature of 37°C was maintained. Cultures of lymphocytes were prepared either with lymphocyte-stimulating phytohemagglutinin (PHA) or with a medium as follows:

The lymphocytes were separated by the use of Histopaque gradients (1.119 g/ml and 1.077 g/ml). After centrifugation (700 × *g*, 30 min), the separated lymphocytes were transferred to another vial and washed twice with phosphate-buffered saline (PBS) (250 × *g*, 10 min). Microscopic morphological assessment of cell population was performed, and no differences were found between the groups. No significant contamination by other cells was found in the samples.

A suspension of 2 MM lymphocyte cells/ml of medium (Roswell Park Memorial Institute (RPMI) 1640, 10% bovine serum, penicillin 100 U/ml, and streptomycin 100 µg/ml) was prepared. 0.5 ml of this suspension was added to a 0.5 ml of PHA solution (20 µg PHA/ml of medium) and for no-stimulation samples, 0.5 ml of the suspension to a 0.5 ml of medium. These suspensions were incubated for 24 h in 37°C, 5% CO<sub>2</sub> atmosphere, and 99% humidity. After incubation and centrifugation (250 × *g*, 10 min), the supernatant was collected into the Eppendorf vials and stored at -80°C.

Assessed panels included chemotactic factors: eotaxin, interleukin 8 (IL-8), macrophage inflammatory protein 1 A and 1B (MIP-1A and MIP-1B), interferon gamma-induced protein (IP-10), monocyte chemoattractant protein-1 (MCP-1), and GFs: interleukin 5 (IL-5), fibroblast growth factor (FGF), granulocyte colony-stimulating factor (G-CSF), granulocyte-macrophage colony-stimulating factor (GM-CSF), platelet-derived growth factor-BB (PDGF-BB), and vascular endothelial growth factor (VEGF).

The samples were thawed directly before the Bio-Plex assay. The assay uses magnetic beads with anticytokine immunoglobulins to assess simultaneously the concentrations of many cytokines. The samples were processed following the manufacturer's instructions (Bio-Plex Pro™ Human Cytokine Assays, Bio-Rad Laboratories) and read using Bio-Rad Bio-Plex™ 200 System with Bio-Plex Manager™ Software. The statistical analysis was performed with the use of STATISTICA 10.0 software. The cytokine data were not normally distributed; therefore, nonparametric tests were applied. Mean/median differences were analyzed by Student's paired *t*-test, the Wilcoxon signed-rank test, or the Mann-Whitney *U* test. The leukocyte count and lymphocyte percentage had normal distribution; therefore, Student's *t*-test was applied.

## 3. Results and Discussion

**3.1. Results.** The CVD group consisted of 34 patients, 85% of which were women. Median age was 47 ± 25 (21–68). The

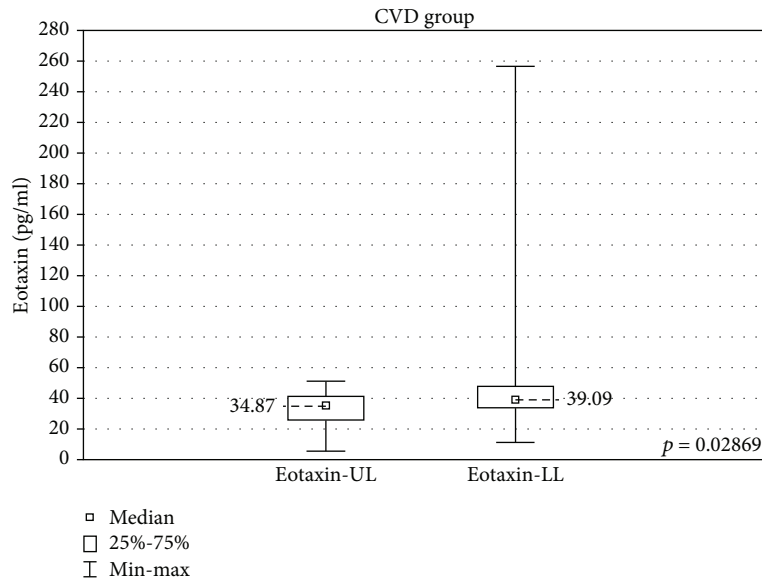


FIGURE 1: Comparison of eotaxin concentrations in the upper (eotaxin-UL) and lower limb samples (eotaxin-LL) in the CVD groups, cultured without stimulation.

patients belonged to clinical CEAP classes C2-C3, with 43% in C2 and 57% in C3. The control group consisted of 12 patients, 92% of which were women. Median age was  $36 \pm 27$  (29-64). The white blood cell count was mean  $5.6 \times 10^3/\mu\text{l}$  ( $3.7-8.8 \times 10^3/\mu\text{l}$ ) in the CVD group and  $5.9 \times 10^3/\mu\text{l}$  ( $4.6-7.5 \times 10^3/\mu\text{l}$ ) in the control group. The lymphocyte percentage was mean 39% (22%-47%) in the CVD group and 36% (23%-45%) in the control group. There were no statistically significant differences between the groups.

In the samples cultured without stimulation, significantly higher concentrations of eotaxin and G-CSF were found in the incompetent GSV samples in comparison with the cubital vein samples of the same patients (results are expressed as median  $\pm$  quartile deviation and range).

Eotaxin:  $39.09 \pm 14.1$  (11.4-256.8) pg/ml vs  $34.87 \pm 15.47$  (5.6-51.34) pg/ml,  $p < 0.05$  and G-CSF:  $107.4 \pm 91.5$  (36.3-1613) pg/ml vs  $89.6 \pm 91.9$  (24.7-1381) pg/ml,  $p < 0.05$ . The above results are presented in Figures 1 and 2.

When the upper limb samples cultured without stimulation were compared between the groups, significantly higher concentrations of MIP-1A and MIP-1B were found in the upper limb samples of the CVD group (MIP-1A:  $181.1 \pm 1633$  (2.18-3163) pg/ml vs  $29.2 \pm 3123$  (2.7-3125) pg/ml,  $p < 0.05$  and MIP-1B:  $1514 \pm 905.1$  (185.6-9142) pg/ml vs  $927.8 \pm 325.1$  (444.3-1396) pg/ml,  $p < 0.01$ ). The CVD group showed lower concentrations of VEGF ( $53.9 \pm 53.3$  (17.4-276.8) pg/ml vs  $76.2 \pm 78.6$  (35.3-263.5) pg/ml,  $p < 0.05$ ). These results are presented in Figures 3-5.

PHA did not cause significant changes in the concentrations of MIP-1B and PDGF-BB in any group. IL-8 and VEGF did not show any difference in concentrations in the control group. PHA did not cause significant changes in the IL-5 concentrations in the CVD group. FGF did not show any significant changes in the

concentrations in the PHA cultures of the lower limb samples in the CVD group. The GM-CSF concentrations were higher in the PHA cultures only in the upper limb samples of the CVD group. The remaining PHA-stimulated samples had significantly higher cytokine concentrations than the unstimulated samples (Table 1).

The magnitude of lymphocyte stimulation by PHA was analyzed and no statistically significant differences were found. The exception is MCP-1 which showed a more significant increase in the concentration after PHA stimulation in the control group, as compared with the examined group (median increase  $899 \pm 1391$  ((-2302)-2681) pg/ml vs  $548 \pm 414$  ((-1341)-2072) pg/ml).

In the samples cultured with stimulation, in the CVD group, the GSV samples had a significantly higher G-CSF concentration as compared with the upper limb samples ( $767.7 \pm 1197$  (160.2-3030) pg/ml vs  $538.4 \pm 747.3$  (115.7-8630) pg/ml,  $p < 0.05$ ) (Figure 6).

When the upper limb samples cultured with stimulation were compared between the groups, a higher concentration of eotaxin was found in the CVD group ( $67.41 \pm 25.9$  (29.0-118.7) pg/ml vs  $54.9 \pm 28.0$  (22.15-73.25) pg/ml,  $p < 0.01$ ) and lower IL-5 and MCP-1 concentrations (IL-5:  $21.59 \pm 24.8$  (1.58-223.6) pg/ml vs  $59.27 \pm 38.65$  (18.5-104.6) pg/ml,  $p < 0.01$ ) MCP-1:  $1351 \pm 531.3$  (918.0-2622) pg/ml vs  $2086 \pm 1269$  (1667-3343) pg/ml,  $p < 0.001$ ) (Figures 7-9).

No significant differences in IL-8, IP-10, FGF, GM-CSF, and PDGF-BB concentrations were found in any of the samples.

**3.2. Discussion.** The results of this study show significant changes in the concentrations of chemokines and GFs in the incompetent GSV and in the general circulation of CVD patients.

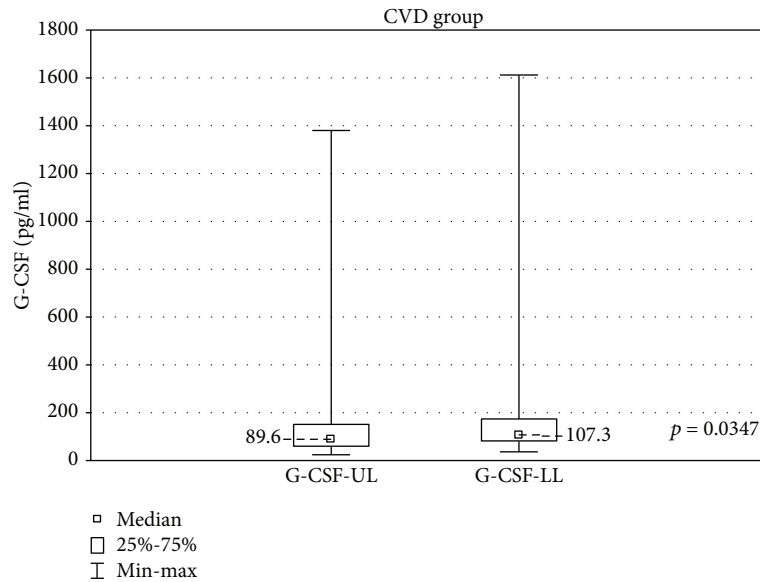


FIGURE 2: Comparison of G-CSF concentrations in the upper (G-CSF-UL) and lower limb samples (G-CSF-LL) in the CVD groups, cultured without stimulation.

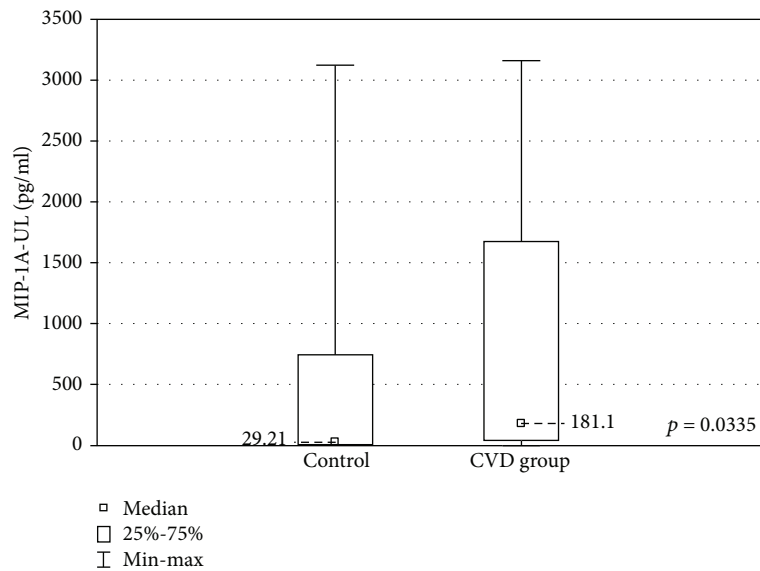


FIGURE 3: Comparison of the MIP-1A concentrations in the upper limb samples (MIP-1A-UL) between the CVD and control groups, cultured without stimulation.

In the nonstimulated samples, higher concentrations of MIP-1A and MIP-1B and a lower VEGF concentration were revealed in the CVD group.

MIP-1 family is responsible for recruiting proinflammatory cells. It also plays a crucial role in the T-cell transendothelial migration [35]. Higher MIP-1A and MIP-1B concentrations in CVD patients were found in a large cytokine profile performed by Tisato et al. [36]. The elevated levels of these factors substantiate the theory of the proinflammatory impact of the turbulent blood flow in incompetent veins.

The concentrations of VEGF, a proangiogenic cytokine which promotes neovascularisation and increases vascular

permeability, were found to be lower in the CVD group. Similar observations were made in a study comparing cytokine concentrations before and after endovenous laser ablation, where VEGF was found in lower concentrations in the blood of the patients before surgery [37]. In other studies, however, the concentrations of VEGF were higher in CVD patients: both in the venous tissue [22] and in the peripheral blood [36, 38]. Further studies including larger groups of patients are required to interpret the role of this factor in venous insufficiency.

Local elevation of proinflammatory markers in GSV was described by Poredos et al. [16] and in our earlier work [17]. Turbulent blood flow, venous stasis, and hypertension are

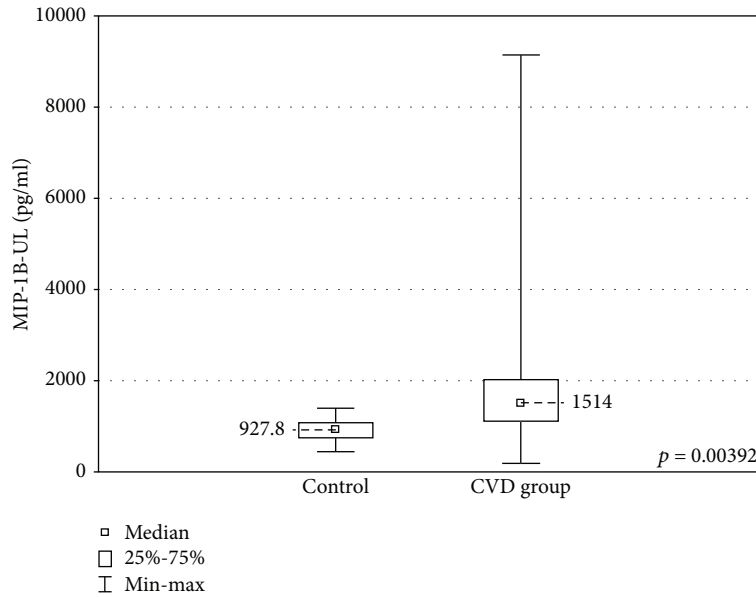


FIGURE 4: Comparison of the MIP-1B concentrations in the upper limb samples (MIP-1B-UL) between the CVD and control groups, cultured without stimulation.

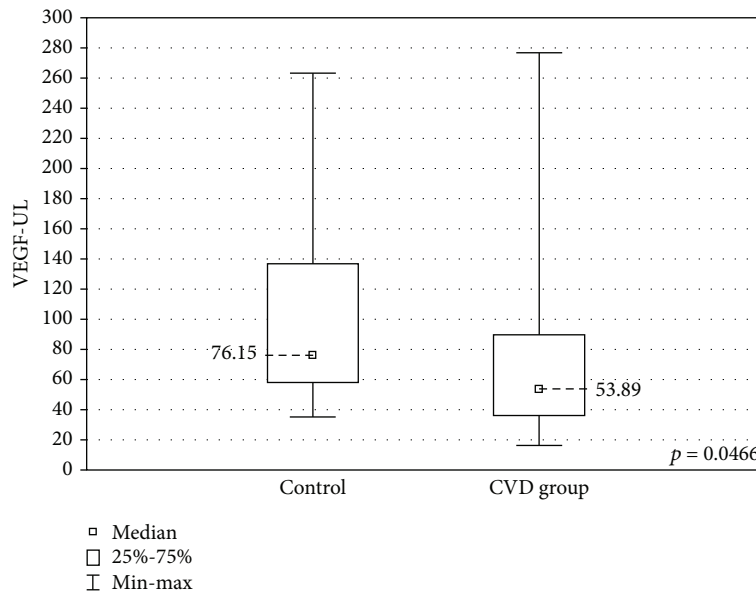


FIGURE 5: Comparison of the VEGF concentrations in the upper limb samples (VEGF-UL) between the CVD and control groups, cultured without stimulation.

well-known factors in CVD pathogenesis. Hemodynamic changes lead to the activation, adhesion, and migration of leukocytes through the venous wall, a so-called “leukocyte trap” [39]. The activated leukocytes damage the endothelium, causing inflammatory response from the endothelial cells [8, 32]. Local increase of inflammatory response is therefore postulated as an important factor of CVD pathogenesis.

In this study, eotaxin and G-CSF had higher concentrations in the incompetent saphenofemoral junction when compared with the same patients’ general circulation. G-CSF stimulates neutrophil production and mobilization,

attracting neutrophils to the inflammation site and restricting their activity in noninflamed regions [40]. Its higher concentration found in the incompetent vein seems to further confirm the proinflammatory effect of nonlaminar blood flow.

Eotaxin is a potent eosinophil chemoattractant, and it has a role in multiple inflammatory diseases such as asthma, atopic dermatitis, or inflammatory bowel disease [41]. It is supposed to have a local impact on tissues in atherosclerosis [41]. In this study, elevated eotaxin concentrations were found in the incompetent vein, while in a study by Sachdev

TABLE 1: Comparison of the cytokine concentrations between samples with PHA-stimulated and unstimulated lymphocytes.

Cytokine	CVD group		Control group—upper limb
	Lower limb	Upper limb	
Eotaxin	$p < 0.001$	$p < 0.001$	$p < 0.05$
IL-8	$p < 0.05$	$p < 0.05$	NS
MIP-1A	$p < 0.001$	$p < 0.001$	$p < 0.05$
MIP-1B	NS	NS	NS
IP-10	$p < 0.000001$	$p < 0.000001$	$p < 0.05$
MCP-1	$p < 0.00001$	$p < 0.0001$	$p < 0.05$
IL-5	NS	NS	$p < 0.05$
FGF	NS	$p < 0.05$	$p < 0.05$
G-CSF	$p < 0.000001$	$p < 0.000001$	$p < 0.05$
GM-CSF	NS	$p < 0.05$	NS
PDGF-BB	NS	NS	NS
VEGF	$p < 0.05$	$p < 0.0001$	NS

Statistically significant increase of concentration in PHA-stimulated samples:  $p \leq 0.05$ . NS: no significant change in cytokine concentration,  $p > 0.05$ .

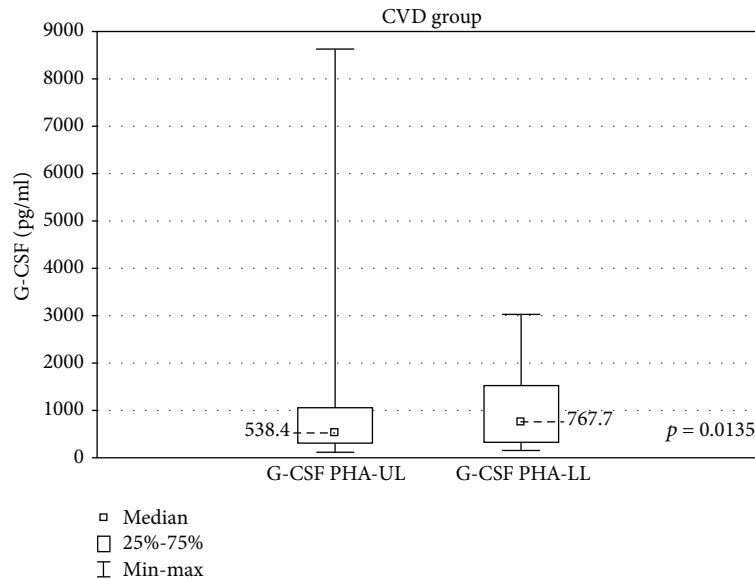


FIGURE 6: Comparison of G-CSF concentrations in the upper (G-CSF PHA-UL) and lower limb samples (G-CSF PHA-LL) in the CVD group, cultured with PHA stimulation.

et al., eotaxin was found in lower concentrations in the general circulation of varicose patients [42]. This might indicate its regional role in the pathogenesis of the disease.

Addition of PHA to the cultures revealed some differences in lymphocyte reaction to stimulation. G-CSF concentration was higher in the GSV when compared with the upper limb of the patients, just as it was in the nonstimulated samples. When stimulated samples were compared between the groups, eotaxin levels were higher in the CVD group and IL-5 and MCP-1 concentrations were lower when compared with controls. The lymphocytes in the control group produced significantly more MCP-1 in reaction to PHA than in the CVD group. No differences in VEGF concentrations were found between the groups. Very few studies discuss the role of the above factors in the CVD. In a study of chronic

venous ulcer wounds, the MCP-1 concentration was elevated in the wound tissue and in the healing process, its concentrations increased [43]. In a study comparing cytokine concentrations in general circulation between a healthy group and CVD patients, MCP had lower concentrations in the CVD group [41]. A study comparing cytokine concentrations before and after surgical flow correction (so-called CHIVA procedure) showed significantly higher MCP-1 concentrations after the surgery [12]. MCP-1 is produced by a multitude of cells and acts not only as a chemotactic agent but also as an angiogenesis promotor [44, 45]. All the above results indicate the importance of MCP-1 in tissue repair [12]. Its lower concentration in the incompetent veins suggests its impact on impaired tissue healing in CVD. However, a study by Tisato et al. showed higher MCP-1 concentrations

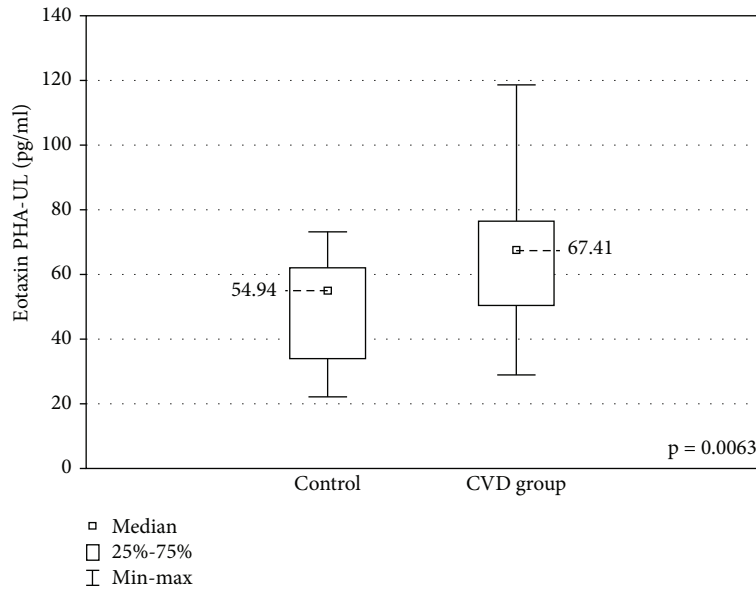


FIGURE 7: Comparison of the eotaxin concentrations in the upper limb samples (eotaxin PHA-UL) between the CVD and control groups, cultured with PHA stimulation.

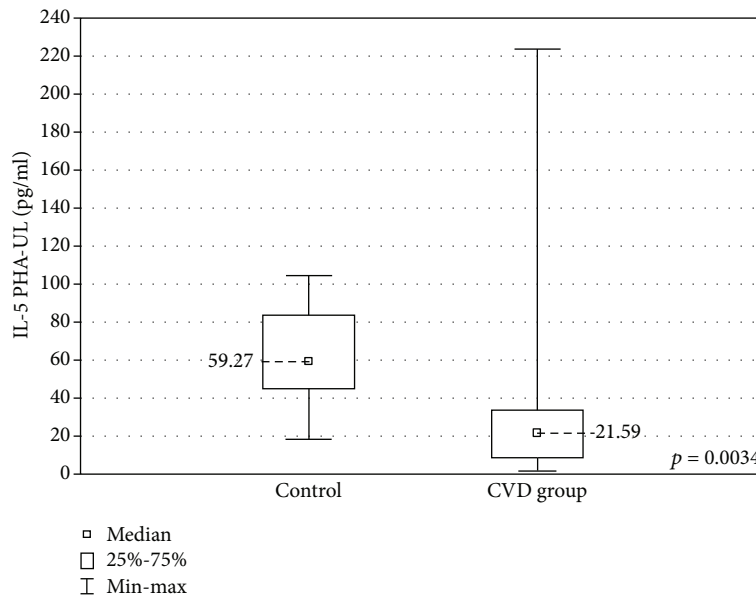


FIGURE 8: Comparison of the IL-5 concentrations in the upper limb samples (IL-5 PHA-UL) between the CVD and control groups, cultured with PHA stimulation.

in CVD group when compared to controls [36]; therefore, more studies would be required to determine the role of these cytokines.

The increased concentration of eotaxin in the stimulated samples of CVD patients supports the hypothesis of the important role of inflammation in this disease. However, in another study, eotaxin was decreased along with other cytokines in varicose patients. The authors of the study concluded that a generally less varied inflammatory network seems to be present in CVD patients [42]. In our study, apart from VEGF (lower concentrations in the

CVD group in the nonstimulated samples), IL-5 was present in significantly lower concentrations in the CVD group in the stimulated samples. This interleukin affects mainly eosinophils, basophils, and mast cells, and it is widely examined as a target in hypereosinophilic conditions [46, 47].

Other cytokines analyzed in this study were IL-8, IP-10, FGF, GM-CSF, and PDGF-BB and they did not show any significant differences in concentrations between samples. Contradictory results concerning PDGF-BB concentration in incompetent veins have been published [13, 42]. The

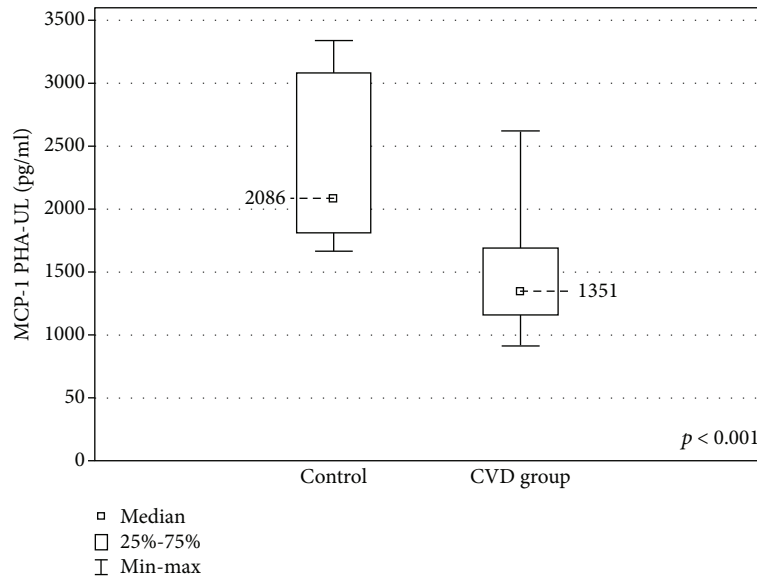


FIGURE 9: Comparison of the MCP-1 concentrations in the upper limb samples (MCP-1 PHA-UL) between the CVD and control groups, cultured with PHA stimulation.

forementioned study assessing the effect of CHIVA on cytokine concentrations described a decrease in IP-10 and its increase after surgical flow correction [12]. Elevated concentrations of GM-CSF have also been noted [36].

In this study, only eotaxin and G-CSF showed significantly higher concentrations locally in the incompetent saphenofemoral junction in comparison with the cubital vein. This suggests that the turbulent flow may have a stimulating impact on the production of these cytokines by lymphocytes in CVD. However, other chemokines and GFs did not show any significant local concentration changes. Samples derived from the calf varices would have been exposed to more stasis and therefore other local changes in the concentrations of chemokines and GFs could have been revealed. However, blood would inevitably come from different tributaries in each patient and therefore we found it less comparable. Drawing the blood from the calf region of the great saphenous vein would also result in less comparable samples as the GSV is not exposed at the same level in all patients. The choice of saphenofemoral junction assured that the samples were obtained from the same anatomical region with most evident oscillatory flow.

Another limitation of this study is that no samples were obtained from the lower limb veins of healthy subjects. Taking blood samples from both the upper and lower limbs of healthy volunteers would expose them to too much distress and therefore has not been suggested. Some researchers have used samples from GSV grafts from patients undergoing cardiac bypass surgery as controls [6]; however, we considered such a group of patients most probably subject to numerous factors altering their immunological state (e.g., atherosclerosis, acetylsalicylic acid intake) and therefore not suitable for this study.

The potential of the lymphocytes in the incompetent veins to respond to activating factors was tested by addition of PHA to the cultures. PHA is a lymphocyte T stimulant.

Therefore, the lymphocyte B response to stimulation was not assessed and requires further study.

The low number of patients is definitely another limitation of this study. The same problem was also met by other authors working on a similar subject [8, 12, 42, 48]. The unanimous results of the studies concerning cytokines in CVD require further investigation with larger groups of patients in order to determine the role of cytokines in CVD and the impact of the oscillatory flow on the functioning of immunological cells.

#### 4. Conclusions

The results obtained in this study show that CVD lymphocytes produce cytokines responsible for recruiting inflammatory cells, angiogenesis, and tissue healing in significantly different concentrations in comparison with a healthy group. The differences are also present when GSV samples are compared with the patients' general circulation. This supports the theory that the turbulent flow present in the incompetent veins affects the functioning of the immunological cells, which may have an important impact on the pathogenesis of the disease. The exact nature of these changes requires further investigation in larger groups of patients.

#### Data Availability

The Bio-Plex data used to support the findings of this study are available from the corresponding author upon request.

#### Conflicts of Interest

The authors declare that there is no conflict of interest regarding the publication of this paper.

## Acknowledgments

Special thanks to Ewelina Szliszka, PhD, D.Sc., for the clinical supervision of the study and to Zygmunt Fiutek, PhD, and his team for giving us access to the patients and the immense help with acquisition of the samples. This work was supported by the Medical University of Silesia (KNW 1-066/N/8/O) and the project “Silesian BIO-FARM-Centre for Biotechnology.”

## References

- [1] E. Rabe, G. Berboth, and F. Pannier, “Epidemiology of chronic venous diseases,” *Wiener Medizinische Wochenschrift*, vol. 166, no. 9-10, pp. 260–263, 2016.
- [2] E. Rabe, J. J. Guex, A. Puskas, A. Scuderi, F. Fernandez Quesada, and VCP Coordinators, “Epidemiology of chronic venous disorders in geographically diverse populations: results from the vein consult program,” *International Angiology*, vol. 31, no. 2, pp. 105–115, 2012.
- [3] F. G. R. Fowkes, C. J. Evans, and A. J. Lee, “Prevalence and risk factors of chronic venous insufficiency,” *Angiology*, vol. 52, Supplement 1, pp. S5–S15, 2001.
- [4] A. Jawień, “The influence of environmental factors in chronic venous insufficiency,” *Angiology*, vol. 54, Supplement 1, pp. S19–S31, 2003.
- [5] A. H. Sprague and R. A. Khalil, “Inflammatory cytokines in vascular dysfunction and vascular disease,” *Biochemical Pharmacology*, vol. 78, no. 6, pp. 539–552, 2009.
- [6] G. L. Sayer and P. D. C. Smith, “Immunocytochemical characterisation of the inflammatory cell infiltrate of varicose veins,” *European Journal of Vascular and Endovascular Surgery*, vol. 28, no. 5, pp. 479–483, 2004.
- [7] T. Ono, J. J. Bergan, G. W. Schmid-Schonbein, and S. Takase, “Monocyte infiltration into venous valves,” *Journal of Vascular Surgery*, vol. 27, no. 1, pp. 158–166, 1998.
- [8] V. Tisato, G. Zauli, R. Voltan et al., “Endothelial cells obtained from patients affected by chronic venous disease exhibit a pro-inflammatory phenotype,” *PLoS One*, vol. 7, no. 6, article e39543, 2012.
- [9] E. Grudzinska and Z. P. Czuba, “Immunological aspects of chronic venous disease pathogenesis,” *Central European Journal of Immunology*, vol. 4, no. 4, pp. 525–531, 2014.
- [10] J. Buján, G. Pascual, and J. M. Bellón, “Interaction between ageing, inflammation process, and the occurrence of varicose veins,” *Phlebology*, vol. 15, no. 4, pp. 123–130, 2008.
- [11] B. Guzik, M. Chwała, P. Matusik et al., “Mechanisms of increased vascular superoxide production in human varicose veins,” *Polskie Archiwum Medycyny Wewnętrznej*, vol. 121, no. 9, pp. 279–286, 2011.
- [12] P. Zamboni, P. Spath, V. Tisato et al., “Oscillatory flow suppression improves inflammation in chronic venous disease,” *Journal of Surgical Research*, vol. 205, no. 1, pp. 238–245, 2016.
- [13] V. Tisato, P. Zamboni, E. Menegatti et al., “Endothelial PDGF-BB produced ex vivo correlates with relevant hemodynamic parameters in patients affected by chronic venous disease,” *Cytokine*, vol. 63, no. 2, pp. 92–96, 2013.
- [14] B. B. Lee, A. N. Nicolaidis, K. Myers et al., “Venous hemodynamic changes in lower limb venous disease: the UIP consensus according to scientific evidence,” *International Angiology*, vol. 35, no. 3, pp. 236–352, 2016.
- [15] J. D. Raffetto and F. Mannello, “Pathophysiology of chronic venous disease,” *International Angiology*, vol. 33, no. 3, pp. 212–221, 2014.
- [16] P. Poredos, A. Spirkoska, T. Rucigaj, J. Fareed, and M. K. Jezovnik, “Do blood constituents in varicose veins differ from the systemic blood constituents?,” *European Journal of Vascular and Endovascular Surgery*, vol. 50, no. 2, pp. 250–256, 2015.
- [17] E. Grudzińska, A. Lekstan, E. Szliszka, and Z. P. Czuba, “Cytokines produced by lymphocytes in the incompetent great saphenous vein,” *Mediators of Inflammation*, vol. 2018, Article ID 7161346, 8 pages, 2018.
- [18] C. Michiels, T. Arnould, and J. Remacle, “Endothelial cell responses to hypoxia: initiation of a cascade of cellular interactions,” *Biochimica et Biophysica Acta*, vol. 1497, no. 1, pp. 1–10, 2000.
- [19] S. Nomura, K. Yoshimura, N. Akiyama et al., “HMG-CoA reductase inhibitors reduce matrix metalloproteinase-9 activity in human varicose veins,” *European Surgical Research*, vol. 37, no. 6, pp. 370–378, 2005.
- [20] A. K. Charles and G. A. Gresham, “Histopathological changes in venous grafts and in varicose and non-varicose veins,” *Journal of Clinical Pathology*, vol. 46, no. 7, pp. 603–606, 1993.
- [21] M. A. Wali and R. A. Eid, “Intimal changes in varicose veins: an ultrastructural study,” *Journal of Smooth Muscle Research*, vol. 38, no. 3, pp. 63–74, 2002.
- [22] A. M. Asbeutah, S. K. Asfar, H. Safar et al., “In vivo and in vitro assessment of human saphenous vein wall changes,” *The Open Cardiovascular Medicine Journal*, vol. 1, no. 1, pp. 15–21, 2007.
- [23] J. Birdina, M. Pilmane, and A. Ligers, “The morphofunctional changes in the wall of varicose veins,” *Annals of Vascular Surgery*, vol. 42, pp. 274–284, 2017.
- [24] J. D. Lee, W. K. Yang, and C. H. Lai, “Involved intrinsic apoptotic pathway in the varicocele and varicose veins,” *Annals of Vascular Surgery*, vol. 24, no. 6, pp. 768–774, 2010.
- [25] Y. Xu, Y. Bei, Y. Li, and H. Chu, “Phenotypic and functional transformation in smooth muscle cells derived from varicose veins,” *Journal of Vascular Surgery: Venous and Lymphatic Disorders*, vol. 5, no. 5, pp. 723–733, 2017.
- [26] P. Sansilvestri-Morel, A. Rupin, C. Badier-Commander et al., “Imbalance in the synthesis of collagen type I and collagen type III in smooth muscle cells derived from human varicose veins,” *Journal of Vascular Research*, vol. 38, no. 6, pp. 560–568, 2001.
- [27] P. Sansilvestri-Morel, F. Fioretti, A. Rupin et al., “Comparison of extracellular matrix in skin and saphenous veins from patients with varicose veins: does the skin reflect venous matrix changes?,” *Clinical Science*, vol. 112, no. 4, pp. 229–239, 2007.
- [28] P. Sansilvestri-Morel, A. Rupin, C. Badier-Commander, J.-N. Fabiani, and T. J. Verbeuren, “Chronic venous insufficiency: dysregulation of collagen synthesis,” *Angiology*, vol. 54, Supplement 1, pp. S13–S18, 2003.
- [29] S. M. H. Ghaderian and Z. Khodaii, “Tissue remodeling investigation in varicose veins,” *International Journal of Molecular and Cellular Medicine*, vol. 1, no. 1, pp. 50–61, 2012.
- [30] M. Kurzawski, A. Modrzejewski, A. Pawlik, and M. Drożdżik, “Polymorphism of matrix metalloproteinase genes (*MMP1* and *MMP3*) in patients with varicose veins,” *Clinical and Experimental Dermatology*, vol. 34, no. 5, pp. 613–617, 2009.

- [31] E. Ascher, T. Jacob, A. Hingorani, B. Tsemekhin, and Y. Gunduz, "Expression of molecular mediators of apoptosis and their role in the pathogenesis of lower-extremity varicose veins," *Journal of Vascular Surgery*, vol. 33, no. 5, pp. 1080–1086, 2001.
- [32] R. Castro-Ferreira, R. Cardoso, A. Leite-Moreira, and A. Mansilha, "The role of endothelial dysfunction and inflammation in chronic venous disease," *Annals of Vascular Surgery*, vol. 46, pp. 380–393, 2018.
- [33] M. Saharay, D. A. Shields, J. B. Porter, J. H. Scurr, and P. D. Coleridge Smith, "Leukocyte activity in the microcirculation of the leg in patients with chronic venous disease," *Journal of Vascular Surgery*, vol. 26, no. 2, pp. 265–273, 1997.
- [34] M. Simka, "Cellular and molecular mechanisms of venous leg ulcers development—the "puzzle" theory," *International Angiology*, vol. 29, no. 1, pp. 1–19, 2010.
- [35] M. Maurer and E. Von Stebut, "Macrophage inflammatory protein-1," *The International Journal of Biochemistry & Cell Biology*, vol. 36, no. 10, pp. 1882–1886, 2004.
- [36] V. Tisato, G. Zauli, E. Rimondi et al., "Inhibitory effect of natural anti-inflammatory compounds on cytokines released by chronic venous disease patient-derived endothelial cells," *Mediators of Inflammation*, vol. 2013, Article ID 423407, 13 pages, 2013.
- [37] N. A. Al-Zoubi, R. J. Yaghan, T. S. Mazahreh et al., "Evaluation of plasma growth factors (VEGF, PDGF, EGF, ANG1, and ANG2) in patients with varicose veins before and after treatment with endovenous laser ablation," *Photomedicine and Laser Surgery*, vol. 36, no. 3, pp. 169–173, 2018.
- [38] S. S. Shoab, J. H. Scurr, and P. D. Coleridge-Smith, "Increased plasma vascular endothelial growth factor among patients with chronic venous disease," *Journal of Vascular Surgery*, vol. 28, no. 3, pp. 535–540, 1998.
- [39] P. D. Smith, "Neutrophil activation and mediators of inflammation in chronic venous insufficiency," *Journal of Vascular Research*, vol. 36, no. 1, pp. 24–36, 1999.
- [40] L. J. Bendall and K. F. Bradstock, "G-CSF: from granulopoietic stimulant to bone marrow stem cell mobilizing agent," *Cytokine & Growth Factor Reviews*, vol. 25, no. 4, pp. 355–367, 2014.
- [41] T. Adar, S. Shteingart, A. Ben Ya'acov, A. Bar-Gil Shitrit, and E. Goldin, "From airway inflammation to inflammatory bowel disease: eotaxin-1, a key regulator of intestinal inflammation," *Clinical Immunology*, vol. 153, no. 1, pp. 199–208, 2014.
- [42] U. Sachdev, L. Vodovotz, J. Bitner et al., "Suppressed networks of inflammatory mediators characterize chronic venous insufficiency," *Journal of Vascular Surgery: Venous and Lymphatic Disorders*, vol. 6, no. 3, pp. 358–366, 2018.
- [43] D. P. Fivenson, D. T. Faria, B. J. Nickoloff et al., "Chemokine and inflammatory cytokine changes during chronic wound healing," *Wound Repair and Regeneration*, vol. 5, no. 4, pp. 310–322, 1997.
- [44] A. Roy and P. E. Kolattukudy, "Monocyte chemotactic protein-induced protein (MCP-1) promotes inflammatory angiogenesis via sequential induction of oxidative stress, endoplasmic reticulum stress and autophagy," *Cellular Signalling*, vol. 24, no. 11, pp. 2123–2131, 2012.
- [45] A. Yadav, V. Saini, and S. Arora, "MCP-1: chemoattractant with a role beyond immunity: a review," *Clinica Chimica Acta*, vol. 411, no. 21–22, pp. 1570–1579, 2010.
- [46] F. Roufousse, "Targeting the interleukin-5 pathway for treatment of eosinophilic conditions other than asthma," *Frontiers in Medicine*, vol. 5, 2018.
- [47] K. Takatsu, "Interleukin-5 and IL-5 receptor in health and diseases," *Proceedings of the Japan Academy, Series B*, vol. 87, no. 8, pp. 463–485, 2011.
- [48] V. Tisato, G. Zauli, S. Giancesini et al., "Modulation of circulating cytokine-chemokine profile in patients affected by chronic venous insufficiency undergoing surgical hemodynamic correction," *Journal of Immunology Research*, vol. 2014, Article ID 473765, 10 pages, 2014.

## Review Article

# Phenotypic and Functional Diversities of Myeloid-Derived Suppressor Cells in Autoimmune Diseases

Huijuan Ma<sup>1</sup> and Chang-Qing Xia<sup>2</sup> 

<sup>1</sup>Department of Nephrology, Jining No. 1 People's Hospital, Jining 272011, China

<sup>2</sup>Department of Pathology, Immunology and Laboratory Medicine, University of Florida College of Medicine, Gainesville, FL 32610, USA

Correspondence should be addressed to Chang-Qing Xia; [cxq65@yahoo.com](mailto:cqx65@yahoo.com)

Received 7 September 2018; Accepted 9 December 2018; Published 23 December 2018

Guest Editor: Qingdong Guan

Copyright © 2018 Huijuan Ma and Chang-Qing Xia. This is an open access article distributed under the Creative Commons Attribution License, which permits unrestricted use, distribution, and reproduction in any medium, provided the original work is properly cited.

Myeloid-derived suppressor cells (MDSCs) are identified as a heterogeneous population of cells with the function to suppress innate as well as adaptive immune responses. The initial studies of MDSCs were primarily focused on the field of animal tumor models or cancer patients. In cancer, MDSCs play the deleterious role to inhibit tumor immunity and to promote tumor development. Over the past few years, an increasing number of studies have investigated the role of MDSCs in autoimmune diseases. The beneficial effects of MDSCs in autoimmunity have been reported by some studies, and thus, immunosuppressive MDSCs may be a novel therapeutic target in autoimmune diseases. There are some controversial findings as well. Many questions such as the activation, differentiation, and suppressive functions of MDSCs and their roles in autoimmune diseases remain unclear. In this review, we have discussed the current understanding of MDSCs in autoimmune diseases.

## 1. Introduction

Myeloid-derived suppressor cells (MDSCs) started to be described more than three decades ago mainly in cancer [1, 2]. The suppressive effects of MDSCs on immune responses lead to the failure of immune surveillance of cancer and promotion of tumor angiogenesis and metastasis. Thus, MDSCs are suggested to be an important cell component for creating tumor immunosuppressive microenvironment [3–7]. In recent years, it has been reported about the involvement of MDSCs in a variety of inflammatory disorders, including autoimmune diseases [8–12]. MDSCs serve as the negative regulator of immune responses, and they are likely to play a protective role in autoimmune diseases by inhibiting T cell-mediated immune responses. Most of the studies of MDSCs in autoimmunity are carried out in animal experiments, and some findings are controversial. The real biological and pathological roles of MDSCs in autoimmune diseases still need to be further characterized. In this review, we summarize the origin, phenotype, and functional

characteristics of MDSCs and their involvement in autoimmune diseases as well as MDSCs as potential targets for therapeutic intervention.

## 2. Origin, Phenotype, and Functional Characteristics of MDSCs

Common myeloid precursor cells derive from hematopoietic stem cells (HSCs) in the bone marrow, and they give rise to “immature myeloid cells” (IMCs) without suppressive features in an unactivated state [13]. In healthy individuals, IMCs can differentiate into mature, functional dendritic cells (DCs), macrophages, and granulocytes [14]. However, in certain pathologic conditions, such as inflammation, tumors, infections, trauma, transplants, sepsis, or autoimmune diseases, the differentiation of IMCs is impaired, and subsequently, IMCs are activated and proliferate in response to diverse endogenous and exogenous factors [13, 15–17]. As a result, IMCs differentiate into MDSCs, resulting in the dramatic expansion and accumulation of a large number of

MDSCs in peripheral tissues. MDSCs can potentially inhibit immune responses through the expressions of suppressive factors [13].

In mice, MDSCs are characterized by the coexpression of CD11b and Gr-1. The CD11b<sup>+</sup>Gr-1<sup>+</sup> cell population is divided into two relatively distinct subsets: M-MDSCs (CD11b<sup>+</sup>Ly6C<sup>hi</sup>Ly6G<sup>-</sup>) with monocytic morphology and G-MDSCs (CD11b<sup>+</sup>Ly6C<sup>low</sup>Ly6G<sup>+</sup>) with granulocytic morphology [18]. Recently, the expressions of CD115, CD80, CD124, F4/80, CD16, and CD31 have also been suggested as markers for identifying MDSCs, although these markers are not specific for MDSCs [19, 20].

Different from murine MDSCs, most human MDSCs express both CD11b and CD33 and have an absent or low expression of HLA-DR. Therefore, human MDSCs can be generally defined as CD11b<sup>+</sup>CD33<sup>+</sup>HLA-DR<sup>low/-</sup>. Within this population, monocytic MDSCs and granulocytic MDSCs can be further characterized by the phenotype of CD14<sup>+</sup>CD15<sup>low/-</sup> and CD14<sup>+</sup>CD15<sup>+</sup>CD66b<sup>+</sup>, respectively, which seems to be consistent with hematologic morphology [13, 21]. Given the heterogeneity of MDSCs populations and the different combinations of markers used, there may be some overlap between the subsets of MDSCs, and these classifications are somewhat controversial [22, 23]. In a recent study, a high level of lectin-type oxidized LDL receptor 1 (LOX-1) was identified in polymorphonuclear MDSCs (PMN-MDSCs) in the peripheral blood and tumor tissues of cancer patients, which was associated with endoplasmic reticulum stress and lipid metabolism [24]. Lately, another study showed that the phenotypic and functional characteristics of MDSCs can shift at different clinical stages of multiple sclerosis (MS) [25].

MDSCs require different signals for their expansion and activation. A variety of factors play important roles in the expansion of MDSCs such as cyclooxygenase-2 (COX-2), prostaglandin E2 (PGE2), granulocyte/macrophage colony-stimulating factor (GM-CSF), macrophage colony-stimulating factor (M-CSF), IL-6, IL-3, vascular endothelial growth factor (VEGF), and stem cell factor (SCF)-1 [13, 26–29]. The activation of MDSCs is associated with IFN- $\gamma$ , TGF- $\beta$ , IL-13, IL-4, etc. [13]. These factors can trigger signaling pathways in MDSCs which are involved in regulating the processes of cell differentiation, proliferation, and apoptosis during hematopoiesis [30–32].

MDSCs can suppress the immune response through a variety of different mechanisms, including close cell-cell contact and soluble mediators, of which the predominant factors are arginase-1 (Arg-1) and inducible nitric oxide synthase (iNOS) [33]. The expressions of Arg-1 and iNOS which generate NO responsible for the MDSCs suppressive function are upregulated by activated MDSCs. The common substrate of Arg-1 and iNOS is L-arginine. Reactive oxygen species (ROS) represent another important mechanism [13, 34–37]. The monocytic MDSCs mainly associated with inflammation were found to express high levels of iNOS and low levels of ROS, whereas the granulocytic MDSCs mainly associated with tumors expressed high levels of ROS and low levels of iNOS [13]. Both subsets expressed Arg-1 [18, 38]. In addition, indoleamine 2,3-dioxygenase (IDO), IL-10, PGE2,

COX-2, program death ligand 1 (PD-L1), and TGF- $\beta$  also are very important to enable MDSCs to inhibit T cell proliferation and cytotoxicity [39–42]. MDSCs also facilitate regulatory T cells (Tregs) to exert suppressive functions. It has been shown that Gr-1<sup>+</sup>CD115<sup>+</sup> MDSCs can promote the development of Foxp3<sup>+</sup> Tregs in vivo and mediate the inactivation of tumor-specific T cells in a tumor mouse model [43]. Further studies are required to demonstrate whether MDSCs are involved and associated with Tregs in a common immune regulatory network. Moreover, a recent study found that Ly6G<sup>+</sup> PMN-MDSCs could control the selective accumulation and cytokine secretion of B cells in the central nervous system (CNS), which facilitated the recovery of disease in experimental autoimmune encephalomyelitis (EAE) [44]. The relationship between MDSCs and B cells also remains to be further studied.

### 3. The Role of MDSCs in Autoimmunity

MDSCs' function has mostly been studied in animal tumor models and cancer patients. Recently, a growing body of evidence has suggested that MDSCs may be actively participating in the development of autoimmune diseases, such as MS [8, 25, 45], systemic lupus erythematosus (SLE) [11, 46], type 1 diabetes (T1D) [47], inflammatory bowel disease (IBD) [9, 48], and rheumatoid arthritis (RA) [49]. However, the in vitro and the in vivo studies are sometimes controversial.

**3.1. In Vitro Study of MDSCs.** Generally speaking, in vitro, CD11b<sup>+</sup>Gr-1<sup>+</sup> cells isolated from autoimmune inflammatory sites are able to inhibit T cell proliferation, typically through the participation of iNOS and Arg-1. In the autoimmune hepatitis (AIH) mouse model, the accumulation of CD11b<sup>+</sup>Gr-1<sup>+</sup> myeloid cells was observed in the BALB/c Tgfb1<sup>-/-</sup> liver. And only the isolated Ly6C<sup>hi</sup> subset was able to efficiently suppress CD4<sup>+</sup> T cell proliferation in vitro by several different mechanisms, including NO, IFN- $\gamma$ , and cell-cell contact [50]. Similarly, in the IBD mouse model, CD11b<sup>+</sup>Gr-1<sup>+</sup> myeloid cells accumulated in the spleens and secondary lymphoid tissues, and only CD11b<sup>+</sup>Ly6C<sup>hi</sup>Ly6G<sup>-</sup> MDSCs suppressed the proliferation and production of cytokines by CD4<sup>+</sup> T cells, which were mediated by NO, cell-cell contact, and partially by IFN- $\gamma$  and PGs [48]. It was shown that CD11b<sup>+</sup>Ly6C<sup>hi</sup>Ly6G<sup>-</sup> MDSCs isolated from the spleen after EAE were induced potentially inhibited CD4<sup>+</sup> and CD8<sup>+</sup> T cell proliferation, and induced apoptosis of proliferating T cell ex vivo, which was mediated by iNOS activity [8]. In line with these findings, MDSCs were also involved in experimental autoimmune uveoretinitis (EAU). These cells expressed CD11b phenotypically resembling monocytes and were accumulated in the inflamed eyes. In vitro, T cell proliferation could be greatly suppressed by these isolated monocyte-like cells [51]. Subsequent research in EAU showed that the intact TNF response axis was responsible for the suppressive function of MDSCs [52]. In line with the above reports, CD11b<sup>+</sup>Gr-1<sup>low</sup> MDSCs were also identified in lupus-prone MRL-Fas<sup>lpr</sup> mice that develop autoimmune organ damages. These cells had a suppressive effect on CD4<sup>+</sup> T cell proliferation

ex vivo, and Arg-1 inhibitor could block the suppression, indicating that arginase served as the dominant suppressive factor of MDSCs in this autoimmune setting [11]. Recently, in the pristane-induced lupus mouse model, we observed that CD11b<sup>+</sup>Ly6C<sup>hi</sup> monocytes sorted from the peritoneal cells greatly inhibited T cell proliferation ex vivo which was mediated by cell-cell contact, NO, and PGE2 and could inhibit Th1 differentiation but enhanced the development of Tregs [53]. Our findings provide a novel insight into the role of Ly6C<sup>hi</sup> monocytes mobilized by pristane injection in the pathogenesis of pristane-induced lupus in mice. We believe the Ly6C<sup>hi</sup> monocytes induced by pristane injection are monocytic MDSCs.

**3.2. In Vivo Study of MDSCs.** Despite that MDSCs can potently inhibit T cell responses in vitro, the presence of MDSCs in autoimmune diseases is different, and current studies have shown conflicting roles for MDSCs in autoimmunity, either as an aggravating or as a curative factor of disease.

EAE is a common mouse model for multiple sclerosis, which is an autoimmune inflammatory neurological disease. Several studies have tried to demonstrate the possible role of MDSCs in EAE. King et al. observed that CD11b<sup>+</sup>CD62L<sup>+</sup>Ly6C<sup>hi</sup> cells were mobilized increasingly and accumulated in the blood and CNS before clinical episodes of the disease, and these cells were subsequently matured into inflammatory macrophages and/or functional DCs. Thus, the study concluded that the accumulation of CD11b<sup>+</sup>Ly6C<sup>hi</sup> monocytes in vivo served as pathologic effectors and was associated with EAE pathogenesis [45]. Similarly, the Mildner study showed that the selective depletion of CCR2<sup>+</sup>Ly6C<sup>hi</sup> monocytes strongly reduced the CNS autoimmunity, indicating a disease-promoting role of CCR2<sup>+</sup>Ly6C<sup>hi</sup> monocytes during autoimmune inflammation of the CNS [54]. Yi et al. also confirmed that the expansion of CD11b<sup>+</sup>Gr-1<sup>+</sup> cells was present in the development of EAE. Although these MDSCs inhibited T cell proliferation, they promoted inflammatory Th17 cell differentiation in vitro mediated by IL-1 $\beta$ . Selective depletion of MDSCs using gemcitabine resulted in a marked reduction in the severity of EAE, and the adoptive transfer of MDSCs after this treatment restored EAE disease progression. The authors also demonstrated that the severity of EAE was correlated with the frequency of Th17 cells and the levels of inflammatory cytokines [55]. All the above findings in EAE indicate that MDSCs in vivo serve as pathologic effectors. However, some other studies had different conclusions about the activity of MDSCs. Ioannou et al. reported that before the disease remission, CD11b<sup>hi</sup>Ly6G<sup>+</sup>Ly6C<sup>-</sup> granulocytic MDSCs were abundantly accumulated in the peripheral lymphoid organs. Adoptive transfer of G-MDSCs potently delayed the development of EAE through the suppressive effect on the priming of Th1 and Th17 cells. The upregulation of PD-L1 upon exposure to the autoimmune milieu both in vitro and in vivo was essential for the suppressive function of G-MDSCs [56]. Taken together, it seems that MDSCs have opposite roles in EAE, having both inflammatory functions and protective functions. The discrepancy of different reports suggests that further characterization of

MDSCs in various autoimmune settings is needed. It is also possible more functionally diverse MDSCs subsets may exist.

Lately, MDSCs have been involved in the development of SLE associated with organ damages. A study reported that the deletion of CD24 in a lupus-like disease model driven by heat shock proteins (HSPs) led to the increase of CD11b<sup>+</sup>Gr-1<sup>+</sup> MDSCs and Tregs that augmented immune tolerance, accompanying with the alleviation of lupus-like renal pathology [57]. On the contrary, it was recently shown that in a humanized SLE model MDSCs contributed to induce Th17 responses and related renal damage which was dependent on Arg-1 [58]. In addition, a recent study demonstrated that there were gender differences about the cellular and functional characteristics of myeloid cells in (NZB $\times$ NZW) F1 mice. The greatly increased Gr-1<sup>hi</sup>Ly6G<sup>+</sup>CD11b<sup>+</sup> myeloid cells in male mice were capable of inhibiting autoantibody production and IL-10 production and slowing the progression of lupus-like disease in vivo. Furthermore, the production of antinuclear autoantibodies was increased after anti-Gr-1 mAb treatment. In vitro Gr-1<sup>hi</sup>CD11b<sup>+</sup> cells could directly inhibit B cell differentiation. The authors postulated that these cells represented an important inhibitory mechanism in male mice and involved in SLE pathogenesis [59]. In Roquin<sup>san/san</sup> SLE mice, sorted MDSCs induced the expansion of IL-10-producing regulatory B cells in vitro via NO. After administration of MDSCs, the regulatory B cells in the spleens of Roquin<sup>san/san</sup> mice were expanded but effector B cells were decreased, accompanied with the reduction of serum anti-dsDNA antibody levels and the improvement of renal pathology. Therefore, MDSCs were likely to be a promising therapeutic target in the pathogenesis of SLE [46]. In our in vivo experiment, the transfer of purified CD11b<sup>+</sup>Ly6C<sup>hi</sup> pristane-induced peritoneal monocytes was able to greatly inhibit anti-keyhole limpet hemocyanin (KLH) antibody production induced by KLH immunization [53], suggesting that these cells may have a protective effect in chronic autoimmune inflammation in pristane-induced lupus.

The role for MDSCs in T1D has been recently studied. The expanded Gr-1<sup>+</sup>CD11b<sup>+</sup> MDSCs induced by anti-CD20 treatment in a mouse model of diabetes were found to suppress T cell proliferation dependent on NO, IL-10, and cell-cell contact and induce Tregs differentiation via TGF- $\beta$ . In vivo, the transient expansion of MDSCs induced by anti-Gr-1 treatment delayed the development of disease in NOD mice. These findings suggested that Gr-1<sup>+</sup>CD11b<sup>+</sup> MDSCs contributed to establish immune tolerance and could be a novel immunotherapeutic target for T1D [47]. A recent study found that CD11b<sup>hi</sup>Gr-1<sup>int</sup> MDSCs were significantly increased in the peripheral blood of diabetic NOD mice. The authors suggested that the expansion of MDSCs was involved in the onset of diabetes [60]. Another study demonstrated that the adoptive transfer of MDSCs had an Ag-specific suppressive function and could prevent the onset of T1D through the induction of CD4<sup>+</sup>CD25<sup>+</sup>Foxp3<sup>+</sup> Tregs development and anergy in autoreactive T cells [61].

MDSCs were also described in other autoimmune diseases. In the mouse model of IBD induced in VILLIN-hemagglutinin (HA) transgenic mice, the significantly

increased CD11b<sup>+</sup>Gr-1<sup>+</sup> MDSCs in the spleen and intestine were found to induce T cell apoptosis and suppress T cell proliferation *ex vivo* in a NO-dependent manner as well. Furthermore, the isolated CD11b<sup>+</sup>Gr-1<sup>+</sup> MDSCs inhibited T cell-mediated colitis in VILLIN-HA mice [9]. The isolated granulocytic MDSCs from the spleens in a collagen-induced arthritis (CIA) mouse model were found to inhibit CD4<sup>+</sup> T cell proliferation *in vitro*. Moreover, these cells could suppress the differentiation of CD4<sup>+</sup> T cells into Th17 cells. Adoptive transfer of MDSCs reduced the severity of joint inflammation *in vivo*, and the removal of MDSCs worsened the disease [49]. Another recent study found that CD11c<sup>-</sup>CD11b<sup>+</sup>GR-1<sup>+</sup> MDSCs separated from the peripheral blood and spleens of CIA mice could inhibit T cell proliferation *in vitro* partly via IL-10 and Arg-1, and *in vivo* infusion of MDSCs significantly ameliorated rheumatoid inflammation [62]. Alopecia areata is an autoimmune skin disease, the characteristic of which is inflammatory immune responses that cause hair loss. In a mouse model of alopecia areata, Gr-1<sup>+</sup>CD11b<sup>+</sup> MDSCs were capable of inhibiting T cell proliferation *in vitro*, and subsequent *in vivo* application led to partial restoration of hair growth [63]. MDSCs were also described in a mouse model of experimental autoimmune myasthenia gravis (EAMG), in which the adoptive transfer of MDSCs was found to effectively reverse the disease progression [64]. Further analysis showed that in MDSCs-treated EAMG mice, acetylcholine receptor (AChR-) specific immune responses were suppressed, serum anti-AChR IgG levels were decreased, and complement activation was reduced, in which various immune-modulating factors, such as PGE2, iNOS and arginase, were actively involved [64].

Up to date, almost all studies about MDSCs in human focus on cancer. There are few about MDSCs in patients with autoimmune diseases. A study performed in T1D patients has shown that in peripheral blood mononuclear cells (PBMC) the frequency of CD11b<sup>+</sup>CD33<sup>+</sup> MDSCs is significantly increased, but these MDSCs are not maximally suppressive in function, suggesting that functional defects in MDSCs may contribute to T1D pathogenesis [60]. Recently, a study on human SLE demonstrated the pathogenic role of MDSCs. Compared to healthy controls, HLA-DR<sup>-</sup>CD11b<sup>+</sup>CD33<sup>+</sup> MDSCs in the peripheral blood of active SLE patients significantly increased. A positive correlation between the frequency of MDSCs and Th17 responses, serum Arg-1 level, and disease severity was observed, which provided new insights into the molecular mechanism targeting MDSCs for the treatment of SLE [58]. This increase of HLA-DR<sup>-</sup>CD11b<sup>+</sup>CD33<sup>+</sup> MDSCs may be mobilized and recruited during the active inflammatory process in SLE, because inflammation can lead to myelopoiesis [65] potentially giving rise to these intermediate stages of myeloid cells. Additionally, the numbers of MDSCs in the peripheral blood and plasma Arg-1 level were greatly increased in RA patients. The elevated frequency of Th17 cells in those patients was observed to be negatively correlated with the plasma Arg-1 level and the frequency of MDSCs. It was also found that there was a negative correlation between the level of plasma TNF- $\alpha$  and MDSCs frequency [66]. Recently, another study

about RA patients has shown that the expansion of MDSCs as a risk factor was associated with disease activity and joint inflammation [67]. Given the important role of MDSCs in modulating immune response, more research needs to be carried out to explore the effect of MDSCs in human autoimmune disorders.

In conclusion, MDSCs possess a variety of activities in autoimmune models and diseases (summarized in Table 1); it is therefore a challenge to draw a definitive conclusion on the roles of MDSCs in autoimmune diseases [68, 69]. Generally speaking, *in vitro*, the isolated CD11b<sup>+</sup>Gr-1<sup>+</sup> MDSCs from inflammatory sites inhibit T cell responses dependent on various mechanisms such as NO and Arg-1. However, *in vivo*, endogenous MDSCs may be proinflammatory and fail to effectively reduce the severity of autoimmune diseases in several systems (e.g. in EAE [45, 54, 55]). By contrast, the adoptive transfer of MDSCs is able to induce immune tolerance to self-Ag and limits autoimmune pathology and has a beneficial effect on the autoimmune disease, as observed in models of IBD [9], T1D [61], and inflammatory eye disease [70]. The reasons that lead to these discrepancies between the activities of endogenous and exogenous MDSCs remain unclear. A possible explanation may be that certain factors coexisting in the same inflammatory microenvironment inhibit the suppressive activity of MDSCs, and the isolation of MDSCs is liberated from this "inhibitory" environment and MDSCs regain their immunosuppressive function upon readministration or addition into *in vitro* culture systems.

#### 4. Therapeutic Potential of MDSCs in Autoimmune Diseases

The application of MDSCs exogenously in certain animal models shows great efficacy in suppressing autoimmune diseases, indicating that MDSCs might be a promising cellular immunotherapeutic target in autoimmune diseases. Several potential cellular sources are available for *in vitro* generated MDSCs. Exogenous MDSCs isolated from the peripheral blood or bone marrow could be markedly expanded *in vitro* by use of growth factor/cytokine regimens [71–73]. In addition, it has been reported that exogenous MDSC populations also can derive from hematopoietic stem cells and embryonic stem cells [74]. More recently, the monocytes isolated from the peripheral blood were cultured *in vitro* supplemented with PGE2, for the generation of high numbers of MDSCs, and their functional stability was established [75]. *In vitro* generated MDSCs share many characteristics with their *ex vivo* isolated counterparts. They have strong suppressive effect on the proliferation of CD4<sup>+</sup> and CD8<sup>+</sup> T cells mediated by the expressions of iNOS and/or Arg-1 and cell-cell contact [72]. All these methods above will be able to provide reliable cellular products for immunotherapy in treating autoimmune diseases. Several groups have shown that the adoptive transfer of *ex vivo* generated MDSCs had the ability to inhibit graft-versus-host disease (GVHD) and prevent allograft rejection in mice [73, 74, 76]. Meanwhile, there are some potential risks associated with the utilization of MDSCs to treat autoimmune diseases. For example, MDSCs utilized

TABLE 1: Myeloid-derived suppressor cells in autoimmune diseases.

Disease	Species	Phenotype	Mechanism of suppression (in vitro)	Effect in vivo	Reference
Multiple sclerosis	Mouse	CD11b <sup>+</sup> Ly6C <sup>hi</sup> Ly6G <sup>-</sup>	NO apoptosis	Not determined	[8]
	Mouse	CD11b <sup>+</sup> CD62L <sup>+</sup> Ly6C <sup>+</sup>	Undetermined	Proinflammatory	[45]
	Mouse	CCR2 <sup>+</sup> CD11b <sup>+</sup> Ly6C <sup>hi</sup>	Unknown	Increase severity	[54]
	Mouse	CD11b <sup>+</sup> Gr-1 <sup>+</sup>	IL-1 $\beta$	Increase severity	[55]
	Mouse	CD11b <sup>hi</sup> Ly6G <sup>+</sup> Ly6C <sup>-</sup>	PD-L1	Reduce severity	[56]
Systemic lupus erythematosus	Mouse	CD11b <sup>+</sup> Gr-1 <sup>low</sup>	Arginase-1	Not determined	[11]
	Mouse	CD11c <sup>-</sup> CD11b <sup>+</sup> Gr-1 <sup>+</sup>	NO	Suppressor	[46]
	Mouse	CD11b <sup>+</sup> Ly6C <sup>hi</sup>	NO, PGE2, cell-cell contact	Possibly protective	[53]
	Human	HLA-DR <sup>-</sup> CD11b <sup>+</sup> CD33 <sup>+</sup>	Unknown	Increase severity	[58]
	Mouse	Gr-1 <sup>hi</sup> Ly6G <sup>+</sup> CD11b <sup>+</sup>	ROS, NO	Suppressor (in males)	[59]
A lupus-like disease driven by HSP	Mouse	CD11b <sup>+</sup> Gr-1 <sup>+</sup>	Unknown	Reduce severity	[57]
Type 1 diabetes	Mouse	CD11b <sup>+</sup> Gr-1 <sup>+</sup>	NO, IL-10, cell-cell contact	Reduce severity	[47]
	Mouse	CD11b <sup>hi</sup> Gr-1 <sup>int</sup>	Cell-cell contact	Proinflammatory	[60]
	Human	HLA-DR <sup>-</sup> CD11b <sup>+</sup> CD33 <sup>+</sup>	Cell-cell contact	Proinflammatory	[60]
	Mouse	Gr-1 <sup>+</sup> CD115 <sup>+</sup>	MHC class II-restricted Ag presentation	Reduce severity	[61]
Inflammatory bowel disease	Mouse	CD11b <sup>+</sup> Gr-1 <sup>+</sup>	NO apoptosis	Reduce severity	[9]
	Mouse	CD11b <sup>+</sup> Ly6C <sup>hi</sup> Ly6G <sup>-</sup>	NO, cell-cell contact, partially IFN- $\gamma$ , PGs	Not determined	[48]
Rheumatoid arthritis	Mouse	CD11b <sup>+</sup> Ly6G <sup>+</sup> Ly6C <sup>low</sup>	Arg-1, NO	Reduce severity	[49]
	Mouse	CD11c <sup>-</sup> CD11b <sup>+</sup> GR-1 <sup>+</sup>	IL-10, Arg-1	Reduce severity	[62]
	Human	HLA-DR <sup>-</sup> CD11b <sup>+</sup> CD33 <sup>+</sup>	Unknown	Suppressor	[66]
	Human	CD11b <sup>+</sup> CD33 <sup>+</sup> HLA-DR <sup>-</sup>	Unknown	Increase severity	[67]
Inflammatory eye disease	Mouse	CD11b <sup>+</sup> Gr-1 <sup>+</sup> Ly6G <sup>-</sup>	TNFR-dependent, arginase	Not determined	[51, 52]
	Mouse	CD11b <sup>+</sup> Gr-1 <sup>+</sup>	IL-6	Reduce severity	[70]
Autoimmune hepatitis	Mouse	CD11b <sup>+</sup> Ly6C <sup>hi</sup> Ly6G <sup>-</sup>	NO, IFN- $\gamma$ , cell-cell contact	Not determined	[50]
Alopecia areata	Mouse	CD11b <sup>+</sup> Gr-1 <sup>+</sup>	T cell apoptosis	Possibly protective	[63]
Experimental autoimmune myasthenia gravis	Mouse	CD11b <sup>+</sup> Gr-1 <sup>+</sup>	PGE2, NO, Arg-1	Reduce severity	[64]

would be nonspecific for antigen-specific T cells. Therefore, the suppressive effects of MDSCs on harmful T cell responses for autoantigens and the protective immune responses to pathogenic microorganisms or tumors exist at the same time. It would also be difficult to control the migration and accumulation of the injected MDSCs. Additionally, the release of inflammatory factors may occur after the administration of MDSCs. Some other unpredictable risks may also exist. Thus, more extensive research in animal models is indispensable before MDSCs therapy moves into clinical studies.

## 5. Concluding Remarks

MDSCs are a highly heterogeneous cell subpopulation. They have multifaceted phenotypic characteristics and may suppress T cell proliferation through various mechanisms. Large numbers of factors are involved in the differentiation, migration, expansion, and activation of MDSCs. However,

there are many unresolved questions in the field of MDSCs research. Up to now, the biological roles of MDSCs are rarely known. The role of endogenous MDSCs in autoimmune diseases in vivo remains controversial. Many questions about the variety of activities for MDSCs remain to be elucidated. It is necessary to understand why the induction and suppressive mechanisms of MDSCs are different between in vivo and in vitro environments. A better comprehension of the role of human MDSCs in autoimmunity and how to manipulate this cell population in patients with autoimmune diseases will be of great clinical significance. Importantly, exogenously prepared MDSCs have a great potential to become an effective immunotherapeutic regimen for autoimmune diseases.

## Conflicts of Interest

The authors declare that they have no conflicts of interest.

## Acknowledgments

This review is supported by the Shandong Science and Technology Development Plan on Medicine and Hygiene in China (2017WS147) and the National Natural Science Foundation of China (No. 81803097).

## References

- [1] M. R. Young, M. Newby, and H. T. Wepsic, "Hematopoiesis and suppressor bone marrow cells in mice bearing large metastatic Lewis lung carcinoma tumors," *Cancer Research*, vol. 47, no. 1, pp. 100–105, 1987.
- [2] S. C. Buessow, R. D. Paul, and D. M. Lopez, "Influence of mammary tumor progression on phenotype and function of spleen and in situ lymphocytes in mice," *Journal of the National Cancer Institute*, vol. 73, no. 1, pp. 249–255, 1984.
- [3] T. Condamine and D. I. Gabrilovich, "Molecular mechanisms regulating myeloid-derived suppressor cell differentiation and function," *Trends in Immunology*, vol. 32, no. 1, pp. 19–25, 2011.
- [4] D. I. Gabrilovich, S. Ostrand-Rosenberg, and V. Bronte, "Coordinated regulation of myeloid cells by tumours," *Nature Reviews. Immunology*, vol. 12, no. 4, pp. 253–268, 2012.
- [5] Y. S. Khaled, B. J. Ammori, and E. Elkord, "Myeloid-derived suppressor cells in cancer: recent progress and prospects," *Immunology and Cell Biology*, vol. 91, no. 8, pp. 493–502, 2013.
- [6] K. De Veirman, E. Menu, K. Maes et al., "Myeloid-derived suppressor cells induce multiple myeloma cell survival by activating the AMPK pathway," *Cancer Letters*, vol. 442, pp. 233–241, 2018.
- [7] A. Pastaki Khoshbin, M. Eskian, M. Keshavarz-Fathi, and N. Rezaei, "Roles of myeloid-derived suppressor cells in cancer metastasis: immunosuppression and beyond," *Archivum Immunologiae et Therapiae Experimentalis (Warsz)*, pp. 1–14, 2018.
- [8] B. Zhu, Y. Bando, S. Xiao et al., "CD11b+Ly-6C(hi) suppressive monocytes in experimental autoimmune encephalomyelitis," *Journal of Immunology*, vol. 179, no. 8, pp. 5228–5237, 2007.
- [9] L. A. Haile, R. von Wasielewski, J. Gamrekelashvili et al., "Myeloid-derived suppressor cells in inflammatory bowel disease: a new immunoregulatory pathway," *Gastroenterology*, vol. 135, no. 3, pp. 871–881.e5, 2008.
- [10] L. B. Nicholson, B. J. Raveney, and M. Munder, "Monocyte dependent regulation of autoimmune inflammation," *Current Molecular Medicine*, vol. 9, no. 1, pp. 23–29, 2009.
- [11] Y. Iwata, K. Furuichi, K. Kitagawa et al., "Involvement of CD11b+ GR-1 low cells in autoimmune disorder in MRL-Fas lpr mouse," *Clinical and Experimental Nephrology*, vol. 14, no. 5, pp. 411–417, 2010.
- [12] A. Wegner, J. Verhagen, and D. C. Wraith, "Myeloid-derived suppressor cells mediate tolerance induction in autoimmune disease," *Immunology*, vol. 151, no. 1, pp. 26–42, 2017.
- [13] D. I. Gabrilovich and S. Nagaraj, "Myeloid-derived suppressor cells as regulators of the immune system," *Nature Reviews Immunology*, vol. 9, no. 3, pp. 162–174, 2009.
- [14] E. Ribechini, V. Greifengberg, S. Sandwick, and M. B. Lutz, "Subsets, expansion and activation of myeloid-derived suppressor cells," *Medical Microbiology and Immunology*, vol. 199, no. 3, pp. 273–281, 2010.
- [15] C. R. Millrud, C. Bergenfelz, and K. Leandersson, "On the origin of myeloid-derived suppressor cells," *Oncotarget*, vol. 8, no. 2, pp. 3649–3665, 2017.
- [16] W. Zhang, J. Li, G. Qi, G. Tu, C. Yang, and M. Xu, "Myeloid-derived suppressor cells in transplantation: the dawn of cell therapy," *Journal of Translational Medicine*, vol. 16, no. 1, p. 19, 2018.
- [17] H. F. Peñaloza, D. Alvarez, N. Muñoz-Durango et al., "The role of myeloid-derived suppressor cells in chronic infectious diseases and the current methodology available for their study," *Journal of Leukocyte Biology*, 2018.
- [18] J. I. Youn, S. Nagaraj, M. Collazo, and D. I. Gabrilovich, "Subsets of myeloid-derived suppressor cells in tumor-bearing mice," *Journal of Immunology*, vol. 181, no. 8, pp. 5791–5802, 2008.
- [19] J. Jiang, W. Guo, and X. Liang, "Phenotypes, accumulation, and functions of myeloid-derived suppressor cells and associated treatment strategies in cancer patients," *Human Immunology*, vol. 75, no. 11, pp. 1128–1137, 2014.
- [20] H. S. Chou, C. C. Hsieh, H. R. Yang et al., "Hepatic stellate cells regulate immune response by way of induction of myeloid suppressor cells in mice," *Hepatology*, vol. 53, no. 3, pp. 1007–1019, 2011.
- [21] P. Serafini, "Myeloid derived suppressor cells in physiological and pathological conditions: the good, the bad, and the ugly," *Immunologic Research*, vol. 57, no. 1–3, pp. 172–184, 2013.
- [22] E. Peranzoni, S. Zilio, I. Marigo et al., "Myeloid-derived suppressor cell heterogeneity and subset definition," *Current Opinion in Immunology*, vol. 22, no. 2, pp. 238–244, 2010.
- [23] D. I. Gabrilovich, V. Bronte, S. H. Chen et al., "The terminology issue for myeloid-derived suppressor cells," *Cancer Research*, vol. 67, no. 1, p. 425, 2007, author reply 426.
- [24] T. Condamine, G. A. Dominguez, J. I. Youn et al., "Lectin-type oxidized LDL receptor-1 distinguishes population of human polymorphonuclear myeloid-derived suppressor cells in cancer patients," *Science Immunology*, vol. 1, no. 2, article aaf8943, 2016.
- [25] E. Iacobaeus, I. Douagi, R. Jitschin et al., "Phenotypic and functional alterations of myeloid-derived suppressor cells during the disease course of multiple sclerosis," *Immunology and Cell Biology*, vol. 96, no. 8, pp. 820–830, 2018.
- [26] K. Fujio, T. Okamura, S. Sumitomo, and K. Yamamoto, "Regulatory T cell-mediated control of autoantibody-induced inflammation," *Frontiers in Immunology*, vol. 3, p. 28, 2012.
- [27] K. Zhu, N. Zhang, N. Guo et al., "SSC(high)CD11b(high)Ly-6C(high)Ly-6G(low) myeloid cells curtail CD4 T cell response by inducible nitric oxide synthase in murine hepatitis," *The International Journal of Biochemistry & Cell Biology*, vol. 54, pp. 89–97, 2014.
- [28] L. Hammerich, K. T. Warzecha, M. Stefkova et al., "Cyclic adenosine monophosphate-responsive element modulator alpha overexpression impairs function of hepatic myeloid-derived suppressor cells and aggravates immune-mediated hepatitis in mice," *Hepatology*, vol. 61, no. 3, pp. 990–1002, 2015.
- [29] Y. Kwak, H. E. Kim, and S. G. Park, "Insights into myeloid-derived suppressor cells in inflammatory diseases," *Archivum Immunologiae et Therapiae Experimentalis (Warsz)*, vol. 63, no. 4, pp. 269–285, 2015.

- [30] J. Bromberg, "Stat proteins and oncogenesis," *The Journal of Clinical Investigation*, vol. 109, no. 9, pp. 1139–1142, 2002.
- [31] K. Imada and W. J. Leonard, "The Jak-STAT pathway," *Molecular Immunology*, vol. 37, no. 1-2, pp. 1–11, 2000.
- [32] D. E. Levy and J. E. Darnell Jr., "Stats: transcriptional control and biological impact," *Nature Reviews Molecular Cell Biology*, vol. 3, no. 9, pp. 651–662, 2002.
- [33] J. M. Haverkamp, S. A. Crist, B. D. Elzey, C. Cimen, and T. L. Ratliff, "In vivo suppressive function of myeloid-derived suppressor cells is limited to the inflammatory site," *European Journal of Immunology*, vol. 41, no. 3, pp. 749–759, 2011.
- [34] C. A. Corzo, M. J. Cotter, P. Cheng et al., "Mechanism regulating reactive oxygen species in tumor-induced myeloid-derived suppressor cells," *Journal of Immunology*, vol. 182, no. 9, pp. 5693–5701, 2009.
- [35] A. C. Ochoa, A. H. Zea, C. Hernandez, and P. C. Rodriguez, "Arginase, prostaglandins, and myeloid-derived suppressor cells in renal cell carcinoma," *Clinical Cancer Research*, vol. 13, no. 2, pp. 721s–726s, 2007.
- [36] C. Bogdan, "Regulation of lymphocytes by nitric oxide," in *Suppression and Regulation of Immune Responses*, M. Cuturi and I. Anegón, Eds., vol. 677 of *Methods in Molecular Biology (Methods and Protocols)*, pp. 375–393, Humana Press, Totowa, NJ, USA, 2011.
- [37] K. Ohl and K. Tenbrock, "Reactive oxygen species as regulators of MDSC-mediated immune suppression," *Frontiers in Immunology*, vol. 9, p. 2499, 2018.
- [38] K. Movahedi, M. Guillemins, J. van den Bossche et al., "Identification of discrete tumor-induced myeloid-derived suppressor cell subpopulations with distinct T cell-suppressive activity," *Blood*, vol. 111, no. 8, pp. 4233–4244, 2008.
- [39] P. Sinha, V. K. Clements, A. M. Fulton, and S. Ostrand-Rosenberg, "Prostaglandin E2 promotes tumor progression by inducing myeloid-derived suppressor cells," *Cancer Research*, vol. 67, no. 9, pp. 4507–4513, 2007.
- [40] A. L. Mellor and D. H. Munn, "IDO expression by dendritic cells: tolerance and tryptophan catabolism," *Nature Reviews Immunology*, vol. 4, no. 10, pp. 762–774, 2004.
- [41] H. Li, Y. Han, Q. Guo, M. Zhang, and X. Cao, "Cancer-expanded myeloid-derived suppressor cells induce anergy of NK cells through membrane-bound TGF- $\beta$ 1," *The Journal of Immunology*, vol. 182, no. 1, pp. 240–249, 2009.
- [42] Y. Liu, B. Zeng, Z. Zhang, Y. Zhang, and R. Yang, "B7-H1 on myeloid-derived suppressor cells in immune suppression by a mouse model of ovarian cancer," *Clinical Immunology*, vol. 129, no. 3, pp. 471–481, 2008.
- [43] B. Huang, P. Y. Pan, Q. Li et al., "Gr-1+CD115+ immature myeloid suppressor cells mediate the development of tumor-induced T regulatory cells and T-cell anergy in tumor-bearing host," *Cancer Research*, vol. 66, no. 2, pp. 1123–1131, 2006.
- [44] B. Knier, M. Hiltensperger, C. Sie et al., "Myeloid-derived suppressor cells control B cell accumulation in the central nervous system during autoimmunity," *Nature Immunology*, vol. 19, no. 12, pp. 1341–1351, 2018.
- [45] I. L. King, T. L. Dickendesher, and B. M. Segal, "Circulating Ly-6C+ myeloid precursors migrate to the CNS and play a pathogenic role during autoimmune demyelinating disease," *Blood*, vol. 113, no. 14, pp. 3190–3197, 2009.
- [46] M. J. Park, S. H. Lee, E. K. Kim et al., "Myeloid-derived suppressor cells induce the expansion of regulatory B cells and ameliorate autoimmunity in the sanroque mouse model of systemic lupus erythematosus," *Arthritis & Rheumatology*, vol. 68, no. 11, pp. 2717–2727, 2016.
- [47] C. Hu, W. Du, X. Zhang, F. S. Wong, and L. Wen, "The role of Gr1+ cells after anti-CD20 treatment in type 1 diabetes in non-obese diabetic mice," *The Journal of Immunology*, vol. 188, no. 1, pp. 294–301, 2012.
- [48] E. Kurmaeva, D. Bhattacharya, W. Goodman et al., "Immuno-suppressive monocytes: possible homeostatic mechanism to restrain chronic intestinal inflammation," *Journal of Leukocyte Biology*, vol. 96, no. 3, pp. 377–389, 2014.
- [49] W. Fujii, E. Ashihara, H. Hirai et al., "Myeloid-derived suppressor cells play crucial roles in the regulation of mouse collagen-induced arthritis," *Journal of Immunology*, vol. 191, no. 3, pp. 1073–1081, 2013.
- [50] J. G. Cripps, J. Wang, A. Maria, I. Blumenthal, and J. D. Gorham, "Type 1 T helper cells induce the accumulation of myeloid-derived suppressor cells in the inflamed Tgfb1 knockout mouse liver," *Hepatology*, vol. 52, no. 4, pp. 1350–1359, 2010.
- [51] E. C. Kerr, B. J. E. Raveney, D. A. Copland, A. D. Dick, and L. B. Nicholson, "Analysis of retinal cellular infiltrate in experimental autoimmune uveoretinitis reveals multiple regulatory cell populations," *Journal of Autoimmunity*, vol. 31, no. 4, pp. 354–361, 2008.
- [52] B. J. Raveney, D. A. Copland, A. D. Dick, and L. B. Nicholson, "TNFR1-dependent regulation of myeloid cell function in experimental autoimmune uveoretinitis," *The Journal of Immunology*, vol. 183, no. 4, pp. 2321–2329, 2009.
- [53] H. Ma, S. Wan, and C. Q. Xia, "Immunosuppressive CD11b+Ly6Chi monocytes in pristane-induced lupus mouse model," *Journal of Leukocyte Biology*, vol. 99, no. 6, pp. 1121–1129, 2016.
- [54] A. Mildner, M. Mack, H. Schmidt et al., "CCR2+Ly-6Chi monocytes are crucial for the effector phase of autoimmunity in the central nervous system," *Brain*, vol. 132, no. 9, pp. 2487–2500, 2009.
- [55] H. F. Yi et al., "Mouse CD11b+Gr-1+ myeloid cells can promote Th17 cell differentiation and experimental autoimmune encephalomyelitis," *The Journal of Immunology*, vol. 189, no. 9, pp. 4295–4304, 2012.
- [56] M. Ioannou, T. Alissafi, I. Lazaridis et al., "Crucial role of granulocytic myeloid-derived suppressor cells in the regulation of central nervous system autoimmune disease," *Journal of Immunology*, vol. 188, no. 3, pp. 1136–1146, 2012.
- [57] J. E. Thaxton, B. Liu, P. Zheng, Y. Liu, and Z. Li, "Deletion of CD24 impairs development of heat shock protein gp96-driven autoimmune disease through expansion of myeloid-derived suppressor cells," *The Journal of Immunology*, vol. 192, no. 12, pp. 5679–5686, 2014.
- [58] H. Wu, Y. Zhen, Z. Ma et al., "Arginase-1-dependent promotion of TH17 differentiation and disease progression by MDSCs in systemic lupus erythematosus," *Science Translational Medicine*, vol. 8, no. 331, article 331ra40, 2016.
- [59] A. Trigunaite, A. Khan, E. der, A. Song, S. Varikuti, and T. N. Jørgensen, "Gr-1(high) CD11b+ cells suppress B cell differentiation and lupus-like disease in lupus-prone male mice," *Arthritis and Rheumatism*, vol. 65, no. 9, pp. 2392–2402, 2013.

- [60] F. Whitfield-Larry, J. Felton, J. Buse, and M. A. Su, "Myeloid-derived suppressor cells are increased in frequency but not maximally suppressive in peripheral blood of type 1 diabetes mellitus patients," *Clinical Immunology*, vol. 153, no. 1, pp. 156–164, 2014.
- [61] B. Yin, G. Ma, C. Y. Yen et al., "Myeloid-derived suppressor cells prevent type 1 diabetes in murine models," *The Journal of Immunology*, vol. 185, no. 10, pp. 5828–5834, 2010.
- [62] M. J. Park, S. H. Lee, E. K. Kim et al., "Interleukin-10 produced by myeloid-derived suppressor cells is critical for the induction of Tregs and attenuation of rheumatoid inflammation in mice," *Scientific Reports*, vol. 8, no. 1, p. 3753, 2018.
- [63] V. Singh, U. Mueller, P. Freyschmidt-Paul, and M. Zöller, "Delayed type hypersensitivity-induced myeloid-derived suppressor cells regulate autoreactive T cells," *European Journal of Immunology*, vol. 41, no. 10, pp. 2871–2882, 2011.
- [64] Y. Li, Z. Tu, S. Qian et al., "Myeloid-derived suppressor cells as a potential therapy for experimental autoimmune myasthenia gravis," *Journal of Immunology*, vol. 193, no. 5, pp. 2127–2134, 2014.
- [65] D. Talabot-Ayer, P. Martin, C. Vesin et al., "Severe neutrophil-dominated inflammation and enhanced myelopoiesis in IL-33-overexpressing CMV/IL33 mice," *Journal of Immunology*, vol. 194, no. 2, pp. 750–760, 2015.
- [66] Z. Jiao, S. Hua, W. Wang, H. Wang, J. Gao, and X. Wang, "Increased circulating myeloid-derived suppressor cells correlated negatively with Th17 cells in patients with rheumatoid arthritis," *Scandinavian Journal of Rheumatology*, vol. 42, no. 2, pp. 85–90, 2013.
- [67] J. Zhu, S. Chen, L. Wu et al., "The expansion of myeloid-derived suppressor cells is associated with joint inflammation in rheumatic patients with arthritis," *BioMed Research International*, vol. 2018, Article ID 5474828, 12 pages, 2018.
- [68] P. A. Barnie, P. Zhang, H. Lv et al., "Myeloid-derived suppressor cells and myeloid regulatory cells in cancer and autoimmune disorders," *Experimental and Therapeutic Medicine*, vol. 13, no. 2, pp. 378–388, 2017.
- [69] M. Zoller, "Janus-faced myeloid-derived suppressor cell exosomes for the good and the bad in cancer and autoimmune disease," *Frontiers in Immunology*, vol. 9, p. 137, 2018.
- [70] Z. Tu, Y. Li, D. Smith et al., "Myeloid suppressor cells induced by retinal pigment epithelial cells inhibit autoreactive T-cell responses that lead to experimental autoimmune uveitis," *Investigative Ophthalmology & Visual Science*, vol. 53, no. 2, pp. 959–966, 2012.
- [71] I. Marigo, E. Bosio, S. Solito et al., "Tumor-induced tolerance and immune suppression depend on the C/EBPbeta transcription factor," *Immunity*, vol. 32, no. 6, pp. 790–802, 2010.
- [72] M. G. Lechner, D. J. Liebertz, and A. L. Epstein, "Characterization of cytokine-induced myeloid-derived suppressor cells from normal human peripheral blood mononuclear cells," *Journal of Immunology*, vol. 185, no. 4, pp. 2273–2284, 2010.
- [73] S. L. Highfill, P. C. Rodriguez, Q. Zhou et al., "Bone marrow myeloid-derived suppressor cells (MDSCs) inhibit graft-versus-host disease (GVHD) via an arginase-1-dependent mechanism that is up-regulated by interleukin-13," *Blood*, vol. 116, no. 25, pp. 5738–5747, 2010.
- [74] Z. Zhou, D. L. French, G. Ma et al., "Development and function of myeloid-derived suppressor cells generated from mouse embryonic and hematopoietic stem cells," *Stem Cells*, vol. 28, no. 3, pp. 620–632, 2010.
- [75] N. Obermajer and P. Kalinski, "Generation of myeloid-derived suppressor cells using prostaglandin E2," *Transplantation Research*, vol. 1, no. 1, p. 15, 2012.
- [76] K. P. A. MacDonald, V. Rowe, A. D. Clouston et al., "Cytokine expanded myeloid precursors function as regulatory antigen-presenting cells and promote tolerance through IL-10-producing regulatory T cells," *Journal of Immunology*, vol. 174, no. 4, pp. 1841–1850, 2005.